

NAVAL POSTGRADUATE SCHOOL Monterey, California

2

AD-A252 932



DTIC
ELECTE
JUL 20 1992
S B D

THESIS

USE OF AN OPTICAL MULTICHANNEL ANALYZER
FOR REFLECTIVITY MEASUREMENTS

by

David T. Moroney

March 1992

Thesis Advisor
Co-Advisor

Oscar Biblarz
David D. Cleary

Approved for public release; distribution is unlimited.

92 7 11 054

92-19046



Unclassified

SECURITY CLASSIFICATION OF THIS PAGE

REPORT DOCUMENTATION PAGE

1a. REPORT SECURITY CLASSIFICATION Unclassified			1b. RESTRICTIVE MARKINGS		
2a. SECURITY CLASSIFICATION AUTHORITY			3. DISTRIBUTION/AVAILABILITY OF REPORT Approved for public release; distribution is unlimited.		
2b. DECLASSIFICATION/DOWNGRADING SCHEDULE					
4. PERFORMING ORGANIZATION REPORT NUMBER(S)			5. MONITORING ORGANIZATION REPORT NUMBER(S)		
6a. NAME OF PERFORMING ORGANIZATION Naval Postgraduate School		6b. OFFICE SYMBOL (If Applicable) 39	7a. NAME OF MONITORING ORGANIZATION Naval Postgraduate School		
6c. ADDRESS (city, state, and ZIP code) Monterey, CA 93943-5000			7b. ADDRESS (city, state, and ZIP code) Monterey, CA 93943-5000		
8a. NAME OF FUNDING/SPONSORING ORGANIZATION		6b. OFFICE SYMBOL (If Applicable)	9. PROCUREMENT INSTRUMENT IDENTIFICATION NUMBER		
8c. ADDRESS (city, state, and ZIP code)			10. SOURCE OF FUNDING NUMBERS		
			PROGRAM ELEMENT NO.	PROJECT NO.	TASK NO.
			WORK UNIT ACCESSION NO.		
11. TITLE (Include Security Classification) USE OF AN OPTICAL MULTICHANNEL ANALYZER FOR REFLECTIVITY MEASUREMENTS					
12. PERSONAL AUTHOR(S) DAVID T. MORONEY, LCDR, USN					
13a. TYPE OF REPORT Master's Thesis		13b. TIME COVERED FROM TO	14. DATE OF REPORT (year, month, day) 1992 March	15. PAGE COUNT 187	
16. SUPPLEMENTARY NOTATION The views expressed in this thesis are those of the author and do not reflect the official policy or position of the Department of Defense or the U.S. Government.					
17. COST CODES			18. SUBJECT TERMS (continue on reverse if necessary and identify by block number)		
FIELD	GROUP	SUBGROUP	Metallic Clusters / Metallic Reflectors / Micro Particles / Reflectance / Fluorescence / Luminescence / Phosphorescence / Copper		
19. ABSTRACT (Continue on reverse if necessary and identify by block number) Current theories that attempt to explain the emission and reflection properties of metallic surfaces still provide some room for conjecture and alternative concepts. This is true particularly for processes in the visible portion of the electromagnetic spectrum. One relatively new theory that has recently received increased attention and support is that of the "native cluster" model. The model proposes that metallic surfaces are populated with small groups of atoms that have been liberated from the crystalline lattice structure of the bulk metal. These colloids possess dielectric qualities that act to modify basic properties of the parent material, such as polarizability, electrical conductivity, thermal emission, and luminescence. While proof of luminescence from metallic surfaces would not significantly detract from existing free electron and quantum theory, it would tend to support the "native cluster" model. Due to its reflectivity characteristics, copper was selected as the metal to be studied in this research. One instrument that is well suited for the collection of reflectivity and emission data is the Optical Multichannel Analyzer. Although a powerful tool for spectral research, the requirement of a significant initial investment of time necessary to gain sufficient user familiarity to become proficient with the equipment has resulted in the instrument being underutilized. Therefore, in addition to the primary aim of this research in evaluating the ability of a polished copper surface to luminesce, a secondary aim was to evaluate the characteristics and applicability of this instrument to support the luminescence research. The results of this research were the development of user friendly checklists for basic operation of the OMA III, a determination of error sources due to experimental equipment and procedures, the magnitudes of those errors, substantiation of the results by reproducing known metallic reflectivity data, and the collection of data indicating the possible existence of luminescence from a copper surface.					
20. DISTRIBUTION/AVAILABILITY OF ABSTRACT <input checked="" type="checkbox"/> UNCLASSIFIED/UNLIMITED <input type="checkbox"/> SAME AS RPT. <input type="checkbox"/> DTIC USERS			21. ABSTRACT SECURITY CLASSIFICATION Unclassified		
22a. NAME OF RESPONSIBLE INDIVIDUAL Oscar Biblarz			22b. TELEPHONE (Include Area Code) (408) 646-3096	22c. OFFICE SYMBOL AA/Bi	

DD FORM 1473, 84 MAR
PAGE

83 APR edition may be used until exhausted SECURITY CLASSIFICATION OF THIS

All other editions are obsolete

Unclassified

Approved for public release; distribution is unlimited.

**Use of an Optical Multichannel Analyzer for
Reflectivity Measurements**

by

David T. Moroney
Lieutenant Commander, United States Navy
B.S., United States Naval Academy, 1979

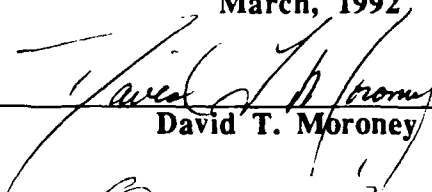
Submitted in partial fulfillment of the requirements for the degree of
MASTER OF SCIENCE IN ASTRONAUTICAL ENGINEERING

from the

NAVAL POSTGRADUATE SCHOOL

March, 1992

Author:




David T. Moroney

Approved by:



Oscar Biblarz, Thesis Advisor



David D. Cleary, Thesis Co-Advisor



Daniel J. Collins, Chairman
Department of Aeronautics and Astronautics

ABSTRACT

Current theories that attempt to explain the emission and reflection properties of metallic surfaces still provide some room for conjecture and alternative concepts. This is true particularly for processes in the visible portion of the electromagnetic spectrum. One relatively new theory that has recently received increased attention and support is that of the "native cluster" model. The model proposes that metallic surfaces are populated with small groups of atoms that have been liberated from the crystalline lattice structure of the bulk metal. These colloids possess dielectric qualities that act to modify basic properties of the parent material, such as polarizability, electrical conductivity, thermal emission, and luminescence. While proof of luminescence from metallic surfaces would not significantly detract from existing free electron and quantum theory, it would tend to support the "native cluster" model. Due to its reflectivity characteristics, copper was selected as the metal to be studied in this research.

One instrument that is well suited for the collection of reflectivity and emission data is the Optical Multichannel Analyzer. Although a powerful tool for spectral research, the requirement of a significant initial investment of time necessary to gain sufficient user familiarity to become proficient with the equipment has resulted in the instrument being underutilized. Therefore, in addition to the primary aim of this research in evaluating the ability of a polished copper surface to luminesce, a secondary aim was to evaluate the characteristics and applicability of this instrument to support the luminescence research.

The results of this research were the development of user friendly checklists for basic operation of the OMA III, a determination of error sources due to experimental equipment and procedures, the magnitudes of those errors, substantiation of the results by reproducing known metallic reflectivity data, and the collection of data indicating the possible existence of luminescence from a copper surface.

Accession For	
NTIS GRA&I	<input checked="" type="checkbox"/>
DTIC TAB	<input type="checkbox"/>
Unannounced	<input type="checkbox"/>
Justification	
By _____	
Distribution/	
Availability Codes	
Dist.	Avail and/or Special
A-1	

TABLE OF CONTENTS

I. INTRODUCTION.....	1
A. GENERAL.....	1
B. BACKGROUND.....	1
1. Free Electron Theory	2
a. Lorentz Model	2
b. Drude Model	2
c. Reflectivity According to Free Electron Theory	3
2. Quantum Theory	5
a. History of Development of the Quantum Theory	5
b. Band Theory of Solids.....	7
c. Reflectivity According to Quantum Theory	9
C. METALLIC CLUSTERS.....	10
1. History of Cluster Research	10
2. "Native Cluster" Model	11
3. Luminescence	12
D. OPTICAL MULTICHANNEL ANALYZER (OMA III).....	16
 II. SCOPE OF RESEARCH.....	 17
A. DESCRIPTION OF EQUIPMENT	17
1. Optical Multichannel Analyzer (OMA III) System	17
a. Spectrograph (MonoSpec 27).....	17
b. Detector (Model 1453A).....	18
c. Detector Controller (Model 1462 and 1462/99).....	20
d. System Processor (Model 1460)	21

e. System Software	22
2. Light Sources.....	24
a. Calibration Source.....	24
b. 100 W Commercial Incandescent Bulb	25
c. 500 W Halogen / Quartz Light Source.....	25
d. Mercury Arc Lamp	25
3. Filters.....	26
4. Metallic Specimens	26
a. Aluminum Specimen.....	26
b. Copper Specimen.....	27
5. Optics Lenses.....	27
6. Optical Bench and Equipment	28
7. Chopper.....	28
8. HP ColorPro Graphics Plotter	28
9. Epson FX-86e Serial Printer	28
B. EXPERIMENT ENVIRONMENT AND CONDITIONS	29
 III. EXPERIMENTAL METHOD.....	 30
A. METALLIC MIRROR SURFACE PREPARATION.....	30
1. Mounting.....	30
2. Grinding	31
3. Polishing.....	31
B. EQUIPMENT SETUP AND EXPERIMENTAL PROCEDURE	32
1. Light Source Radiance	33
2. Sources of Experimental Error	35
a. Wavelength Calibration.....	35
b. Source Intensity Fluctuations	35

c. Dark Current	36
d. Polarization Sensitivity of the OMA III	37
e. Spectrograph Axis Angle Offset Sensitivity.....	37
f. Apparent Detector Sensitivity as a Function of Exposure Time, Data Source Mode and Data Acquisition Mode	38
g. Oxidation of Copper Surface.....	39
3. Sources of Data Reduction Errors	39
a. Background Compensation Mode.....	40
b. Timing of Background Compensation.....	41
4. Filter / Goggle Transmittance.....	42
5. Polished Aluminum Surface Reflectance.....	43
6. Copper Luminescence Experiments	45
a. Filter Method Number 1	46
b. Filter Method Number 2.....	47
c. Chopper Method.....	48
C. DATA REDUCTION AND PRESENTATION.....	50
D. SAFETY.....	50
 IV. RESULTS AND DISCUSSION.....	 52
A. GENERAL.....	52
B. EXPERIMENTAL EQUIPMENT CHARACTERISTICS.....	52
1. Light Source Spectra	52
a. Mercury Sources	52
b. Tungsten Filament Sources	53
2. Sources of Experimental Error	53
a. Wavelength Calibration.....	54
b. Source Intensity Fluctuations	54

c. Dark Current	56
d. Polarization Sensitivity of the OMA III.....	57
e. Spectrograph Axis Angle Offset Sensitivity.....	58
f. Apparent Detector Sensitivity as a Function of Exposure Time, Data Source Mode and Data Acquisition Mode	59
g. Oxidation of Metal Surface.....	61
3. Sources of Data Reduction Errors	61
a. Background Compensation Mode.....	61
b. Timing of Background Compensation and Data Storage	63
4. Twardy Bandpass Filter Transmittance	64
5. Longpass Filter Transmittance	64
6. Safety Goggle Transmittance.....	65
7. Aluminum Reflectance	66
7. Copper Luminescence Using Filter Method 1.....	67
8. Copper Luminescence Using Filter Method 2.....	68
9. Copper Luminescence Using the Chopper.....	68
 V. CONCLUSIONS AND RECOMMENDATIONS	70
A. CONCLUSIONS.....	70
B. RECOMMENDATIONS	71

APPENDIX A.....	75
APPENDIX B.....	79
APPENDIX C.....	94
REFERENCES.....	171
INITIAL DISTRIBUTION LIST	173

LIST OF TABLES

Table I	QUANTUM THEORY OF THE ATOMIC ELECTRON BAND STRUCTURE OF SOME OF THE NOBEL METALS	8
Table II	SPECTROGRAPH GRATING SPECIFICATIONS.....	18
Table III	TWARDY FILTER MANUFACTURER SPECIFIED CHARACTERISTICS.....	27
Table IV	BASELINE PROCEDURES	33
Table V	SOURCE TO SPECTROGRAPH DISTANCES FOR RADIANCE MEASUREMENTS (as Shown in Figure 6)	34
Table VI	APPARENT DETECTOR SENSITIVITY EXPERIMENTAL SETTINGS...	38
Table VII	ORDER OF DATA STORAGE BY COMPENSATION MODE FOR VARIOUS SOURCES	41
Table VIII	SELECTED LIGHT SOURCE AND SOURCE TO SPECTROGRAPH DISTANCES (as Shown in Figure 6) FOR FILTER / GOGGLE TRANSMITTANCE MEASUREMENTS	43
Table IX	MERCURY CALIBRATION LAMP RADIATED INTENSITY FLUCTUATIONS	55
Table X	MERCURY CALIBRATION LAMP INTENSITY AS A FUNCTION OF WAVELENGTH AND COMPENSATION MODE.....	62

LIST OF FIGURES

Figure 1	Generalized Metallic Reflectivity Curve Based on the Free Electron Theory.....	5
Figure 2	Reflectance of Common Metals at Normal Incidence	6
Figure 3	Band Theory of Solids.....	9
Figure 4	State Energy Diagram Depicting Fluorescence and Phosphorescence	14
Figure 5	Fluorescence Spectrum for Copper	15
Figure 6	Setup for Light Source Emittance and Filter Transmittance Experiments (Side View)	34
Figure 7	Setup for Spectrograph Axis Angle Offset Sensitivity Measurements (Top View).....	37
Figure 8	Setup for Copper Surface Reflection Degradation Experiment (Top View)....	40
Figure 9	Setup for the Aluminum Reflectance Experiment.....	44
Figure 10	Setup for the Copper Luminescence Experiments Using Longpass and Bandpass Filters.....	47
Figure 11	Setup for the Copper Luminescence Experiments Using a Light Chopper.....	49

ACKNOWLEDGEMENT

The research performed for this thesis required the involvement and assistance of members of four separate curricula at the Naval Postgraduate School. Everyone was extremely supportive and helpful. Without each of their individual contributions, this thesis would not have been possible.

In addition to the insight and guidance they provided in planning, reviewing, and reporting on experimental procedures and results, my Advisor, Prof. Oscar Biblarz, and Co-Advisor, Prof. Dave Cleary, were the only two people at NPS who had any prior experience with the OMA III.

From the Physics Department, Mr. Bob Sanders provided unparalleled service in his capacity as laboratory technician. He gladly made available every piece of laboratory equipment that he had in his inventory, and took the time to conduct familiarization training when I needed it. Prof. Scott Davis' experience in the field of spectroscopy was an invaluable resource that allowed the research to progress when stumbling blocks from unexpected results presented themselves. Prof. Jerry Lentz's previous endeavors in the area of fluorescence research provided many suggestions for alternative experimental methods, which proved potentially fruitful.

The Material Science Department provided the highly pure metal specimens and the training, support and equipment necessary for the proper preparation of the metallic surfaces. Profs. Alan Fox and Roy Crooks acquired and made available the sheet of chemical grade copper and aluminum ingot from which the specimens were taken. Mr. Doug Shelton made his grinding and polishing facilities and supplies available around the clock and demonstrated the proper techniques for using the necessary equipments.

Finally, Mr. Dan Sakoda, of the Space Systems Engineering Curriculum provided access to word processing facilities and administrative support.

I. INTRODUCTION

A. GENERAL

Reflectivity measurements from metallic surfaces pose many challenges and is an area of great practical interest. Much care must be exercised in the collection of the data and measurement apparatus are typically complex. One instrument that is well suited for the collection of reflectivity data is the Optical Multichannel Analyzer (OMA). OMAs, however, are sophisticated instruments, the use of which requires a significant initial investment of time and research to gain the user familiarity necessary to properly operate them and minimize the introduction of errors in the acquired data. Consequently, although they are a very powerful tool, they have historically tended to be underutilized.

Reflectivity from metallic surfaces is a broad area of study with many applications and areas of specialized emphasis. Virtually any aspect of this vast field could have been chosen for the topic of this thesis; however, the thrust of the research discussed herein is designed to support a relatively new theory of metallic surface composition based on the possible existence of "native clusters". The specific aspect of metallic surface reflectivity that is the ultimate goal of this research is the observation of luminescence from metallic copper surfaces.

B. BACKGROUND

Currently there are two principal theories that attempt to explain the optical properties of metallic surfaces. The free electron theory seems to hold well for incident wavelengths in the infrared portion of the electromagnetic spectrum and greater, and the quantum theory is mostly applicable to the regions of ultraviolet wavelength and lower. Consequently, no

one theory is thought to adequately explain the optical characteristics of metals in the near visible spectrum.

1. Free Electron Theory

Free-electron theory was first proposed by H.A. Lorentz to explain the atomic structure of insulators, or dielectrics as they are also known. The Lorentz model was modified by P.K.L. Drude for applicability to free-electron metals and later both models were refined by A. Sommerfield [Ref. 1:p. 42]. The result of the theory is the model of a metal as a conducting medium in which both bound and unbound electrons play a role.

a. Lorentz Model

In a dielectric material, the Lorentz model contends that negatively-charged electrons are bound to the positively-charged atomic nuclei by quasi-elastic forces. The existence of these forces is based on the fact that a charge equilibrium position exists between the positive and negative particles. If the electrons are displaced from their charge equilibrium position, a restoring force equal and opposite to the product of the charge and the displacement distance is generated bringing the electrons back to their bound equilibrium position. [Ref. 2:p. 91] The response of a dielectric material to an externally induced electromagnetic field is due primarily to these bound electrons.

b. Drude Model

According to the Drude model, in a conducting material such as a metal, there exist "free electrons." Drude modified the Lorentz model by eliminating the restoring force, applicable to bound electrons, from the model of the free electrons [Ref. 1:p. 53]. The free electrons, also called valence electrons, are thus free to move randomly throughout the surface of the metal, relatively independent of atomic nuclei or the other free valence electrons. Thus, the random motion of electrons produces no net current flow; however,

when an externally induced electromagnetic field is applied to the metal, the free electrons flow in a more orderly fashion giving rise to an electric current.

c. Reflectivity According to Free Electron Theory

All of the electromagnetic energy incident on the surface of a material may be acted upon by only three mechanisms; it may be reflected from, absorbed by, or transmitted through the material. The reflectance of a material is a function of wavelength and temperature $\{\rho(\lambda, T)\}$ and is defined to be the ratio of the intensities of the light reflected by the material (R) to the intensity of the light incident on the material (I), as shown in Equation (1). Similarly, the absorbance $\{\alpha(\lambda, T)\}$ and transmittance $\{\tau(\lambda, T)\}$ are defined as the ratios of the intensities of the absorbed (A) or transmitted (T) energies to the intensity of the incident energy as shown in Equations (2) and (3). The relationship between the magnitudes of these energy mechanisms is depicted in Equation (4).

$$\rho(\lambda, T) = \frac{R}{I} \quad (1)$$

$$\alpha(\lambda, T) = \frac{A}{I} \quad (2)$$

$$\tau(\lambda, T) = \frac{T}{I} \quad (3)$$

$$1 = \rho(\lambda, T) + \alpha(\lambda, T) + \tau(\lambda, T) \quad (4)$$

The transmittance of metals is sufficiently small so that it may, for practical purposes, be neglected from Equation (4). Indeed, the transmittance of copper at 300° K is typically only of the order of 3E-13 [Ref. 1:p. 93]. Thus, Equation (5) defines the more effective relationship between metallic reflectance and absorbance.

$$\rho(\lambda, T) = 1 - \alpha(\lambda, T) \quad (5)$$

If over a discrete frequency range, a metal is considered to behave as a graybody, such that its absorptance $\{\alpha(\lambda, T)\}$, which is equal to its emittance $\{\epsilon(\lambda, T)\}$, is less than unity then Equation (6) is applicable.

$$\alpha(\lambda, T) = \epsilon(\lambda, T) > 1 \quad (6)$$

From work done by Drude [Ref. 3:p. 122], and also by Hagen and Rubens [Ref. 2:p. 622], in accordance with the free electron theory, the emittance of a body is related to the wavelength of the incident energy and the resistivity of the body. Thus,

$$\epsilon(\lambda, T) = 36.50 \sqrt{\frac{r(T)}{\lambda}} \quad (7)$$

where $r(T)$ is the resistivity as a function of temperature in ohm-cm and λ is the wavelength in μm .

Combining Equations (5), (6), and (7) for a constant temperature yields Equation (8) which defines the relationship between the reflectance of a material and wavelength.

$$\rho(\lambda) = 1 - \sqrt{\frac{\text{constant}}{\lambda}} \quad (8)$$

Thus, the generalized shape of a metal's reflectivity curve according to the free-electron theory is as depicted in Figure 1.

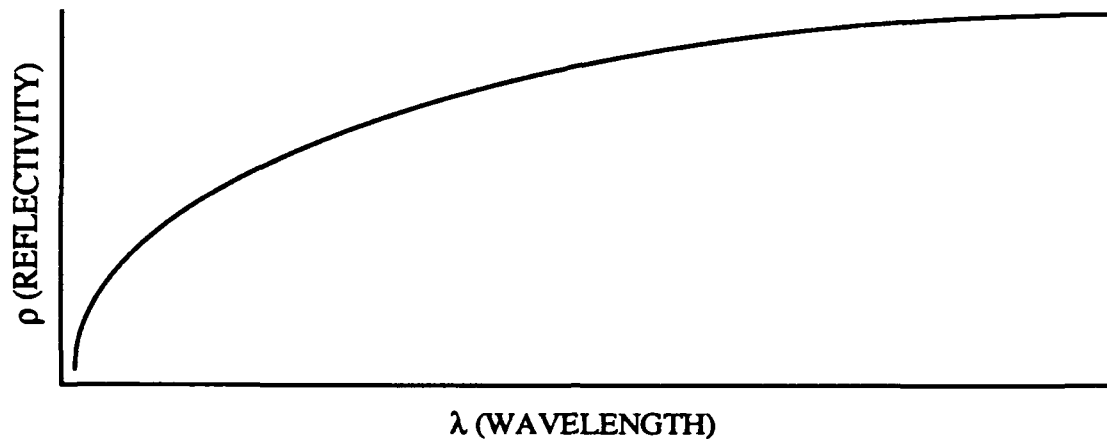


Figure 1 Generalized Metallic Reflectivity Curve Based on the Free Electron Theory

Work by Hagen and Rubens, as well as others, indicates that the relation defined in Equation (8) agrees closely with results of reflectivity experiments for many metals, so long as the wavelength of the incident energy is not allowed to decrease below about 1 μm . [Ref. 2:p. 622] Therefore, the free electron theory does not adequately explain the optical properties of metals for visible wavelengths and below. This fact is evident when comparing the theoretical reflectivity curve of Figure 1 with the experimental reflectance data presented in Figure 2 [Ref. 4].

2. Quantum Theory

a. History of Development of the Quantum Theory

Max Planck introduced a concept in October 1900 before the German Physical Society that was to be the beginnings of "Quantum Mechanics." Albert Einstein expanded on Planck's ideas, and in 1905 he proposed that light consisted of discrete particles or quanta of radiant energy, which he later named "photons." The photon's energy

(e) is directly proportional to its frequency ($\nu = C/\lambda$, where C is the speed of light), as shown in Equation (9). The constant of proportionality is known as Planck's constant (h).

$$e = h \nu \quad (9)$$

The theory was verified and expanded upon through the works of Bohr, Schrodinger, Dirac and others. Postulates expounded by Wolfgang Pauli in 1930, and later experimentally verified in 1950, suggested that certain characteristics of light could best be explained in terms of wave properties, and others in terms of particle properties. Thus was born the wave-particle duality principle, that light acts both as a wave and as a particle, depending on the particular application. [Ref. 5:p. 8]

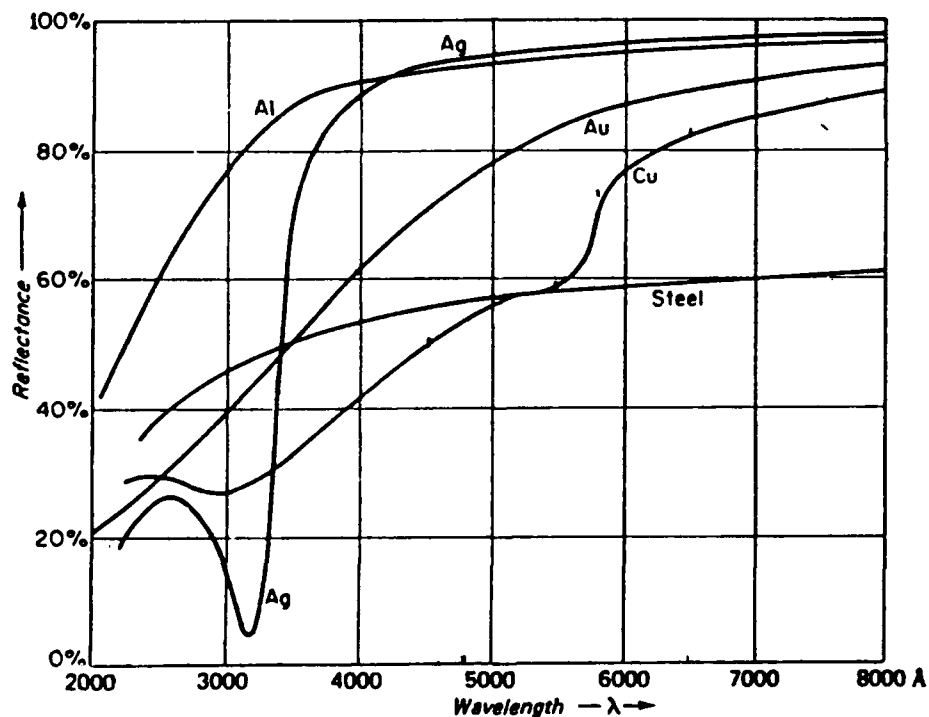


Figure 2 Reflectance of Common Metals at Normal Incidence
[Ref. 4:p. 536]

b . Band Theory of Solids

From this original quantum theory evolved a new concept for solids based on a model of the atom in which its electrons were allowed to exist only within restricted levels or bands of energy. The model of the atom proposed by Niels Bohr represents three postulates: 1) electrons are held to the nucleus of an atom by the Coulomb force; 2) electrons move around the parent atomic nucleus only in certain stable orbits representing discrete energy levels, with the only possible orbits being those for which the electron angular momentum is equal to Planck's constant divided by 2π ; and 3) when an electron transitions from one stable orbit to another, emission or absorption of light may occur such that the difference of energy in the two stable orbital states is equal to the product of the frequency of the light and Planck's constant (or the energy of the absorbed or emitted photon, as defined in Equation (9)). [Ref. 6:p. 978-981]

Due to their close proximity, the electrons of adjacent atoms in the crystalline lattice structure of metals interact with each other, altering their energy states and effectively broadening the allowable energy levels of the orbiting electrons into allowable energy "bands" of varying width. Just as allowable energy bands exist, so to do forbidden bands, or energy levels in which electrons theoretically cannot exist. The allowable bands are given names (eg. s, p, d, f, g). Table I presents the location of the atom's electrons within these various bands for some of the noble metals.

Within each band are allowable energy orbitals and states. According to the Pauli Exclusion principle, only one electron may occupy each allowable state, and two electrons of opposite spin direction may occupy each orbital [Ref. 7:p. 929] and [Ref. 8:p. 4-5]. Spin is a term that indicates the intrinsic angular momentum of the electron [Ref. 9]. Therefore, each band depicted in Table I consists of an even number of electrons since

there may be a maximum of two electrons of opposite spin within each integral number of orbitals per band. The energy of the electrons increases as the state, orbital, and band number increases. Hence, the two electrons in band 1S possess less energy than do the two electrons in band 2S. Similarly, the first two copper electrons in band 3D possess less energy than do the next two, which occupy the same band but are in a higher orbital.

**Table I QUANTUM THEORY OF THE ATOMIC ELECTRON BAND
STRUCTURE OF SOME OF THE NOBEL METALS**

	1S	2S	2P	3S	3P	3D	4S	4P	4D	4F	5S	5P	5D	5F	6S
Cu	2	2	6	2	6	10	1	-	-	-	-	-	-	-	
Ag	2	2	6	2	6	10	2	6	10	-	1	-	-	-	
Au	2	2	6	2	6	10	2	6	10	14	2	6	10	-	1

An important energy level for solids is the Fermi energy, which is not an energy band but the highest occupied discrete electron energy level of a bound atom, at a temperature of absolute zero. Another way of saying the same thing is the Fermi energy is the lowest energy, or ground state of a metal.

In conductors, such as metals, the most energetic band is only partially filled with electrons. Consequently, energy levels above the Fermi energy and within the same band are available to the highest energy electron should it become "excited" by an applied external energy field, such as by the addition of thermal or electromagnetic energy. Insulators, in their ground state fill the highest energy band, directly above which exists a forbidden band. Only if sufficient energy is applied to the insulator to allow the highest energy electron to reach a vacant energy level in the conduction band above the forbidden

band, will that electron be able to gain any energy from an external source. A semiconductor is similar to an insulator in that the highest existing energy band is filled, but the forbidden band above it is sufficiently narrow to allow excited electrons to move across the forbidden band to another conduction band above it. Figure 3 depicts the energy band locations for the three described materials.

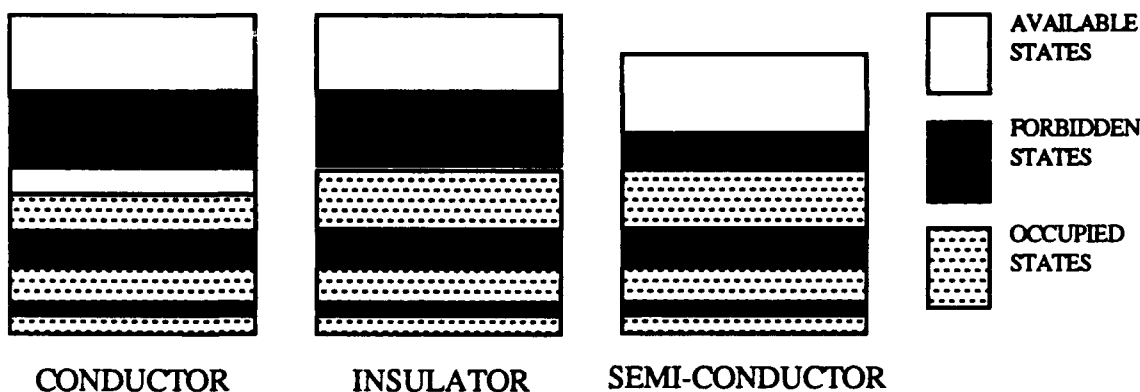


Figure 3 Band Theory of Solids

c. Reflectivity According to Quantum Theory

The sharp drops in the reflectance of metals at visible and ultraviolet wavelengths, as shown in Figure 2, is not adequately predicted by the free electron theory and the Drude / Hagen and Rubens expression defined in Equation (8). Additional information provided by the quantum theory offers one possible explanation of the mechanisms responsible for the reflectance characteristics of metals in these regions.

For noble metals such as copper, silver and gold, the highest energy "d band" lies well below the Fermi energy level. Therefore, low energy incident radiation at infrared wavelengths and above provide only sufficient excitation energy to stimulate intraband transitions; whereas, visible and ultraviolet energies allow for transitions to

higher level conduction bands. The quantum model predicts the deviations in experimental observations from the results provided by the free electron theory in the region below the short visible wavelengths. This is accomplished through analysis of both the inter- and intra-band transitions and of the proximity of the frequency of the incident energy to the solid's plasma frequency [Ref. 1:p. 55-64]. The reflectance of metals in the visible region is not, however, sufficiently well described by free electron theory, quantum theory, or a combination of the two to preclude interpretation based upon other theory.

C. METALLIC CLUSTERS

One possible theory to explain the optical properties of metallic surfaces in the region of the electromagnetic spectrum not adequately described by existing theories, is based on postulated properties of clusters of atoms located on metallic surfaces [Ref. 10].

1. History of Cluster Research

As early as 1661 the British chemist Robert Boyle, in his *Sceptical Chymist*, referred to "minute masses or clusters [that] were not easily dissapable into such particles as composed them" [Ref. 11]. In 1861 another British chemists, Thomas Graham, studying the nature of particles with diameters of between 1 and 100 nm, labeled such particles as "colloids", and founded the discipline of colloidal chemistry. These cluster particles have been found to exhibit properties differing from those displayed by either larger or smaller groups of atoms. Physicists began to research the properties of colloids around the turn of the next century. In the 1960's Ryogo Kubo noted that for metallic particles smaller than 10 nm it was difficult to either add or remove an electron, and hence such particles tend to remain electrically neutral. He also reported that the electrons of particles of this size, because of the small number of electrons present, do not obey Fermi statistics. By the 1980's, much research began to be devoted to the production of these "ultrafine particles." [Ref. 12]

In the 1950's a method of forming free clusters for study was developed. A bulk metal was vaporized in an oven and then precipitated onto a substrate. This process allowed the production of only three to five atom clusters for metals with high transition temperatures. Due to the extremely small number of atoms present in these man made clusters, they provided little information about the relationship between the material properties of the clusters and their size. In 1981 the process was refined using a laser to vaporize the metal, allowing for the production of free clusters containing over 100 atoms.

The relatively recent capability to artificially produce metallic clusters has resulted in the majority of the research currently being performed centering around the properties of individual free clusters. Duncan and Rouvray contend that clusters may be viewed almost as a distinct phase of matter, with characteristics that separate them from solids, liquids, or gases, and that this conventional phase independence is a function of the number of atoms that compose the cluster. They also indicate that experimental evidence suggests that the ionization potential or electron binding energy of cluster atoms is inversely proportional to the number of atoms in the cluster. Thus clusters tend to hold their electrons to a greater extent than do the bulk metal atoms. Supporting this claim is the observation that the average atomic spacing of copper atoms in clusters is significantly smaller than in solid copper, with the spacing approaching that of the solid for clusters of approximately 50 atoms. Additionally, clusters exhibit the ability to change shape spontaneously. [Ref. 11]

2. "Native Cluster" Model

The model proposed by Biblarz [Ref. 10] postulates that clusters of atoms always exist on the surface of a solid material and that they act in such a way as to modify the emission properties of the bulk material. These clusters, although bound to the bulk material, exhibit separate and distinct properties from the atoms that make up the crystalline lattice structure of the solid. They are not atoms of a foreign deposit on the metallic

surface, but rather small groups of atoms that have been "partially liberated" from the bulk material's crystalline lattice structure, although still attached to it. Clustered atoms are covalently bonded together and possess a discrete electron state spectrum, perhaps even having an energy band structure. Cluster size, defined to be between 1 nm (approximately 100 atoms) and 1 μm , imparts a dielectric quality to the small aggregates of atoms. Clustering occurs only on a fraction of the surface with the value of this fraction varying from metal to metal. [Ref. 10]

If in fact clusters behave as dielectrics, then one would expect them to possess dielectric characteristics such as no electrical conductivity, polarizability, different emission characteristics from the conducting bulk metal and luminescence. Indeed, work based on the native cluster model with dielectric characteristics, demonstrates close agreement between the modeled polarization characteristics of various metals and those experimentally obtained. [Ref. 13]

3. Luminescence

Luminescence is a general term to describe a two phase process by which initially shorter wavelength radiation incident on a surface is absorbed by atoms or molecules, exciting their electrons to a higher energy state. Later, as the electrons return to their stable states, energy is emitted by the excited particles as photons of longer wavelengths. Phosphors in fluorescent lamps for example, absorb the ultraviolet spectral lines of the mercury vapor, re-emitting in the visible spectrum. Usually the initial unexcited state is the ground electronic state, and the particle returns to this state after emission occurs, however it frequently remains in a vibrationally excited form.

Luminescence is subdivided into two categories, fluorescence and phosphorescence, depending on the emission mechanism. Returning momentarily to the discussion of band theory in solids, it is necessary to define two additional terms that are

applicable to luminescence. Whether an emission from an excited state is termed fluorescence or phosphorescence depends on the net spin (S) of the electrons within the atom, or the difference between the number of electrons of one spin direction and the other. Another term necessary to properly classify the type of emission is "multiplicity" which is defined in Equation (10).

$$\text{Multiplicity} = 2S + 1 \quad (10)$$

As an example, consider an atom with an even number of electrons. The net spin is zero, and therefore the multiplicity is one. For such a condition, the state is referred to a singlet state. If the atom were excited such that one of its electrons were transferred to a higher state, and in the process reversed its spin direction, the net spin would be one ($S = 1$) since the spin of one electron is $1/2$. Therefore, the multiplicity would be three. Such a state is called a triplet state. Figure 4 depicts energy absorption by an atom, and the possible mechanisms by which the excited atom can return to its ground state. Processes by which radiation is emitted in the form of a photon are fluorescence and phosphorescence. Radiationless processes of internal conversion and intersystem crossings, result from conversion of electronic energy into vibrational energy of the atom. [Ref. 8:p. 1-6]

Absorption can occur to any excited state. However, the internal conversion process is 10^3 times more likely to occur from any state other than the first excited singlet than is fluorescence or intersystem transfer, which is necessary for phosphorescence to occur. Thus, luminescence nearly always occurs from the lowest excited state (S_1) to the ground state (S_0). [Ref. 8:p. 87-88] The change of electronic to vibrational energy through internal conversion from the first excited singlet state competes with the fluorescence and

intersystem transfer mechanisms, thus reducing the intensity of the photon-emitting processes. [Ref. 8:p. 2-3] If the lowest triplet state is below that of the lowest excited singlet state, then phosphorescence occurs at a longer wavelength than does fluorescence [Ref. 8:p. 76].

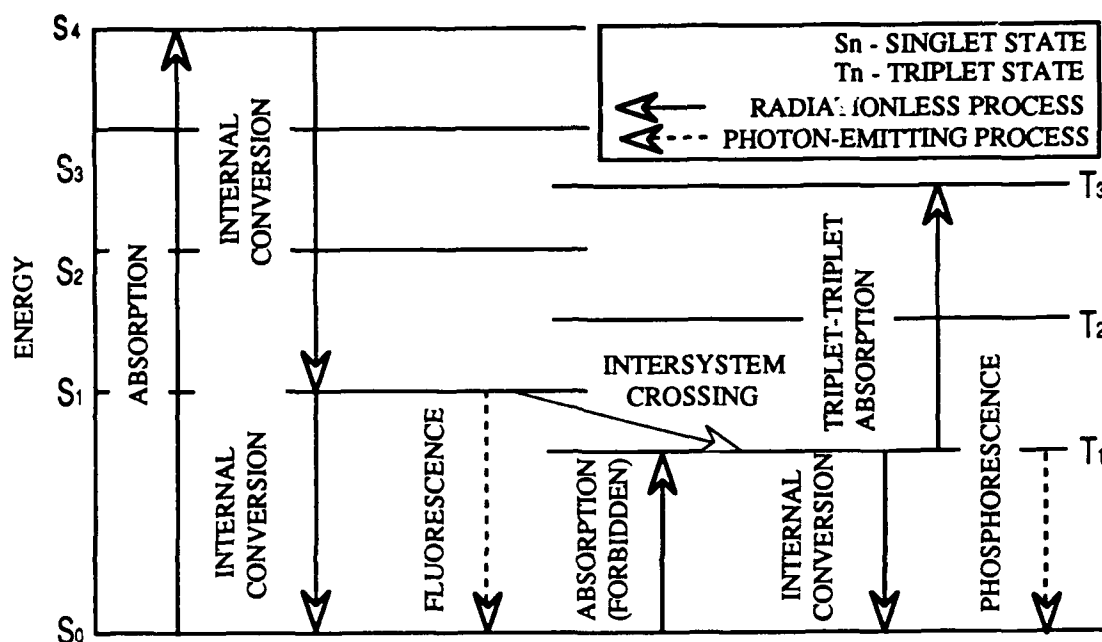


Figure 4 State Energy Diagram Depicting Fluorescence and Phosphorescence [Ref. 8:p. 2]

A transition from a singlet to a singlet is allowed whereas a triplet to singlet transition is forbidden. Hence, the lifetime for fluorescence, which is based on the amount of time the electrons remain in their excited states is extremely short. Observed durations for photon emission via fluorescence are 10^{-7} to 10^{-10} seconds. The lifetime for phosphorescence is relatively long with the duration of the emission having been measured at 10 to 10^{-3} seconds. Observations indicate that the intensity of the emission process

decays following the removal of the source of the excitation energy. Experimental data show that the emission decays at a first-order exponential rate.

Absorption and emission may occur at discrete wavelengths or they may be spread over a range of wavelengths known as absorption and fluorescence or emission bands. The shape of the fluorescence band is often the mirror image of the absorption band. Although it is frequently located immediately adjacent to the absorption band on the long wavelength side, the emission band is sometimes displaced to an even greater wavelength, with the displacement shift being known as the "Stokes shift." [Ref. 8:p. 77-78]

The previous definition of the mechanisms and characteristics of the luminescence processes combined with the reflectivity data presented in Figure 3 and the relationship between reflectance and absorptance (and hence emittance) from Equations (5) and (6), produce the depiction of the conjectured fluorescence spectrum for metallic copper presented in Figure 5.

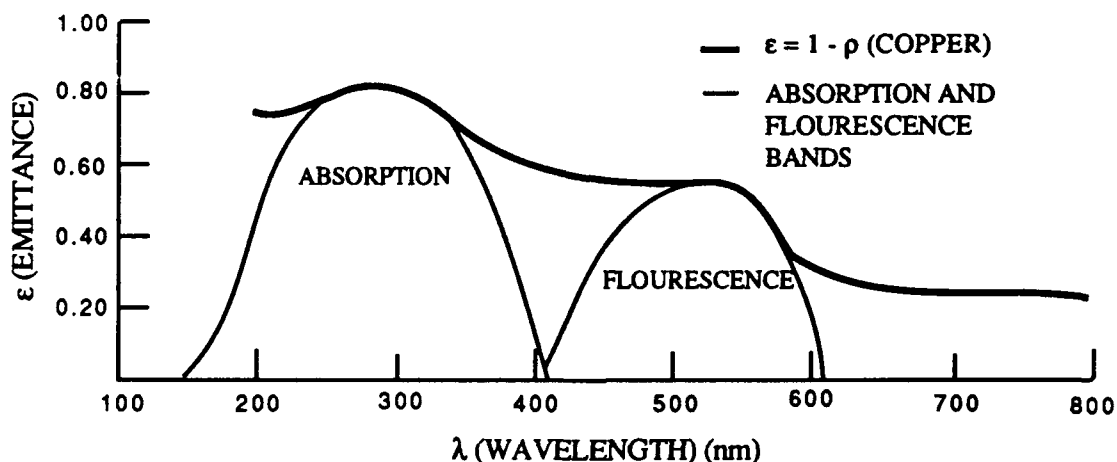


Figure 5 Fluorescence Spectrum for Copper

Thus, a combination of accepted models for metallic materials with the theory that the optical properties of metallic surfaces are due, in part, to contributions from dielectric "native clusters", which include the capability to luminesce, points to the possible existence of a copper fluorescence band in the visible region that is excited by absorption of ultraviolet radiation.

D. OPTICAL MULTICHANNEL ANALYZER (OMA III)

An instrument that is owned by the Naval Postgraduate School (NPS) and is well suited for experimental research into the existence of luminescence in metallic copper, is the Department of Physics' Optical Multichannel Analyzer. The instrument has been in the school's possession since 1988 but has been underutilized because of its complexity. The only documentation available at NPS on the operation of the OMA III is contained in the contractor supplied manuals for the various individual components. Such publications are not known for clarity.

Recently interest in use of this asset at NPS has been on the increase. As part of the research into the dielectric nature of metallic clusters and their influence on the emission properties of metallic surfaces, an investigation into the capabilities and operation of the OMA III is not only essential to the primary research, but also aids in the understanding and future usage of the OMA III by other students and faculty members at NPS. Thus a secondary aim of this research is an evaluation of the OMA III operating characteristics, error sources and capabilities as applicable to this area of research.

II. SCOPE OF RESEARCH

A. DESCRIPTION OF EQUIPMENT

Laboratory equipment consisted primarily of the Optical Multichannel Analyzer 1460-XD Diode Array System Configuration as described in the System's Configuration Manual [Ref. 14]. This configuration is composed of a system processor (OMA III Model 1460), a photodiode detector (Model 1453A), and a detector controller (Model 1462). These are connected to a spectrograph to provide for data acquisition, processing, storage and data reduction. Additionally, various light sources, metal samples, bandpass and polarization filters, lenses, plotters and printers were used for data collection and presentation.

1. Optical Multichannel Analyzer (OMA III) System

The basic OMA III configuration was used, consisting of a spectrograph, a detector, a detector controller, and a system processor.

a. Spectrograph (MonoSpec 27)

The Jarrell-Ash MonoSpec 27 Monochromator/Spectrograph Model 12976300 (serial number 13105), was manufactured by Allied Analytical Systems of Waltham, MA. The spectrograph is designed to measure absorption, transmission, emission, reflection, polarization, photometry, and spectral isolation. The unit is designed to function in the infrared, visible, and ultraviolet portions of the electromagnetic spectrum, and incorporates a Czerny-Turner design, using turning, focusing and collimating mirrors, in order to minimize reentry spectra. Appendix A, Figure 1 depicts the path taken by light from the light source through the spectrograph to the detector face.

Three user selectable gratings are cement mounted in an adjustable triple bracket to allow for alignment and selection. The gratings are selected by rotating the grating turret knob atop the instrument. Each grating is blazed at a specific wavelength and groove frequency. Gratings incorporated in the spectrograph and used in this experiment are detailed in Table II. The 18 mm high by 25 μm wide entrance slit is designed to provide a spectral resolution of 0.3 nm with the 1200 grooves/mm grating. A wavelength counter crank and wavelength counter window are also provided for course adjustment of the spectra presented on the Model 1460 display screen. The factors (x) by which the window reading are to be multiplied to give the center wavelength of the displayed spectrum, based on the grating in use are designed to be: 1) 1200 grooves/mm grating, $x=1$; 2) 600 grooves/mm grating, $x=2$; and 3) 150 grooves/mm grating, $x=8$. A detailed description of the Jarrell-Ash MonoSpec 27 is contained in the system's operator's manual. [Ref. 15:p. 7]

Table II SPECTROGRAPH GRATING SPECIFICATIONS [Ref. 15]

RULING (grooves / mm)	BLAZE (nanometers)	RANGE (nanometers)	DISPERSION (nm / mm)
1200	400	300-900	3.0
600	500	480-1200	6.0
150	450	360-720	24.0

b. Detector (Model 1453A)

The Model 1453A detector (serial number 21102) manufactured by the EG & G Princeton Applied Research Corporation of Princeton, NJ, is mounted directly to the exit port of the spectrograph.

1. Theory of Operation. The detector incorporates a large aperture linear silicon photodiode array. The photodiodes are reversed biased so that they act as charged capacitors. Initially each diode is charged to a designed voltage of +5 V. When the photodiode is exposed to light, electrons are freed discharging the capacitor and dropping the voltage across the diode proportionally to the excitation falling upon it during the exposure period. Control is obtained via CMOS logic driven by signals from the detector controller. The array consists of 1024 photodiode elements each connected to an individual Field-Effect-Transistor (FET) switch. Two two-phase MOS detector shift registers are connected to the gates of the FET switches such that one register controls access to the even-numbered elements while the other register controls access to the odd-numbered elements. Each individual photodiode measures 25 μm wide by 2.5 mm high, providing a total array width of slightly over 25 mm.

Wavelength response is designed to cover from approximately 180 nm to 1100 nm as shown in the manufacturer provided data depicted in Figure 2, Appendix A.

2. Dark Current. A leakage or "dark current" occurs in photodiodes as a result of thermally generated charge carriers. Since the dark current discharges the voltage of the photodiode, and is integrated over the exposure interval, it directly limits the exposure time. The dark-current inducing thermally generated charge carriers are reduced by approximately 50% for every 7° C drop in operating temperature. To minimize dark current and to maintain a cold and stable operating temperature, a two-staged closed-loop Peltier thermoelectric cooler is incorporated to allow for normal operation at temperatures down to 5° C and for operation down to -30° C by circulating liquid coolant. Temperature control of the detector array is user selectable at the Model 1460 via the Model 1462 detector controller. The default "PRESET" setting (selected by

typing the command DT 5 at the Model 1460 keyboard) is designed to maintain the detector at the normal "COOLER LOCKED" operating temperature of 5° C in most laboratory environments. For optimum performance, and ensured repeatability of experimental data, Ref 16 recommends that users wait to acquire data a minimum of 30 minutes from receiving a "COOLER LOCKED" message on the Model 1460 display screen, to ensure temperature stability within the system.

3. *Detector Purging.* The thermoelectric cooler can cause condensation on the photodiode array and other sensitive components, degrading signal-to-noise ratio and possibly leading to eventual catastrophic failure. It is therefore essential that before using, the detector be flushed with dry nitrogen and a slight backpressure maintained by constant gas flow during operation (a manufacturer specified minimum of five cubic feet per hour), to purge the detector of atmospheric moisture.

Applicable manufacturer provided detector specifications are presented in Table I, Appendix A. A detailed description of the Model 1453A detector is provided in the system's instruction manual. [Ref. 16]

c. Detector Controller (Model 1462 and 1462/99)

The Model 1462 Detector Controller, manufactured by the EG&G Princeton Applied Research Corp. is a VME card designed to control the Model 1460 Optical Multichannel Analyzer System Processor. Timing circuitry uses a primary 16 MHz crystal oscillator located internal to the 1460 with a backup located on-board the 1462. A Model 1462/99 14-bit Analog-to-Digital Converter (ADC) operates in conjunction with the Model 1462 as well as various latches and amplifiers to control the acquisition of spectral data. The unit is capable of acquiring a 1024 pixel spectrum at a user selectable scan time of 20 ms or 30 ms and then temporarily storing the data for processing and data reduction. The ADC dynamic range is 16,383 counts at full scale.

The Model 1462 and 1462/99 perform the following six primary functions:

1) analog signal processing, 2) pixel timing, 3) scan timing, 4) cooler control, 5) high voltage power supply drive, and 6) addressing functions. Analog signals received from the detector are amplified, integrated and temporarily stored in a sample-and-hold circuitry before being applied to the ADC.

A detailed description of the Model 1462 Detector Controller and the Model 1462/99 ADC is contained in that unit's instruction manual. [Ref. 17]

d. System Processor (Model 1460)

The Model 1460 System Processor (serial number 24119), manufactured by the EG&G Princeton Applied Research Corp., is contained in a 57 X 47 X 28.5 cm plastic housing. The processor incorporates solid state electronics including VME bus circuitry and two 68000 microprocessors. A 23 cm diagonal, touch-sensitive, monochrome display screen is located on the front of the processor to display data and the menu-driven control format, as well as providing a means of inputting user information. A single internal, double-sided, double density 5 1/4 inch floppy disk drive with a 385K byte formatted storage capacity is located on the front of the processor to allow for system programming software access and for data storage to disk. Internal memory consists of 512K bytes of Random Access Memory (RAM). In addition to the touch-sensitive screen, additional user control is provided via 13 front panel pushbutton keys and a connected external modular keyboard. Separate VME cards control the RS232C serial port and the IEEE-488 GPIB port which are provided for connection to additional data collection and presentation equipment.

A complete description of the Model 1460 System Processor is contained in the system operating manual. [Ref. 18]

e. System Software

1. General. System programming software, which provides the functions of data acquisition, manipulation, display and storage is provided on a 5 1/4 inch diskette. System operating program code is contained in the PARCSAM.BIN file and the file PARCSYS.PRM contains the the default operating instructions and the data acquisition parameters. A modular menu-driven format allows the user to access all system functions. From the "Main Menu" of user selectable control options addressed via the touch-sensitive screen on the Model 1460, the user can access the following modes 1) Disk Operating System, 2) Calibration, 3) Data Acquisition, 4) Curve Calculation, 5) X Y Plotter, 6) Return to Setup, 7) Utility Menu, 8) Y:T Operation, 9) PIA Setup, 10) Detector/Pulser Setup, 11) Printer Routines, and 12) Keystroke Programming. Only the first seven of the above mentioned modes were used in this thesis.

The software version used in this research was Optical Multichannel Analyzer (OMA III) Revision 2.3. A complete description of the system software is contained in the system operating manual. [Ref. 18]

2. Compensation Modes (Comp Modes). Six software modes are included which are designed to provide a means to correct for the effects of background lighting and internal noise or dark current present in acquired data. The modes are identified as Comp Mode B and Comp Modes 0 through 4.

The default mode is Comp Mode B, which is designed to perform a point-by-point subtraction of the background data stored using the "Background Set" softkey from the acquired data. The contractor warns that since the set background data is stored in 16 bit format, rounding errors may occur.

Selection of Comp Mode 0 allows the raw acquired data to be stored to disk without compensating for background effects. Comp Modes 1 through 4 all

perform a point-by-point subtraction of the background data file from the acquired data as the data are being stored to disk. These modes, therefore, require an additional initial step of acquiring and storing the background data to disk as a separate data file. The only designed difference between Comp Modes 1 and 2 is that the background and acquired data file need not have the same number of memory spaces for Comp Mode 2, as they must for Comp Mode 1. Comp Modes 3 and 4 are designed to operate identically to Comp Modes 1 and 2, with the additional feature that they use the Source Compensation Value (SCV) for each file as well. The SCV is determined by using a single detector element to detect the overall amplitude of the light source, which is then stored with the data file. Thus in addition to compensating for background effects, Comp Modes 3 and 4 are designed to compensate for fluctuations in the overall intensity of the light source by multiplying the background corrected value of the acquired data by the ratio of the background and data SCVs. The manufacturer recommends use of these last two modes if the source fluctuations occur slowly compared to the scanning rate.

One final method of correcting for background effects in acquired data is through the use of the "Curve Calculations" menu described in paragraph II.A.1.e.4. [Ref. 18:p. 10.9-10.20]

3. Data Acquisition Modes (DA Modes). Fifteen data acquisition modes are provided to allow for different user controlled methods of data acquisition. The only DA Mode used in this research was DA Mode 1, which was designed to add numerous scanned sets of data. The algorithm allows the user to determine the number of data scans (I) to be added together per data set. The number of sets (J) to be added together is also user selectable, with each set requiring one memory location. Provisions are incorporated to allow the user to ignore a specified number of scans (K) after each added scan. [Ref. 18:p. 12.1-12.4]

4. Curve Calculations. The "Curve Calculations" menu allows the Model 1460 to be used to reduce and manipulate data files, and to either store the results to disk or to various single value "V-Registers" or 1025 value "Ram Buffers." A wide variety of left- and righthand operands, mathematical and logical operands and Boolean algebra expressions are programmed for use by the operator to allow for customized data reduction. [Ref. 18:p. 16.1-16.7]

2. Light Sources

A variety of light sources were used throughout the research. Selection of the various sources was based upon considerations of best available spectral output, required intensity and economy of operation.

a. Calibration Source

Prior to collecting data with the OMA III, the system must be calibrated to enable the user to read wavelength (or wavenumber) and intensity directly from the Model 1460 display screen. Due to the lack of an available intensity calibration source, no intensity calibration was performed during this research. The source used for wavelength calibration of the OMA III was a standard low pressure, cold cathode mercury (Hg) discharge lamp. The Model 11SC-1-90-0012-01 Pen-Ray lamp manufactured by Ultra-Violet Products, Inc. of San Gabriel, CA provides a lighted tube $2 \frac{1}{16}$ inches long by $\frac{1}{4}$ inch in diameter. The lamp envelope is fused double bore quartz to allow for good transmission in the ultraviolet spectrum as well as the visible. The manufacturer specifies that the radiation intensity is uniform to within 2% after allowing the lamp to reach thermal equilibrium following a 30 minute warm up period. A voltage regulator was used to control the voltage supplied to the lamp. A complete description of the calibration light source is contained in the manufacturer's product catalogue. [Ref. 19]

b. 100 W Commercial Incandescent Bulb

A 100 W "Extended Life" incandescent light bulb produced by Sylvania, was mounted in a commercial lighting fixture to provide a low wattage blackbody source. The operating voltage was rated at 130 V. The lighting fixture consisted of a 1 1/2 foot long arm extending from a circular base to the socket. No material, in any way, shielded nor contributed by reflection to the emitted spectrum of the source.

c. 500 W Halogen / Quartz Light Source

A 500 W halogen floodlamp manufactured by Regent Lighting Corp. of Burlington, NC, was used as a white light source when high output power was a consideration. Designed as an outdoor floodlamp, the fixture contained a 500 watt halogen bulb with a quartz envelope enclosed in an aluminum fixture with an internal aluminum reflector and a glass cover plate. To prevent any attenuation of the available ultraviolet output spectrum by the glass coverplate, to correct for the inconsistent light spectrum emitted from the shaped reflector surfaces, and to reduce the overall size of the light source, the external housing was removed and only the bulb, bracket and wiring were used. The heat emitted by the 500 watt bulb required that an external fan be used to cool the source and the area around it.

d. Mercury Arc Lamp

A mercury arc lamp, manufactured by Oriel Optics Corp. of Stamford, CT, was used as a high power ultraviolet source. The arc lamp consisted of the lamp (model C-60-30, serial number 71966), an ignitor and a power supply (model C-72-20). The lamp is rated at 200 watts for DC operation and provides a 0.100 x 0.070 inch arc generating 9500 lumens. Design limitations require that the lamp be operated vertically with the anode down, limiting possible experiment setups.

A separate power supply was required to provide a constant operating DC current of 4.0 amps at 57 volts. The arc lamp is air convection cooled by means of an internal cooling fan. Focus adjustment is provided for by an externally mounted adjustable quartz lens.

3. Filters

A set of five band pass filters were obtained for use in this research from Twardy Technology Incorporated, of Darien, CT. The five filters are constructed from Schott glass and strengthened to withstand temperatures below approximately 250° C without sustaining any damage. No additional temperature strengthening was performed on the filters. Contractor provided design specification data for each of the 2 inch square, 3 mm thick filters is listed in Table III.

Additional long pass and band pass filters of unknown manufacture were provided by the NPS Physics Department and were used in this research.

4. Metallic Specimens

Both high grade copper and aluminum metallic specimens were selected and prepared for use in this research.

a. Aluminum Specimen

A ingot of chemical grade (99.9% pure) aluminum was cut, ground and polished to produce a 23 x 25 mm reflective surface 22 mm thick. Comparison of the reflectivity data obtained from the aluminum specimen and known reflectivity data for aluminum was used to substantiate results of the experiments involving copper. Due to the casting process which formed the original ingot, interior imperfections in the solid aluminum bar prevented the attainment of a highly polished surface free of visible surface imperfections. Structural grain features were visible on the polished surface.

Table III TWARDY FILTER MANUFACTURER SPECIFIED CHARACTERISTICS

SCHOTT TYPE	PRODUCT NUMBER	DESCRIPTION	PEAK TRANSMISSION (1% TRANSMISSION POINTS)
UG 5	3172	UV TRANSMITTING BLACK GLASS	290-320 nm (1% T @ 220 & 420 nm)
UG 11	3174	UV TRANSMITTING BLACK GLASS	320-340 nm (1% T @ 215 & 380 nm)
UG 1	3176	UV TRANSMITTING BLACK GLASS	350-360 nm (1% T @ 315 & 395 nm)
BG 1	3178	UV & RED TRANSMITTING BLUE-VIOLET GLASS	350-367.5 nm (1% T @ 225 & 495 nm)
BG 3	3180	UV & RED TRANSMITTING BLUE-VIOLET GLASS	360-380 nm (1% T @ 220 & 475 nm)

b. Copper Specimen

A $\frac{1}{16}$ inch thick sheet of chemical grade copper obtained from Fischer Scientific Company as Cat No. C-424, F.W. 63.54 was cut, mounted, ground and polished to produce a highly reflective copper surface measuring 33 x 43 mm.

5. Optics Lenses

Two 21 cm focal length rectangular (51 x 99 mm) glass lenses were used in the initial reflectivity experiments, for which transmission of the ultraviolet portion of the spectrum was not crucial. The lenses provided a means to minimize errors produced by slight angle misalignments and inconsistencies by increasing the distance from the light source to the detector without reducing the detected light intensity in the visible portion of the spectrum.

6. Optical Bench and Equipment

A six-foot-long steel optical bench provided the basis for maintaining proper alignment between all optical equipments. Magnetic stands and brackets were used to position and support the metallic specimens, light sources, lenses, filters and the OMA III. A 55 x 99 cm rectangular shield with a 4 cm high slit of adjustable width was used to prevent undesired source light from entering the spectrograph while providing a means to minimize errors induced by inconsistent light angles of arrival at the detector face. Slit edges were constructed of razor blades to ensure a uniform slit width along its length.

7. Chopper

A metal rotary chopper (serial number 1137591), manufactured by Bodine of Chicago IL, was used to "chop" the light source output to the copper specimen and the reflected spectrum to the spectrograph. The chopper wheel is 14.0 cm in diameter with a single 2° wide slit open between 8.0 and 12.3 cm from the wheel center. An electric motor (model V10) rated at 115 volts and a maximum of 5000 rpm, rotates the wheel at a constant rate. Wheel rotation speed is user selectable via a rheostat at the base of the motor.

8. HP ColorPro Graphics Plotter

Connected to the Model 1460 GPIB port to provide for data presentation is a ColorPro graphics plotter manufactured by the Hewlett-Packard Co. of San Diego, CA. Eight different colored fine line felt tip marking pens are stored in a carousel for user selection to trace graphics file data onto bond paper. A detailed description of the HP ColorPro Graphics Plotter is presented in the system operation manual. [Ref. 20]

9. Epson FX-86e Serial Printer

The Epson FX-86e dot matrix printer, manufactured by Seiko Epson Corp. of Nagano, Japan, is connected to the Model 1460 RS232C serial port. The printer operates

at 240 and 200 character per second print rates depending on font and quality selections. The printer provides rapid low quality hardcopy prints of stored and displayed OMA III data for initial data analysis. A complete description of the Epson FX-86e dot matrix printer is presented in the system user's manual. [Ref. 21]

B . EXPERIMENT ENVIRONMENT AND CONDITIONS

A baseline laboratory environment and set of conditions were established for the collection of all data in this experiment. Unless specifically otherwise addressed, all data were taken at night with dark cloth curtains drawn over all exterior windows, and all interior lights extinguished except for the light source used in the applicable experiment and the monochromatic light from the Model 1460 display screen. The axis of the spectrograph was defined as an imaginary line drawn through the center of the entrance slit of the spectrograph, and perpendicular to the front face of the Model 1460. The display screen was positioned perpendicular to the axis of the spectrograph and behind the instrument, such that light from the display screen neither entered the spectrograph directly, nor by reflection. Laboratory temperature and humidity were maintained at approximately 50° - 70° F and 60% - 80% humidity.

All data were recorded, stored, reduced and displayed using the OMA III configuration described in this chapter.

III. EXPERIMENTAL METHOD

A. METALLIC MIRROR SURFACE PREPARATION

A variety of surface preparation techniques were initially considered, including chemical, electrolytic, and mechanical polishing. Although the purity of both the aluminum and the copper samples were at least 99.9% pure, some impurities did exist and the exact concentrations and composition of those impurities were not known. For electropolishing, the electrolyte, voltage, current density, electrolyte temperature and duration of electropolishing, are all dependent on the impurities present in the specimen. Echants used to chemically prepare the metallic surface also depend on the bulk metal impurities. Nearly one hundred possible methods for chemical etching and electropolishing are listed in Refs 22 and 23. Although electrolytic polishing and chemical etching do provide some distinct advantages over mechanical polishing, there are also some disadvantages to their use, and the determination of the proper chemical solution and conditions for the subject specimen can be a long and arduous process.

Consequently, both chemical and electropolishing procedures were determined to be too complex to warrant their use, and mechanical polishing was selected as the method of surface preparation. The polishing procedure described in Ref 22 for aluminum and copper and copper alloys was used.

1. Mounting

The size of the ingot of aluminum allowed a specimen to be prepared that was sufficiently large that mounting of the aluminum sample was not required. The specimen cut from the copper sheet, however, had to be mounted to a larger object to facilitate its

grinding, polishing and spectrographic study. Compression-mounting using a Buehler Speed Press II mounting machine with Bakelite mounting material required the specimen fit within the machine's one inch diameter cylindrical mounting chamber and be subjected to extreme heat and pressure. A mixture of two parts by volume of Buehler "Sampl-Kwick Powder" to one part "Sampl-Kwick Liquid" poured over the specimen placed in the bottom of a larger cylindrical container, alleviated the heat and pressure requirements of the previous method and offered greater flexibility in the size of the specimen. Both of these mounting methods required that the excess mounting material be removed from around the edges of the specimen in order to prevent metallic reflectance and luminescence data from being corrupted by the mounting material's contribution. That excess mounting material was needed, however, to hold the metal specimen to the mounting base, so that removal of the unwanted material resulted in loss of the mounting structure. The specimen cut from the copper sheet was, therefore, epoxied to cubic pieces of steel that were of smaller frontal dimension than the copper.

2. Grinding

Initial wet grinding was used to remove metal that had been cold worked, and was followed by finish grinding to provide a suitable surface for polishing. Initial grinding was performed beginning with 180 grit silicon carbide on a wet belt grinder. Finish grinding using progressively finer grits (240, 320, 400, and 600) was accomplished by hand. The specimens were rotated 90° between consecutive grinding stages, from one grit stage to the next, to ensure that scratches due to the coarser grit were removed by the subsequent grinding stage.

3. Polishing

Because both copper and aluminum are relatively soft metals, they required a polishing material that provided maximum cutting and minimum rubbing characteristics.

Therefore, rough polishing was accomplished on an eight inch polishing wheel covered with a Buehler "Rayvel" polishing cloth using an abrasive of 1.0- μ m alumina and distilled water at a polishing wheel speed of 160 rpm. Finish polishing was performed on a 12 inch polishing wheel at a wheel speed of 160 rpm, using a Buehler "Mastertex" polishing cloth for the aluminum specimen and "Microcloth" polishing cloth for the copper specimen. Finish polishing was accomplished using a combination of polishing abrasive and Buehler "Metadi" (polyglycol ether). The abrasives used in final polishing were 1.00 μ m followed by 0.25 μ m diamond paste. Use of alumina as the abrasive medium for finish polishing resulted in the rapid formation of an oxide film layer on the surface of the specimen and was therefore not used. Minimal pressure was applied to the specimens to hold them against the polishing surface, and they were rotated around the polishing surface opposite the direction of wheel spin in order to ensure consistent polishing from all directions.

Following each polishing phase, the specimens were rinsed with an Alconox soap solution, water and ethanol to remove surface deposits from the polishing process. During the rinsing process special care was taken to ensure that no part of the surface was allowed to dry prior to being completely rinsed with ethanol. The specimens were then cold air blown dried.

B. EQUIPMENT SETUP AND EXPERIMENTAL PROCEDURE

The experimental setup, including combination of the selection of light source, specimen, and filter type, use of optical lenses and shields to minimize the possibility of light from unwanted sources or reflections from entering the OMA III and the physical geometry of the equipment locations were all experiment dependent and unique.

Experimental procedures, including use of selected OMA III operating modes and functions, closely followed the procedures suggested in the OMA Operating Manual with minor exceptions. Due to the contractor reported non-linear wavelength response of the

detector, peak intensities of acquired data were usually maintained at approximately one half the dynamic range of the system, or 8000 counts. The set of baseline experimental procedures, listed in Table IV, was established for consistency and repeatability purposes. Only deviations from these baseline procedures to those used in individual experiments are noted in the following paragraphs. Detailed checklists for OMA III operations are presented in Appendix B.

Table IV BASELINE PROCEDURES

PARAMETER	BASELINE SETTING
Spectrograph Grating	150 grooves / mm
Wavelength Calibration	Performed Using a Mercury Lamp
Intensity Calibration	Not Performed
Background Data	Calibrated, Set and Stored to Disk
Data Source	Live-B
Exposure Time	30 msec
High / Slow Speed	Slow Speed
Compensation Mode	Comp Mode 2
Data Acquisition Mode	Mode 1 (J=1, K=0, I=333)
Data Reduction Method	OMA III "Curve Calculation" Software

1. Light Source Radiance

Initial evaluation of the radiated intensity of each light source as a function of wavelength, was accomplished by placing the light source on the axis of the spectrograph directly in front of the entrance slit, as shown in Figure 6. No filters were positioned at the spectrograph entrance slit for source radiance experiments. Distances from the light source to the spectrograph entrance slit were selected to prevent the source intensity from exceeding the dynamic range of the detector. Applicable distances for each light source, as

defined in Figure 6, are presented in Table V. The slitted shield was used only for the 500 W halogen / quartz and 200 W mercury arc lamps due to their significantly greater radiated intensities. For these experiments, the shield slit width was adjusted to 1.0 mm. The focus control on the mercury arc lamp was adjusted to focus the maximum amount of light on the shield slit.

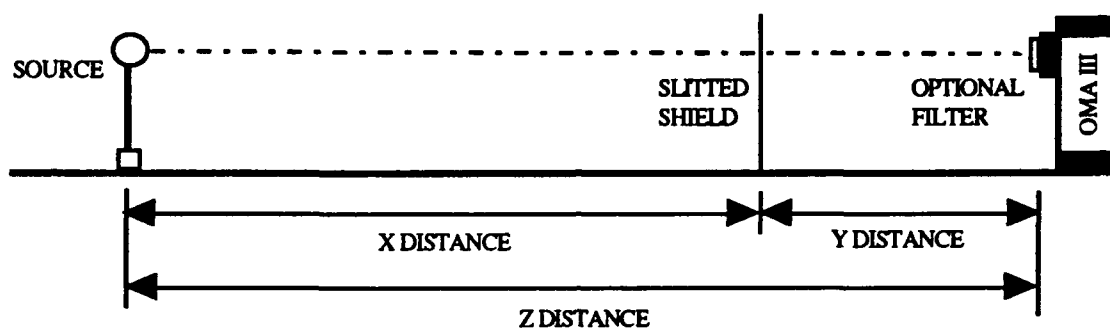


Figure 6 Setup for Light Source Emittance and Filter Transmittance Experiments (Side View)

Table V LIGHT SOURCE TO SPECTROGRAPH DISTANCES FOR RADIANCE MEASUREMENTS (as Shown in Figure 6)

LIGHT SOURCE	X DISTANCE	Y DISTANCE	Z DISTANCE
Mercury (Hg) Calibration Lamp	N/A	N/A	2.0 cm
100 W Incandescent Light Bulb	N/A	N/A	25.0 cm
500 W Halogen / Quartz Bulb	60.0 cm	5.0 cm	95.0 cm
200 W Mercury (Hg) Arc Lamp	750.0 cm	100.0 cm	850.0 cm

The amount of time between application of electrical power to the source and recording the radiance data varied for each source, but the source spectral output was allowed to equilibrate a minimum of one hour before acquiring data.

Background data for those experiments in which the shield was used were acquired with the source radiating and the shield slit covered. For those sources for which the shield was not used, the background data were taken for the ambient lighting conditions and experiment setup with the source not radiating.

2. Sources of Experimental Error

A variety of error sources were evaluated to determine their effects on the experimental setup, data storage and reduction techniques and experimental results. Subsequent experimental procedures and setups were modified so as to minimize the error present in the final results.

a. Wavelength Calibration

Before acquiring any data, and as part of the initial OMA operations, the system was initially wavelength calibrated using the mercury calibration lamp and following the procedures delineated in the "Background Level and Calibration Checklist" presented in Appendix B. Wavelength data input for the peak mercury spectral lines are reproduced from Ref 18, and presented in Appendix B, Figure 1.

The ability of the OMA III to maintain wavelength calibration throughout data acquisition and reduction was evaluated for both the initial calibration performed as part of the "Background Level and Calibration Checklist", and on subsequent "reboot" of the system using the stored calibration lamp data curve to recalibrate the system. At various times throughout the course of the research, the wavelengths of the spectra peaks of freshly acquired data for the mercury sources were spot checked for comparison between OMA presented wavelengths and the known data upon which the calibration was based.

b. Source Intensity Fluctuations

The amount, rate and characteristics of radiated intensity fluctuations were evaluated qualitatively throughout all experiments. Quantitative short interval data for all

sources except the halogen / quartz bulb were taken during the light source radiance experiments. Long term effects were evaluated for the mercury arc lamp during the filter transmittance experiments. The physical geometry of the laboratory setup and procedures used to acquire the quantitative data were, therefore, the same as those described in paragraphs III.B.1 and III.B.4. Data were stored to disk using Comp Mode 0 and later, appropriate background data files were subtracted out using the "Curve Calculations" software.

Before taking any qualitative data, all sources were allowed to equilibrate during an initial "warm-up period" of at least 30 minutes, during which time the spectral output of all sources appeared to stabilize to the maximum extent possible. Quantitative data were acquired after sources had been radiating continuously for between four and seven hours. Due to the time necessary to store data to disk, the minimum interval between subsequent data acquisitions was approximately 16 seconds. Since the OMA III displayed 30 msec frames of acquired data much faster than that, frame-to-frame fluctuations were observed and their variations noted but were not stored to disk.

c. Dark Current

The consistency of amplitude of the dark current and internal noise within the OMA III were evaluated using two different experimental methods. First, the spectrograph entrance slit was covered with an opaque material so that no external light could enter the instrument. Data were acquired and stored to disk using Comp Mode 0 at intervals from 17 seconds to over an hour. The second method was performed concurrently with the filter transmittance experiments by acquiring and storing Comp Mode 0 background data for a completely darkened laboratory, and then for the mercury arc lamp source radiance following the procedures defined in paragraph III.B.4.

d. Polarization Sensitivity of the OMA III

Procedures and setup for evaluation of the sensitivity of the OMA III to polarization of incident light are defined in paragraph III.B.4 as applicable to the transmittance of the polarizing filter. Data were initially taken using only the halogen / quartz source, and were later repeated, using the same setup with the 100 W incandescent source to ensure repeatability.

e. Spectrograph Axis Angle Offset Sensitivity

The 500 W halogen / quartz bulb was used to evaluate the effect of light entering the spectrograph from directions other than directly along the axis of the spectrograph. Figure 7 depicts the physical geometry of the experimental setup. The shield slit width was constant at 4.0 mm for all angles of incidence, which were varied from 0° - 7° in one degree increments. A protractor was mounted to the top of the Model 1460 parallel to the face of the spectrograph entrance slit. A string was then run from the center grommet of the protractor through the center of the shield slit and to the center of the light source to measure the offset angle. The shield remained perpendicular to the source-spectrograph line at each angle for which data were collected.

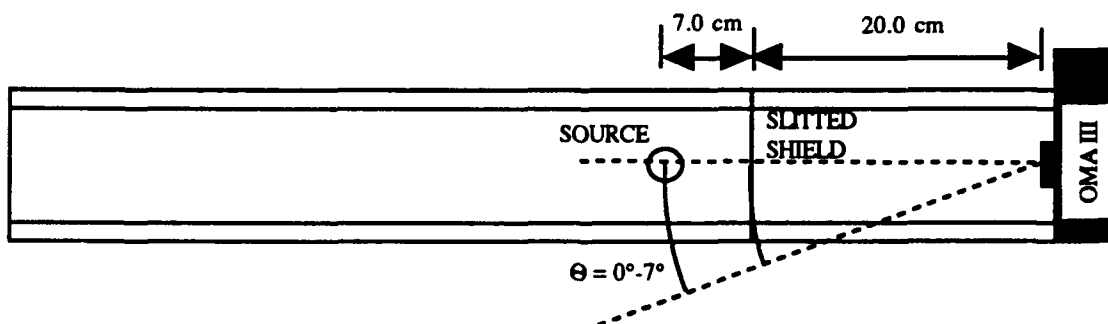


Figure 7 Setup for Spectrograph Axis Angle Offset Sensitivity Measurements (Top View)

Background data were acquired and stored for each location of the shield and source for which data were taken. Background data were acquired with the shield slit covered and the source radiating. Angle sensitivity data were stored to disk using Comp Mode 2, based on the applicable background data file collected for the specific setup being evaluated.

f. Apparent Detector Sensitivity as a Function of Exposure

Time, Data Source Mode and Data Acquisition Mode

The effects of the detector exposure time, the Data Source Mode (LIVE or ACCUM) and the Data Acquisition Mode (D.A. Mode) on apparent detector sensitivity were evaluated by comparing detected background data for a darkened laboratory with data taken with all laboratory overhead fluorescent lights on. Data for lighting conditions were acquired and stored to disk using Comp Mode 0. Background data with all laboratory lights extinguished were then subtracted from the lighted laboratory background data using the "Curve Calculation" software. Experimental mode and exposure time combinations evaluated are presented in Table VI.

Table VI APPARENT DETECTOR SENSITIVITY EXPERIMENTAL SETTINGS

SETTING	COMBINATION 1	COMBINATION 2	COMBINATION 3
DATA SOURCE MODE	LIVE	LIVE	ACCUM
DATA ACQUISITION MODE	N/A	N/A	D.A. MODE 1
D. A. MODE SETTINGS (J,I,K)	N/A	N/A	J=1, I=330, K=0
EXPOSURE TIME	30 msec	9989.999 msec	30 msec
ACQUISITION TIME	0.03 sec	9.99 sec	9.99 sec

g. Oxidation of Copper Surface

The effects of constant exposure to the ambient laboratory atmosphere on the reflectivity of metallic surfaces was evaluated using a freshly polished copper specimen that was allowed to remain exposed to the ambient laboratory atmosphere for a period of six days. A maximum of one hour elapsed between completing the polishing process and initial data acquisition. The 200 W mercury arc lamp source was encased in a box with a two cm high by 1 cm wide exit slit, to minimize chances of stray reflections entering the spectrograph. The source was allowed to equilibrate for four hours before data were acquired. Background data were acquired for both data acquisition periods and were used as the reference for the Comp Mode 2 stored experimental data. Experimental setup was the same as that used for the first copper luminescence experiments as shown in Figure 8. The copper specimen was positioned on the axis of the spectrograph and rotated so as to provide the greatest intensity of reflected light at the detector, based on the intensity shown on the OMA III display screen for the "Live " Data Source Mode. The setup was not disturbed over the course of the next six days. Following another 4 hour warm-up period for the mercury arc lamp, data were recorded 144 hours after the initial data were taken.

To ensure repeatability of the results, and to minimize the net effect of errors that would influence the final conclusions drawn from the data, the experiment was performed twice.

3. Sources of Data Reduction Errors

Two sources of data reduction errors were evaluated to determine their effects on selection of experimental procedures and on interpretation of the final results. These error sources derived from the operating and data reduction software loaded in the system processor. The two sources specifically evaluated were, 1) the methods available to correct

data for the affects of background illumination and internal dark current, and 2) the mathematical operations accessed through the "Curve Calculation" menu.

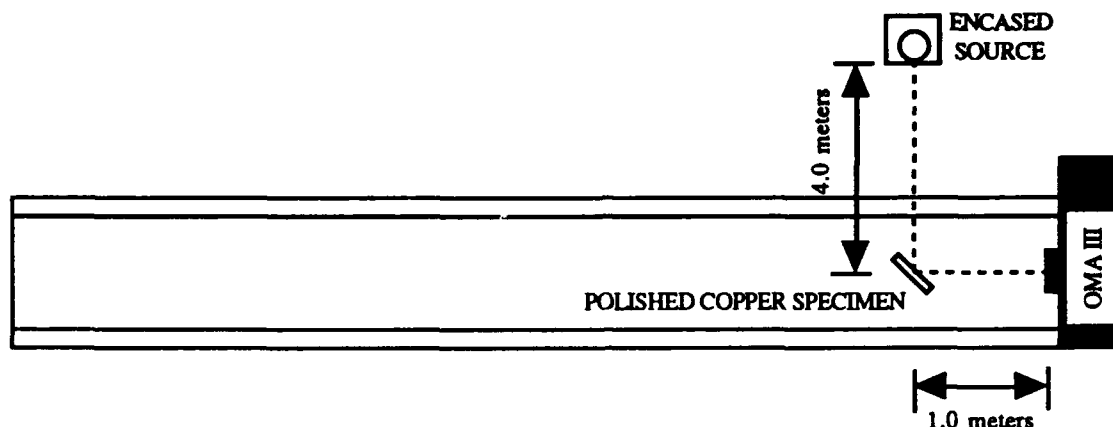


Figure 8 Setup for Copper Surface Reflection Degradation Experiment (Top View)

a. Background Compensation Mode

All available Background Compensation Modes were evaluated to determine their utility for this research and their overall accuracy. The data for this evaluation were collected during the light source radiance experiments for all sources, using the setup and procedures defined in paragraph III.B.1. Following collection of the initial data, data were stored using the various compensation modes in the order listed in Table VII. Background data were subtracted from the Comp Mode 0 data manually using an HP-48SX hand calculator to verify the validity of the data thus stored to disk.

In all cases the first six modes listed in Table VII were stored while the initial acquired data were still in the OMA memory; that is, before any new data were acquired. Seventh and subsequent entries in Table VII were later stored to disk by either the "Curve Calculation" software or, in the case of Comp Modes B and 0-4, by fetching the

stored Comp Mode 0 curve for the desired source and saving it using the desired new Comp Mode and referencing the applicable background data file.

Table VII ORDER OF DATA STORAGE BY COMPENSATION MODE FOR VARIOUS SOURCES

100 W Hg CALIBRATION LAMP	100 W COMMERCIAL BULB	500 W HALOGEN BULB	200 W MERCURY ARC LAMP
Comp Mode 0	Comp Mode B	Comp Mode B	Comp Mode 0
Comp Mode B	Comp Mode 0	Comp Mode 2	Comp Mode B
Comp Mode 1	Comp Mode 1	Comp Mode 4	Comp Mode 1
Comp Mode 2	Comp Mode 2	Comp Mode 1	Comp Mode 2
Comp Mode 3	Comp Mode 3	Comp Mode 3	Comp Mode 3
Comp Mode 4	Comp Mode 4	Comp Mode 0	Comp Mode 4
Comp Mode 0 - Background	Comp Mode 0 - Background	Comp Mode 0 - Background	Comp Mode 0 - Background
Comp Mode 2	Comp Mode 2	Comp Mode 2	Comp Mode 2
Comp Mode 4	Comp Mode 4	Comp Mode 4	Comp Mode 4
Comp Mode B	Comp Mode B	Comp Mode B	Comp Mode B

b. Timing of Background Compensation

As part of the evaluation of the accuracy and utility of the Background Compensation Modes, the effects of timing of data storage using the selected modes were also evaluated. Data stored to disk using the modes and timing indicated in rows 8 through 10 of Table VII were compared to their counterparts that had been stored to disk immediately after data acquisition, and before other data were read into the system memory.

4. Filter / Goggle Transmittance

The transmittances of the polarizing filter, the bandpass filters and the safety goggles, as functions of wavelength, were measured using all four light sources. Experimental setup is depicted in Figure 6, with applicable source and distance information listed in Table VIII. The shield was used for the 500 W halogen / quartz bulb and the 200 W mercury arc lamp. Shield slit widths for these measurements were 2.0 mm and 1.0 mm respectively.

The source was initially positioned on the axis of the spectrograph and the output spectral response allowed time to equilibrate following application of electrical power to the source. To minimize long term fluctuation errors, source radiance data were recorded using Comp Mode 2 for all sources immediately prior to acquisition of transmission data for each filter. After the source radiance data were recorded, the applicable filter or goggle was placed directly in front of the spectrograph entrance slit such that only light passing through the filter or goggle could enter the spectrograph. Again data were recorded using Comp Mode 2 based on the same initial background lighting conditions used for the source radiance data.

Data for the polarizing filter were recorded first for vertical and then for horizontal polarization. Since light from the source could leak around the shield or otherwise be reflected into the spectrograph, additional background data were acquired and stored with the source radiating and the shield slit closed for the experiments in which the polarizing filter was used. These data were collected for setups with no filter and for the vertical and horizontal polarization axes of the filter and then stored for use with the applicable data compensation modes.

Following data storage, the "Curve Calculation" menu software was used to calculate the transmittance data file for each filter by dividing the data file obtained with the filter in place by the applicable source radiance data file.

Table VIII SELECTED LIGHT SOURCE AND SOURCE TO SPECTROGRAPH DISTANCES (as Shown in Figure 6) FOR FILTER / GOGGLE TRANSMITTANCE MEASUREMENTS

FILTER	SOURCE	X DISTANCE	Y DISTANCE	Z DISTANCE
Polarized	500 W Halogen	10.0 cm	50.0 cm	60.0 cm
	100 W Sylvania	N/A	N/A	20.0 cm
3172	200 W Hg Arc	650.0 cm	100.0 cm	750.0 cm
3174	200 W Hg Arc	650.0 cm	100.0 cm	750.0 cm
3176	200 W Hg Arc	650.0 cm	100.0 cm	750.0 cm
3178	200 W Hg Arc	650.0 cm	100.0 cm	750.0 cm
3180	200 W Hg Arc	650.0 cm	100.0 cm	750.0 cm
Longpass Filters 1-7	200 W Hg Arc	650.0 cm	100.0 cm	750.0 cm
	Hg Calibration	N/A	N/A	6.0 cm
	100 W Sylvania	N/A	N/A	N/A
Safety Goggles	200 W Hg Arc	650.0 cm	100.0 cm	750.0 cm

5. Polished Aluminum Surface Reflectance

The aluminum reflectance experiment was conducted to determine a method, using the OMA III, to accurately measure the reflectivity of a metallic surface for comparison against the known reflectance data presented in Figure 2, and to thus substantiate the results of the copper luminescence experiments. Reflectance measurements for the aluminum specimen were, therefore conducted using the 500 W halogen / quartz source, since it provided the most consistent radiance with respect to time, and since an ultraviolet source was not required.

After allowing the source to equilibrate during an initial warmup period of over one hour, background data were acquired using Comp Mode 0 with the source radiating and the shield slit closed for the setup shown in Figure 9. Light from the source was shielded from directly entering the spectrograph by extending the slitted shield. Shield slit width was maintained at 2.0 mm throughout the experiment.

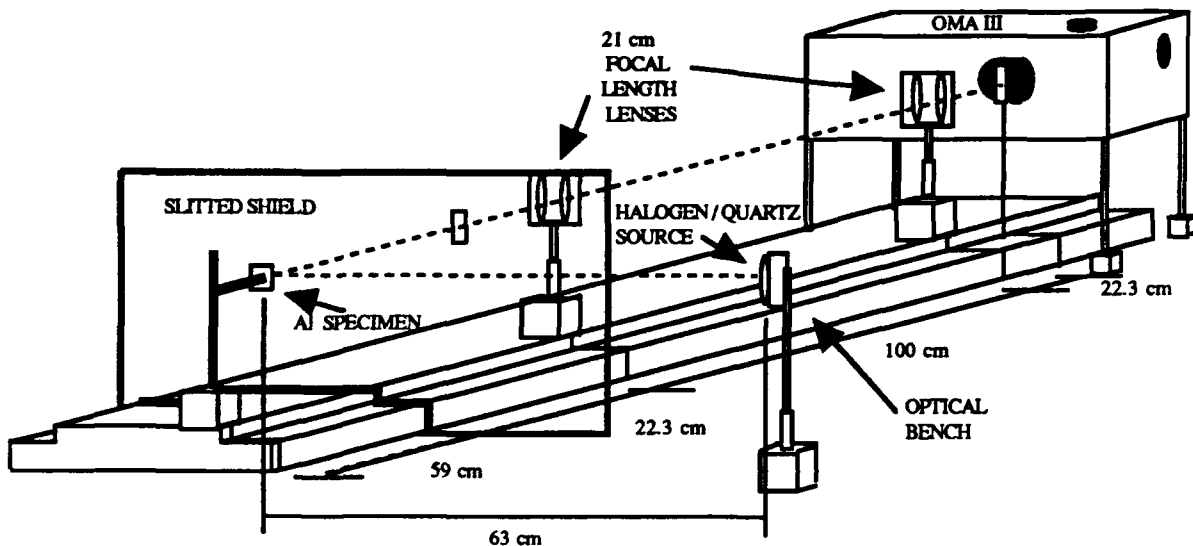


Figure 9 Setup for the Aluminum Reflectance Experiment

The aluminum specimen which had been freshly polished within 30 minutes of taking the first data, was positioned so as to reflect the maximum amount of light from the source to the entrance slit as reported on the OMA III display screen while acquiring "Live" data. A protractor, positioned directly below the aluminum specimen and oriented with 0° pointing directly along the axis of the spectrograph, was used to measure the angle of the metallic surface with respect to the axis of the spectrograph. Initial specimen angle was measured at 45°.

Since two types of reflection, spectral and diffuse, occur when light strikes a surface, the experimental method was devised to measure the total contributions of both mechanisms. Spectral reflection obeys Snell's Law in which the angle of incidence equals the angle of reflection. Diffuse reflection results in a more omnidirectional scattering of light due to surface roughness. Although every effort was made to ensure the metallic surfaces were polished as smoothly as possible, the finest polishing abrasive diameter of 0.25 μm , or 250 nm was of the same order of magnitude as the wavelength of the reflected light of interest. Therefore, a significant amount of the light incident on the surface was diffusely scattered. Thus, the experimental method was devised to "capture" as much of the diffuse, as well as the spectral, reflected energy as possible. Data were therefore taken, using Comp Mode 2, for 1° incremental decreases in the angle of reflection until no more reflected light was detected by the OMA III. The 1° increment was selected since this was the approximate angle subtended by the source at the aluminum surface.

Following the acquisition of all reflected light data, the specimen was removed from the setup and the source was positioned on the axis of the spectrograph such that the path lengths travelled by the light from the source to the spectrograph entrance slit for the two setups were identical. Background data were again taken with the shield slit closed for the new setup and used to correct the radiance data obtained from the source directly using Comp Mode 2. Reflected data for all angles were summed using the "Curve Calculation" software representing the total of the spectral and diffuse reflected energies. This total was then divided by the direct source radiance to yield the reflectance of the aluminum surface.

6. Copper Luminescence Experiments

Two experimental methods were used to evaluate the ability of a highly polished copper surface to luminesce. The first method relied on the ability of selected longpass and bandpass filters to allow light of certain wavelengths to pass while blocking the

transmittance of other wavelengths, thus allowing or preventing the excitation process necessary for luminescence to occur. The second method keyed on the fact that luminescence is a delayed reaction to excitation from an external source, and hence a chopper was employed to look at the emission intensity after, not during, surface excitation.

a. Filter Method Number 1

Based on the transmittances of the Twardy bandpass filters that allow certain wavelengths of ultraviolet radiation (where excitation should occur) to pass but block nearly all of certain portions of the visible spectrum (where luminescence should occur) an experimental method was devised whereby a filter was placed such that the light radiated by the source had to pass through the filter prior to being reflected off the copper specimen. In this manner, the filter allowed light energy of the proper excitation wavelength to pass through and stimulate the luminescence process while it filtered out most of the visible light energy at the anticipated emission wavelengths. Thus, assuming the intensity of the luminescence were sufficiently great, the emitted energy should be readily apparent in the reflected data.

The corresponding setup is depicted in Figure 10, however, for method 1 no filters were placed at filter position 2. The 200 W mercury arc lamp was selected as the source for this method because of its strong radiance in the ultraviolet region, which provides a more broadband spectrum than the mercury calibration lamp of much lower radiated power.

As with the copper reflectance degradation experiment, the source was encased in the slitted box to minimize the likelihood of unfiltered light from the source from being reflected into the spectrograph. Background data with the slit covered were taken using the "ACCUM" Data Source Mode and D.A. Mode 1 with a 30 msec exposure time

and $J=1$, $K=0$, $I=333$, thus providing a total acquisition time of 9.99 sec. The high intensity of the spectral peaks of the reflected mercury source precluded use of the "Live" Data Source Mode with a long exposure time in order not to exceed the detector dynamic range. The copper specimen was positioned along the axis of the spectrograph at an angle of 45° , which provided the greatest reflected intensity at the detector. Data were acquired using the same Data Source and Acquisition Modes as were used to acquire the background data. Reflected data were stored to disk using Comp Mode 2 referencing the previously mentioned background data file.

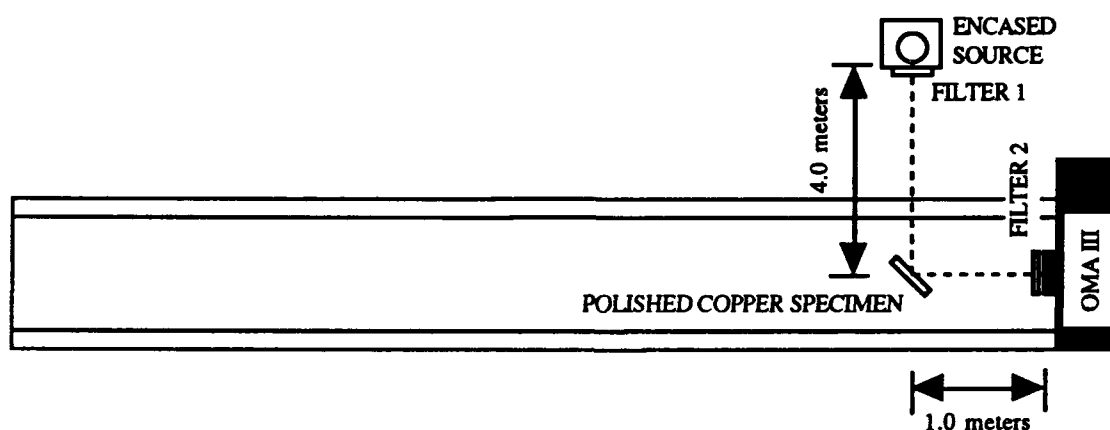


Figure 10 Setup for the Copper Luminescence Experiments Using Longpass and Bandpass Filters

b. Filter Method Number 2

Longpass filters were used in the second filter method employed to evaluate the luminescence characteristics of copper. The setup for this method is presented in Figure 10. The basis for this method centered around the placement of the same filter at the two different specified points along the light path and comparison of the two resulting

reflected spectra. If luminescence mechanisms were excited by ultraviolet light from the source that was allowed to strike the surface when the filter was placed at position 2, the visible wavelength light that passed through the filter to the detector should contain reflected contributions due to both reflection of the visible light radiated by the source, and contributions due to luminescence. If then the longpass filter were located at position 1, the source ultraviolet radiation would be prevented from striking the surface and, hence from exciting the luminescence process. Thus, visible wavelength reflection data for the longpass filter at position 1 should contain only contributions due to reflection of the visible light radiated by the source. The difference between the visible wavelength data taken for the two filter locations should represent the intensity of the luminescence.

Data acquisition procedures including modes and settings defined in paragraph III.B.6.a. were duplicated for this experimental method.

c. Chopper Method

Since the emission of photons during the luminescence process is delayed in time from the excitation phase, it is not only possible to observe the emissions in the absence of the source light, but it is in fact preferable to do so. This can be accomplished by using a chopper. The Model 1462 detector controller does incorporate provisions to synchronize detector scans to external electrical signals, such as those from a chopper. Consequently, an experimental setup had to be devised to allow the chopper to physically synchronize the source radiance and detector scan patterns so as to not overlap. The geometry depicted in Figure 11 allowed for such synchronization.

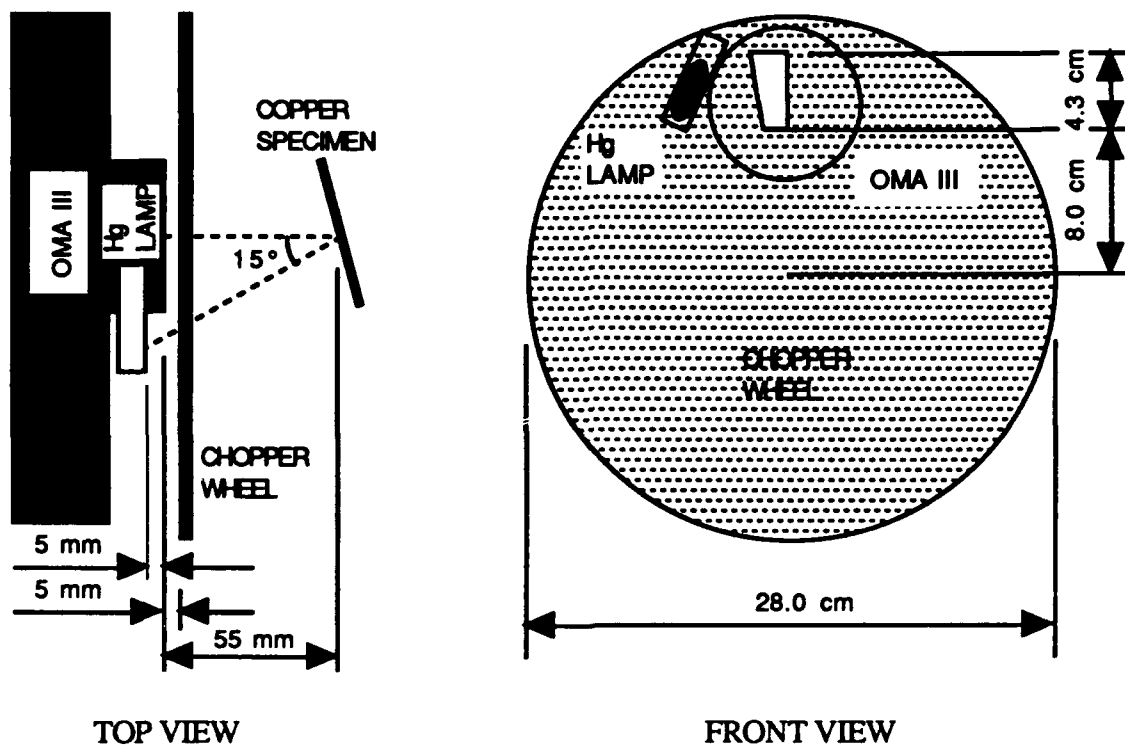


Figure 11 Setup for the Copper Luminescence Experiments Using a Light Chopper

The 2° wide chopper slit and offset location of the mercury calibration lamp source ensured that the copper surface could not be in view of the detector and the source at the same time. Placement of the source behind the plane of the spectrograph entrance slit minimized scattering into the spectrograph. In this configuration a 30 second exposure time could be used without exceeding the dynamic range of the detector. To further enhance the acquisition of low intensity luminescence emissions spectral summing was employed ("ACCUM" Data Source Mode with D.A. Mode 1 and J=1, K=0, and I=10 were used to provide a total data acquisition time of 5 minutes). Background data for a darkened laboratory using these modes and settings were acquired for the setup with the mercury

calibration lamp radiating and the chopper not rotating. Initial source warmup exceeded six hours. The chopper was then brought up to maximum rotational speed and allowed to stabilize. Because the chopper wheel had been modified to close one 90° sector that had originally been a window and to reduce the opening of the remaining window to 2°, a wheel imbalance at high rotational speeds caused the chopper to vibrate, and required that it be manually held in place while data were being acquired. Data were stored to disk using Comp Mode 2.

C. DATA REDUCTION AND PRESENTATION

Data were primarily reduced using the software resident in the OMA III Model 1460 System Processor. OMA III data reduction software employed in this research was available from two sources. Firstly, in the "Data Acquisition" menu, the desired background compensation mode was selected following data acquisition which was then applied to the data being stored to disk. Secondly, software in the "Curve Calculation" menu was used to perform basic mathematical operations on the stored data. This consisted primarily of addition, subtraction, multiplication, and division. The logical operands and Boolean algebra expressions available in this menu were not used for reduction of any of the data presented in this thesis.

Additionally, spot checks of OMA III software data reduction results were conducted using a Hewlett-Packard Model HP-48SX handheld calculator. Data presentation using the Epson FX-86e serial printer were used during the experiments to provide a quick hardcopy results, but the final data plots presented in this thesis were drawn using the HP ColorPro graphics plotter.

D. SAFETY

Because of their relatively higher ultraviolet output, use of mercury light sources required safety considerations which were not necessary for the tungsten filament sources.

The human body is extremely sensitive to ultraviolet radiation, which can cause irritation and burning of both skin tissues and the eyes, and even blindness. Consequently, when working with the ultraviolet light sources, the skin and eyes were always protected from the harmful rays of the mercury source. Ultraviolet radiation blocking goggles and sunscreen were worn whenever the mercury sources were operating, and care was taken so as not to look directly at the radiating sources.

IV. RESULTS AND DISCUSSION

A. GENERAL

Before measurements of metallic reflectivity and luminescence can be made, the capabilities, utility and possible sources of error of the equipment must be evaluated. Only after the characteristics of all experimental equipment have been determined is it possible to develop a proper experimental method for acquiring and reducing reflectivity and luminescence data.

B. EXPERIMENTAL EQUIPMENT CHARACTERISTICS

1. Light Source Spectra

The radiated spectra of the mercury calibration lamp, 200 W mercury arc lamp, 100 W commercial incandescent light bulb and 500 W halogen / quartz lamp sources were evaluated using the OMA III to provide a baseline reference against which other measurements could be compared and to determine their applicability for other experiments conducted in the course of this research. Comp Mode 2 background corrected data for the four sources are presented in Appendix C, Figures 1 through 4.

a. Mercury Sources

The radiated output of the low pressure mercury calibration lamp consisted primarily of energy concentrated in spectral lines at distinct wavelengths with little radiated intensity at other wavelengths. In comparison, the spectral lines of the 200 W mercury arc lamp were broadened and a significantly greater radiated intensity was provided at all wavelengths covered, for the same intensities of the peak spectral lines. The calibration lamp produced a spectral line at 253 nm that was not present in the output of the arc lamp. Since the 507 nm line is the second harmonic for the 253 nm line, it too was missing from

the output of the arc lamp. Similarly, the 296 nm, and its harmonic at 592 nm, were either pressure broadened or significantly reduced in the output of the arc lamp compared to the calibration lamp. Although the calibration lamp did provide source coverage over a wider range of wavelengths than did the arc lamp (beginning at approximately 253 nm vs 280 nm), the radiated power of the arc lamp provided much more flexibility in laboratory set up, and was therefore the primary ultraviolet source used in this research.

b. Tungsten Filament Sources

The 100 W incandescent bulb and the 500 W halogen / quartz lamp provided a continuous spectrum of radiated output, beginning from approximately 300 nm through all visible wavelengths. Both sources displayed definite peaks of intensity at certain wavelengths, however, of all the available sources, their radiated spectra most nearly approximated "white light" for the range of wavelengths covered. Based on their consistent output across the portion of the spectrum covered, the tungsten filament sources were used in experiments not requiring an ultraviolet source output below approximately 400 nm. Since the service life of the halogen bulb was significantly shorter than that of the 100 W incandescent bulb, and the heat generated by the halogen source made it difficult to use, the lower wattage bulb was used when radiated intensity was not a factor in a given experiment.

2. Sources of Experimental Error

An evaluation of the limitations and constraints imposed by the experimental equipment was performed to first determine the optimum method of conducting subsequent experiments and then to define the total error contributions to the final results. Errors that affected experimental results during the course of this research came from a variety of sources including OMA III system hardware and software.

a. Wavelength Calibration

The ability of the OMA III to maintain wavelength calibration throughout data acquisition and reduction was evaluated during other dedicated experiments by spot checking system displayed wavelengths for peak mercury spectral lines against the known values upon which the initial calibration was based. In all cases evaluated, the calibration remained correct to within the accuracy capabilities of the selected grating, so long as neither the Grating Select Knob nor the Wavelength Counter Crank on the spectrograph were disturbed, or electrical power was removed from the system.

b. Source Intensity Fluctuations

The magnitude of the fluctuations in radiated intensity was evaluated qualitatively for all sources, and quantitatively for the two mercury lamps and the 100 W commercial incandescent light bulb. Qualitatively, the intensities of the two tungsten filament bulbs exhibited the same relative fluctuations in terms of rate, character and amount of change. Curves depicting ratios between source radiance data collected 16 to 17 seconds apart are presented in Appendix C, Figures 5 through 7, and a similar ratio curve for the mercury arc lamp data taken one hour and 35 minutes apart is presented in Appendix C, Figure 8. Table IX presents per cent change between minimum and maximum intensities of the mercury calibration lamp, at specified wavelengths, over a one minute period.

For all light sources, the amount of change in the intensities of the radiated output was not constant across the spectrum but was a function of wavelength. Although the intensities at all wavelengths varied from one 30 msec scan to the next, as a general rule, the mercury source spectral peaks exhibited greater changes in intensity than did the spectral valleys. Intensity changes in the incandescent bulbs did not appear to exhibit any significant long term characteristics once the bulb had reached thermal equilibrium with its

surroundings, but the inconsistent nature of the electric arc and, to a lesser extent the calibration lamp, resulted in long term periodic changes in the radiance characteristics of the mercury sources.

**Table IX MERCURY CALIBRATION LAMP RADIATED INTENSITY
FLUCTUATIONS**

WAVELENGTH	PERCENT CHANGE
254.3 (Spectral Peak)	8.19196
296.9 (Spectral Peak)	12.41005
312.8 (Spectral Peak)	13.91762
364.9 (Spectral Peak)	14.00828
403.9 (Spectral Peak)	0.49038
419.3 (Spectral Valley)	6.03976
435.9 (Spectral Peak)	0.62729
472.0 (Spectral Valley)	4.12371
507.5 (Spectral Peak)	0.71305
529.9 (Spectral Peak)	8.59106
565.4 (Spectral Valley)	5.65553
579.0 (Spectral Peak)	6.03908

The maximum short term error due to light source intensity fluctuations was approximately $\pm 15\%$ for the mercury sources and approximately $\pm 5\%$ for the tungsten filament sources. Long term source fluctuations, which include the errors due to short term changes in intensity are estimated at a maximum of approximately $\pm 10\%$ for tungsten filament sources. Long term errors due to mercury source intensity fluctuations are estimated at approximately $\pm 90\%$ at short wavelengths where the source output is quite low

and measurements are inaccurate, and approximately $\pm 40\%$ at longer ultraviolet and visible wavelengths.

The significantly less stable radiated intensity of the mercury sources further made the tungsten filament bulbs the preferred source when experimental data in the ultraviolet region were not required. When radiated power was not a primary consideration in experiments in the ultraviolet spectrum, the mercury calibration lamp was the preferred light source.

c. Dark Current

The dark current and internal noise within the OMA III were evaluated for fluctuations in the amplitude of the signals. Ratios of data taken with the spectrograph entrance slit covered permitting no external light to illuminate the detector, are presented in Appendix C, Figures 9 and 10. Fluctuations in the amplitude of the dark current signal at all positions were random and not time or wavelength dependent. The maximum fluctuation in the signal at any wavelength was 2% . This was over twice the average fluctuation.

Appendix C, Figures 11 and 12 present uncompensated data for ambient darkened laboratory conditions and, on the same scale, corresponding data for illumination by the mercury arc lamp. An increase in intensity at short wavelengths, below the portion of the electromagnetic spectrum in which the source radiated, were consistently present regardless of the type source used, but were dependant on the intensity of the source at short wavelengths. The 3% increase in dark current at short wavelengths may be induced by the stimulation or leakage of other nearby photodiodes. The combination of the two effects results in a maximum combined dark current error of approximately 10 to 15 counts, which is relatively insignificant for moderate or greater levels of external signal intensity. However, at low levels of external signal intensity (eg below about 250 nm for

the mercury calibration lamp, 300 nm for the mercury arc lamp and 330 nm for the tungsten filament bulbs) the errors can be significant if the magnitudes of two such low-level background-corrected signals are ratioed. If a background data file containing only dark current and its associated errors is subtracted from a data file in a portion of the spectrum in which no source radiation exists, so that the only contributions present are due solely to dark current and errors, the remainder is effectively the sum of the two original errors. If two such background corrected data files are then ratioed, large fluctuations due to the errors result. This explains the short wavelength portion of the filter transmittance curves such as the one depicted in Appendix C, Figure 13.

d. Polarization Sensitivity of the OMA III

The sensitivity of the OMA III to vertically and horizontally polarized light was evaluated by placing a polarizing filter at the spectrograph entrance slit and acquiring transmittance data for both polarizations using the tungsten filament sources. Similar data for the halogen / quartz and 100 W incandescent sources are presented in Appendix C, Figures 13 and 14, showing plots of (in order from top to bottom), 1) vertical transmittance, 2) horizontal transmittance, and 3) the difference between the two. Data were repeatable for different orientations of the source. In the visible spectrum, the OMA III detection sensitivity to horizontally polarized light is between approximately 1% and 8% less than for the same intensity of vertically polarized light.

The difference in the sensitivity for different polarizations may be significant for reflectivity studies in which unpolarized light becomes partially polarized upon reflection from a metallic surface. The percentages of reflected light that are horizontally and vertically polarized upon reflection vary as functions of the reflected wavelength. Thus, depending on the reflectivity characteristics of the metal being studied, care must be

taken to orient the specimen and source to minimize the effects of the error caused by the OMA III's sensitivity to vertically and horizontally polarized light.

e. Spectrograph Axis Angle Offset Sensitivity

The sensitivity of the OMA III to the angle at which light enters the spectrograph was evaluated using the 100 W incandescent light bulb for entry angles of between 0° - 7° from the axis of the spectrograph. Detected source radiance data for increasing angles of incidence from top to bottom, are presented in Appendix C, Figure 15, and ratio data between offset and direct intensity data files are presented for increasing angles of incidence in Appendix C, Figures 16 through 22. In addition to a decrease in the detected source intensity with increasing angle offset, Figure 16 distinctly shows an apparent shift in wavelength to the left, as evidenced by the gradual movement of the peaks and valleys of the radiance spectrum to shorter wavelengths as offset angle increases. These phenomena, known as "channelled spectrum" are the result of the source light passing through a dielectric medium of finite thickness prior to reaching the detector. [Ref. 2:p. 260-269] The flat thin film may be due to a coating applied to the grating surfaces, a glass plate placed between the spectrograph exit port and the detector to allow for purging of the detector or, as in the case of later experiments, by the placement of a glass filter between the source and spectrograph.

Appendix C, Figures 16 through 22 demonstrate the results of ratioing data files that were taken with different angles of incidence from the source to the spectrograph. The amplitude of the variations in these data curves, due to the apparent shift in the wavelengths at which the spectral peaks and valleys occur, increase from approximately $\pm 5\%$ at 1° offset to approximately $\pm 8\%$ at 3° offset.

In addition to the variations present in the ratio data curves, the slope of the curves also change, from slightly positive, to slightly negative (ratio of $4^{\circ}/0^{\circ}$ data), to

slightly positive again. These phenomena were constantly observed throughout the source radiance and reflectivity experiments, during which lateral movement of the source caused the final slope of the longest wavelength portion of the detected spectrum (the tail) to radically change from negative to positive.

To prevent, or at least minimize, the channelled spectrum errors due to varying angles of incidence of light at the spectrograph entrance slit, the setup using the slitted shield and optical lenses was devised to increase the path length between source and detector without decreasing the intensity of the source at the detector. This setup allowed greater accuracy in the angular positioning of the source. Due to the absorption of ultraviolet radiation by the glass lenses, the setup was not employed for experiments in which the mercury sources were utilized.

f. Apparent Detector Sensitivity as a Function of Exposure Time, Data Source Mode and Data Acquisition Mode

Various combinations of detector exposure time, Data Source Mode and Data Acquisition Mode (D.A. Mode) were evaluated for their effects on apparent detector sensitivity by comparing background data acquired for darkened and overhead lighted laboratory conditions. Data are presented in Appendix C, Figure 23 through 25 using a 30 msec exposure time and "Live" Data Source Mode for , 1) darkened laboratory data, 2) laboratory data with the fluorescent overhead lights on and 3) the difference between the two previous data files. Similarly, Appendix C, Figures 26 through 28 present data acquired using a 30 msec exposure time and the "ACCUM" Data Source Mode with D.A. Mode 1 selected for values of J=1, K=0 and I=333; and Figures 29 through 31 present data using a 9.99 second exposure time and the "Live" Data Source Mode.

The dark current errors masked the low intensity contributions of the fluorescent light source hidden in the lighted data. Hence, visual comparison of the lighted

and unlighted data curves for the "Live" 30 msec mode setting, as well as similar comparison of the "ACCUM" mode data, failed to detect the influence of the florescent lights. Their contribution became apparent in the "Live" 30 msec data only after subtracting out the darkened laboratory data. A much clearer indication of the overhead fluorescent lights' radiated spectrum was obtained by adding 333 consecutive 30 msec scans of the two background conditions as performed by the "ACCUM" mode and subtracting the resulting darkened laboratory data from the lighted data. The total time that data acquisition occurred using this mode was 9.99 sec.

By using the "Live" Data Source Mode and expanding the exposure time to 9.99 seconds, the same total acquisition period was achieved as by the use of the "ACCUM" mode, however the results were quite different. By increasing the exposure time, the influence of the overhead fluorescent lights' radiated spectrum was immediately noticeable in the uncorrected data, and became much more clearly defined after subtracting out the dark current errors present in the darkened laboratory data.

The presence of low intensity radiation in the ultraviolet and visible portions of the electromagnetic spectrum may be detected by increasing the acquisition time of the detector. Two possible methods of achieving this end, are to either increase the exposure time using the "Live" Data Source Mode, or to add multiple short duration scans by use of the "ACCUM" Data Source Mode in conjunction with appropriate selection of D.A. Mode and applicable parameters. Of the two, the first provides the best results, however the intensity of the total radiation entering the spectrograph must be extremely low since the dynamic range of 16383 counts is the maximum observable intensity per scan. Thus, the "ACCUM" mode allows for the amplification of weak spectral contributions in the presence of stronger intensity radiation.

g. Oxidation of Metal Surface

The effects on the reflectivity of a highly polished copper surface due to extended exposure to the ambient laboratory environment were evaluated over a six day period using the mercury arc lamp source. Initial data acquired as part of the filter luminescence experiments were repeated 144 hours later and the two results ratioed. To ensure repeatability of the data and to reduce the total error, the experiment was performed twice with the same results. The results presented in Appendix C, Figure 32 and 33 represent the ratio of the original polished data divided by the data acquired after the six day exposure period. A minor decrease in the reflectance of the copper surface resulted from exposure to the atmosphere. To minimize this source of error, the metallic surfaces were repolished, to remove any build up of surface oxidation immediately prior to conducting any reflectivity or luminescence experiments.

3. Sources of Data Reduction Errors

a. Background Compensation Mode

The OMA III software capability to compensate acquired data for the effects of background and internal noise was evaluated by storing individual data files using each of the six Compensation Modes (Comp Modes). Each file was allocated one "memory." Comparison of the recorded output intensity of the mercury calibration lamp at various wavelengths using each of the Comp Modes is presented in Table X. Comp Modes 0, 1, 2, 3, and 4 as well as the "Curve Calculation" software file generated by subtracting the background data file from the Comp Mode 0 data file all functioned as the manufacturer claimed. Table X and Appendix C, Figure 34 present data showing the proper identical results for files containing the same number of "memories." Identical results to those presented in Appendix C, Figure 34 were obtained for ratios of Comp Mode 1 and 2 data

files as well as for Comp Mode 1 and background subtracted data files using the "Curve Calculation" software.

Table X MERCURY CALIBRATION LAMP INTENSITY AS A FUNCTION OF WAVELENGTH AND COMPENSATION MODE

$\lambda =$	BKGND	CM 0	HP $\Delta =$	CM B	CM 1	CM 2	CM 3	CM 4	O - BKGND
150.2	209	218	9	-1872	9	9	7.8	7.8	9
175.0	203	213	10	-1817	10	10	8.6	8.6	10
200.4	206	221	15	-1839	15	15	13.0	13.0	15
225.2	200	215	15	-1785	15	15	13.0	13.0	15
250.0	207	288	81	-1782	81	81	70.0	70.0	81
274.9	197	238	41	-1732	41	41	35.4	35.4	41
300.3	201	268	67	-1742	67	67	57.9	57.9	67
325.1	210	268	58	-1832	58	58	50.1	50.1	58
349.9	201	275	74	-1735	74	74	63.9	63.9	74
375.3	202	457	255	-1563	255	255	220.3	220.3	255
400.1	196	555	359	-1405	359	359	310.0	310.0	359
424.9	205	468	263	-1582	263	263	228.0	228.0	263
449.8	196	379	183	-1581	183	183	158.1	158.1	183
475.2	200	345	145	-1655	145	145	125.3	125.3	145
500.0	201	781	580	-1229	580	580	501.0	501.0	580
525.4	200	506	306	-1494	306	306	264.3	264.3	306
550.2	200	581	381	-1419	381	381	329.1	329.1	381
575.0	197	399	202	-1571	202	202	174.5	174.5	202
599.9	204	283	79	-1757	79	79	68.2	68.2	79
625.3	200	3136	2936	1136	2936	2936	2536.1	2536.1	2936
650.1	201	235	34	-1775	34	34	29.4	29.4	34
674.9	201	226	25	-1784	25	25	21.6	21.6	25
699.7	207	229	22	-1841	22	22	19.0	19.0	22
725.1	204	227	23	-1813	23	23	19.9	19.9	23

Data storage using Comp Mode B, however, consistently resulted in the majority of the spectral data being presented as having large negative values of intensity as depicted in Appendix C, Figures 35 and 36, which show (in order from top to bottom), 1) the uncompensated data, 2) the background data, 3) the compensated data using Comp Modes 1 through 4, and 4) the results of Comp Mode B corrections. This characteristic was evident regardless of the order in which the Comp Mode B file was stored. The

significant error caused by the inaccurate correction of data for background effects by the Comp Mode B data reduction software resulted in that compensation mode not being used during this research. It is recommended that Comp Mode B not be used for the software and hardware configuration specified for this research.

b. Timing of Background Compensation and Data Storage

The time dependency of data storage using the various Comp Modes was evaluated by comparing the results of data files stored immediately after data acquisition, to those stored using the same Comp Mode, but by applying the compensation to the original Comp Mode 0 data file recalled from disk. Appendix C, Figure 37 presents on one plot Comp Mode 2 radiance data for the 500 W halogen / quartz bulb for (in order from top to bottom), 1) data stored after performing the background compensation on the recalled file of the original Comp Mode 0 data, 2) data stored after performing the background compensation on the uncompensated data just acquired, and 3) the difference between the two. Data compensation was accurately performed using all Comp Modes, except Comp Mode B, so long as the raw data to be corrected had not been erased from and then recalled to the system processor's volatile memory. The intensities of spectral data stored using background compensation performed on recalled data was in error by 50%. To ensure proper application of the desired background compensation mode, data had to be stored using each of the desired Comp Modes immediately after the uncorrected data were acquired. Since at the time of data acquisition the required compensation mode was not always known, either files using each available Comp Mode had to be stored, wasting disk storage space, or the possibility existed that the experiment would have to be repeated to obtain the desired Comp Mode corrected data.

4. Twardy Bandpass Filter Transmittance

The transmission characteristics of the Twardy bandpass filters were evaluated for comparison with contractor supplied data and to determine which filter or filters would best be used for the copper luminescence experiments. Background compensated transmittance data for each of the filters (3172 through 3180) using the 200 W mercury arc lamp source are provided in Appendix C, Figures 38 through 42.

Due to the errors caused by short term source fluctuations and dark current, the short wavelength values are unreliable and provide no information on the transmittance of the filters below about 280 nm. Allowing for experimental error, the transmittances of the Twardy filters were in close agreements with the contractor values presented in Table III. The contractor's performance statements, however did not mention the second and sometimes third transmission windows that existed in all five of the Twardy filters in the visible region. Although filters 3174 and 3176 exhibited practically no transmittance at wavelengths between approximately 400 nm and 550 - 600 nm, the other filters allowed different ultraviolet wavelengths to pass. Consequently, based on these data, all five of the Twardy filters were used in both of the copper luminescence experiments.

5. Longpass Filter Transmittance

The transmission characteristics of the longpass filters were evaluated to determine which filter or filters would best be used for the second copper luminescence experiment. Transmittance data using the 200 W mercury arc lamp and the 100 W incandescent bulb are presented for each of the longpass filters 1 through 7 in Appendix C, Figures 43 through 56. There are clearly differences between the transmittances obtained from use of the two sources. The causes of these differences are not fully understood. The transmittance data obtained using the mercury arc lamp appears to provide a good

indication of filter transmittance between 300 nm and 400 nm while the incandescent source provides more accurate transmittance data at wavelengths above 400 nm.

The Twardy filters were obtained new from the manufacturer for this research whereas the longpass filters had been used for student classroom and laboratory studies for many years. Additionally, the Twardy filters were of a much better quality than the longpass filters, some of which contained air bubbles and other imperfections or had rough surfaces. Consequently, the transmittance curves for the Twardy filters using the mercury arc lamp were smoother and contained fewer spikes than did the similar data for the longpass filters. The jaggedness of the transmittance curves using the mercury sources, and the variations in the curves obtained using the incandescent source are primarily due to the "Channelled spectrum" effect discussed in paragraph IV.B.2.e.

The data for the filters presented in this paragraph represent only a small portion of the total number of longpass filters evaluated. The seven filters discussed here have been presented in order of increasing initial cut-off wavelength. These cut-off wavelengths effectively divide the expected excitation region into seven sections. Consecutive measurements using the second copper luminescence method with each of these longpass filters individually, could determine if fluorescence does occur in copper. In addition it may also provide a range of wavelengths within which the excitation energy must exist.

6. Safety Goggle Transmittance

The transmittance of the safety goggles was evaluated using the mercury arc lamp to determine their effectiveness in offering eye protection against ultraviolet radiation. Data presented in Appendix C, Figure 57 indicates that the goggles prevent the transmission of all but a trace amount of radiation in the 300 - 400 nm region, which closely agrees with contractor supplied data. The large fluctuations in the transmittance data below approximately 300 nm have been previously explained in this section, and are

most likely due to the effects of ratioing very small numbers such as those in which only errors exist. As a result of these data, the safety goggles were worn at all times during which the ultraviolet sources were operated. It is further strongly recommended that the goggles be worn in future experiments involving the use of ultraviolet sources. A warning to that effect has been included in the OMA III operating checklists presented in Appendix B.

7. Aluminum Reflectance

Reflectance data for the aluminum specimen using the 500 W halogen / quartz source was evaluated by comparison with the normal incidence aluminum reflectance curve, reproduced from Ref 1 and presented in Figure 2, to substantiate the results obtained from the copper luminescence experiments. Presented in Appendix C, Figure 58 are overlaid aluminum reflectance data for the following angles of incidence (from the top to the bottom), 1) all angles for which reflection was observed (ie 30° through 45°), 2) 43° through 45° and 3) 44° and 45° only. The procedure used in this experiment with the slitted shield and optical lenses was validated by the relative absence of small scaled variations in the data curves indicating that the angles of incidence for the two ratioed data files, those for the reflected and radiated energies, were the same. As expected, the vast majority of the reflected energy was concentrated in angles of reflection at or near the angle of incidence, indicating that the surface was indeed quite smooth and the majority of the incident energy was spectrally reflected. The fact that the reflectance values did not increase at long visible wavelengths as data obtained for additional angles were added indicates that the depth of the imperfections on the polished copper surface was less than 700 nm. The effects of diffuse reflection, due to surface roughness of approximately the same magnitude as the 250 nm diamond polish abrasive used to polish the surface, were evident at shorter visible wavelengths.

The total reflectance curve obtained for the aluminum specimen closely agrees with the accepted data to within approximately 3%. Differences between the two could arise from a wide variety of sources. Many error sources have already been discussed and are possibly applicable to these results. The sensitivity of the OMA III to the polarization of incident light, errors due to dark current and source intensity fluctuations, method of surface preparation and surface smoothness may all contribute the slightly lower reflectance obtained by the experimental data than from those presented by Jenkins and White. Additionally, errors due to inconsistent experimental methods may be present. Examples might be the difference between normal and 45° incidence reflectance and the possibility that the accepted reflectance data may have been smoothed or have even been acquired with the specimen in a vacuum, preventing the formation of an aluminum oxide layer which is known to form almost instantly on aluminum surfaces exposed to air.

Regardless of possible error sources that might explain the differences between the experimental and the accepted aluminum reflectivity data, the key point is that the differences between the two were small and thus the ability of the OMA III to measure reflectivity from metal surfaces was substantiated.

7. Copper Luminescence Using Filter Method 1

The ability of a highly polished copper surface to luminesce when irradiated by an ultraviolet source was evaluated using the Twardy filters. Specifically, they were used to filter the radiation produced by the mercury arc lamp before being reflected off the copper surface. The "ACCUM" Data Source mode with a total acquisition time of 9.99 seconds was used to increase the apparent sensitivity of the OMA III. Data presented in Appendix C, Figures 59 through 63 depict the reflected spectra using each of the Twardy filters, respectively. Also plotted in these figures are the filter's transmittance curve. There

were no emission features in these spectra that could be attributed to luminescence. The results of the first copper luminescence experiment were therefore inconclusive.

8. Copper Luminescence Using Filter Method 2

Following the inconclusive results of the first copper luminescence experiment using the Twardy filters, the second filter method was devised to further evaluate the ability of the copper surface to luminesce. Data representing the difference between the reflectance measured with each of the 13 filters in the two positions, are presented in Appendix C, Figures 64 through 75. Also plotted on each curve, in arbitrary units, is the radiated spectrum of the source. Large amplitude positive to negative or negative to positive spikes were present in the data at or near the spectral peaks of the radiating source. These spikes are artifacts of the measurement process and are not considered valid. This effect was present for every major spectral peak. No peaks in the difference data were observed at wavelengths other than those associated with strong source radiation. Thus, the results of the second copper luminescence experiment to employ the use of filters were also inconclusive.

9. Copper Luminescence Using the Chopper

After the results of the two luminescence experiments in which filters were used to search for signs of luminescence from copper surfaces, a method was devised to take advantage of the time delay between the excitation and emission phases of the luminescence process. Again, the ability of a polished copper surface to luminesce after being radiated by an ultraviolet source was evaluated, but this time, using a chopper and the mercury calibration lamp. The combination of a 30 second exposure time and use of the "ACCUM" Data Source Mode to effectively add 10 consecutive detector scans, allowed a five minute acquisition period to be used to greatly increase the apparent sensitivity of the OMA III. The combination of the chopper and the extended acquisition time allowed for detection of

low intensity emissions while eliminating many of the error sources caused by filters, fluctuating light sources, and inconsistent angles of incidence.

Data from the chopper method using Comp Mode 2 for background compensation are presented in Appendix C, Figure 76 with the spectrum of the mercury calibration lamp plotted at the bottom. Chopper experimental data are again presented in Figure 77, but with an expanded vertical scale. Vibration of the chopper assembly during rotation of the wheel while data were being collected caused the wheel to drift away slightly from the face of the spectrograph. This allowed more light from the source to be reflected back into the detector than during the acquisition of the background data. After the background data were subtracted out, there remained a contribution due to this reflected source light. All of known spectral lines for the mercury calibration source appear in the data curve of Figure 76. In addition to these spikes the chopped spectra contains a spike at 445.2 nm. One possible explanation for the existence and characteristics of this spike may be a luminescence emission from the copper surface. Although by no means conclusive, the possibility that copper exhibits a luminescence peak at 445.2 nm warrants additional investigation.

V. CONCLUSIONS AND RECOMMENDATIONS

A. CONCLUSIONS

The Optical Multichannel Analyzer is a powerful tool that can be successfully used for many applications in spectral studies including radiance, transmission, absorption, and even reflection and emission. With sufficient user familiarity and training, the configuration used in the conduct of this research; consisting of the spectrograph, detector, detector controller, system processor and system software; can be rapidly and easily manipulated to acquire and reduce data for analysis and presentation. The menu format permits the user to quickly access various functions as needed, however the many user selectable options that give the instrument its versatility and flexibility also make it somewhat complicated to use initially. Proper use of the system to maximize its capabilities requires a substantial initial investment of time.

The checklists presented in Appendix B attempt to provide a more detailed list of step-by-step procedures to aid future users of the system in initial orientation. It is hoped that these checklists avoid some of the ambiguity in the procedures provided by the manufacturer. These checklists should be used only as a starting point however, for although they define the basic common procedures used in the acquisition and storage of data for this experiment and they are applicable to any generic experiment using this equipment, they do not attempt to cover many of the more complicated procedures necessary to utilize the full potential of the OMA.

Although the OMA does provide a relatively easy to use means of collecting and manipulating spectrographic data, it does have some notable shortcomings. Many sources of error were discovered and evaluated during the course of this research. There are still

probably many more that were not encountered within the scope of this research. Since there is little "corporate knowledge" of the intricacies of OMA at the Naval Postgraduate School future users will still have to be, at least initially, a bit wary of the results provided by the system.

While the results of the research regarding the ability to make a polished copper surface luminesce by irradiating it with an ultraviolet source are far from definitive, they should spark enough interest to keep the area of research alive. The data supporting the theory of the existence of "native clusters" and their contributions to the surface emission properties of the bulk crystalline material of the parent metal continues to increase. Although the possibility of copper to luminesce when excited by ultraviolet radiation does not entirely dispute existing theories of metal surface reflectance properties, it does nevertheless support the "native cluster" theory without necessarily contradicting quantum theory. Thus luminescence can be viewed as an essential, but not sufficient, argument for the "native cluster" model.

Use of the OMA to obtain very accurate measurements of reflection and emission properties, while possible to perform, requires extensive and painstaking planning and preparation. Specific conclusions drawn from this research are discussed in the following paragraphs along with recommendations for future research based on those findings.

B . RECOMMENDATIONS

The first and foremost recommendation to come out of the research conducted to date is that it be continued. A more definitive answer as to the existence of luminescence in copper needs to be made using more capable and more accurate equipment. If indeed luminescence is determined to occur, many additional questions should be answered. Exactly which wavelengths excite the process, and precisely where does the emission or emissions occur? What is the relative intensity of the emission and what is its radiative

lifetime? The answers to these questions could provide valuable insight into the nature of the surface composition of metals. Research need not be restricted to only copper, but metals with postulated high cluster to surface area ratios should also be candidates for luminescence studies, for example gold.

Future studies must build on the results obtained from this research. Clearly, the use of optical filters for luminescence studies required cumbersome and error inducing procedures that were not present in experiments employing a chopper. Since the one window of the chopper wheel used in these experiments spanned only 2° out of 360° of the chopper wheel's circumference, the vast majority of the detector acquisition time was used not to illuminate the copper surface or to open the detector to possible emitted spectra, but rather to detect source spectra reflected off the back of the chopper wheel. Future chopper wheels should incorporate the maximum number of open detection windows consistent with the experimental setup and procedure. To avoid the vibration of the chopper assembly that occurred at high rotational speeds, chopper wheels used in future research must be balanced.

If a chopper is to be used in future research, a better setup could be designed than was used in these experiments. Use of a detector controller that could be synchronized to an external chopper signal would allow for such a setup. According to the the manufacturer's detector controller instruction manual, the EG&G Model 1463 may be one such possible candidate.

Since the luminescence process requires excitation by incident radiation, a high intensity source may prove useful. For use with optical filters a continuum light source produced the least errors. With a chopper arrangement this should not be necessary. Lasers, such as a helium-cadmium laser, provide a high-powered monochromatic ultraviolet radiance that may stimulate luminescence in certain metals. The difficulty with

individual monochromatic sources, however, is that they must radiate at the correct wavelength to excite the surface electrons to the proper higher states. A high intensity source that could be swept through the range of wavelengths that compose the ultraviolet region would be highly desirable for these experiments.

The intensity of the possible luminescence emission discussed in paragraph IV.B.9. was of an intensity of only approximately 100 counts after compensating for the background data. Although the percentage of the acquisition time that the detector was actually exposed to the surface during the chopper experiment was extremely small (approximately $2^\circ/360^\circ = 0.6\%$), the total exposure time was approximately 1.67 sec (.006 * 5 minutes). Thus, the intensity of the possible emission was significantly less than the direct intensity of the mercury calibration lamp at that wavelength. If the intensity of emissions are indeed as small as research tends to indicate, methods to increase their effective intensities would ease future data acquisition efforts. Increasing detector exposure time and summing numerous consecutive scans of data have proven effective in this regard. Use of a photomultiplier at the entrance to the detector may prove to better serve the purpose.

To further reduce diffuse scattering caused by surface roughness, electropolishing may be employed. While the process is a timely and laborious one, its proper application will produce a much smoother surface and improve the accuracy of the results while simplifying the experimental procedure for data acquisition.

All of the above recommendations are not necessarily based on continued use of the OMA III as the data collection and reduction instrument. There may well be other equipment better suited to this type of research and future researchers should explore that possibility. If, however, additional research is to be conducted using the OMA III, whether in this area of study or in another, it is strongly recommended that the preventive

maintenance described in the manufacturer's manuals be performed on the equipments. A technical representative from the manufacturer should be immediately contacted to repair the spectrograph wavelength counter crank assembly which currently does not function properly.

To reduce the level of, and hence the errors associated with dark current, use of liquid coolant to lower the cooler and detector operating temperature may also prove valuable. Before this is done however, care must be taken to ensure that the process does not cause condensation to form within the system that would prove catastrophic to the instrument.

Due to inaccurate compensation for background and dark current effects in acquired data, it is strongly recommended that Comb Mode B not be used for operating software version 2.3. Future revisions should be evaluated for corrections to this deficiency.

Data collected during this research indicate the presence of a dielectric film in the light path within the instruments which tends to produce an apparent wavelength shift. To alleviate resulting errors, care must be taken to minimize inconsistencies between angles of incidence at the spectrograph entrance slit for different sources of data that will be ratioed or differenced.

APPENDIX A

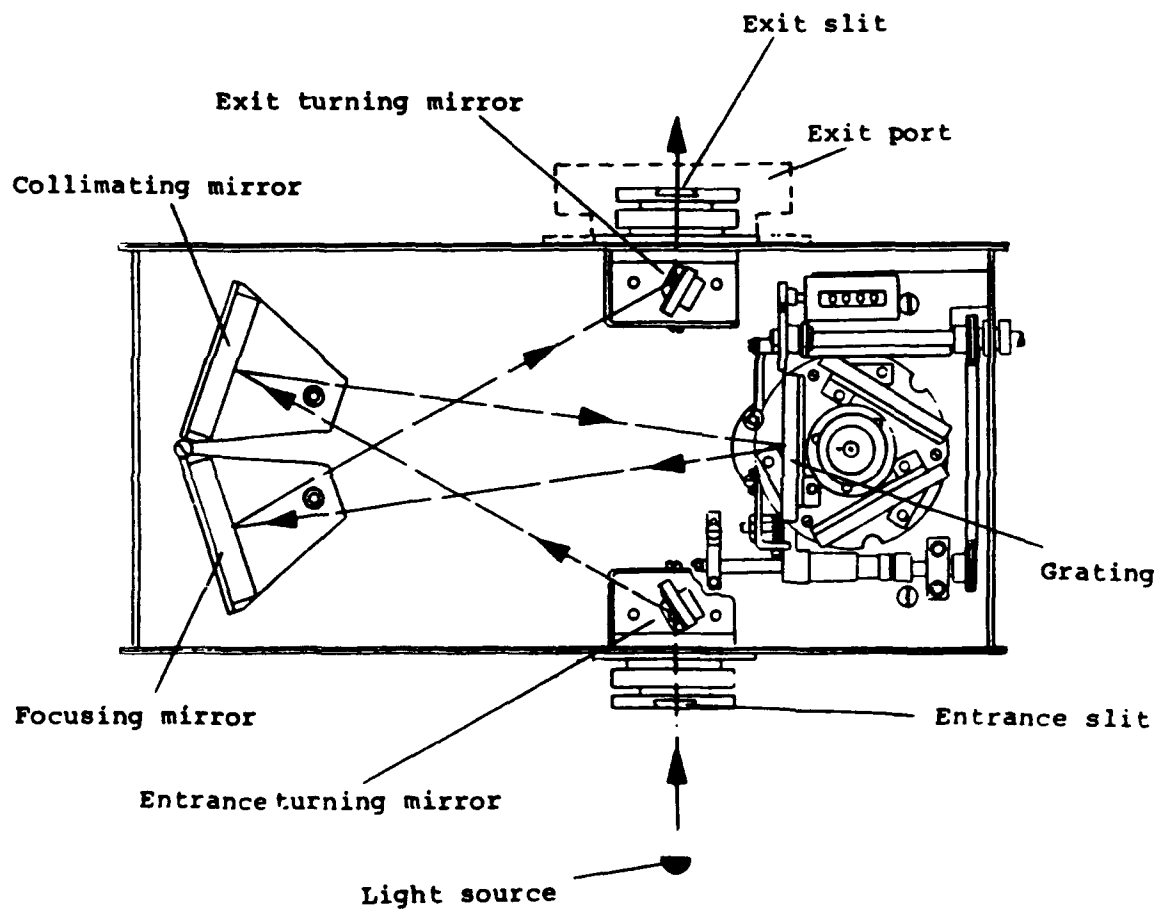


Figure 1 Spectrograph Optical Design [Ref. 15:p. 8]

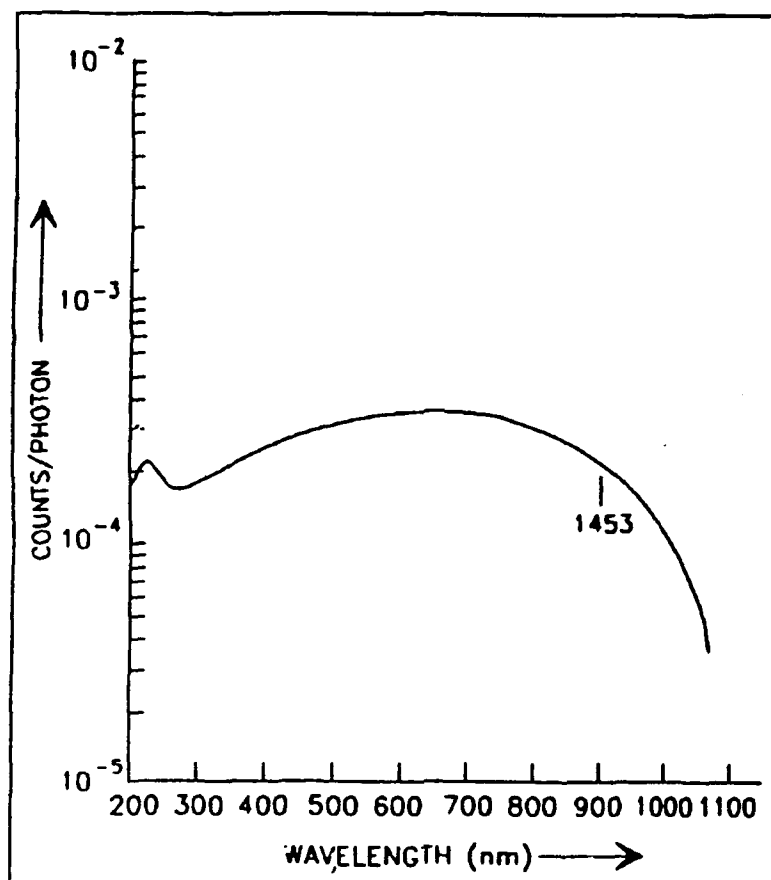


Figure 2 **Manufacturer Provided Typical Spectral Response of the**
Model 1453A Detector [Ref. 16:p. 4]

**Table I MANUFACTURER SPECIFICATIONS FOR THE MODEL 1453A
DETECTOR [Ref. 16]**

Detector Type	Silicon Photodiode Array
Photosensitive Material	Silicon behind fused silica face plate.
Wavelength Range	180-1100 nm
Quantum Efficiency ¹	70% @ 650 nm
Gain	0.00032 counts / photoelectron 3100 photoelectrons / count
Sensitivity @ 550 nm	4500 photons / count
Deviation from Linear Response	<1%
Uniformity of Sensitivity Across the Detector	± 5%
Geometric Distortion	<1 channel
Pixel Number	1024
Pixel Size	25 μm x 2.5 μm on 25 μm centers
Array Length	25 mm

**Table I MANUFACTURER SPECIFICATIONS FOR THE MODEL 1453A
DETECTOR (cont) [Ref. 16]**

Dark Current ² 800 ms @ 5° C Maximum Typical	2500 counts 913 counts
1 sec @ 5° C Typical	1123 counts
1 sec @ -20° C Typical	95 counts
Temperature Range	-30° C to 5° C
System noise ³	<1 count / $\sqrt{\text{scan}}$
Gas Requirements	Must be flushed with dry nitrogen before and during operation at 5 cubic feet per hour.
Power Requirements	Provided by Model 1462 installed in Model 1460.

1. Detector is located behind a fused silica plate in the detector housing. Under proper conditions, with the face plate removed, Quantum Efficiency percentages greater than 75% can be achieved.

2. Measured by subtracting 0.8 dark signal from 1.6 sec dark signal. Some arrays have a few pixels with dark currents that rise above the normally smooth baseline. As long as the dark pattern is stable and the highest point is below the specification, the array is allowed. Dark current decreases about a factor of 2 for every 7° C drop in temperature.

3. Measured by subtracting the results of two, 50 scan dark signal accumulations (5° C and 20 ms/scan), taking the square root, and then dividing by 10.

APPENDIX B

A. GENERAL

The following checklists are provided not only to accurately define the methods and procedures used in the experiments discussed in this thesis, but are also intended to provide a clear and succinct reference for future OMA III users at the Naval Postgraduate School. The checklists were developed from a combination of the procedures identified throughout the Model 1460 Optical Multichannel Analyzer Reticon Operating Manual [Ref. 18] contractor provided information, and from a user familiarity with the system. The procedures defined herein, are applicable to simple experiments using the OMA III 1460-XD Diode Array System Configuration used in this research.

For conciseness, the following abbreviations and symbols are used throughout the checklists and are similar to those used in Ref. 18:

- 'MENU' - Menus displayed on the touch-sensitive screen.
- "SOFTKEY" - Softkey displayed on the touch-sensitive screen.
- "HARDKEY" - Hardkey located on the front panel of the Model
1460 System Processor.
- [PROMPT] - System prompt displayed on the touch-sensitive
screen.
- <COMMAND> - Command entry using the external keyboard
followed by pressing the ENTER key on the
external keyboard.

B. START-UP CHECKLIST

The following START-UP checklist is, in part reproduced from the OMA III Operating Manual pages 7-1 thru 7-3.

1. Nitrogen Tank Stem Valve ADJUST full open
2. Nitrogen Valve Regulator ADJUST below first mark on left gauge
3. SCFH Air Flow A) ADJUST flow to 1.0 for 3 minutes then;
B) ADJUST to 0.1-0.2
4. OMA III POWER Switch ON
5. [Insert disk] Prompt A) INSERT OMA III System Operating Disk into Model 1460 disk drive;
B) LOWER Disk Drive Control Lever

Note: [Booting :

*****] message will be displayed followed by a

[Drives check OK!] message and then an [Interface is 1462] message.

After the system has booted up and the disk drive has been checked ok, the 'STARTUP' Screen is displayed. Steps 6 through 9 are performed to properly label data files that will be stored to the disk.

6. "DATE" Softkey SELECT
7. [Enter Date as 1 Jan 1988 :) Prompt INPUT current date using either the keypad displayed on the screen or the external keyboard, in the format DD MON YY. Date entry is followed by pressing either the "ENTER" Softkey or the Return key on the external keyboard.
8. "TIME" Softkey SELECT
9. [(HH:MM:SS)] Prompt INPUT current time using either the keypad displayed on the screen or the external keyboard, in the format HH:MM:SS. Time entry is followed by pressing either the "ENTER" Softkey or the Return key on the external keyboard.

10. 'SYSTEMS SETTINGS' Menu SELECT
11. Verify the following settings:
- | | |
|------------------------|----------|
| "SECTOR BUFFERS" | 12 |
| "PLOTTER" | HP7440 |
| "RAM CURVES" | 0 |
| "RS 232 PORT" | CPU |
| "GPIB ADDRESS" | 5 |
| "TEST ECHO" | OFF |
| "TERMINATOR" | <Cr> |
| "BAUD RATE" | 9600 |
| "DATA BITS" | 8 |
| "STOP BITS" | 1 |
| "PARITY" | DISABLED |
| "AUTO RUN" | DISABLED |
| "BEEP" | ON |
| "LINE FREQ" | 60 Hz |
12. Verify the following pairs of settings by pressing the "I/O FUNCTION" Softkey to view the next pair:
- | | |
|---------------------|--------------------|
| "I/O FUNCT'N" | REAR PANEL CONTROL |
| "PORT SELECT" | ETHER |
| "I/O FUNCT'N" | PRINTER |
| "PORT SELECT" | CPU SERIAL |
| "I/O FUNCT'N" | PLOTTER |
| "PORT SELECT" | GPIB |
| "I/O FUNCT'N" | I/O LINK |
| "PORT SELECT" | CPU SERIAL |
13. "DISK LABEL" Softkey SELECT
14. [DISK LABEL] Prompt INPUT desired disk label using either the keypad displayed on the screen or the external keyboard, followed by pressing either the "ENTER" Softkey or the Return key on the external keyboard.
15. "RETURN" SELECT
16. 'MAIN MENU' SELECT

C. FORMATTING, INITIALIZING, AND BACK-UP CHECKLIST

The FORMATTING, INITIALIZING, AND BACK-UP checklist starts from the 'MAIN MENU' selection. The OMA III uses a standard 5 1/4" double-sided, double density floppy computer disk. In order to prepare a new disk for the OMA III Operating System, it must first be formatted and initialized. The formatting process erases all previously stored information from the disk and restructures it by writing magnetic tracks of housekeeping information pertaining to sectors and timing functions. The initializing process creates the disk directory and allocates sectors for system and data files. The "FORMAT" softkey performs both of these functions. By copying the OMA III system operating software, as a backup, onto the new data disk, the Master disk need not be used and instead the single disk upon which experimental data will be recorded is the only disk that is required.

1. "DISK OPERATING SYSTEM" SELECT
2. Original System Disk REMOVE from Model 1460 Disk Drive.
3. New blank floppy disk A) INSERT into Model 1460 disk Drive; and
B) LOWER Disk Drive Control Lever.
4. "DISK OPS" Column "FORMAT" SELECT
5. [DRIVE?] Prompt SELECT "ENTER" Softkey or the RETURN key on the external keyboard. This will input the default drive, which for this configuration is the only disk drive.
6. [# DATA SECTORS] ENTER <383> followed by pressing either the "ENTER" Softkey or the Return key on the external keyboard.

Note: The default and maximum available number of data sectors is 385, however, 383 allows space to copy the PARCSYS>PRM program onto the disk and to assign and store a label to the disk.

7. [DRIVE 0, UPPER WILL BE ERASED!]

CONTINUE?] Prompt SELECT "YES" Softkey
 followed by pressing
 either the "ENTER"
 Softkey or the Return key
 on the external keyboard.

Note: Selection of "NO" will result in return to the Disk Operating System Menu.

A [BUSY] Prompt will flash at the top of the screen and a [FORMATTING ...] Prompt will be displayed during the formatting process. An [INITIALIZING] Prompt will be displayed during the initializing process since this function is also performed at this time. A [TESTING] Prompt will be displayed until self test is complete at which time the Disk Operating System Menu will be displayed.

8. "DISK OPS" Column "BACKUP" SELECT

9. [WARNING! WILL REQUIRE REBOOT
 CONTINUE?] PROMPT SELECT "YES" Softkey
 followed by pressing
 either the "ENTER"
 Softkey or the Return key
 on the external keyboard.

10. [INSERT MASTER IN UPPER DRIVE, PRESS CONTINUE] A) Remove newly formatted
 floppy disk from Model
 1460 disk drive;

 B) Insert Master Disk into
 Model 1460 disk drive; and

 C) LOWER Disk Drive
 Control Lever.

11. "CONTINUE" Softkey SELECT

Note: A [LOADING] Prompt will be displayed as the Model 1460 loads the information on the Master Disk into its memory.

12. [REMOVE DISK FROM UPPER DRIVE!] Prompt Remove master disk from
 disk drive.

13. [TO COPY: INSERT BLANK IN UPPER DRIVE
 TO STOP: TOUCH ANY SOFTKEY.] Prompt A) Insert newly formatted
 floppy disk into Model
 1460 disk drive; and

 C) LOWER Disk Drive
 Control Lever.

Note: A [COPYING] Prompt will be displayed as the Model 1460 copies the information from its memory onto the newly formatted floppy disk.

14. [REMOVE DISK FROM UPPER DRIVE] Prompt A) Remove newly copied
 disk from Model 1460 disk
 drive.

Note: The system will loop back to step 13 and continue to repeat as long as formatted floppy disk is reinserted into the disk drive and the Disk Drive Control Lever is lowered. To get out of the loop the last disk is copied and removed from the disk drive, touch any softkey and the system returns to step 5 of the START-

UP CHECKLIST.

D. BACKGROUND LEVEL AND CALIBRATION CHECKLIST

Proper calibration of the OMA III allows wavelength and intensity of acquired spectral data to be read directly from the display screen instead of pixel number and detected counts as displayed for uncalibrated curves. The procedures delineated herein were derived from those presented in Ref 18, Chapter 14. A standard test lamp with known spectral emittance is required to perform the system calibration. For this experiment, a low pressure Mercury test lamp was used. Use of a Mercury-Argon test lamp, as discussed in Ref 18, would provide calibration of the visible and near infrared regions as well as the ultraviolet region obtained by the Mercury lamp alone, but was not available for this experiment. The CALIBRATION checklist starts from the 'MAIN MENU'.

1. 'DATA ACQUISITION' Menu SELECT

Note: Wavelength calibration may be performed either from newly acquired "LIVE" data or from a previously stored data file.

IF CALIBRATION DATA HAVE BEEN PREVIOUSLY STORED TO DISK:

2. "SET DISPLAY" Softkey SELECT
3. "FETCH CURVE " Softkey SELECT
4. [] Prompt INPUT stored calibration data file number in format XXXXXXXX followed by pressing either the "ENTER" Softkey or the Return key on the external keyboard.

5. GOTO STEP OF 10 THIS CHECKLIST.

IF CALIBRATION DATA ARE TO BE NEWLY ACQUIRED:

2. "ACQUIRE DATA" Softkey ENSURE the "ACQUIRE DATA" Softkey is highlighted.
3. "LIVE" ENSURE the "LIVE" softkey is displayed at the left center of the screen. If

"LIVE-B", "ACCUM",
or "ACCUM-B" is
displayed, repeatedly press
that Softkey until "LIVE"
is displayed.

4. "START" Softkey SELECT

NOTE: A combination of background or ambient light detected by the system and "dark current" or internal noise will be displayed on the screen. This should appear as a fuzzy horizontal line at approximately 100 - 200 counts.

SAFETY: BEFORE OPERATING AN ULTRAVIOLET LIGHT SOURCE, SUCH AS A MERCURY TEST LAMP, PROPER EYE PROTECTION MUST BE WORN TO PREVENT RADIATION DAMAGE TO THE EYES.

5. MERCURY TEST LAMP A) POSITION directly in front of the spectrograph entrance slit and ;
B) TURN ON.

NOTE: The Mercury test lamp consists of a metal cover placed over an outer glass tube which contains two inner tubes filled with Mercury vapor. Ensure that the slit in the metal cover is aligned with the two inner tubes such that when viewed through the cover slit one tube is directly behind the other.

As the test lamp heats up, the intensities of the various spectral lines will gradually increase and finally stabilize. As the intensity of the mercury test lamp output increases, it will become necessary to press the "AUTOSCALE" Hardkey on the front of the Model 1460 to automatically adjust the range of the vertical axis of the display. Although the detected output intensities will always fluctuate to some extent after approximately 2 minutes the source is sufficiently equilibrated that it may be used for calibration purposes. Long before this point, however, the distinct spectral lines of the Mercury source may be easily identified. Steps 8-10 may be performed while waiting for the source spectral intensities to equilibrate.

If the Mercury test lamp is too close to the detector slit, the detector may become saturated, as evidenced by flattening of the spectral peaks at the top of the display curve and by a displayed magnitude reading of those peaks of 16383 counts. If this occurs, move the source back from the detector slit until the all spectral peaks are less than 16383 counts.

6. DISPLAY CURSOR position ADJUST to the wavelength position, as shown on the display screen X-axis and the pixel number at the top of the screen, of an identifiable Mercury spectral line (eg 365.015 nm). Adjustment of the DISPLAY CURSOR position is accomplished using the left-most left and right arrow hardkeys on the front panel of the Model 1460.

Note: Simultaneous depression of the left or right arrow hardkey and the "FAST" Hardkey will increase the

speed with which the cursor moves across the screen.

7. SPECTROGRAPH WAVELENGTH COUNTER CRANK ADJUST until the peak of the chosen identifiable Mercury spectral line is positioned under the display cursor position.

NOTE: The grating turret knob and the wavelength counter crank must not be adjusted following the calibration process, or the system will require recalibration for the new settings.

8. WAVELENGTH COUNTER RECORD counter reading.
9. "STOP" Softkey SELECT
10. "RETURN" Softkey SELECT to return to the 'Main Menu'.
11. 'CALIBRATION' Menu SELECT
12. "IN WAVELENGTH / WAVENUMBERS" Softkey ENSURE
"IN WAVELENGTH" is displayed. If
"IN WAVENUMBER" is displayed, press that Softkey to change the label to display
"IN WAVELENGTH".
13. "LINEAR / CUBIC FIT" Softkey ENSURE "LINEAR FIT" is displayed. If
"CUBIC FIT" is displayed, press that Softkey to change the label to display
"LINEAR FIT".
14. "WvLNGTH CALIBR." Softkey SELECT. "WvLNGTH CALIBR." Softkey should now be highlighted.
15. [POSITION CURSOR, THEN ENTER WAVELENGTH] A) POSITION CURSOR, using the front panel left and right arrow hardkeys, to the peak of a displayed spectral line whose wavelength is known;

B) SELECT " λ =" Softkey;

C) INPUT appropriate wavelength (in nanometers) for selected spectral line using the external keyboard or displayed keyboard, followed by pressing either the "ENTER" Softkey or the Return key on the external keyboard.

DATA" Softkey should no longer be highlighted and the **"STORE DATA"** Softkey will become highlighted.

26. **"DISK STORE"** Softkey **SELECT**
27. **[STORE LIVE UNCORRECTED DATA
IN DESTINATION]** Prompt **INPUT <XXXXXXX>**
(desired file number) up to 7
digits maximum using
either the keypad displayed
on the screen or the external
keyboard.
28. **[;DRIVE]** Prompt **SELECT** either the
"ENTER" Softkey or press
the **RETURN** Hardkey on the
external keyboard.

NOTE: Steps 18 through 28 store the calibration data in the data file **FXXXXXXX.DAT**. Once calibrated, using the above procedure, the stored calibration data may be used to calibrate the screen for future experimental data or for curve data already stored to disk.

NOTE: Steps 29 through 40 acquire and store a combination of background light and "dark current" onto disk so that they may be compensated for when data are acquired. Consequently, it is vital that the ambient lighting conditions during the acquisition of Background data remain constant throughout the experiment, or the following procedure will have to be repeated for each different set of conditions that exist during the acquisition of spectral data.

29. **"ACQUIRE DATA"** Softkey **SELECT**
30. **"LIVE"** **ENSURE** the **"LIVE"**
softkey is displayed at the
left center of the screen. If
"LIVE-B", **"ACCUM"**,
or **"ACCUM-B"** is
displayed, repeatedly press
that Softkey until **"LIVE"**
is displayed.
31. **"START"** Softkey **SELECT**

NOTE: A combination of background or ambient light detected by the system and "dark current" or internal noise will be displayed on the screen. This should appear as a fuzzy horizontal line at approximately 200 counts.

32. **"STOP"** Softkey **SELECT**
33. **"STORE DATA"** Softkey **SELECT** to activate the Data
Storage Display.
34. **"BKGND SET"** Softkey **SELECT**
35. **[DATA SOURCE: LIVE, OR FILE]** Prompt **SELECT "LIVE"** Softkey
36. **"COMP MODE 0"** Softkey **ENSURE** the
"COMP MODE 0"

softkey is displayed at the
left center of the screen.

37. "LABEL" Softkey SELECT
38. [CURVE LABEL:] Prompt INPUT desired labeling
information, using either
the keyboard displayed on
the screen or the external
keyboard.
39. "DISK STORE" Softkey SELECT
40. [STORE LIVE UNCORRECTED DATA
IN DESTINATION FILE NUMBER?] Prompt INPUT <YYYYYYY>
(desired file number) up to 7
digits maximum using the
external keyboard and press
the "ENTER" Softkey.
41. [DRIVE?] Prompt PRESS "ENTER" Softkey

NOTE: Steps 36 through 41 store the background data in the data file FYYYYYYY.DAT. Once stored, using the above procedure, the background data may be used to compensate future experimental data for both background lighting and "dark current" effects.

42. "RETURN" Softkey SELECT

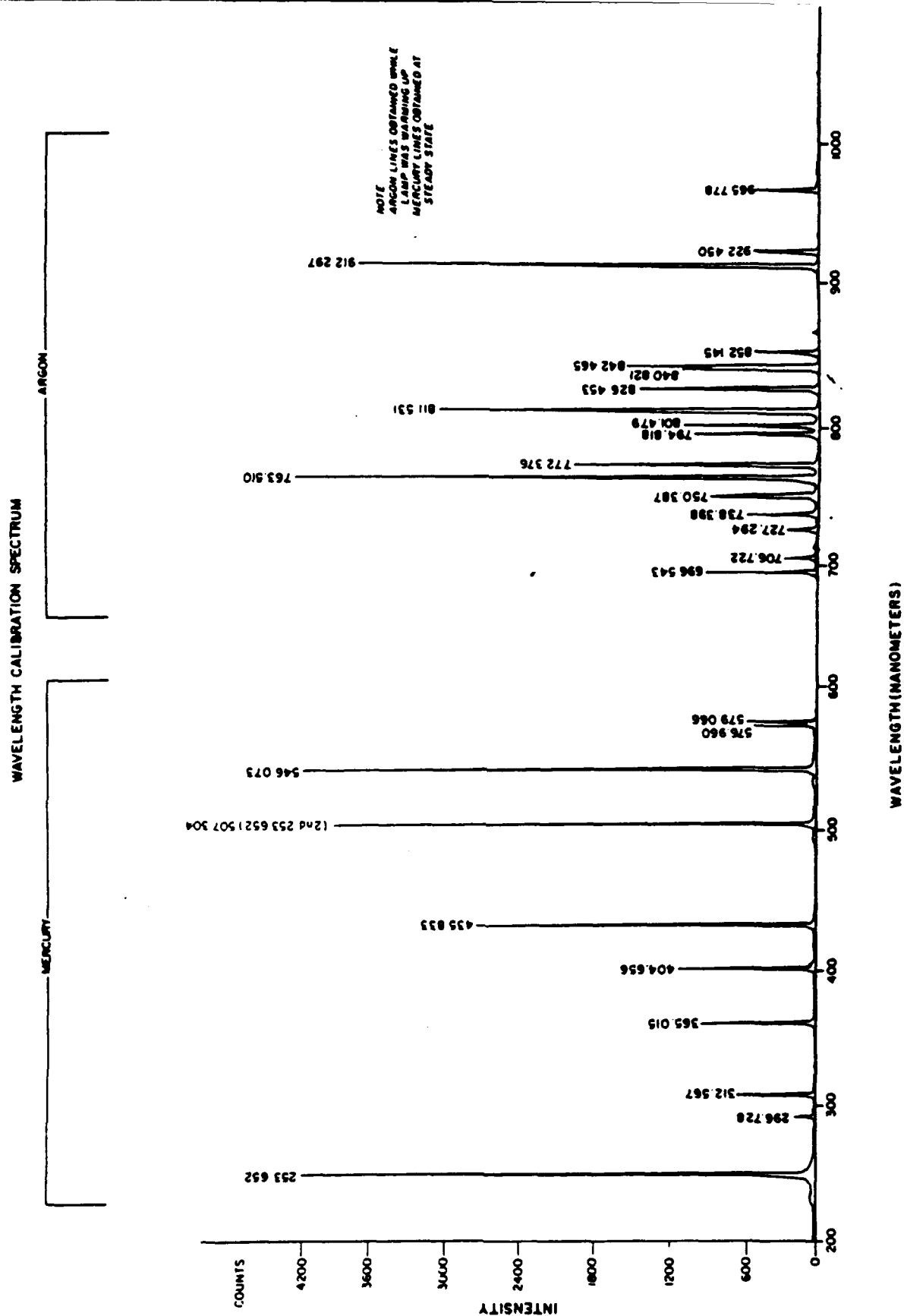


Figure 1 Mercury Calibration Lamp Spectral Data [Ref. 18]

E. DATA ACQUISITION CHECKLIST

The DATA ACQUISITION checklist starts from the 'MAIN MENU' selection. The checklist includes a method of compensating stored data for the effects of background laboratory ambient lighting conditions so that only the desired data without background effects saved.

1. 'DATA ACQUISITION' Menu SELECT
2. "ACQUIRE DATA" Softkey SELECT (When selected, the "ACQUIRE DATA" Softkey will remain highlighted).
3. "LIVE-B" ENSURE the "LIVE-B" softkey is displayed at the left center of the screen. If "LIVE", "ACCUM", or "ACCUM-B" is displayed, repeatedly press that Softkey until "LIVE-B" is displayed.

NOTE: Selection of the "LIVE-B" data acquisition / display mode allows background corrected data to be displayed on the screen. Consequently, with the only light entering the spectrograph being the ambient lighting conditions present at the time of acquisition and storage of the background data, and with the above procedures in effect, the display should show only a low amplitude, near-level line representing fluctuations in the ambient lighting conditions, and more importantly, the internal noise and fluctuations within the system.

4. "START" Softkey SELECT

SAFETY: BEFORE OPERATING AN ULTRAVIOLET LIGHT SOURCE, PROPER EYE PROTECTION MUST BE WORN TO PREVENT RADIATION DAMAGE TO THE EYES. CARE MUST ALSO BE TAKEN TO PREVENT LONG TERM EXPOSURE OF SKIN TO ULTRAVIOLET RADIATION BY WEARING LONG SLEEVED SHIRTS AND / OR SUNSCREEN.

5. EXPERIMENT SET-UP
 - A) Adjust as desired for data acquisition;
 - B) Light source TURN ON.

NOTE: As the light source heats up, the intensities of the various spectral lines will gradually increase and finally stabilize. Although the detected output intensities will always fluctuate to some extent after

approximately 2-20 minutes (source dependant) the source is sufficiently equilibrated that it may be used for data acquisition purposes.

- 6. "STOP" Softkey SELECT
- 7. "STORE DATA" Softkey SELECT to activate the Data Storage Display.
- 8. "DISK STORE" Softkey SELECT

NOTE: Selection of the "COMP MODE 0" data storage mode provides for storage of raw uncorrected data. Thus, if the ambient or internal conditions change during the course of the experiment, the existing background data may be stored and corrected for later using the data reduction software resident on the system disk. To use other than Comp Mode 0, background reference data must have previously been stored to the same disk to which the current data will be stored.

- 9. "COMP MODE 0" Softkey SELECT
- 10. [COMP MODE B; NEW MODE?] Prompt INPUT number of desired Comp Mode using either the keyboard displayed on the screen or the external keyboard followed by pressing either the "ENTER" Softkey or the RETURN key on the external keyboard.
- 11. [REFERENCE FILE VVVV;
NEW REFERENCE FILE? Prompt INPUT the file number of the desired background reference data file using either the keyboard displayed on the screen or the external keyboard followed by pressing either the "ENTER" Softkey or the RETURN key on the external keyboard.
- 12. "DISK STORE" Softkey SELECT
- 13. [STORE LIVE-B DATA
IN DESTINATION FILE NUMBER?] Prompt INPUT desired file number , consisting of a maximum of 7 alphanumeric characters (eg. <ZZZZZZZ>) using the external keyboard, and press the "ENTER" Softkey. The actual data file will be named FZZZZZZ.DAT.
- 14. [DRIVE?] Prompt PRESS "ENTER" Softkey

NOTE: Steps 1 through 14 store the data file FZZZZZZ.DAT. If a data compensation mode other than Comp Mode 0 is desired for data storage, the current data may be stored using that mode under a different file number.

Source: F22205.DAT. Mem 1

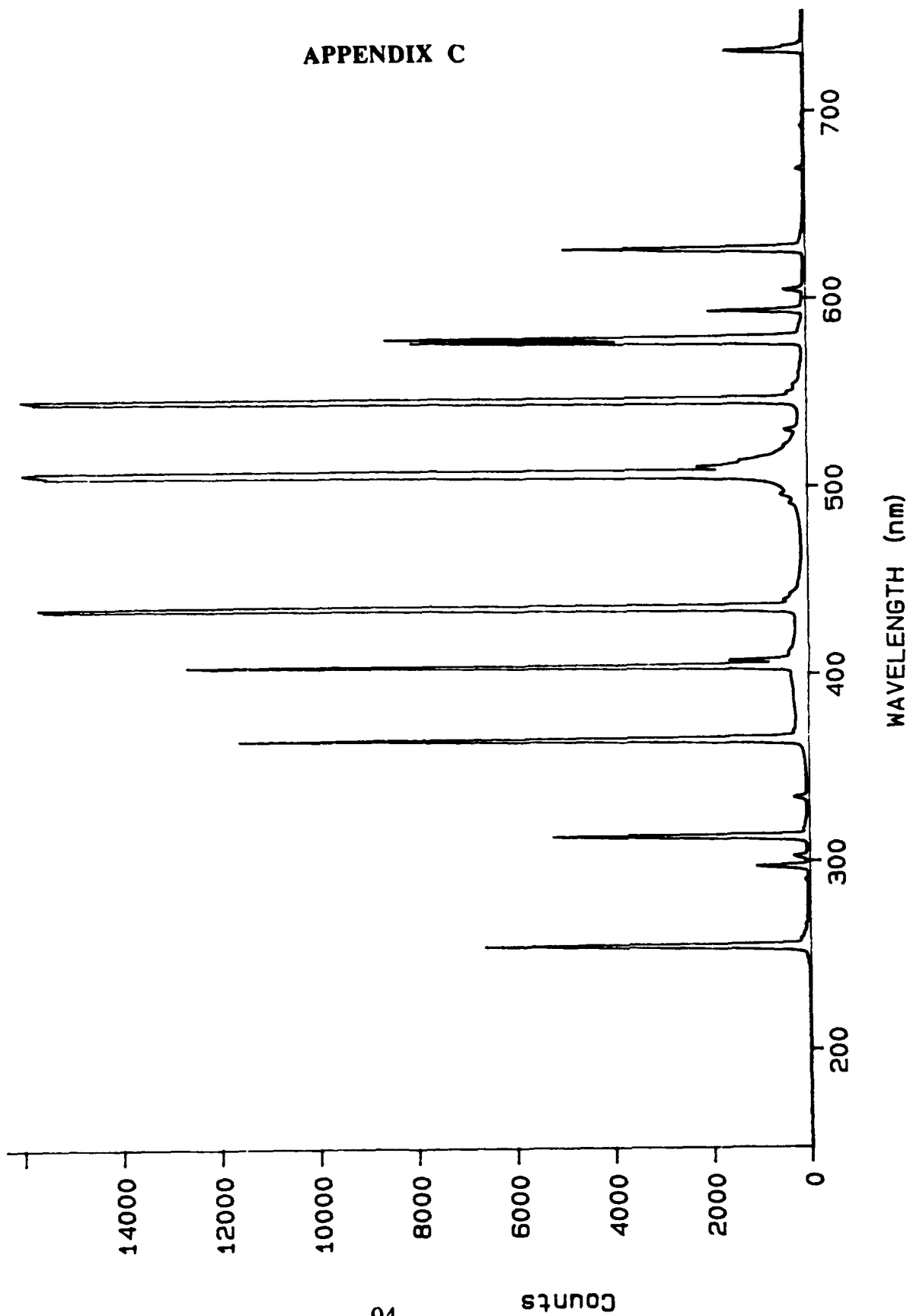


Figure 1
Mercury Calibration Lamp Radiated Spectrum

Source: F22234.DAT, Mem 1

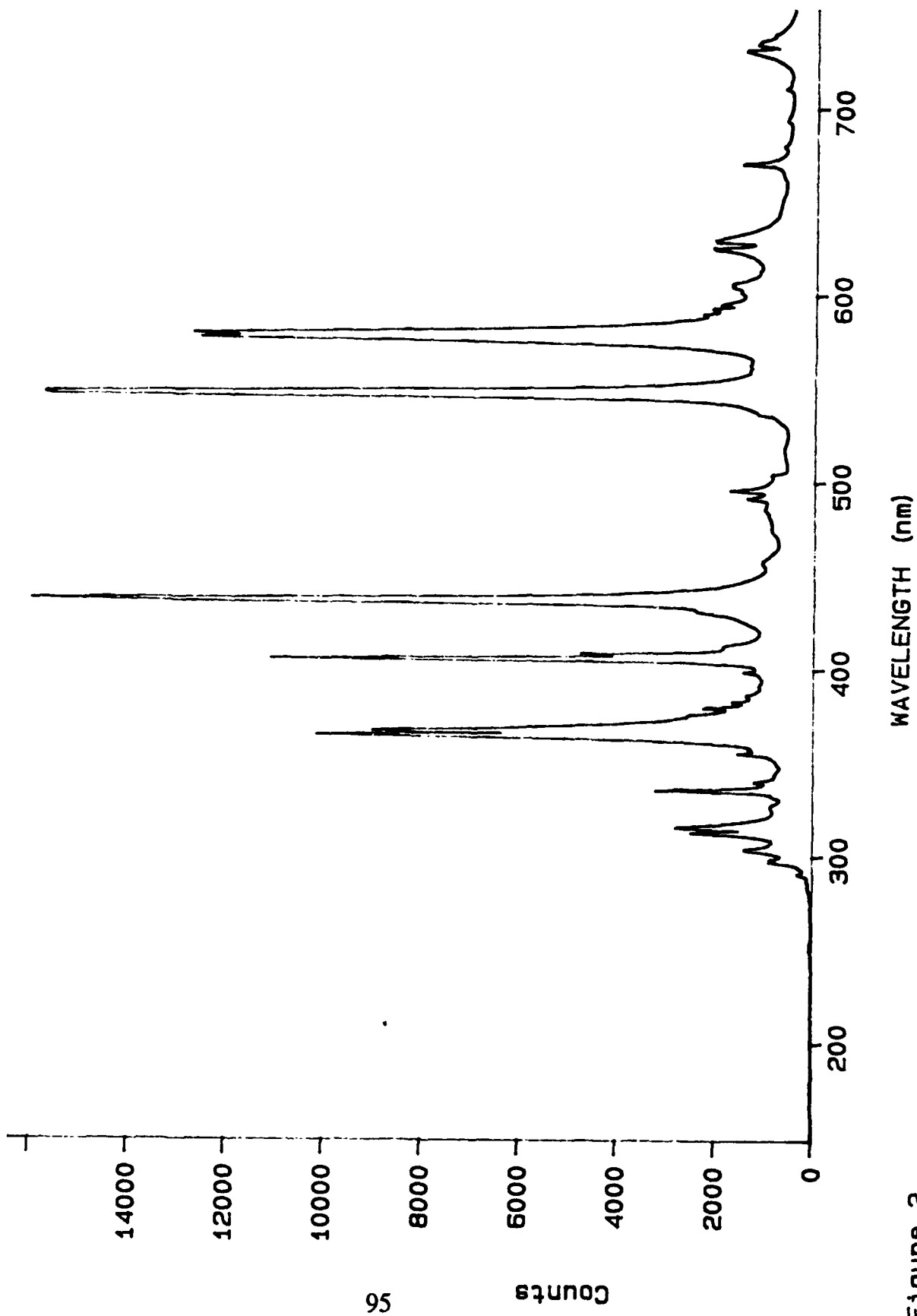


Figure 2
200 Watt Mercury Arc Lamp Radiated Spectrum

Source: F22215.DAT, Mem 1

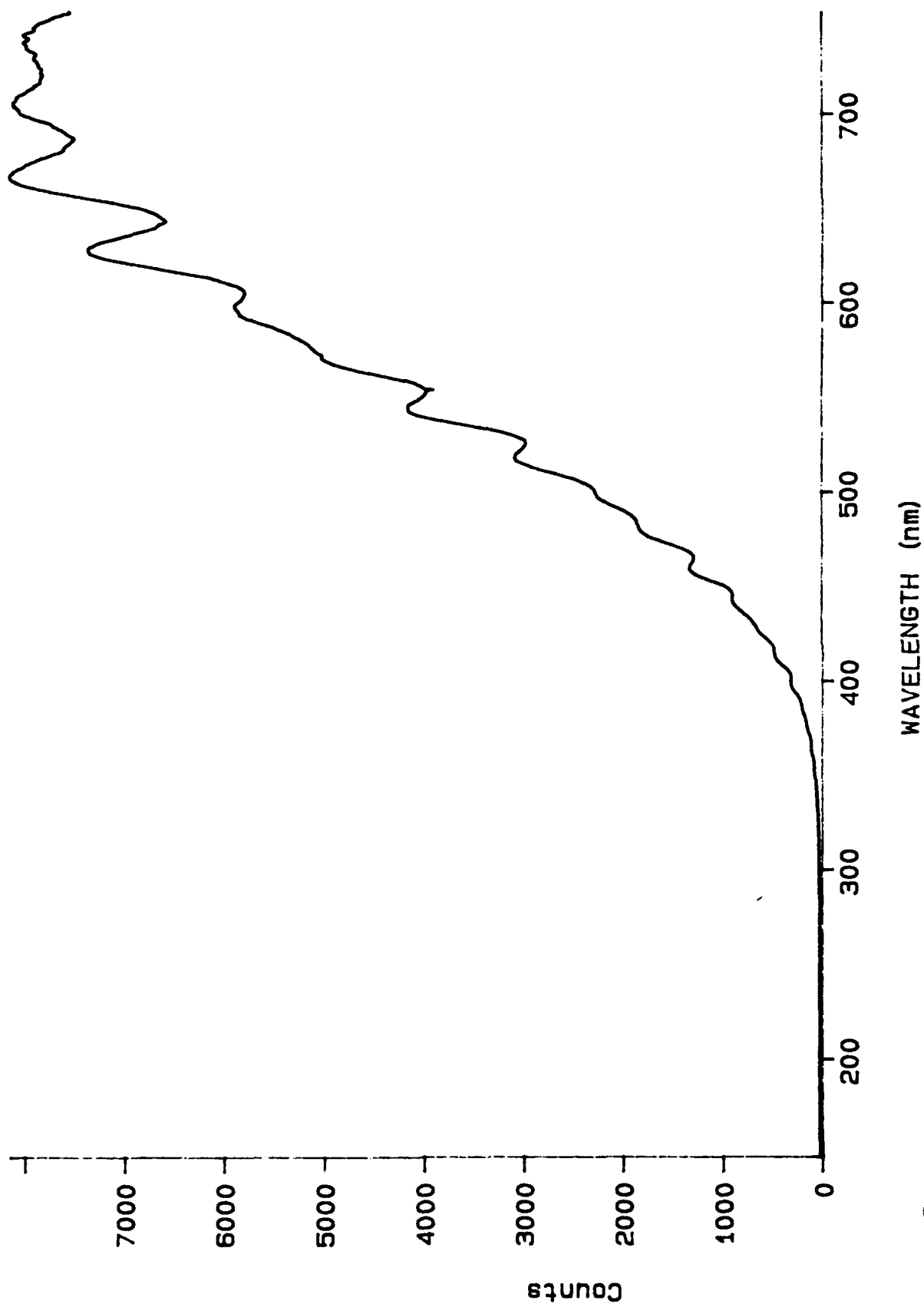


Figure 3
100 Watt Sylvania Extended Service Light Bulb Radiated Spectrum

Source: F22612.DAT, Mem 1

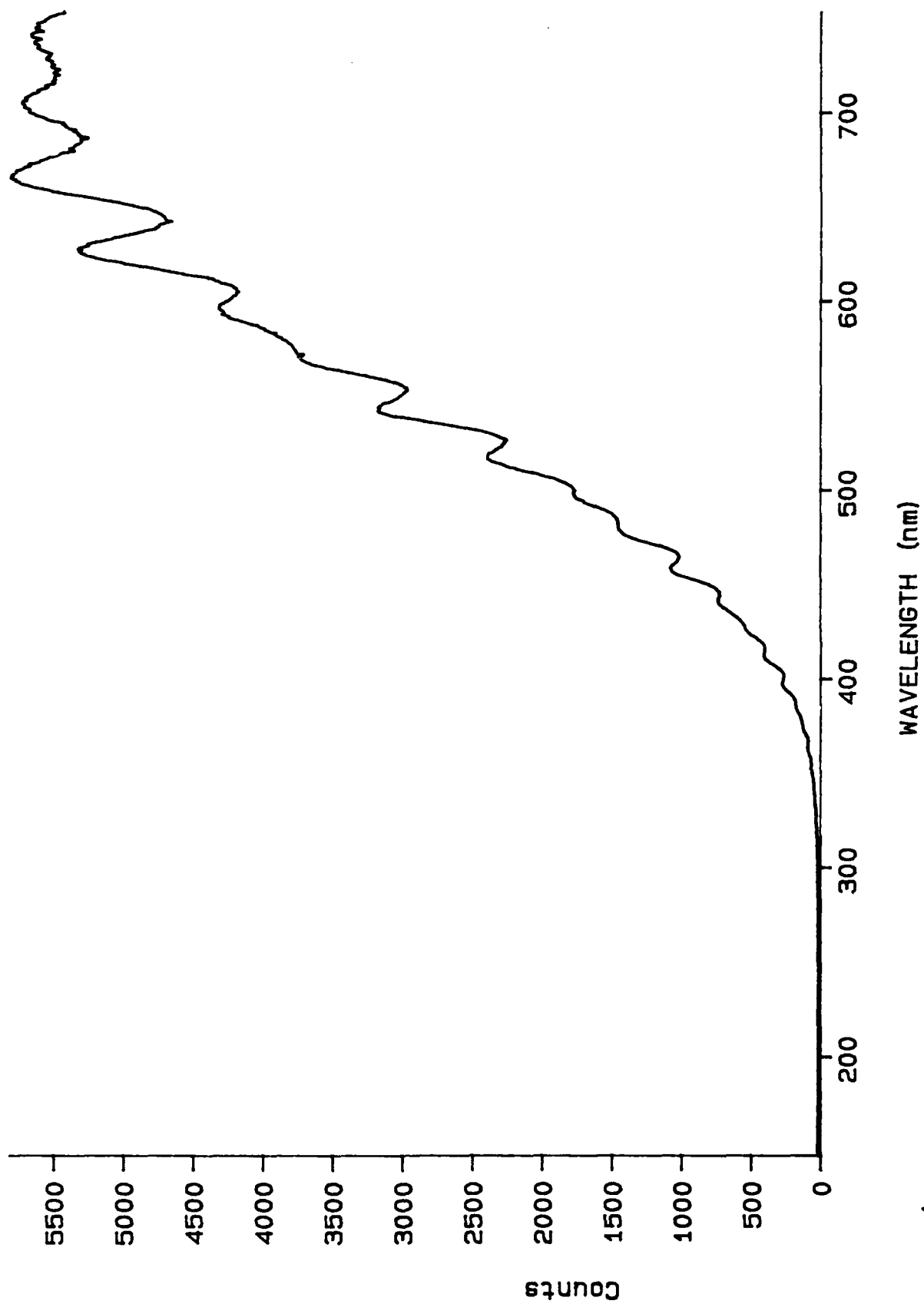


Figure 4
500 Watt Halogen / Quartz Bulb Radiated Spectrum

Source: F30601.DAT, Mem 1

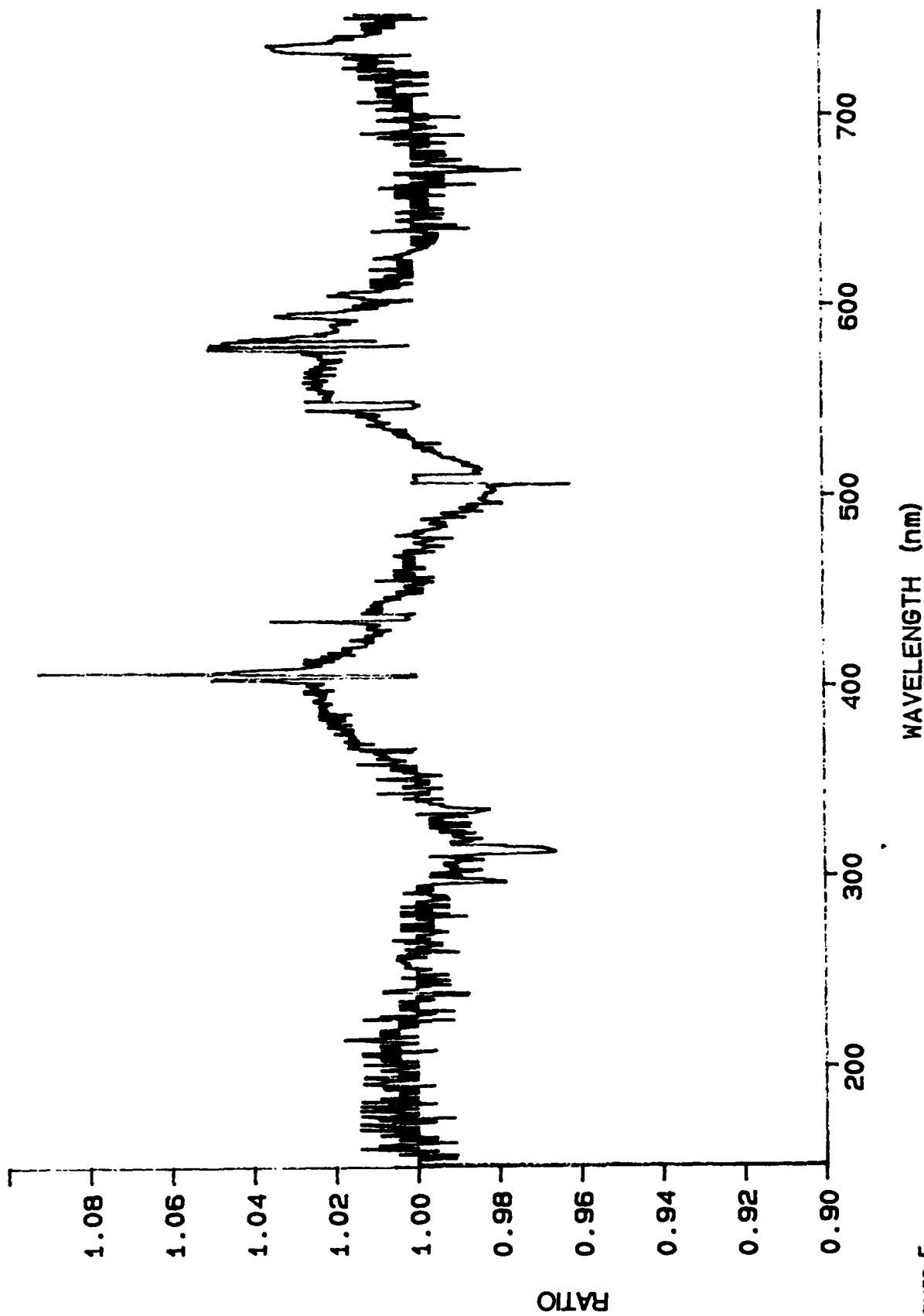


Figure 5
Ratio of Mercury Calibration Lamp Intensities Taken 16 sec Apart

Source: F22291.DAT, Mem 1

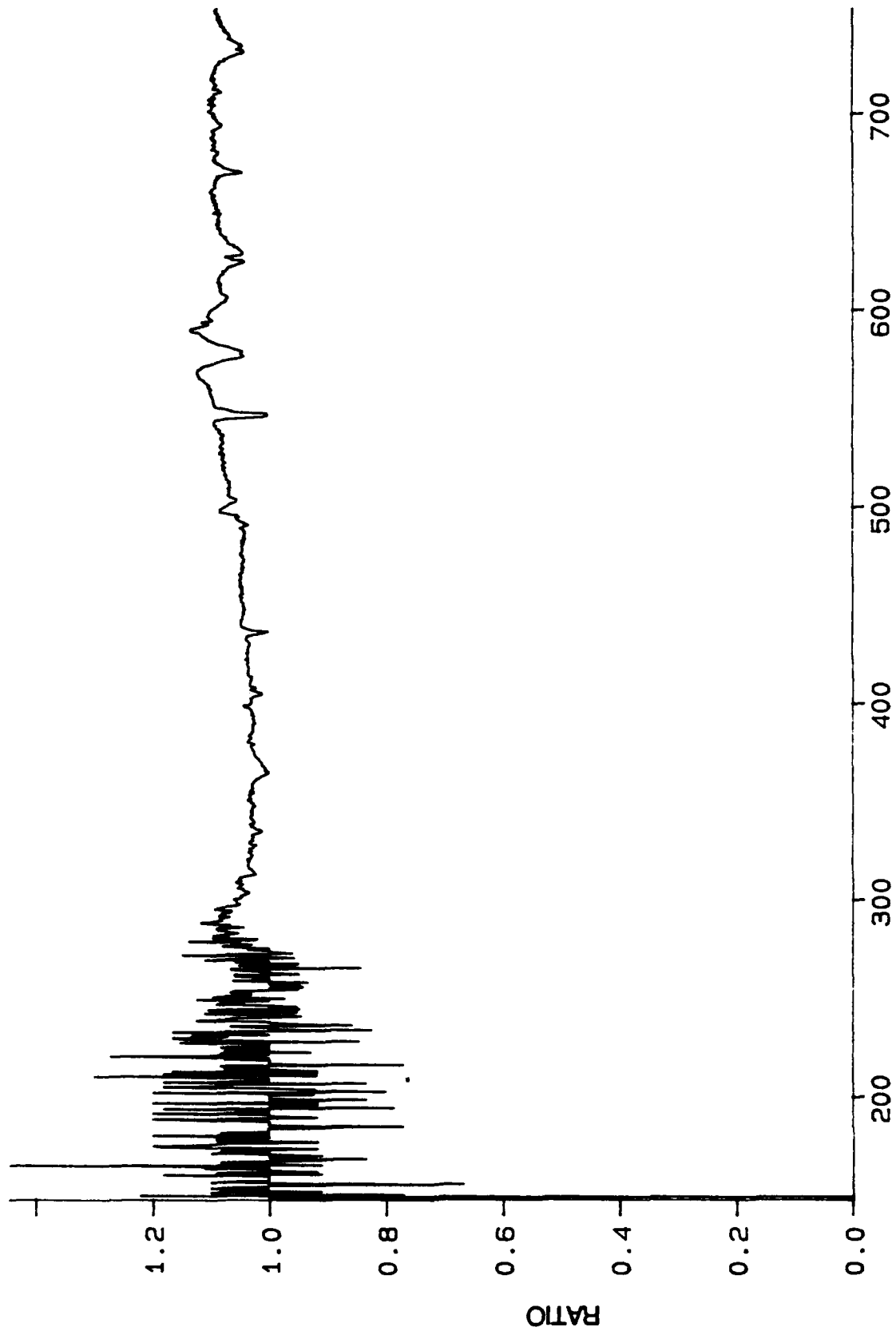


Figure 6
Ratio of Mercury Arc Lamp Intensities Taken 100 μ c Apart

Source: F224373.DAT, Mem 1

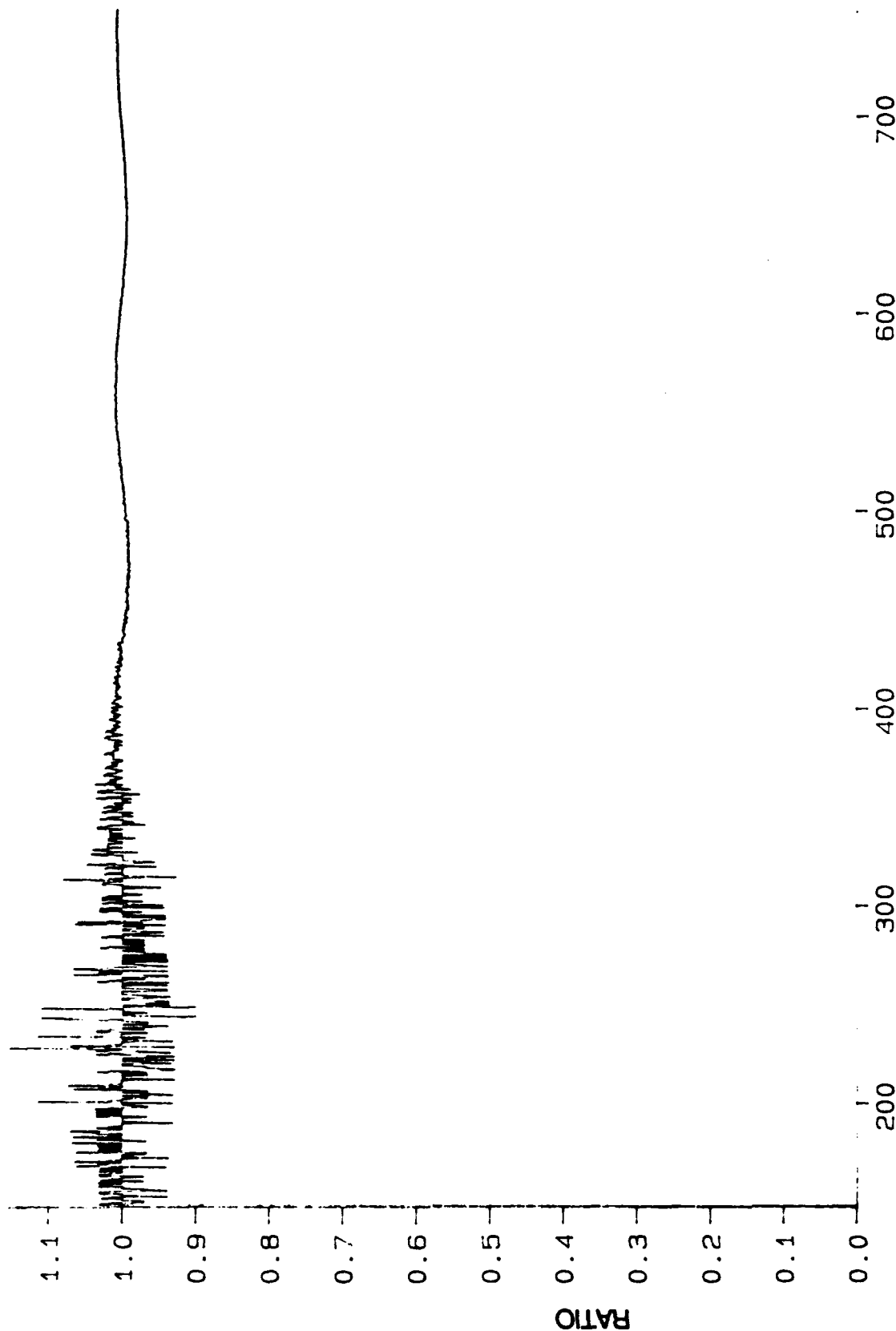


Figure 7

Ratio of 100 W Sylvania Bulb intensities to Talon 22 Sec Aperture

Source: F22290.DAT, Mem 1

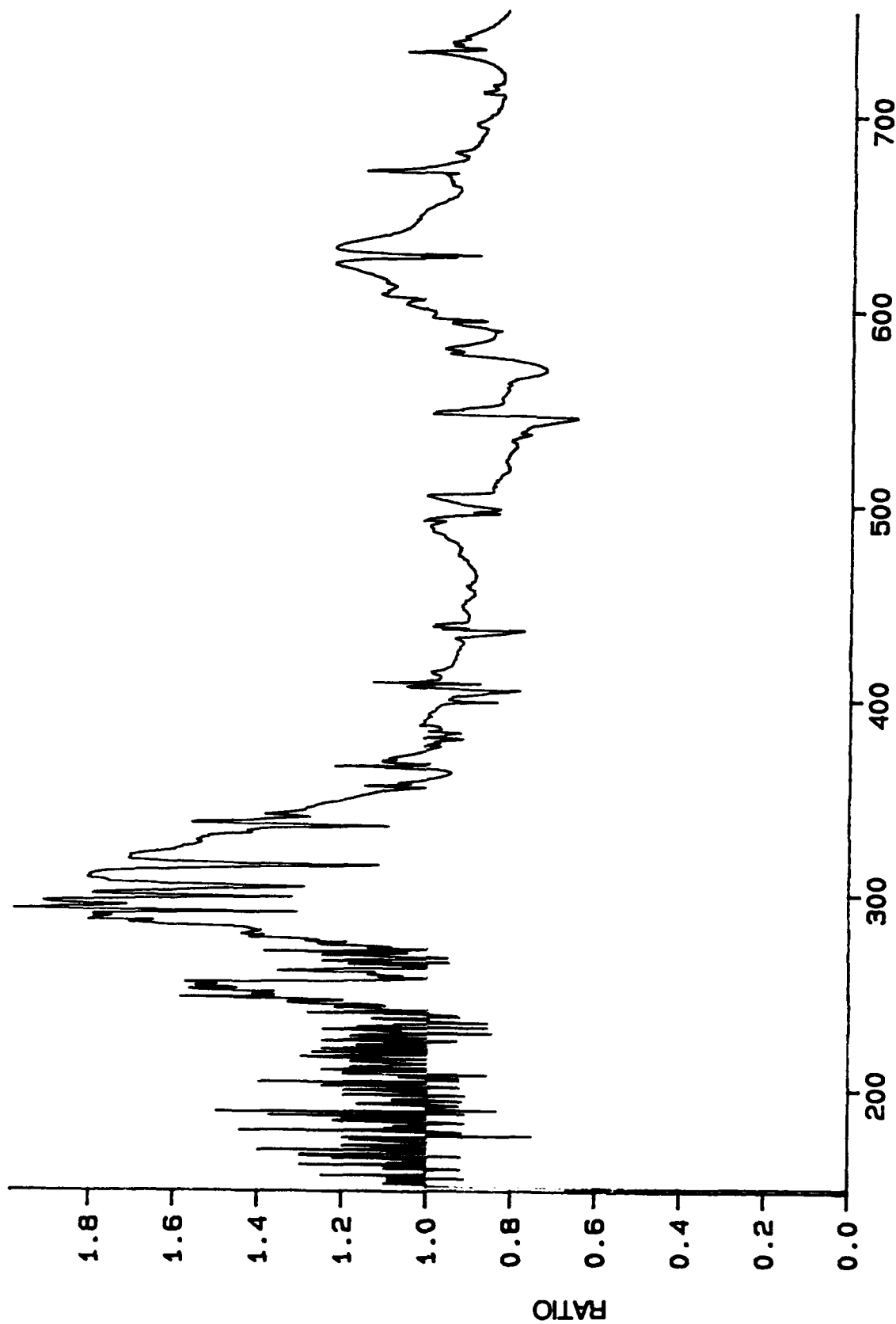


Figure 8

Ratio of Mercury Arc Lamp Intensities Tak. Hr 35 Min Ap. 1

Source: F22650.DAT, Mem 1

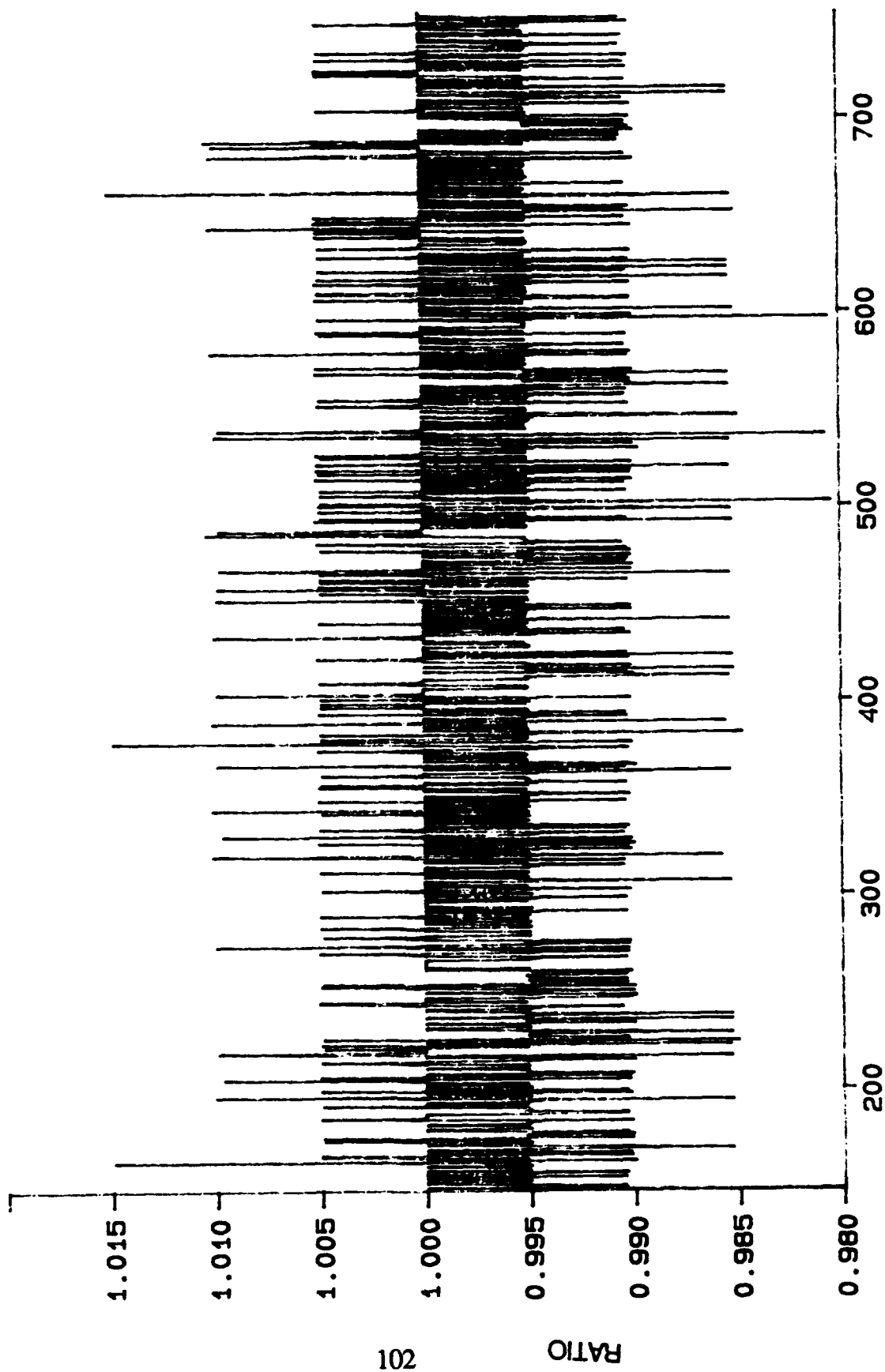


Figure 9

Ratio of Dark Background Data (30 msec Exposure Time, 2 Min 00 Sec Apart)

Source: F2.DAT, Mem 1

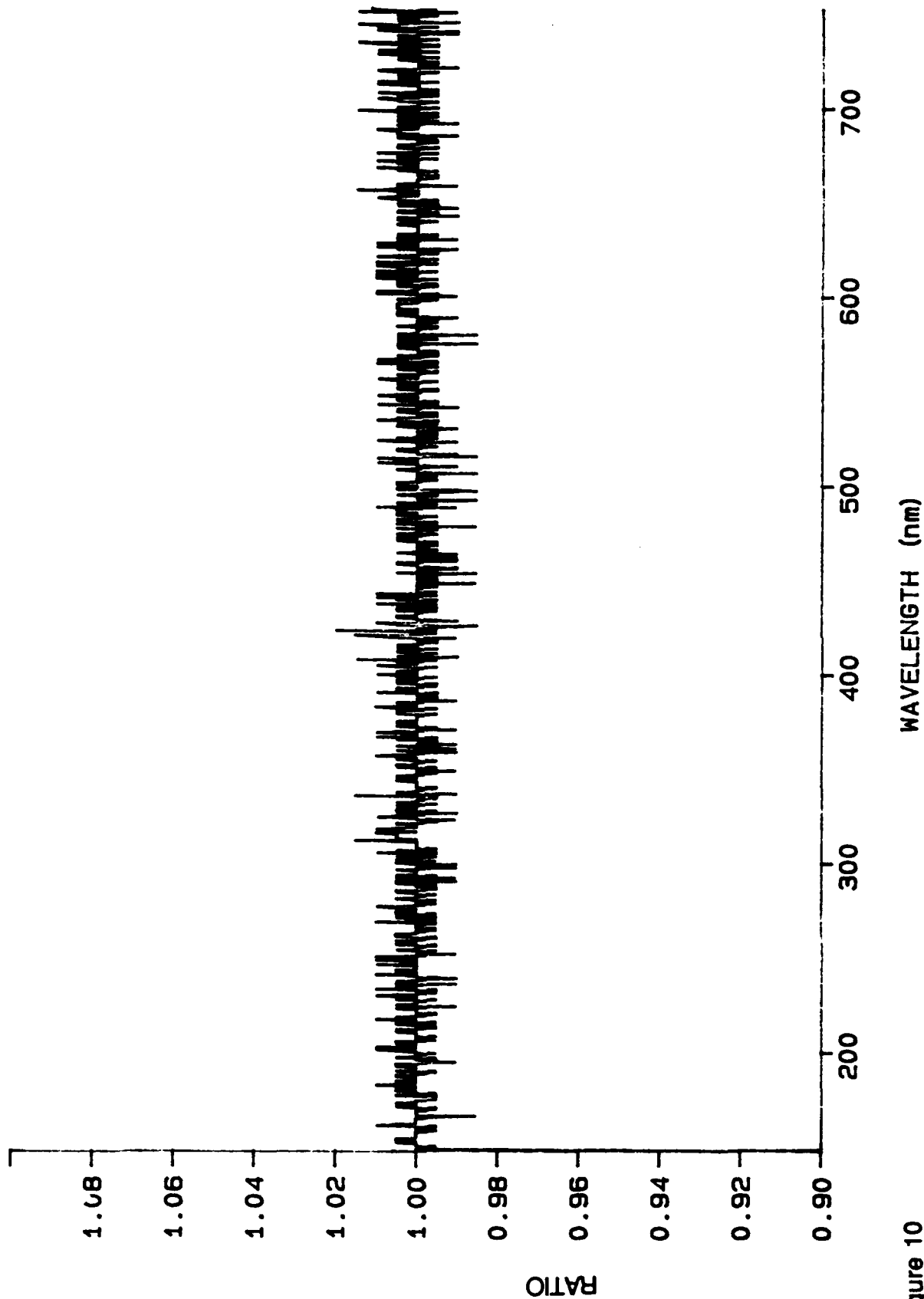


Figure 10

Ratio of Background Data Taken 17 Minutes , Second Apart

Source: F22401.DAT, Mem 1

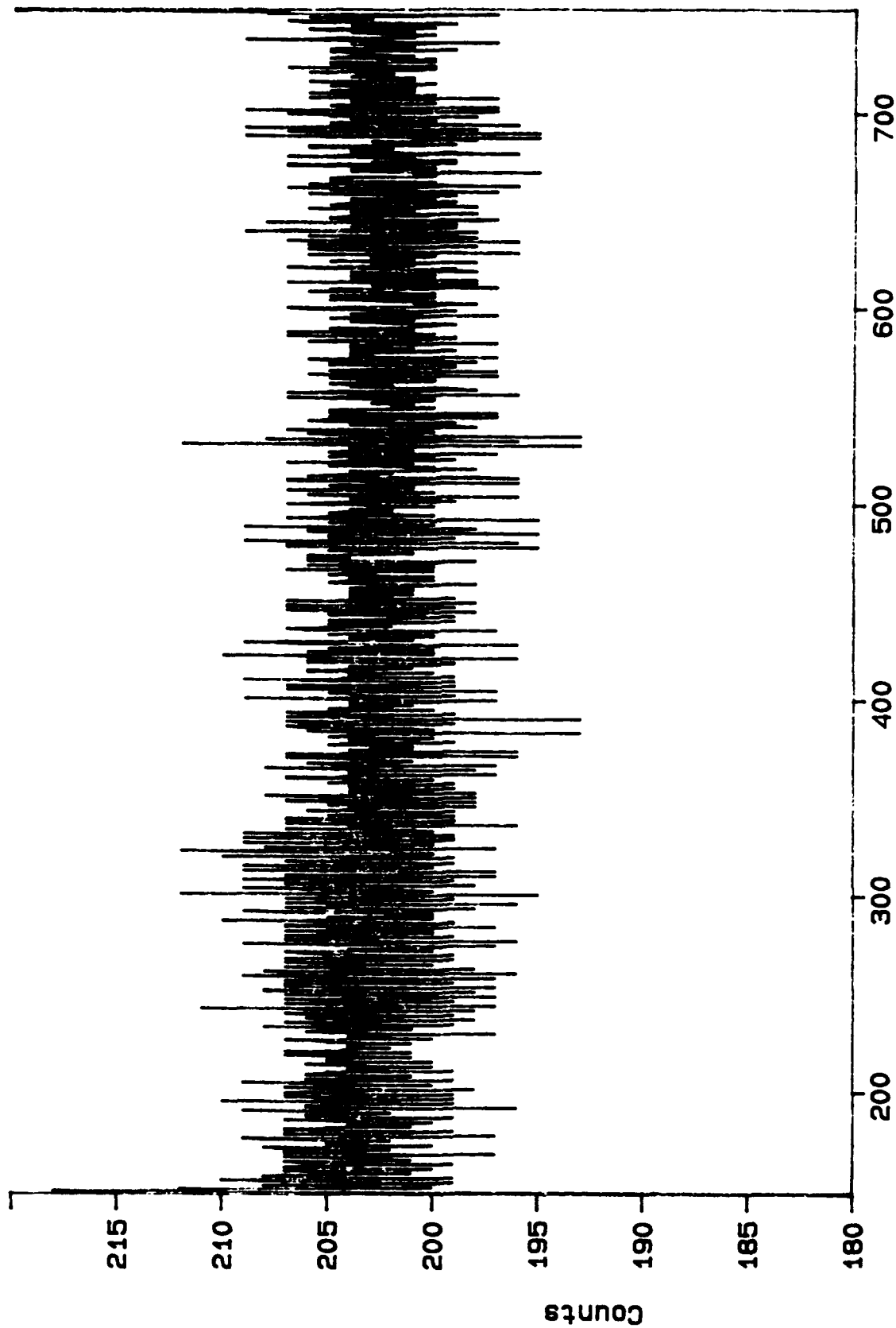


Figure 11
Background Data for Filter Transmittance Experiments

Source: F22408.DAT, Mem 1

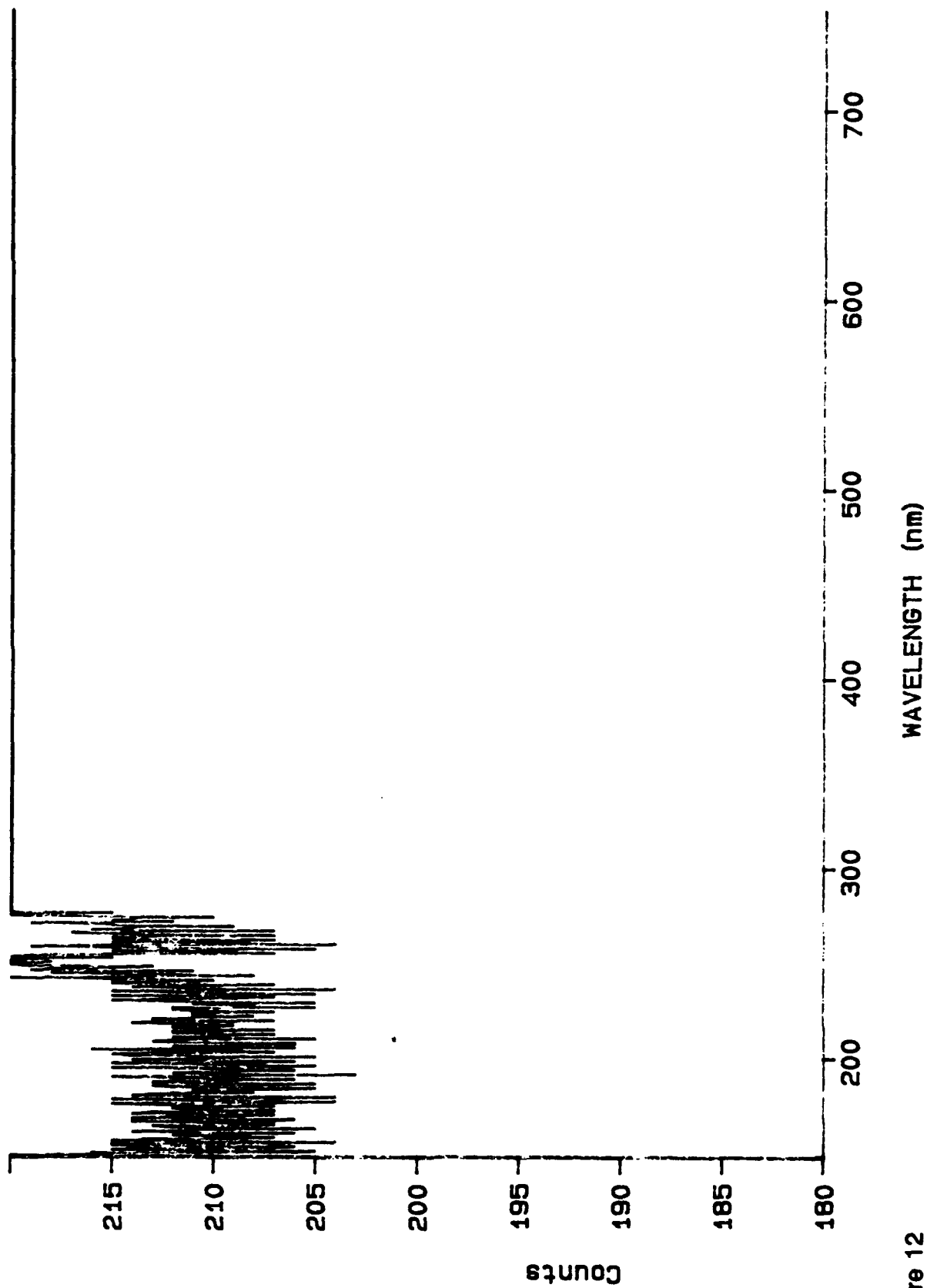


Figure 12

Uncompensated 200 W Hg Arc Lamp Source

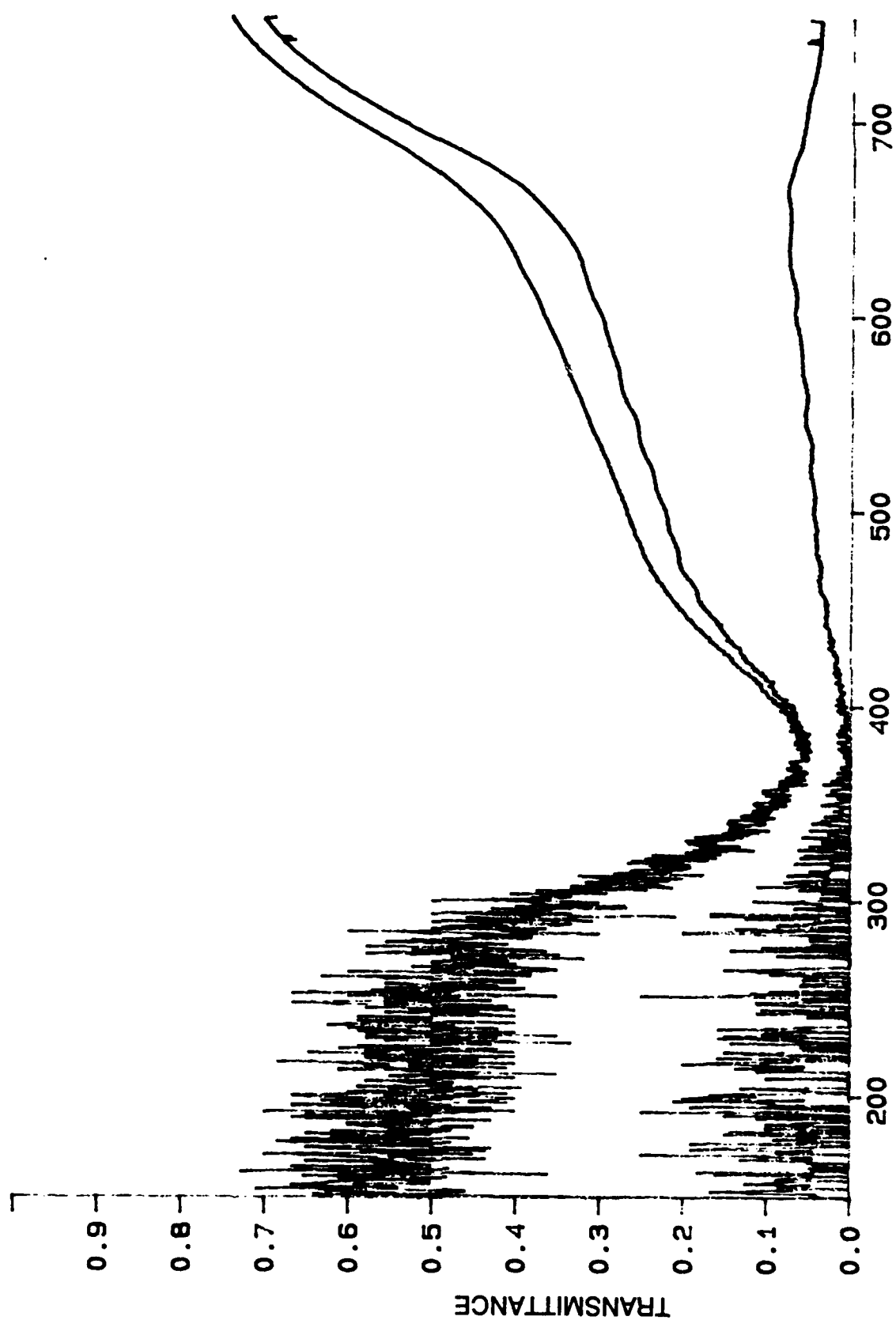


Figure 13

Polarizing Filter with Halogen Lamp (Vertical, Horizontal, Reference).

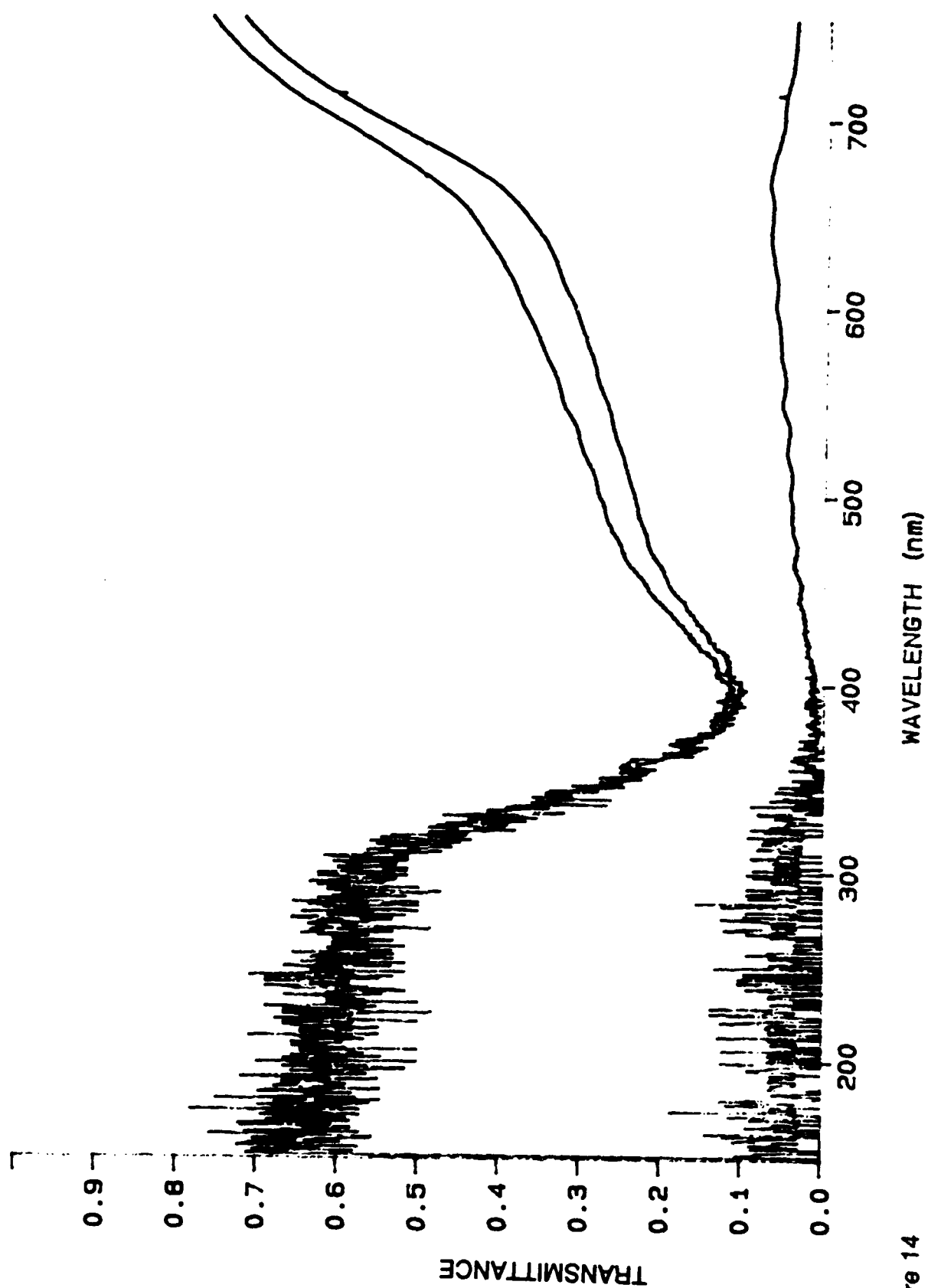


Figure 14
Polarizing Filter with Sylvania Bulb (Vertical, Horizontal, Reference)

Source: F20503.DAT. Mem 1

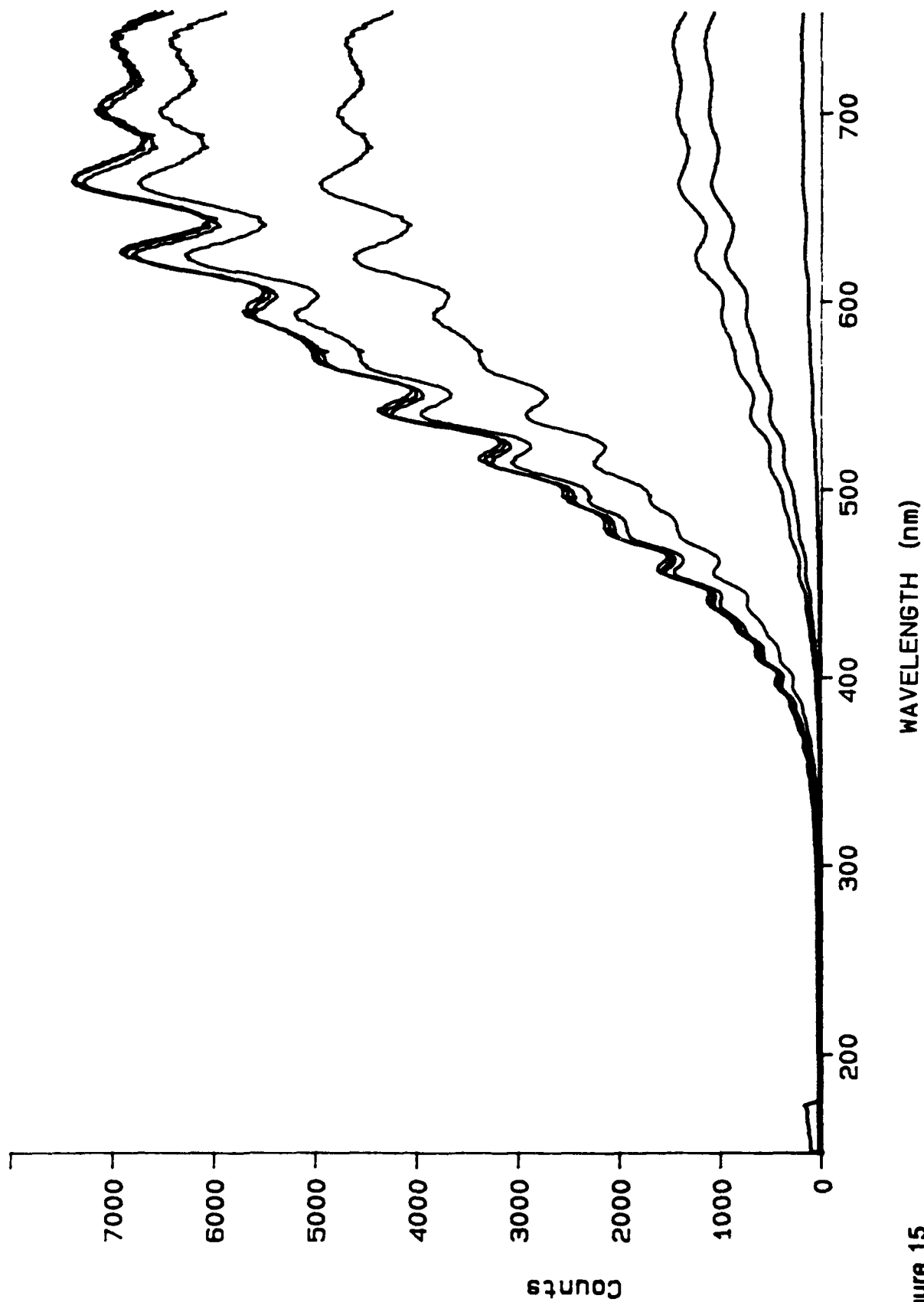


Figure 15
Spectrograph Axis Offset Angle Sensitivity (0 - 7 Degrees)

Source: F20521.DAT, Mem 1

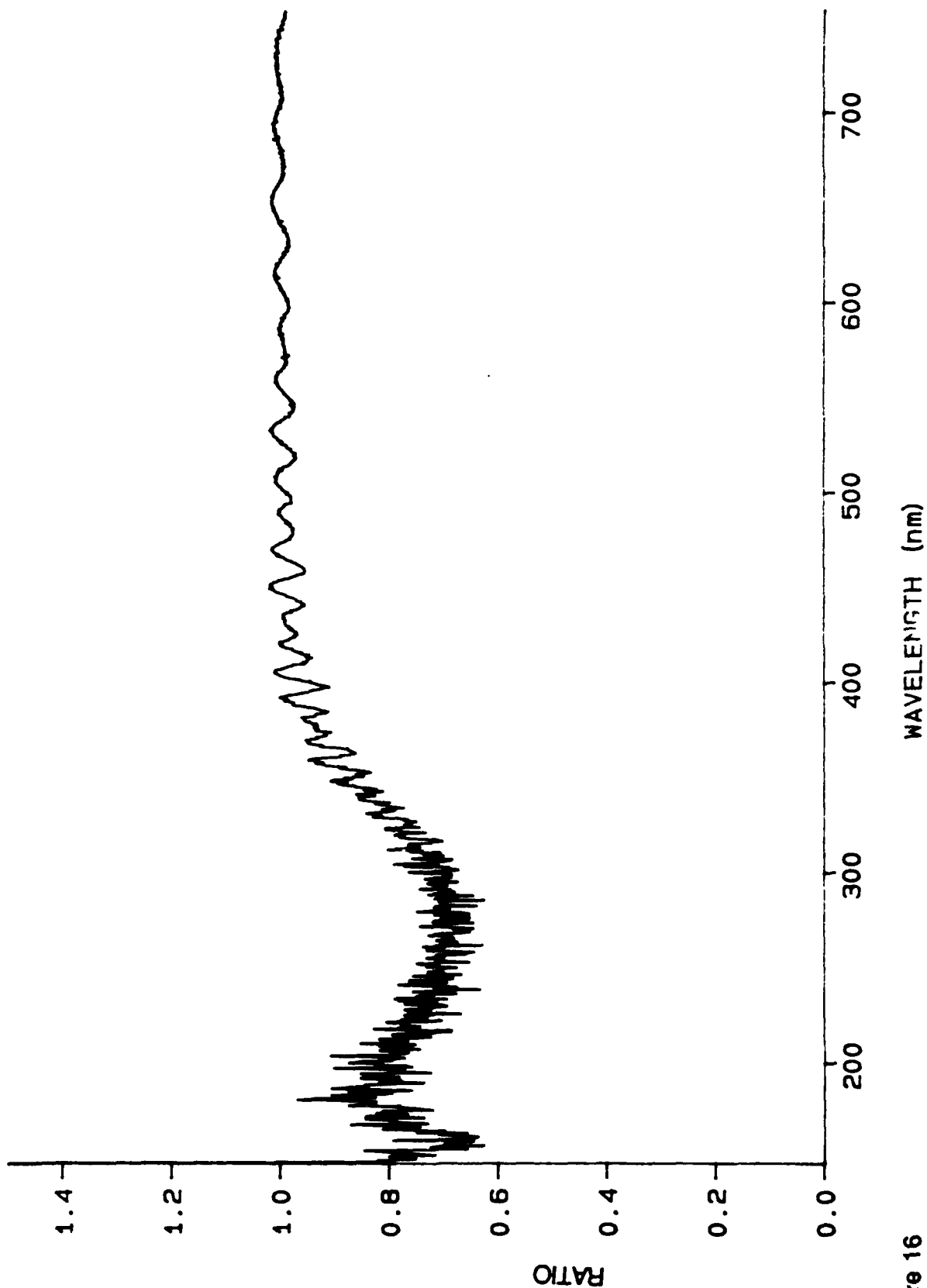


Figure 16

Ratio of Spectrgraph Axis Offset Angle Da1 / 0 Degrees)

Source: F20522.DAT, Mem 1

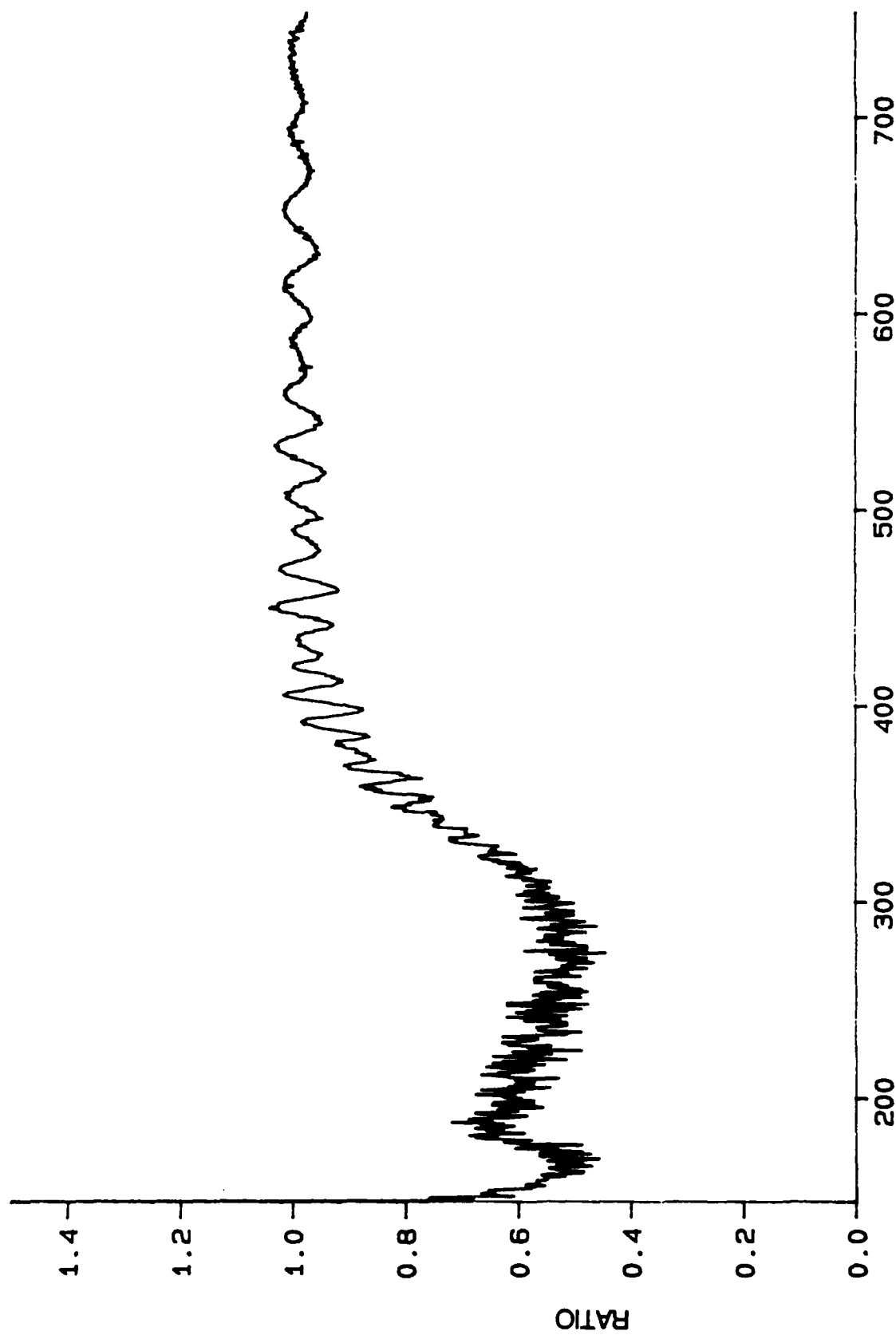


Figure 17
Ratio of Spectrograph Axial Offset Angle $\Delta\alpha$ (2 / 0 Degrees)

Source: F20523.DAT, Mem 1

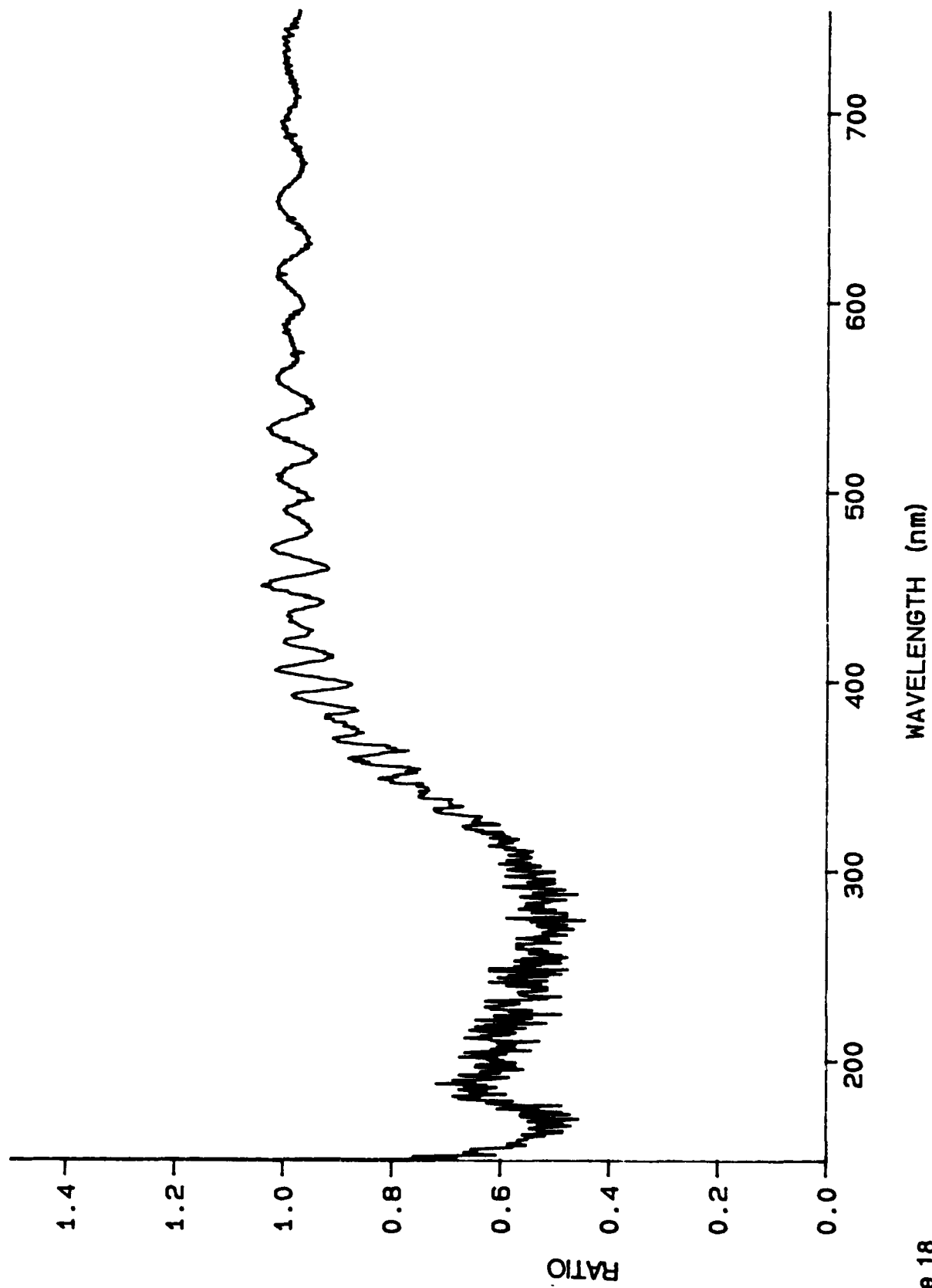


Figure 18

Ratio of Spectrograph Axial Offset Angle Data / 0 Degrees)

Source: F20524.DAT, Mem 1

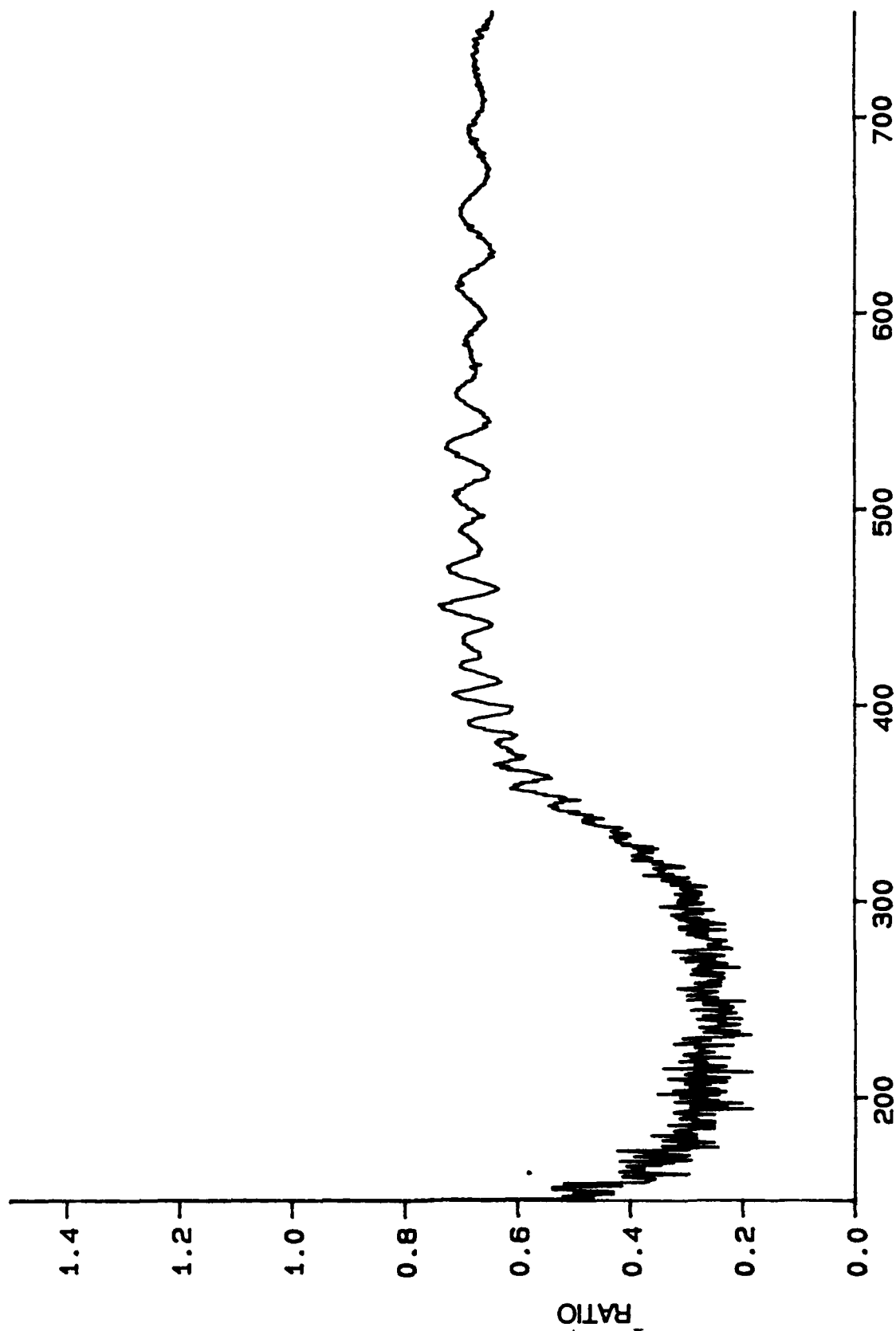


Figure 19

Ratio of Spectrograph Axis Offset Angle D (4 / 0 Degrees)

Source: F20525.DAT, Mem 1

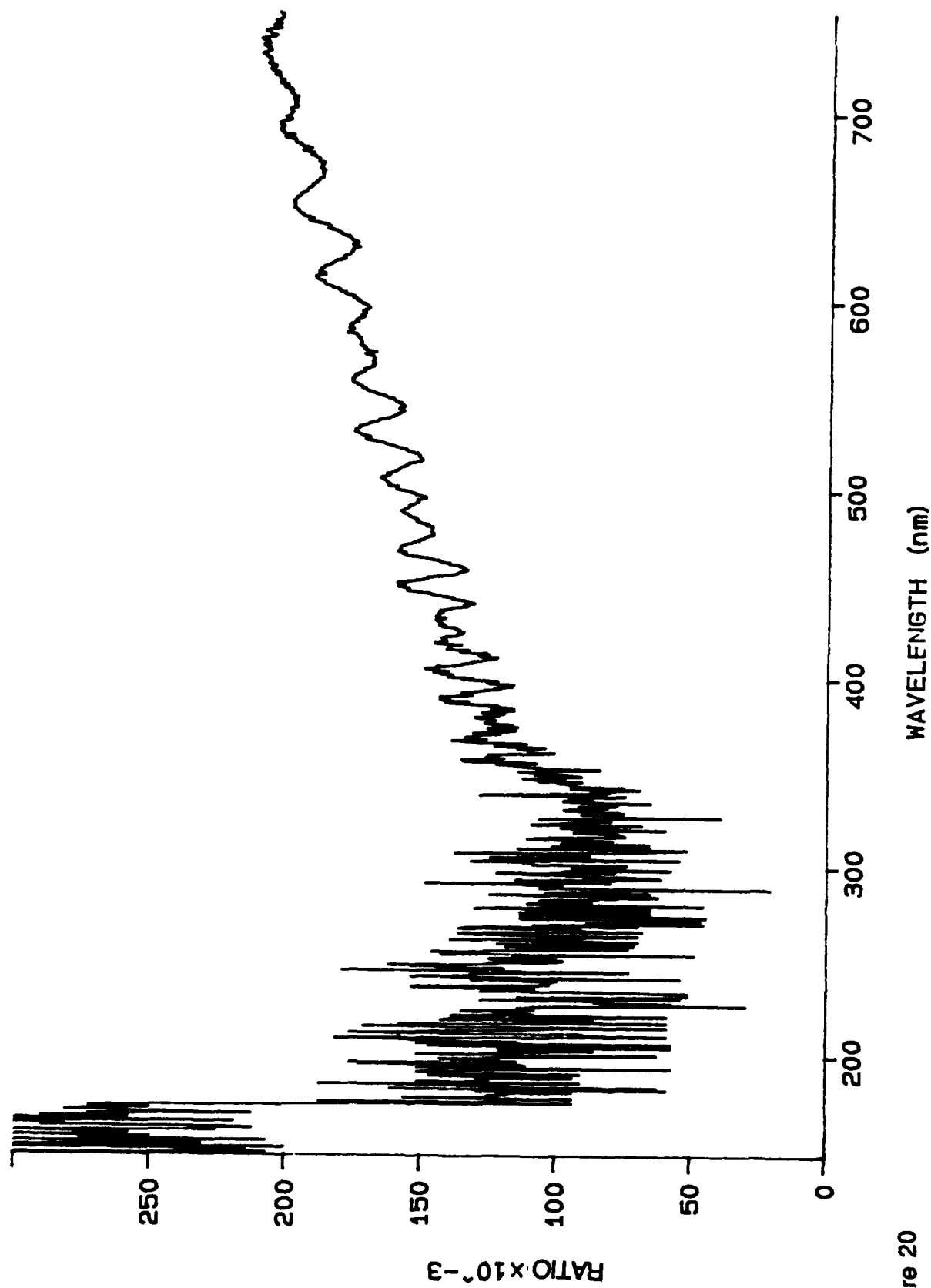


Figure 20
Ratio of Spectrograph Axis Offset Angle Difference / 0 Degrees)

Source: F20526.DAT, Mem 1

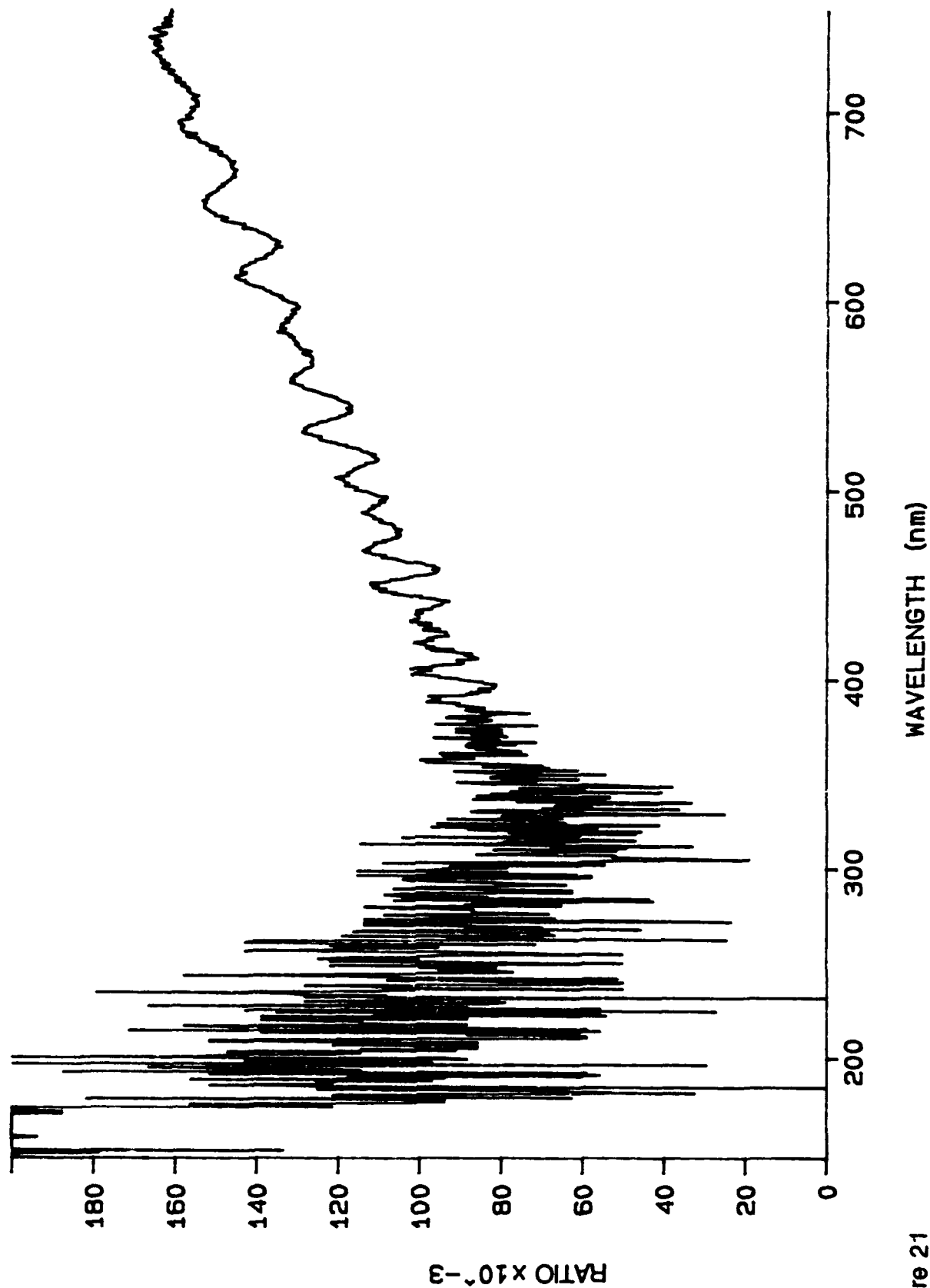


Figure 21

Ratio of Spectrograph Axis Offset Angle Data (° / 0 Degrees)

Source: F20527.DAT, Mem 1

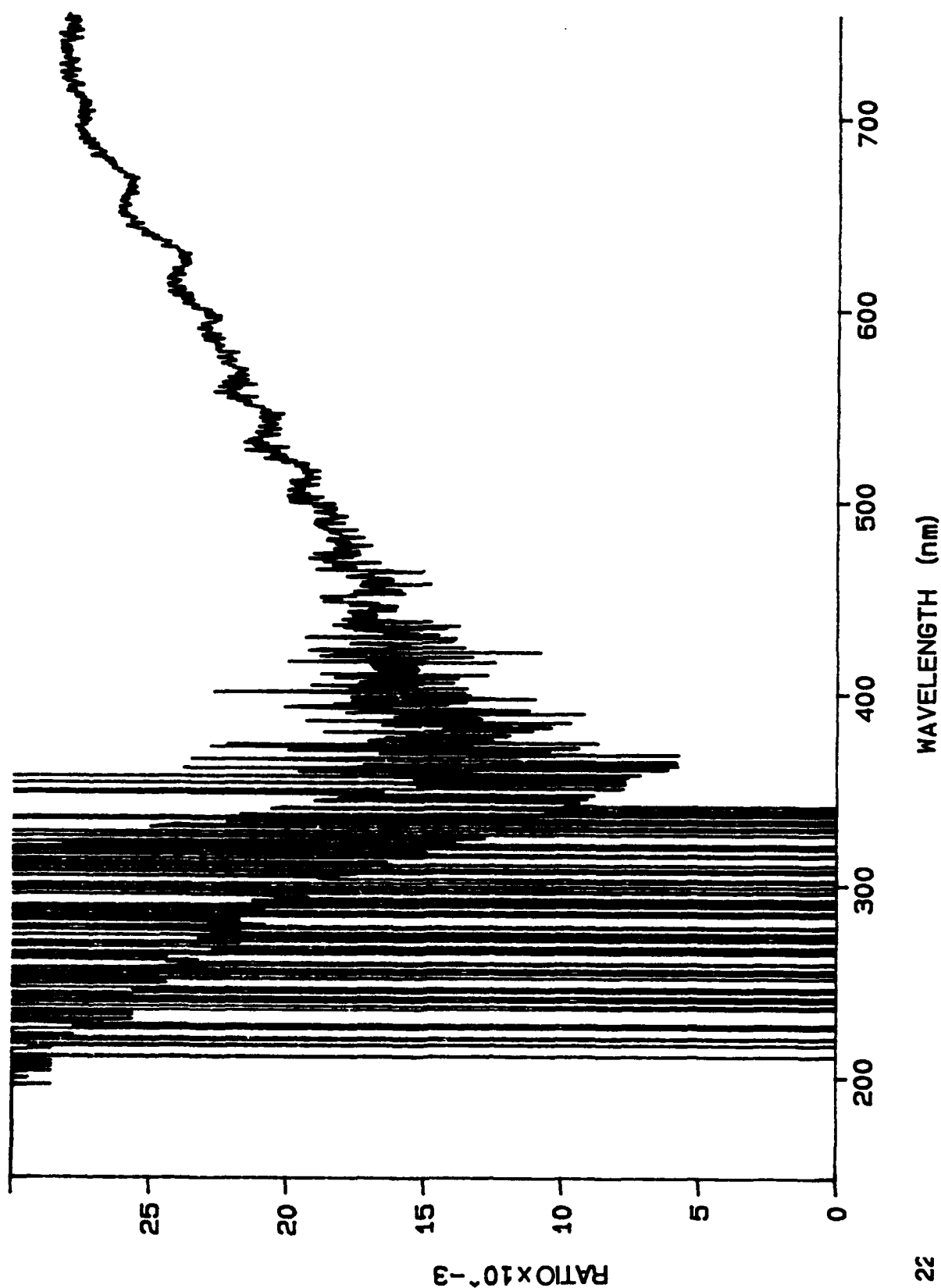


Figure 22
Ratio of Spectrograph Axis Offset Angle Data (7 / 0 Degrees)

Source: F22602.DAT, Mem 1

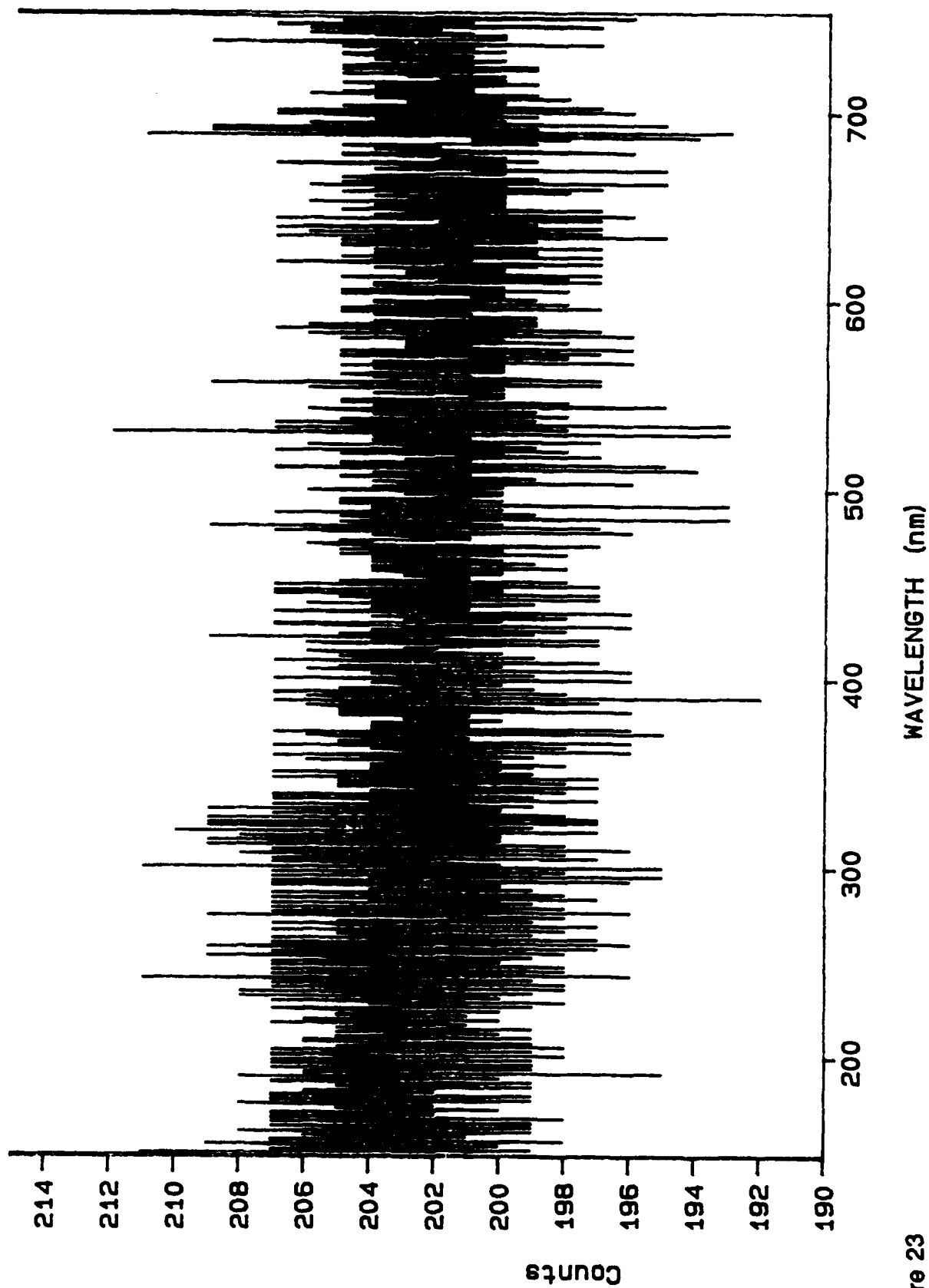


Figure 23
Background Data with All Lights Out (Live, 30 msec Exp Time)

Source: F22603.DAT, Mem 1

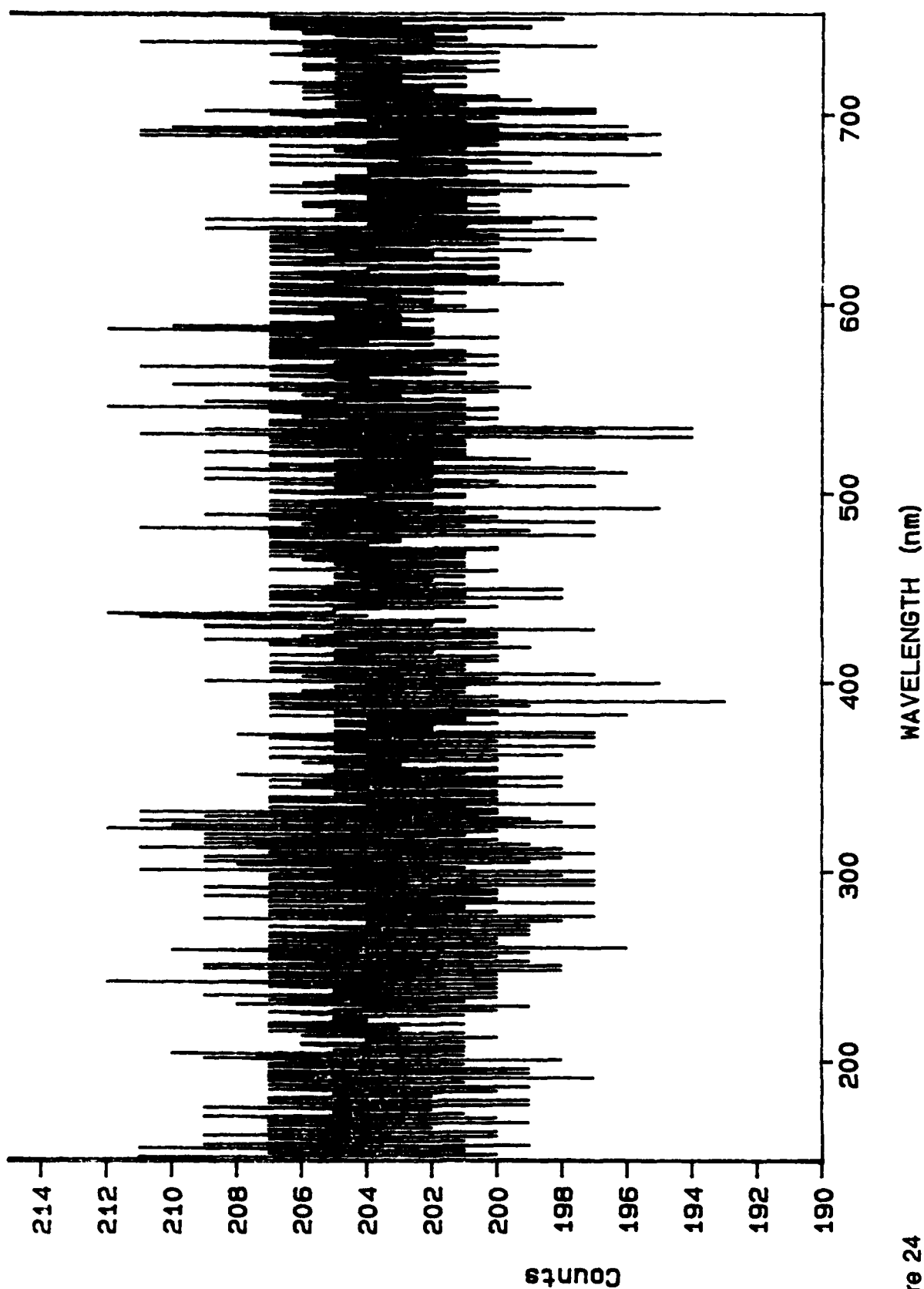


Figure 24
Background Data with All Overhead Lights On (Live, 30 msec Exp Time)

Source: F22651.DAT, Mem 1

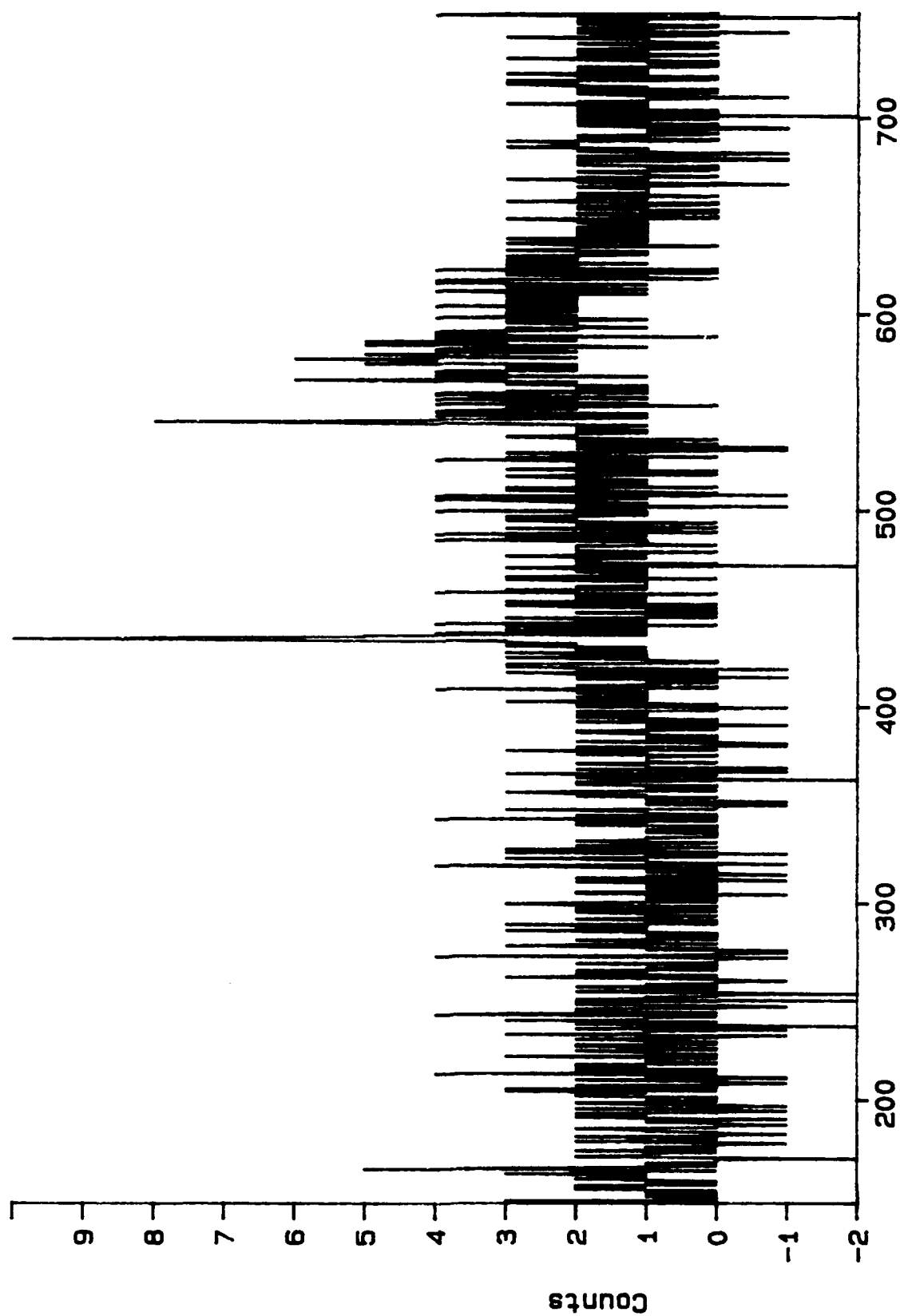


Figure 25

WAVELENGTH (nm)

Difference Between Background Lights On & Out Data (Live, 30 msec)

Source: F22607.DAT, Mem 1

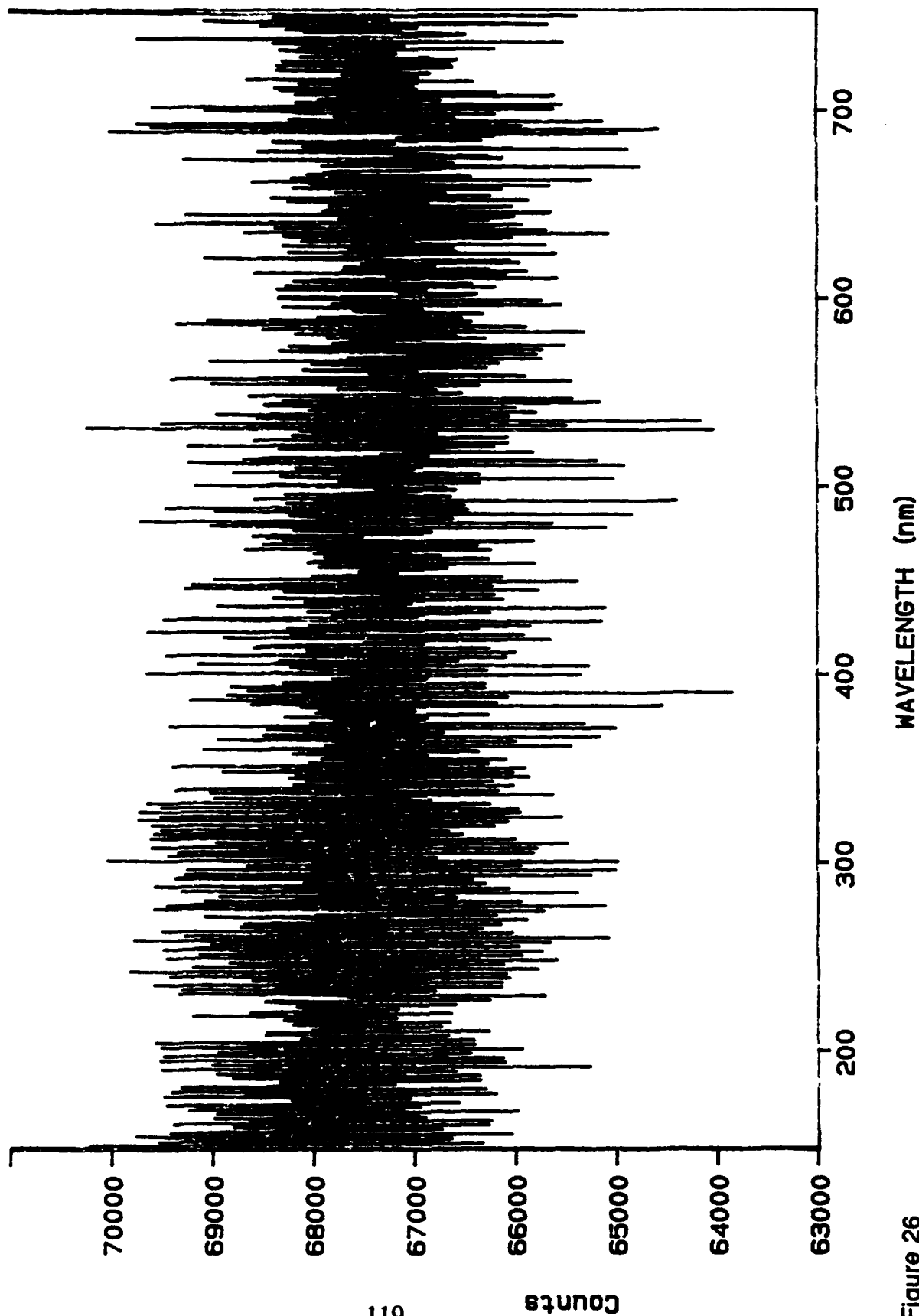


Figure 26

Background Data with All Lights Out (ACCUM. 9.99 sec Acq Time)

Source: F22606.DAT, Mem 1

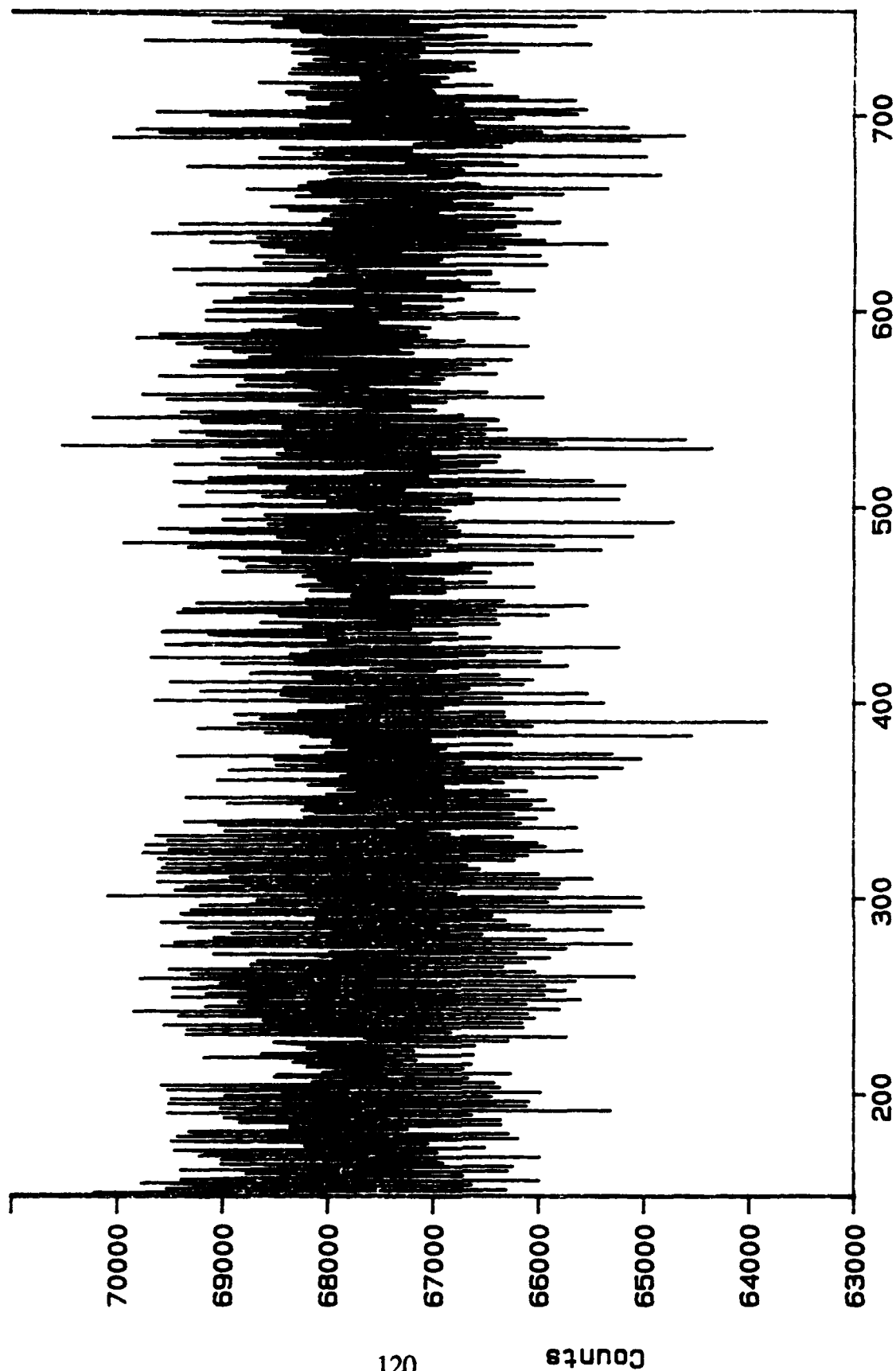


Figure 27

WAVELENGTH (nm)

Background Data with All Overhead Lights On (ACCUM. 9.99 sec Acq Time)

Source: F4.DAT, Mem 1

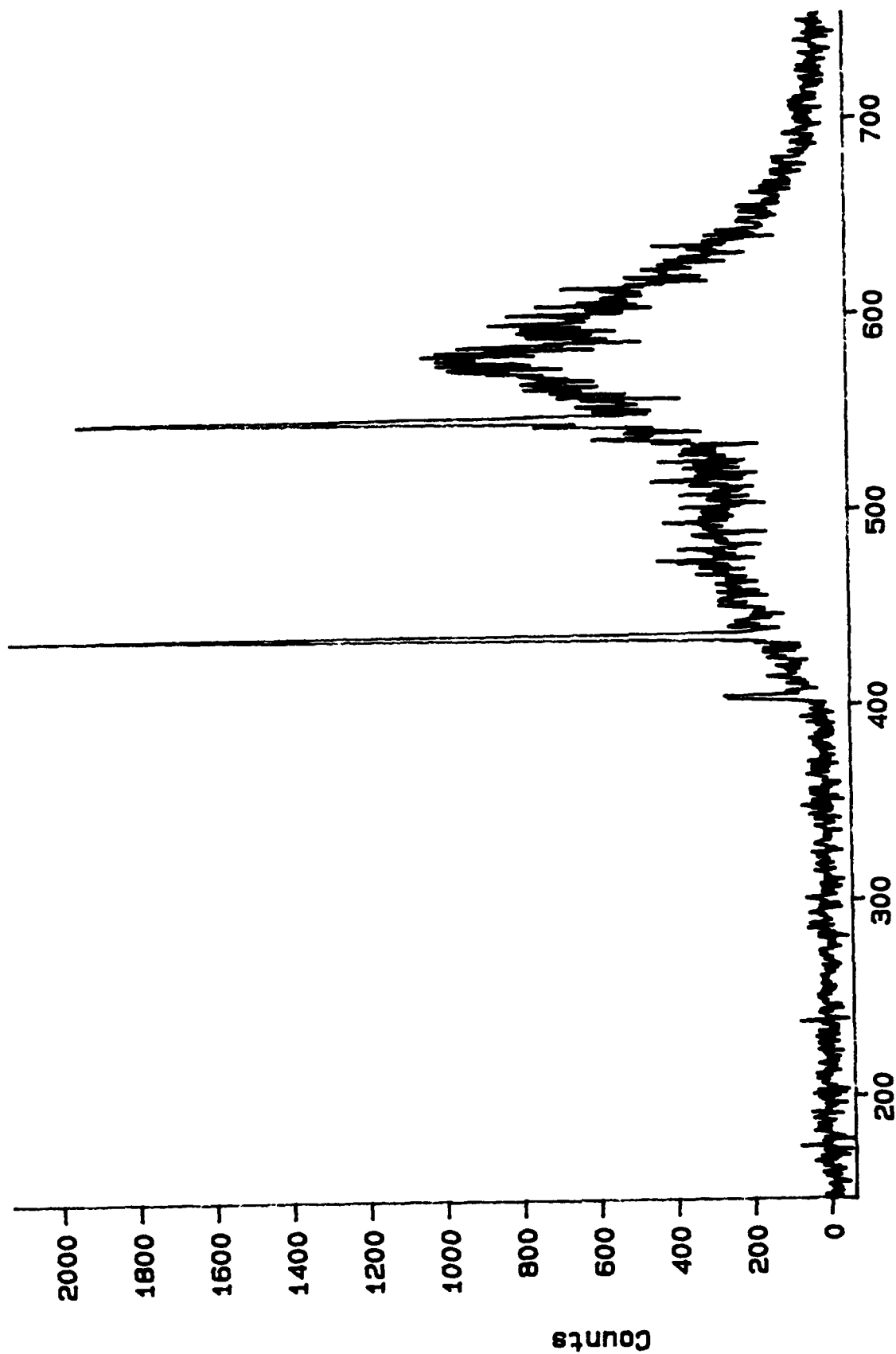


Figure 28

Difference Btwn Background Lts On & Out Data (ACCUM, 9.99 sec Acq Time)

Source: F22604.DAT, Mem 1

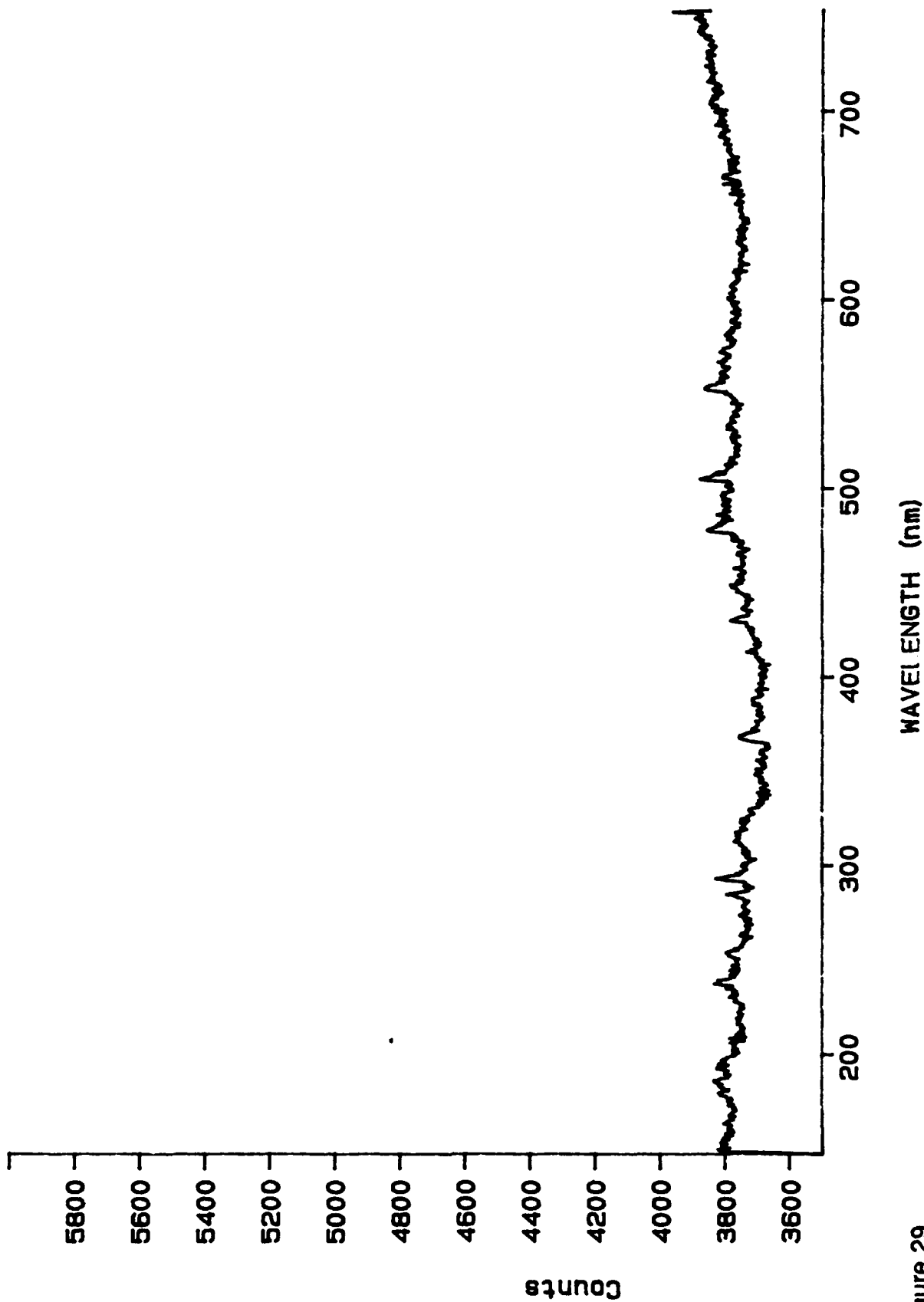


Figure 29

Background Data with All Lights Out (Live, 1989.999 msec Exp Time)

Source: F22605.DAT, Mem 1

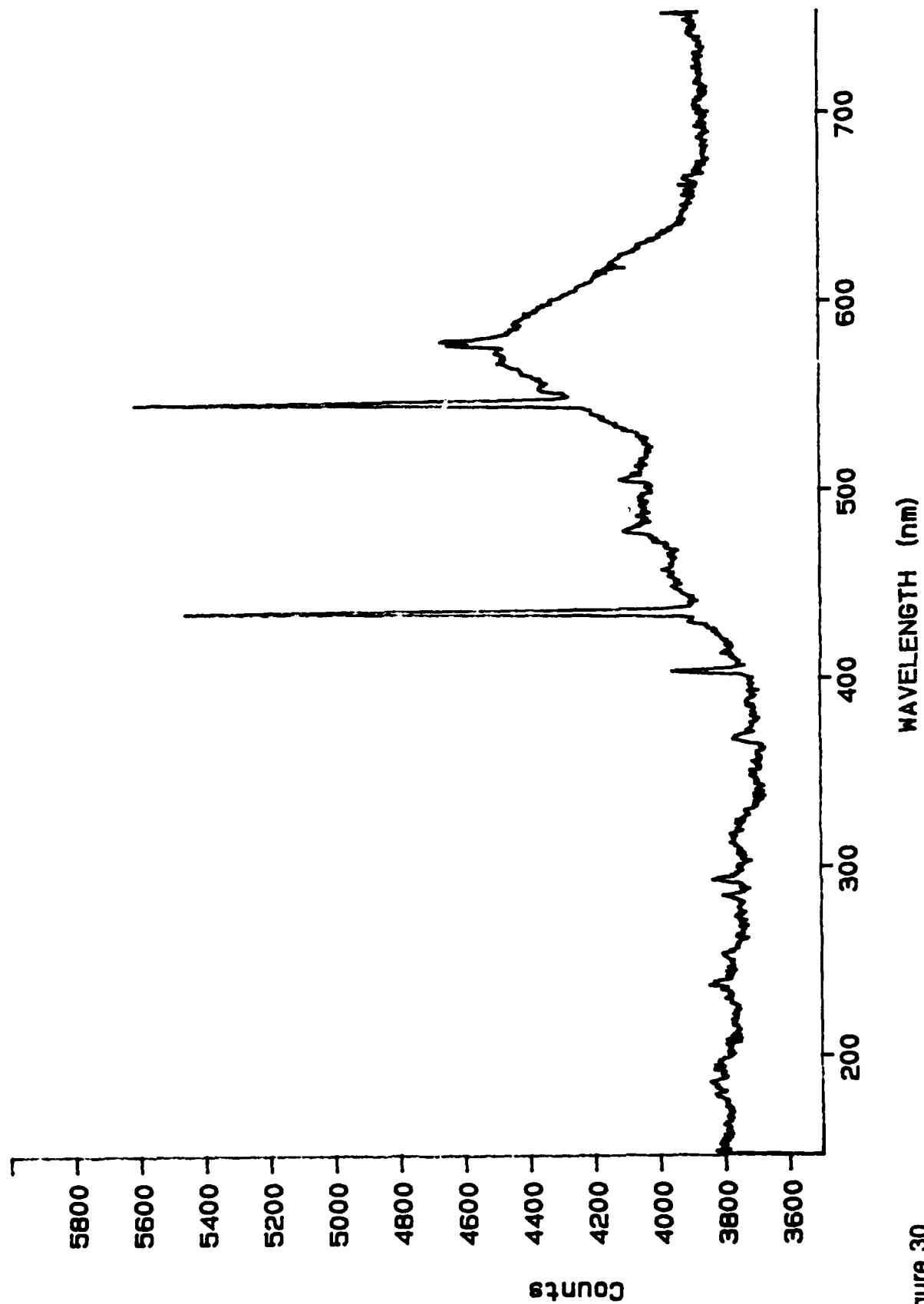


Figure 30

Background Data with All Overhead Lights On (live, 9989.99 sec Exp)

Source: F6.DAT, Mem 1

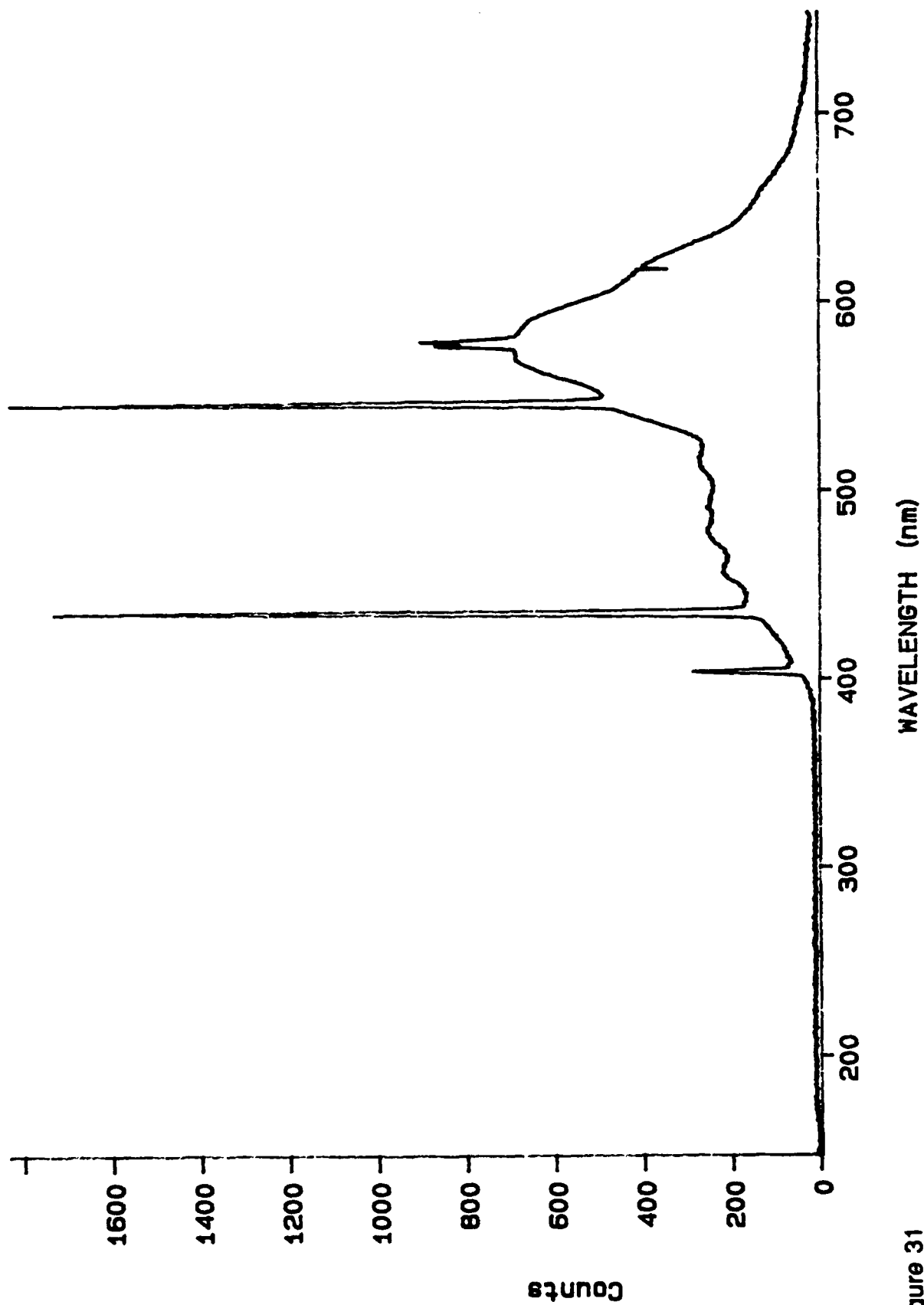


Figure 31

Difference Btwn Background Lts On & Out Dn (Live, 9989.999 msec Exp)

Source: F22801.DAT, Mem 1

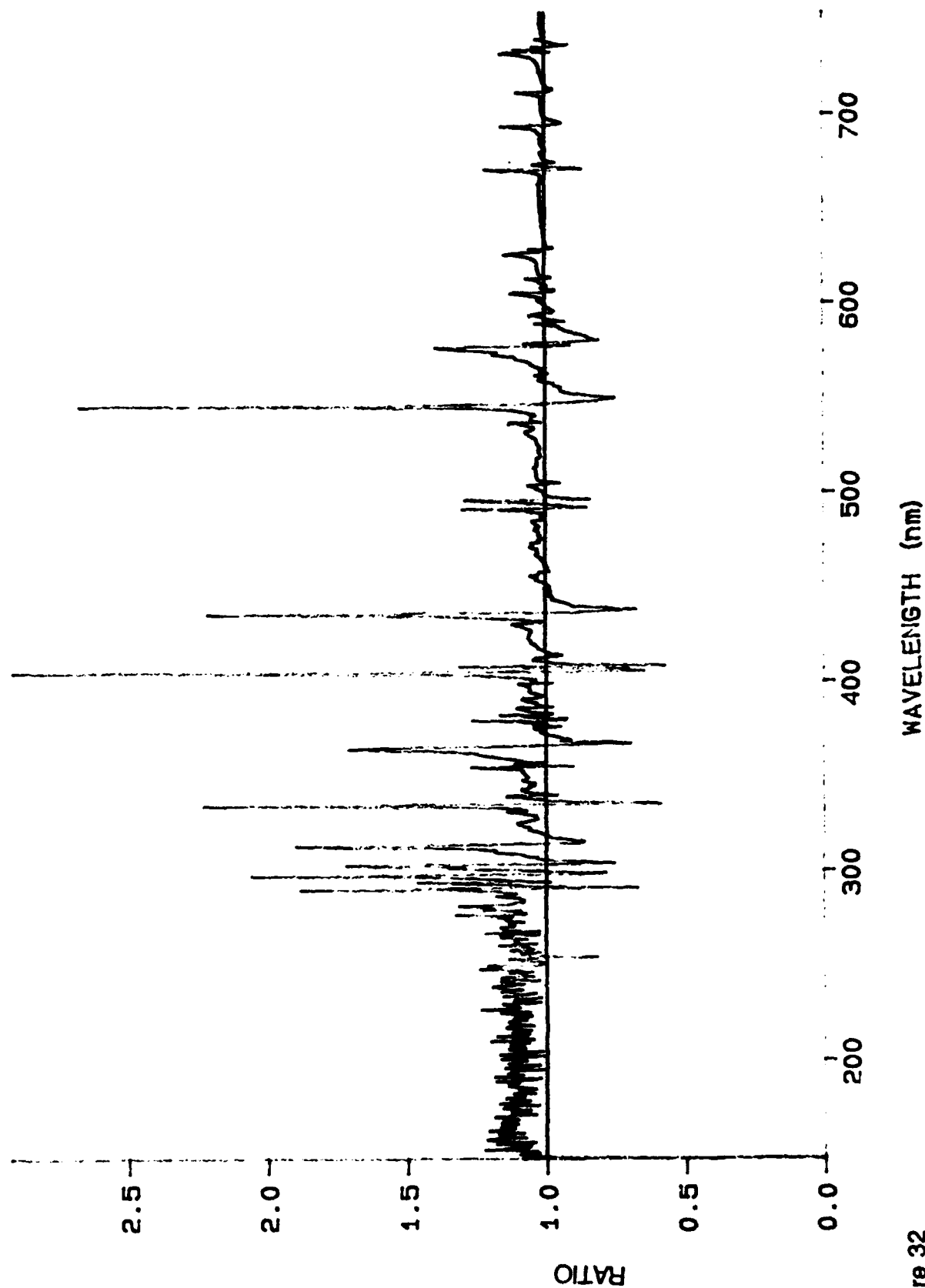


Figure 32
Ratio of Mercury Arc Lamp Reflected Intensities Off Copper (6 Days)

Source: F22803.DAT, Mem 1

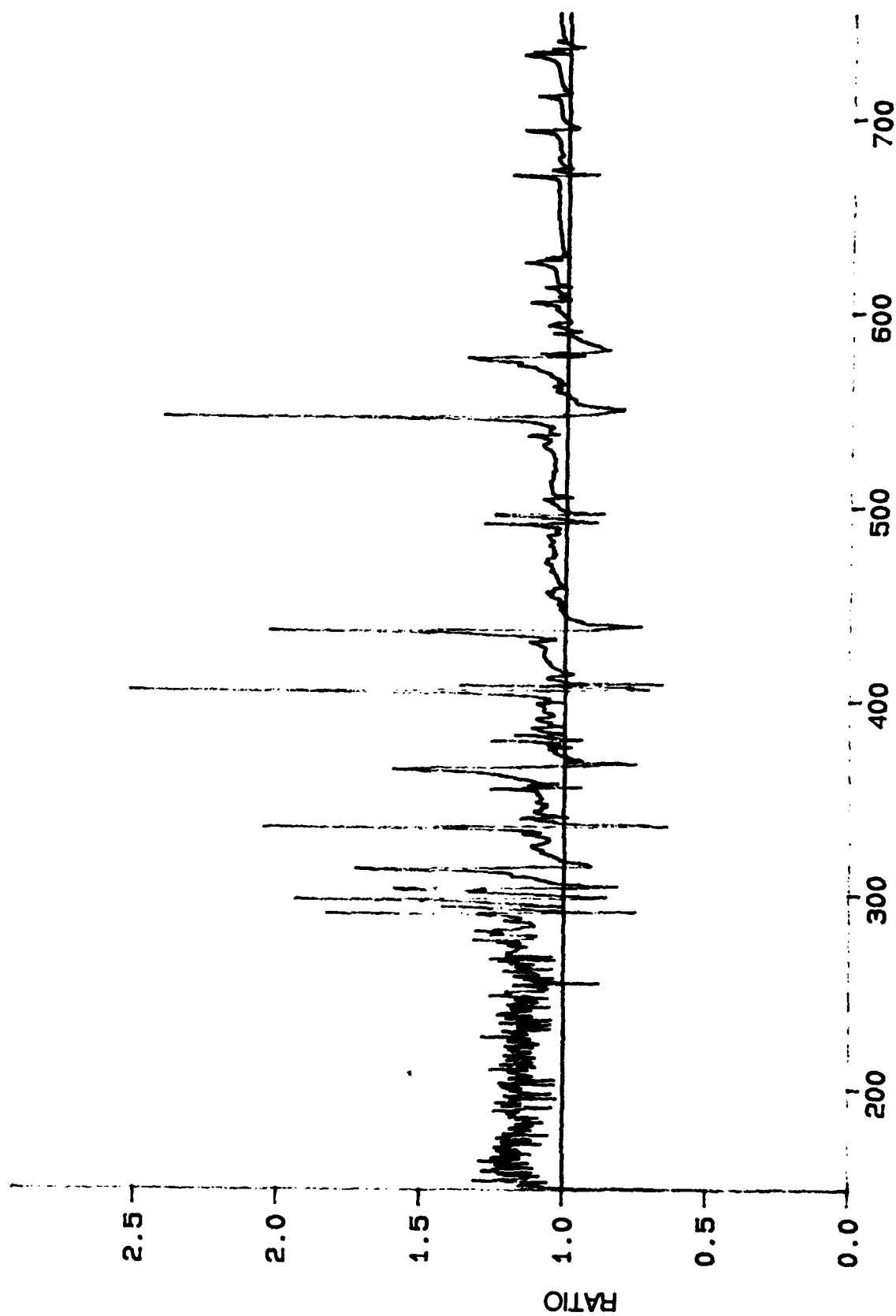


Figure 33

Ratio of Mercury Arc Lamp Reflected Intensities Off Copper (6 Days II)

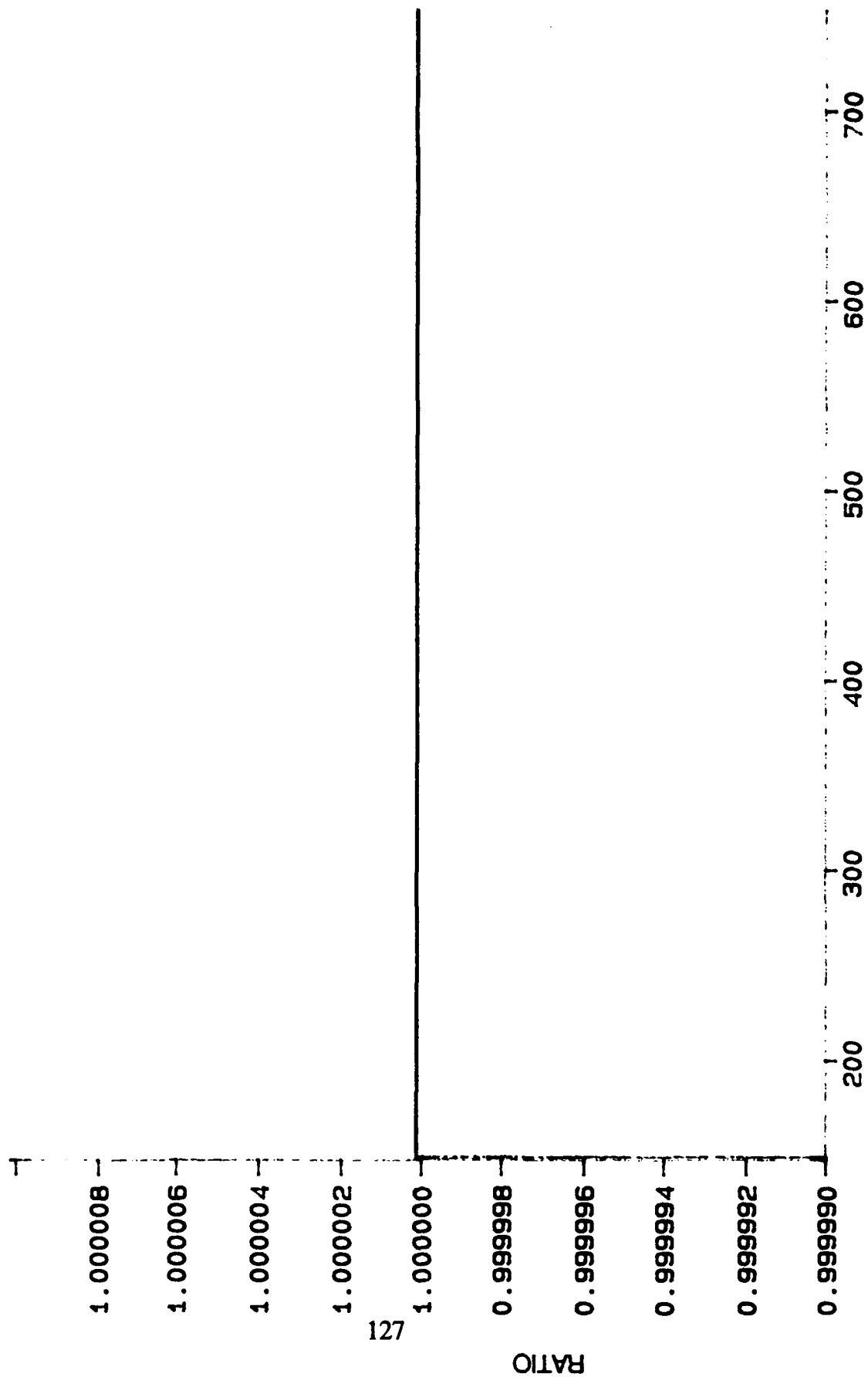


Figure 34

Ratios of Comp Mode 2 and Curve Calculation Subtracted Background

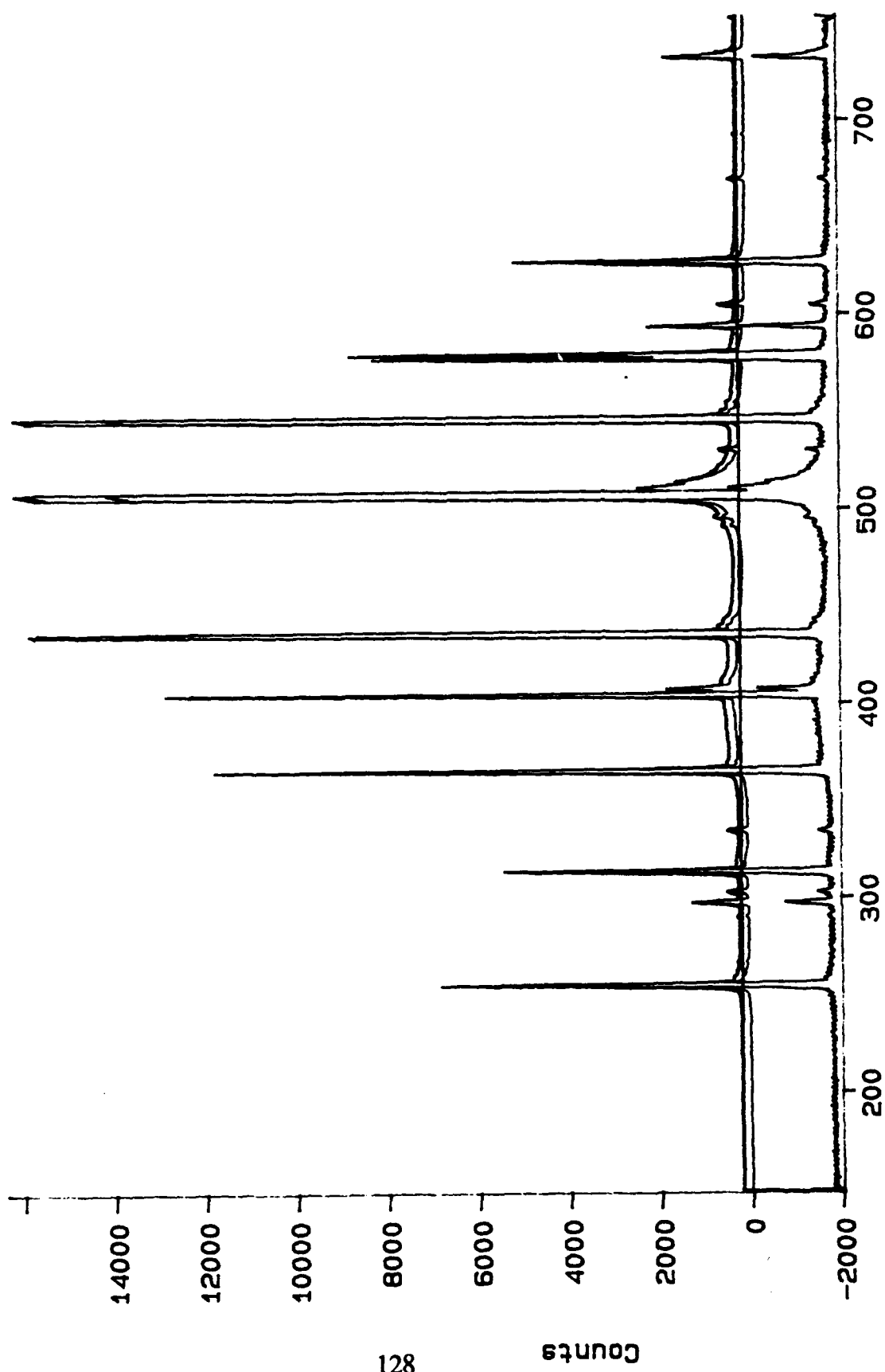


Figure 35
Mercury Calibration Lamp (MO, Background, 11/2/3/4, CMB)

Source: F30702.DAT, Mem 1

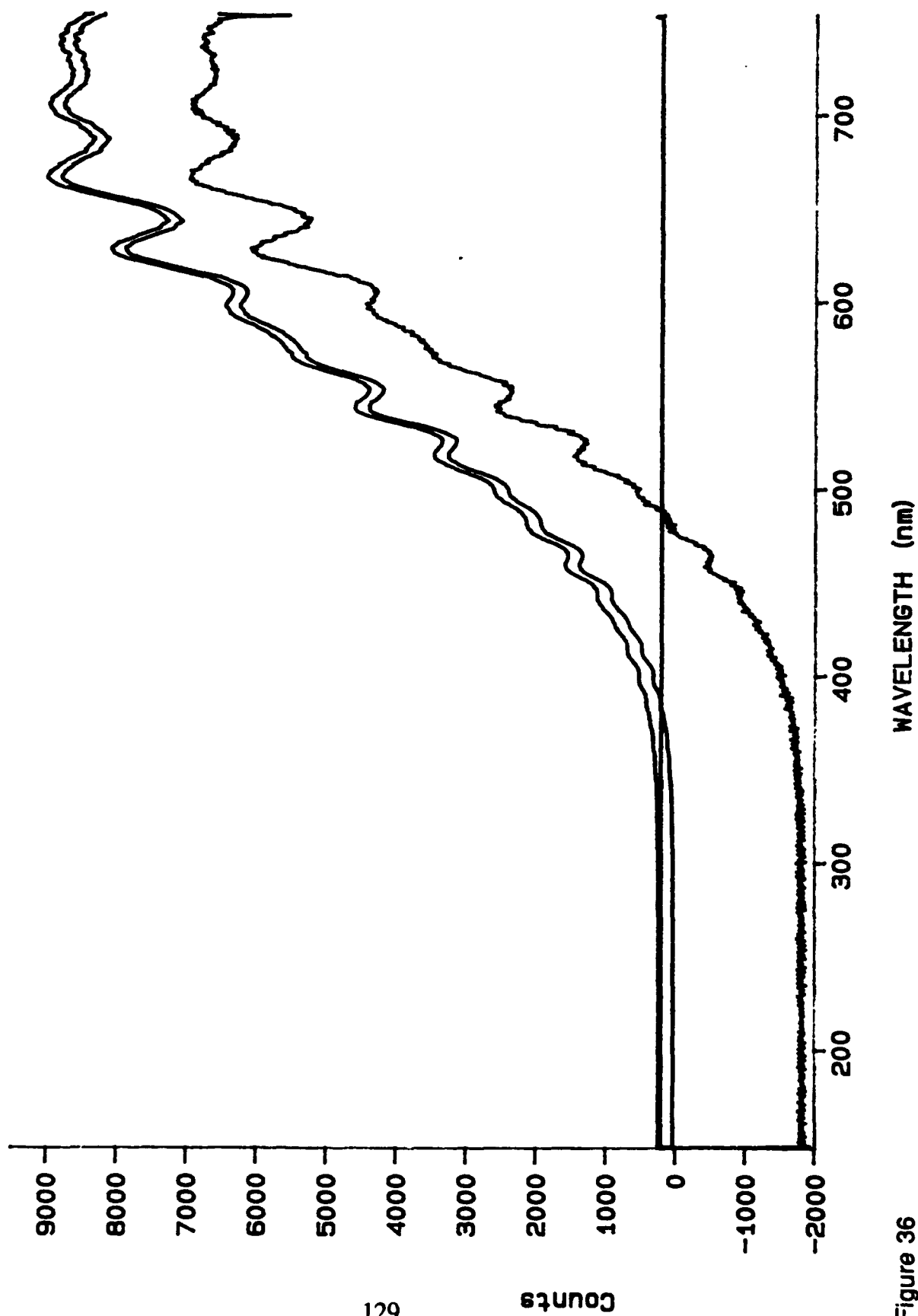


Figure 36

100 Watt Sylvania Light Bulb (CM0, Background, CM1/2, CMB)

Source: F22609.DAT, Mem 1

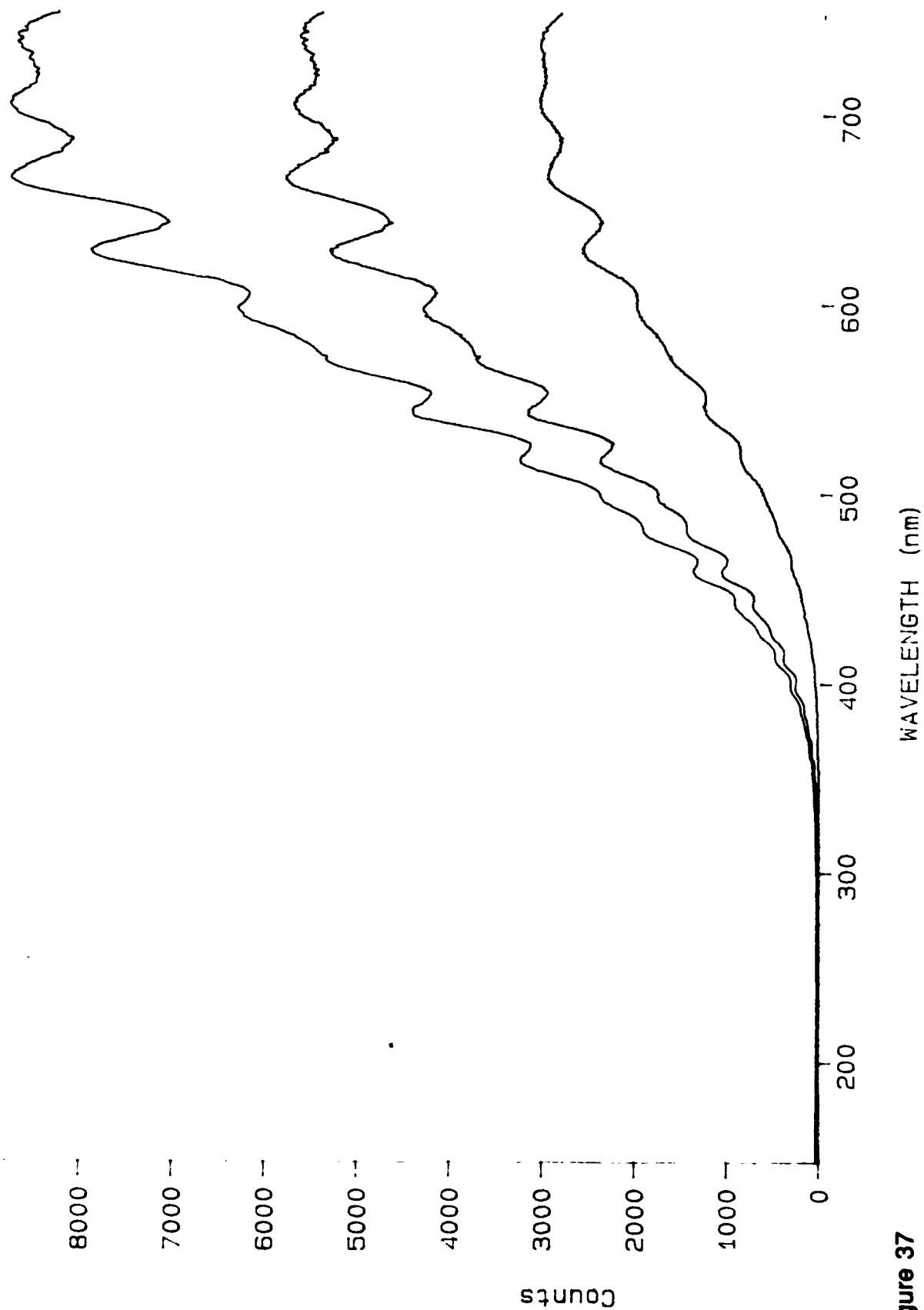


Figure 37

Timing of Background Compensation Storage (Revisited, Original, Delta)

Source: F5.DAT, Mem 1

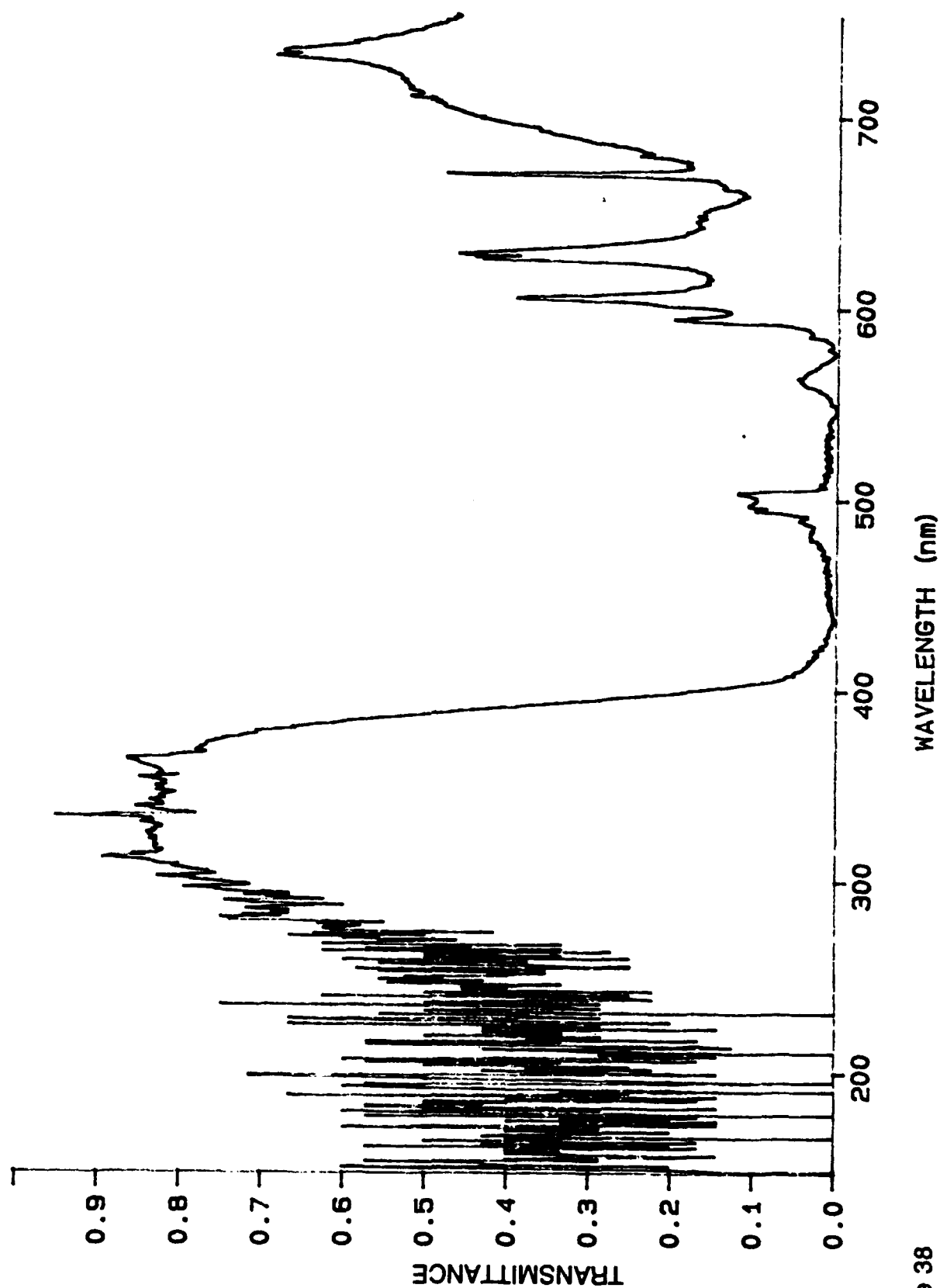


Figure 38
Transmittance of Filter 3172 Using a 200 W Mercury Arc Lamp Source

Source: F6.DAT, Mem 1

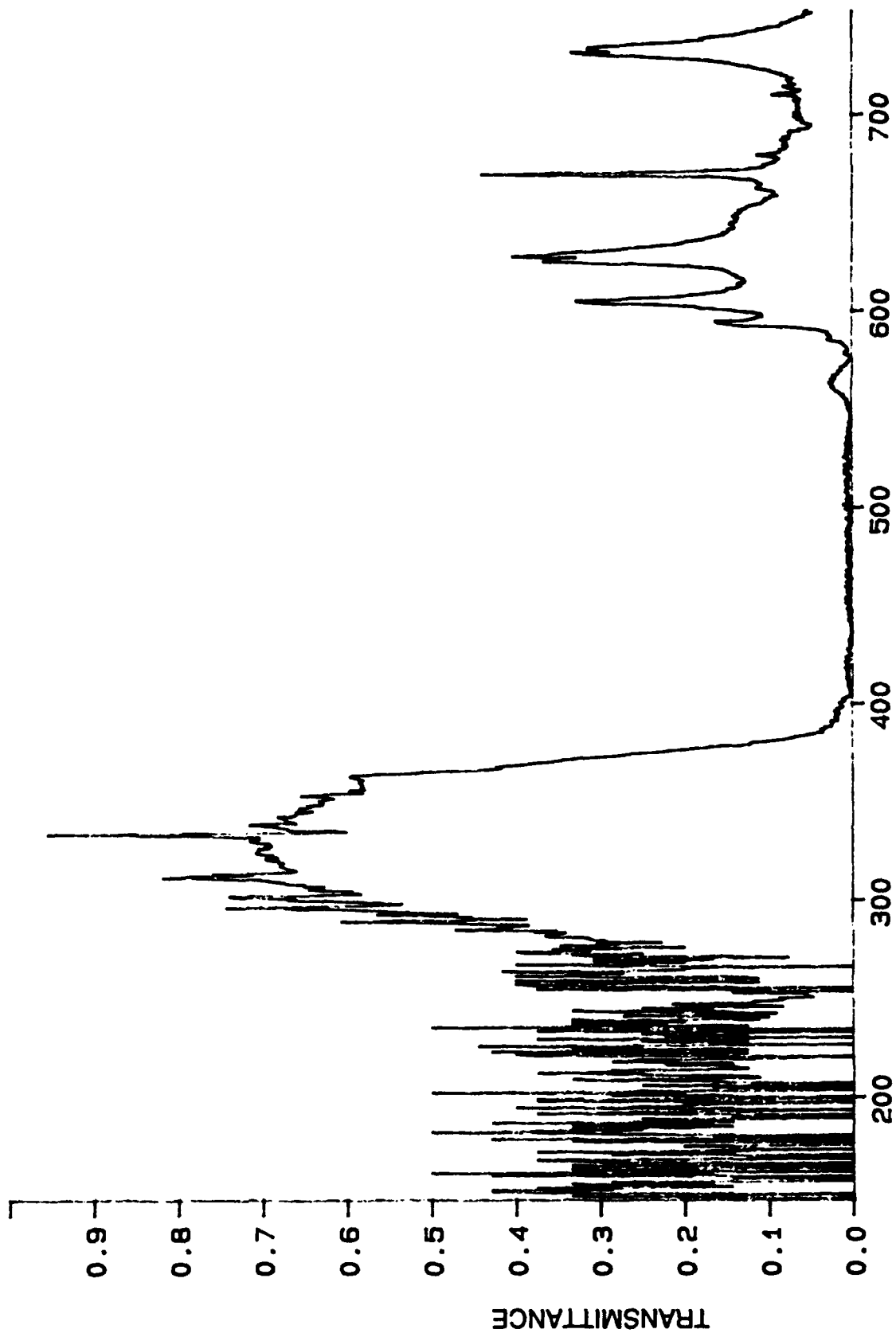


Figure 39
Transmittance of Filter 3174 Using a 200 W Mercury Arc Lamp Source

Source: F10.DAT, Mem 1

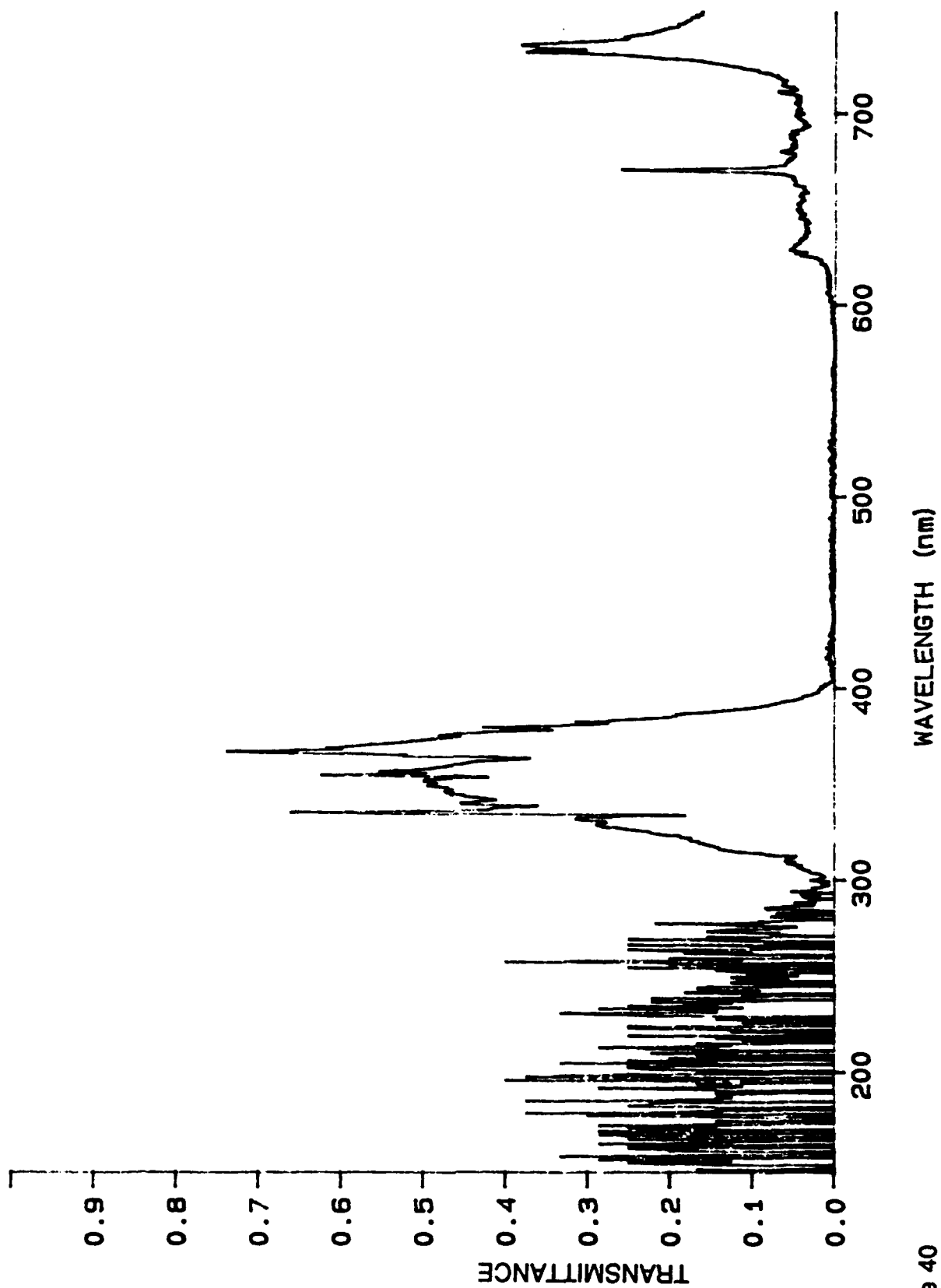


Figure 40
Transmittance of Filter 3111. Using a 200 W Mercury Arc Lamp Source

Source: F11.DAT, Mem 1

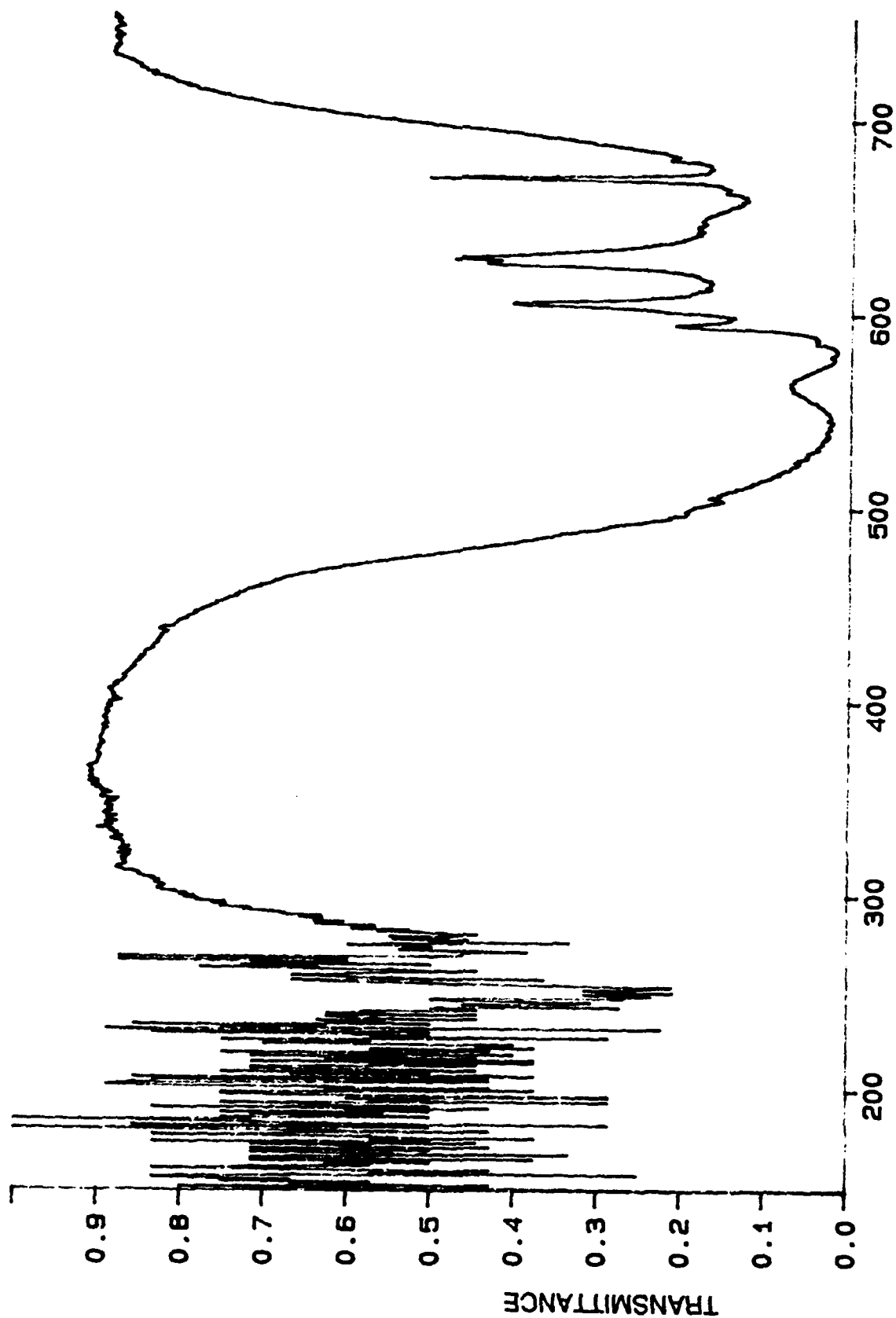


Figure 41
Transmittance of Filter 317A Using a 200 W Mercury Arc Lamp Source

Source: F12.DAT. Mem 1

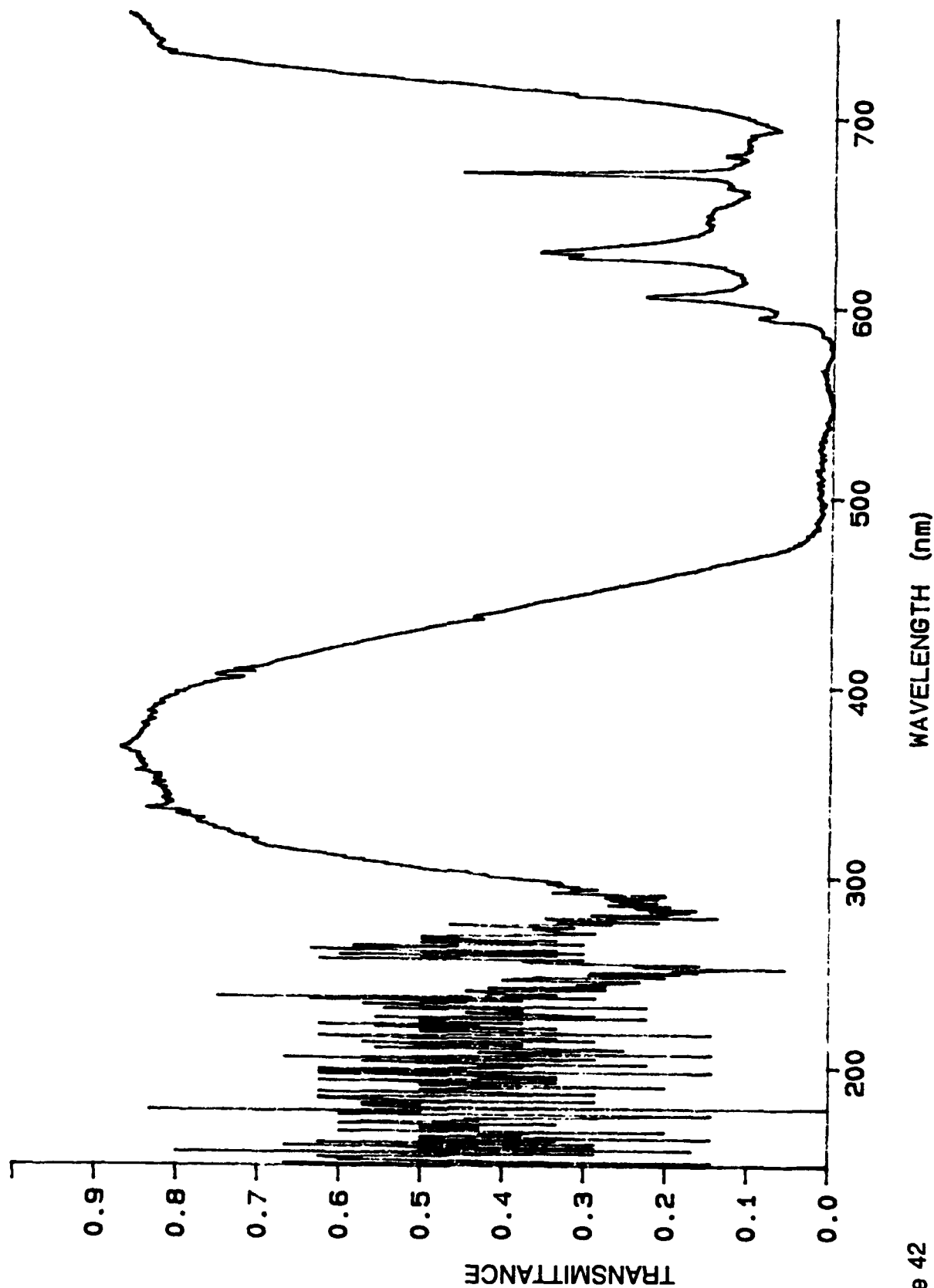


Figure 42
Transmittance of Filter 3180 Using a 200 W Mercury Arc Lamp Source

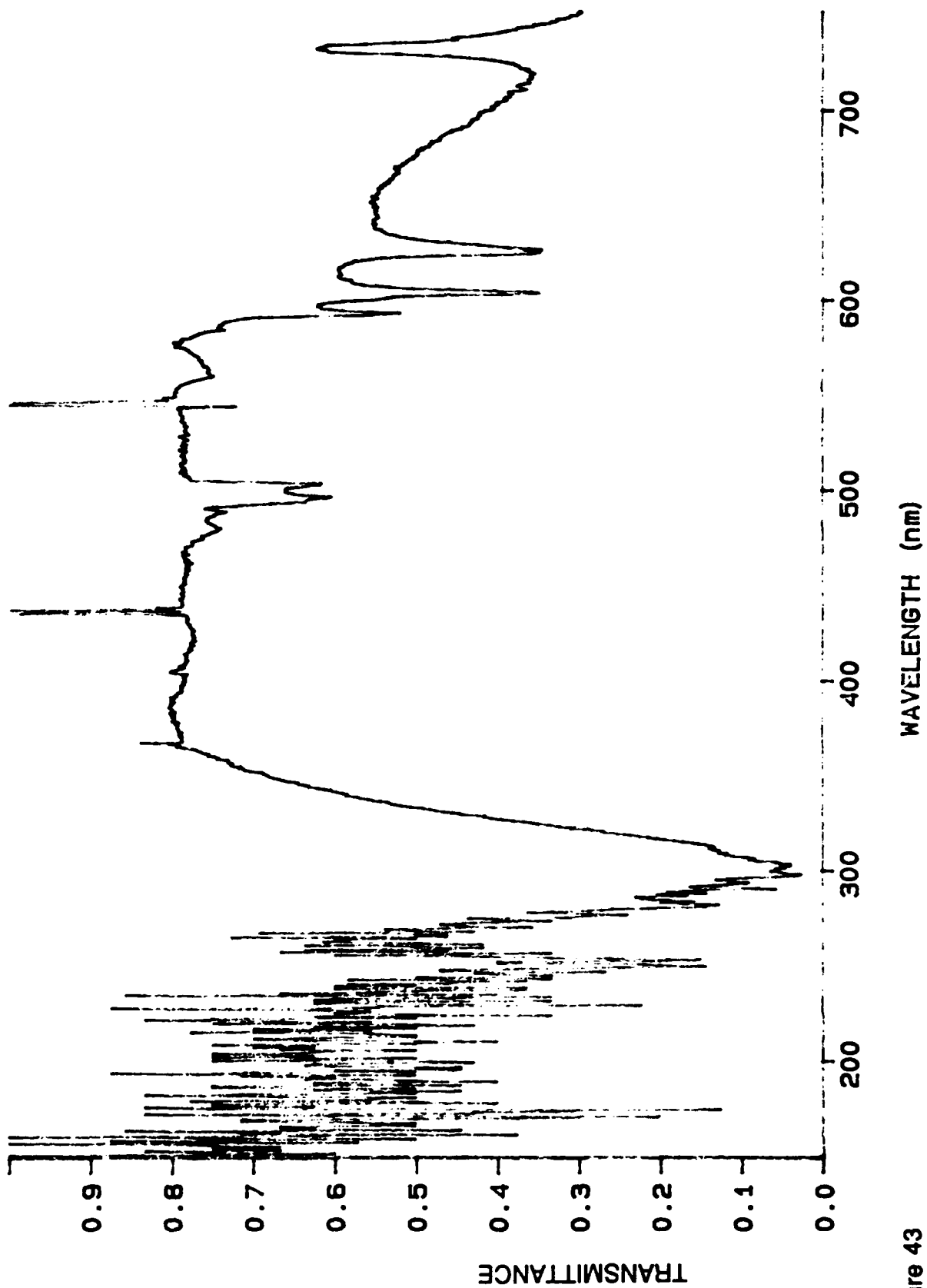


Figure 43
Transmittance of Long Pass Filter 1

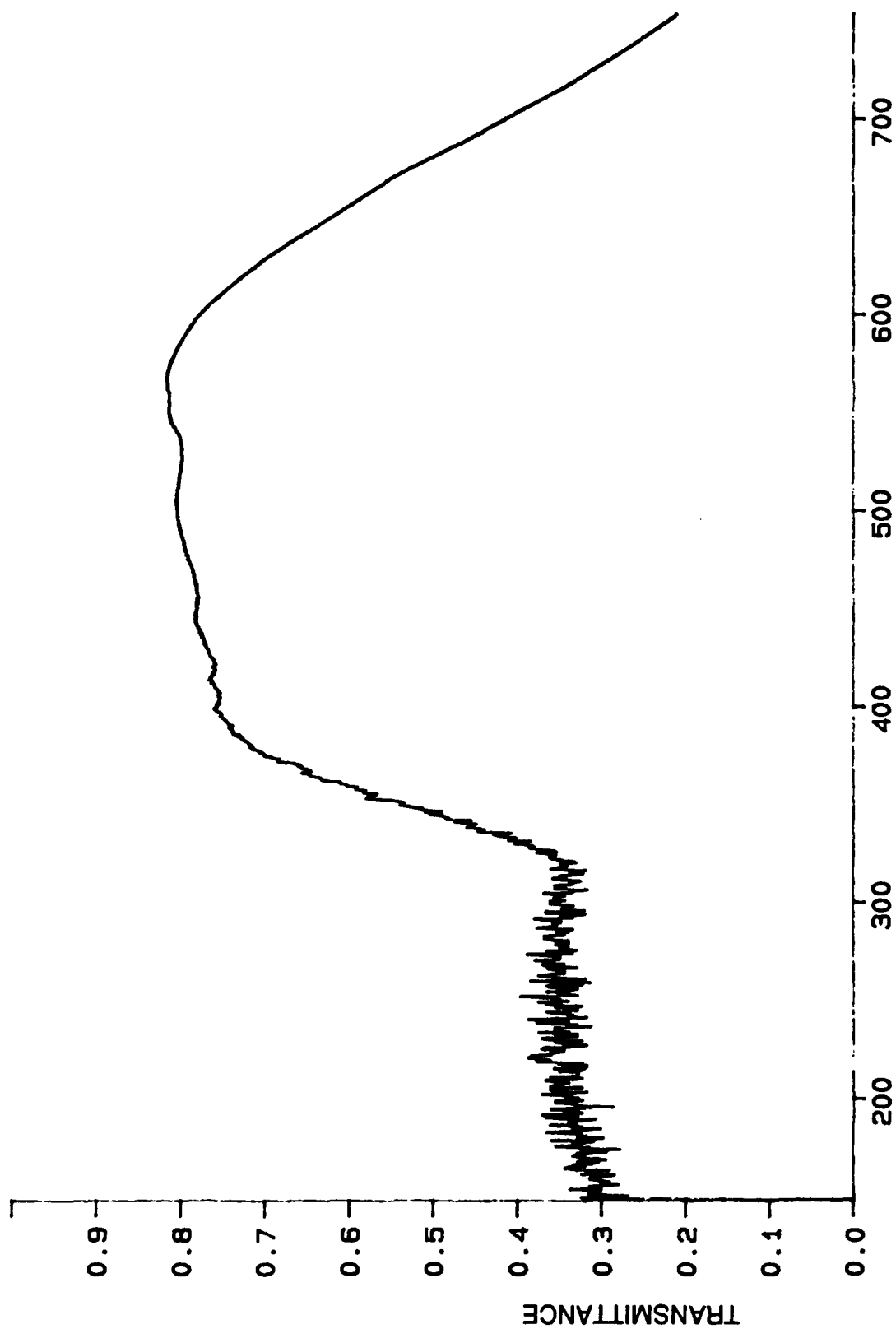


Figure 44
Transmittance of Filter 1 Using 100 W Sylva-lan Bulb

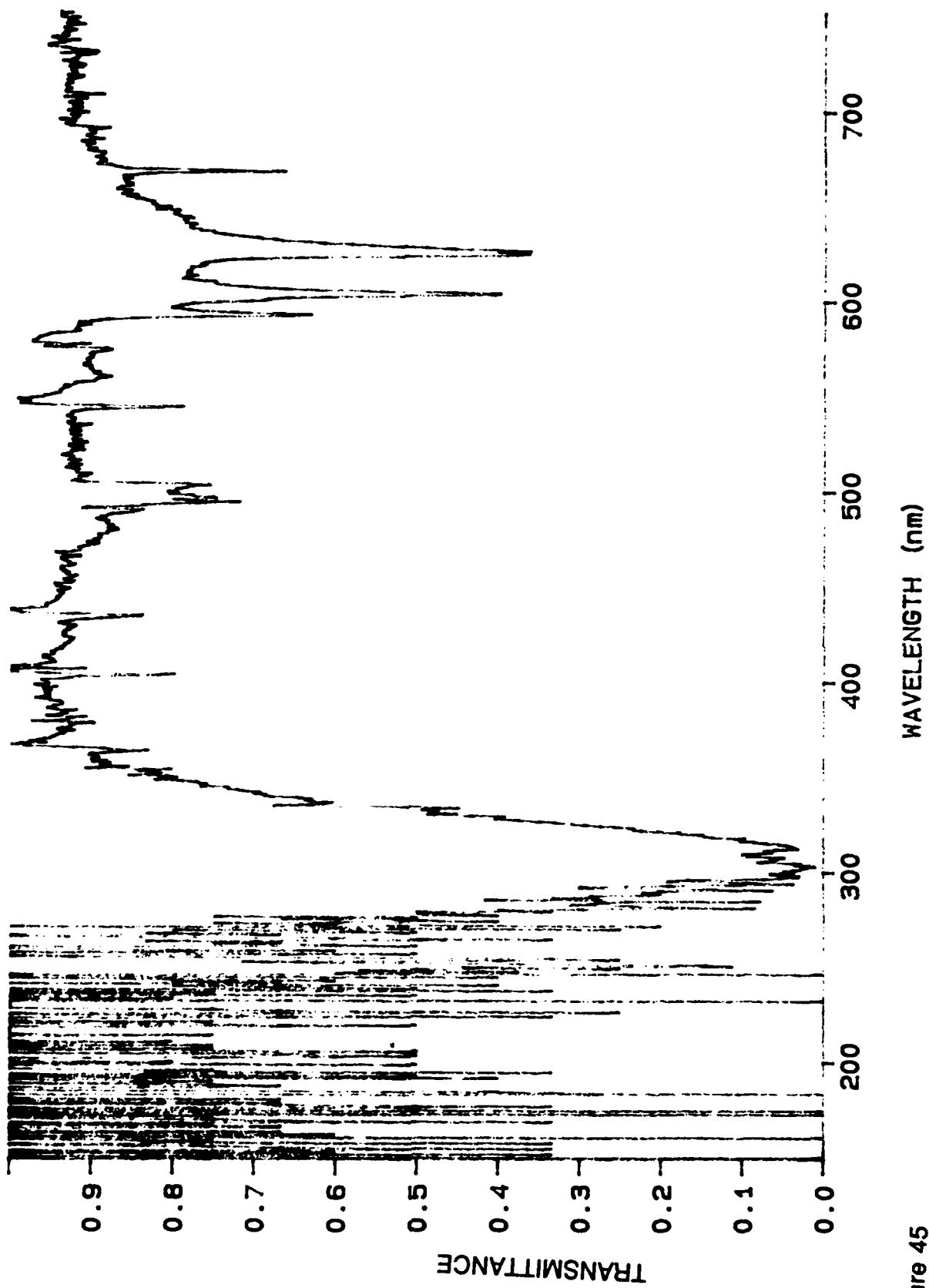


Figure 45
Transmittance of Long Pass Filter 2

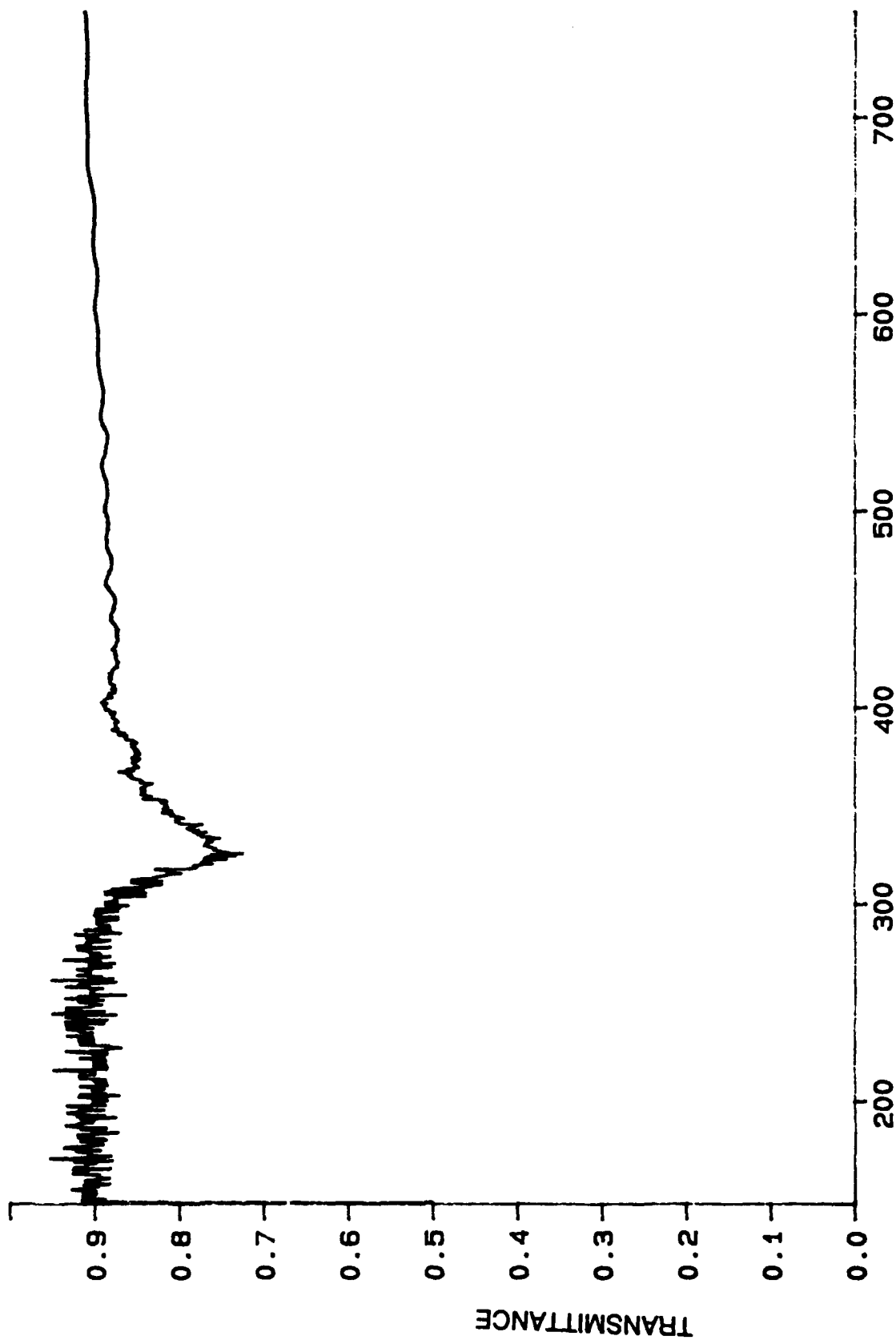


Figure 46
Transmittance of Filter 2 Using 100 W Sylvania Bulb

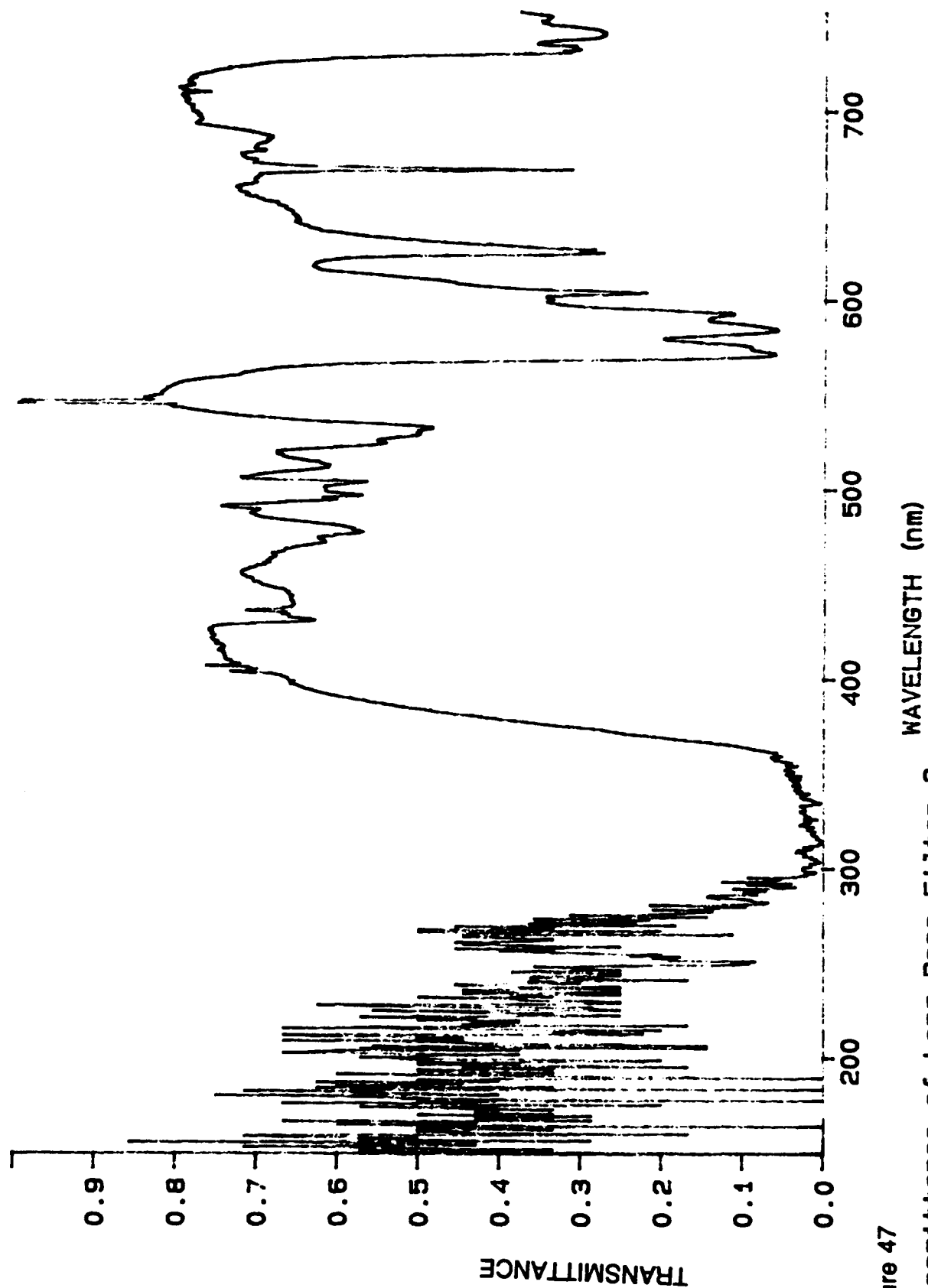


Figure 47
Transmittance of Long Pass Filter 3

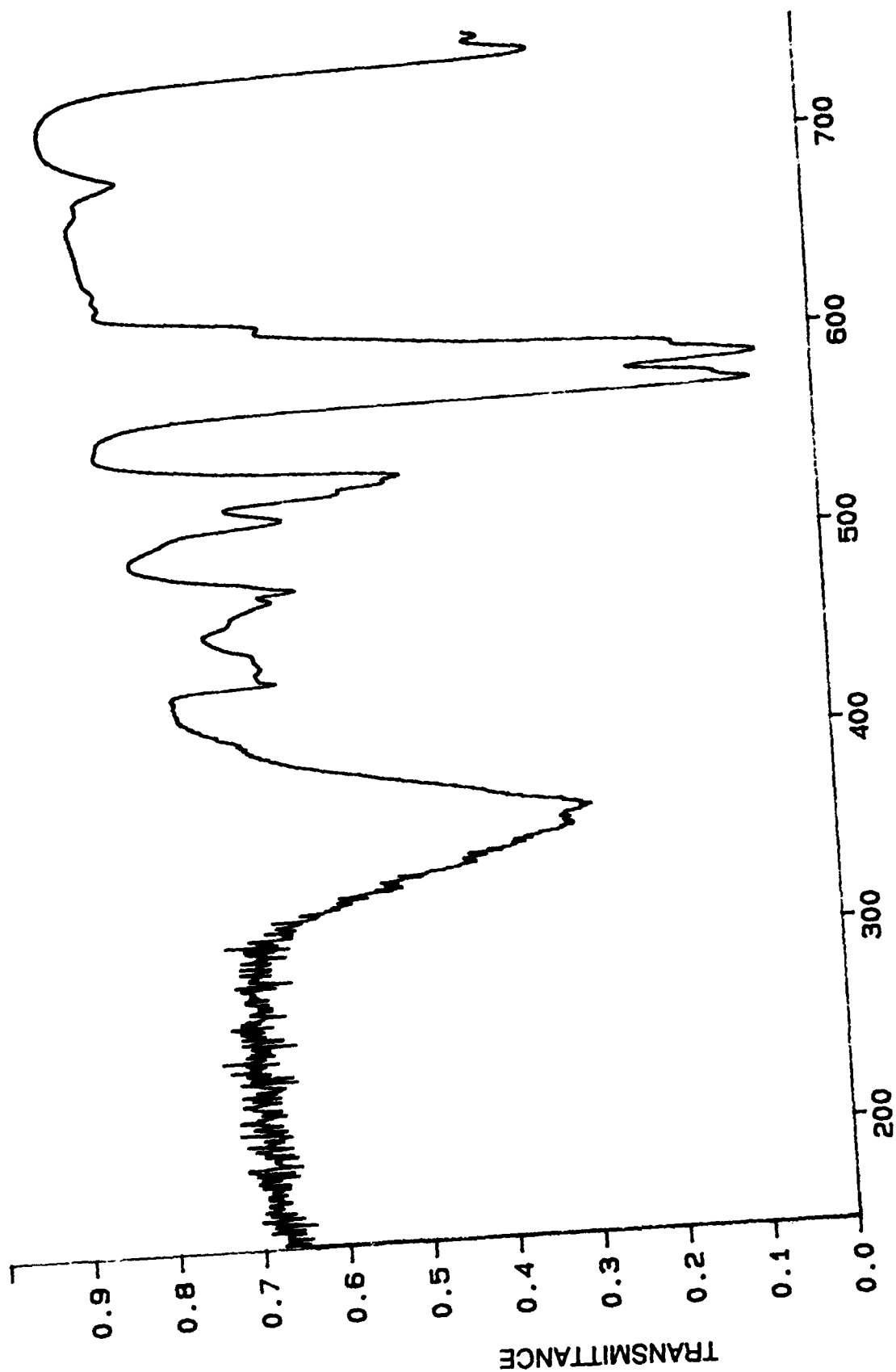


Figure 48
Transmittance of Filter 3 lining 100 W Sylvania Bulb

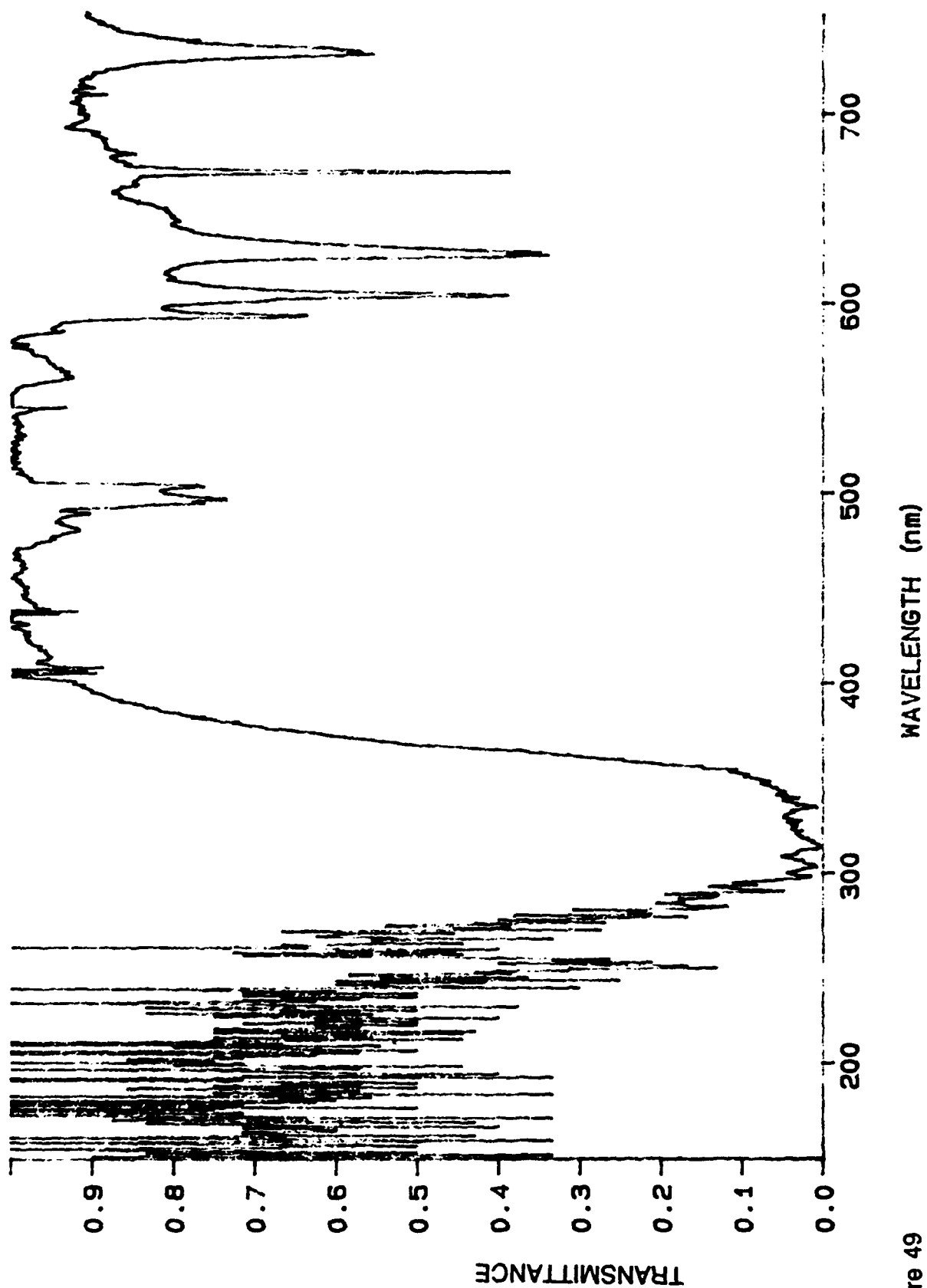


Figure 49

Transmittance of Long Pass Filter 4

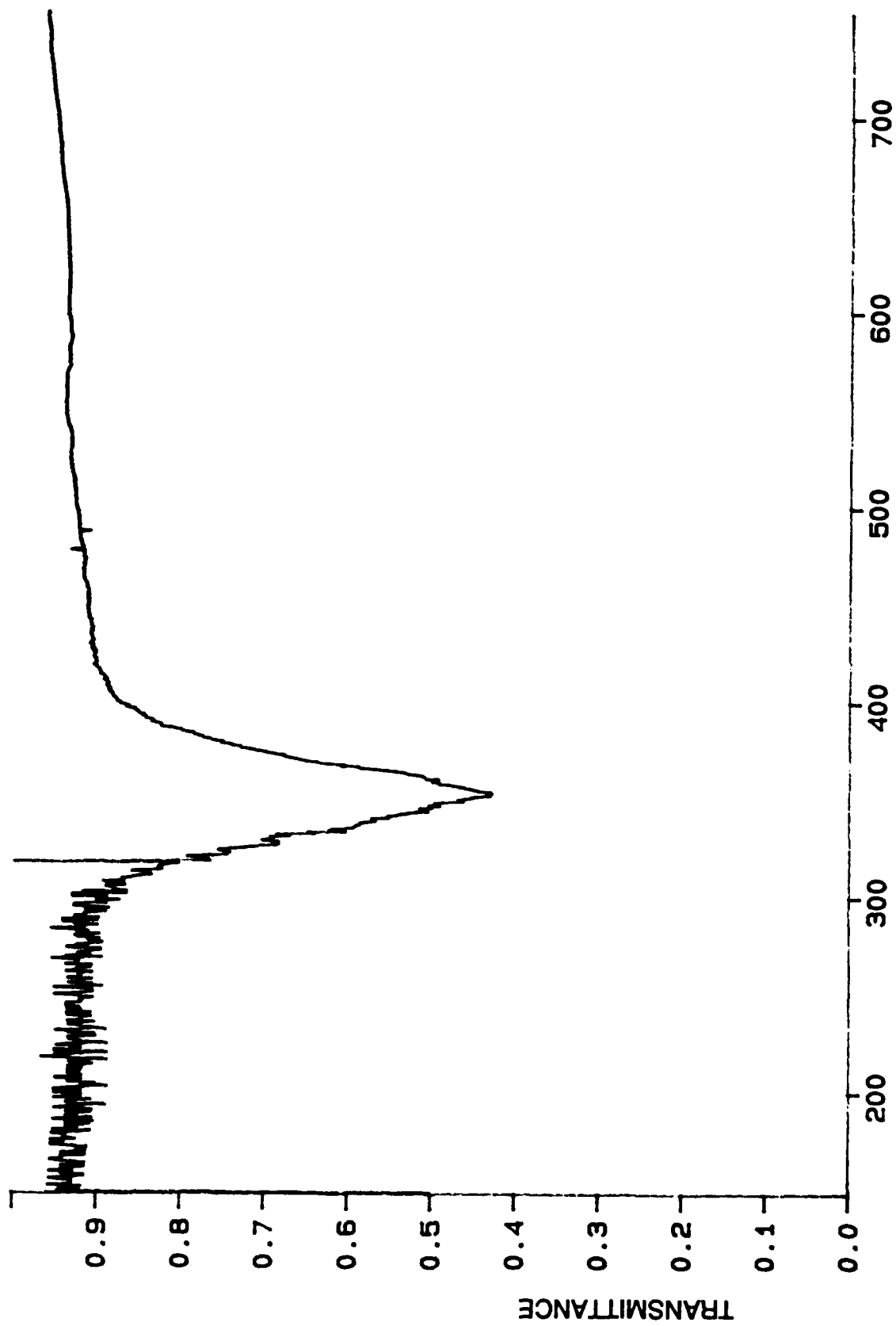


Figure 50

Transmittance of Filter 4 Using 100 W Sylvania Bulb

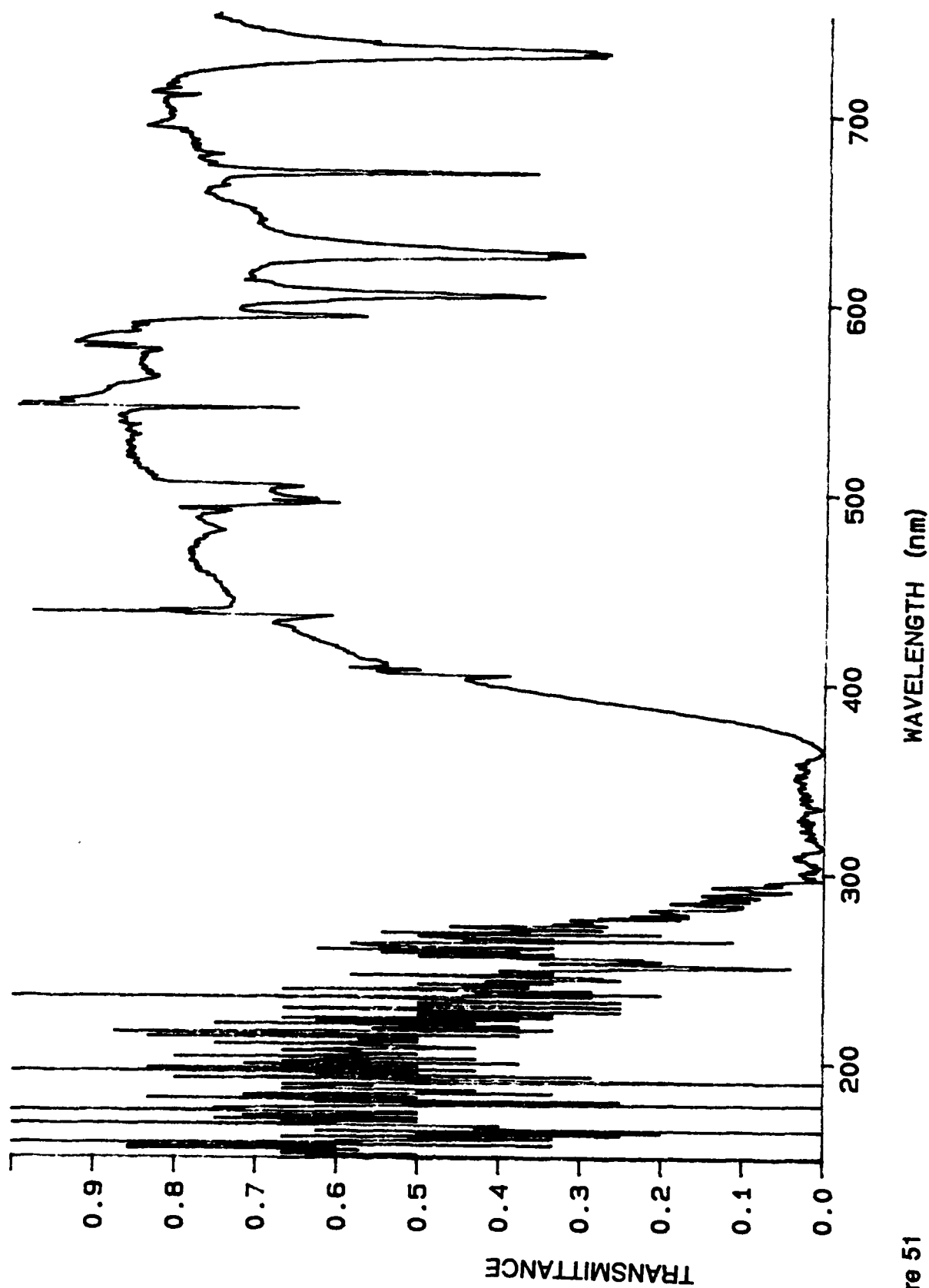


Figure 51
Transmittance of Long Pass Filter 5

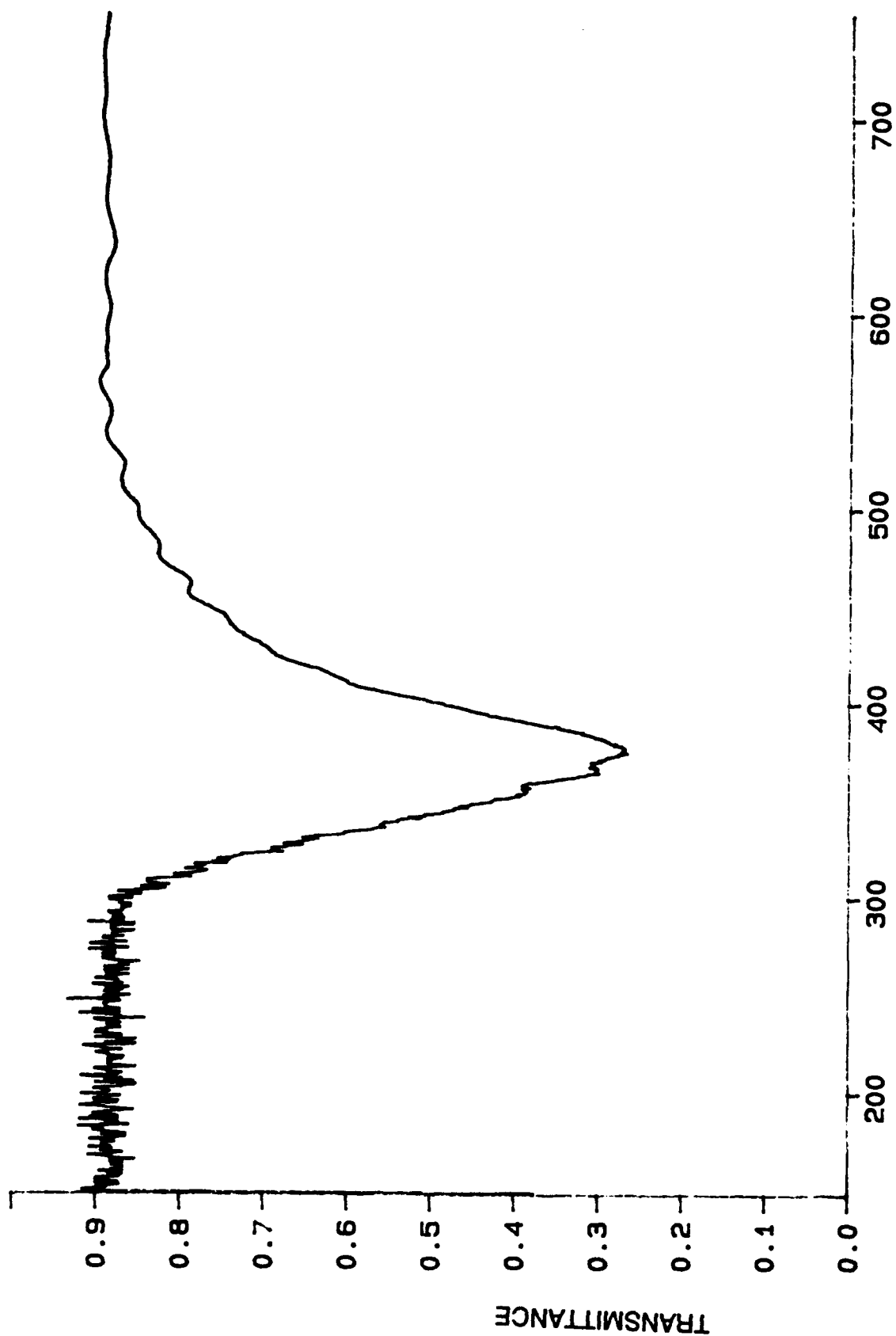


Figure 52
Transmittance of Filter 5 Using 100 W Sylvania Bulb

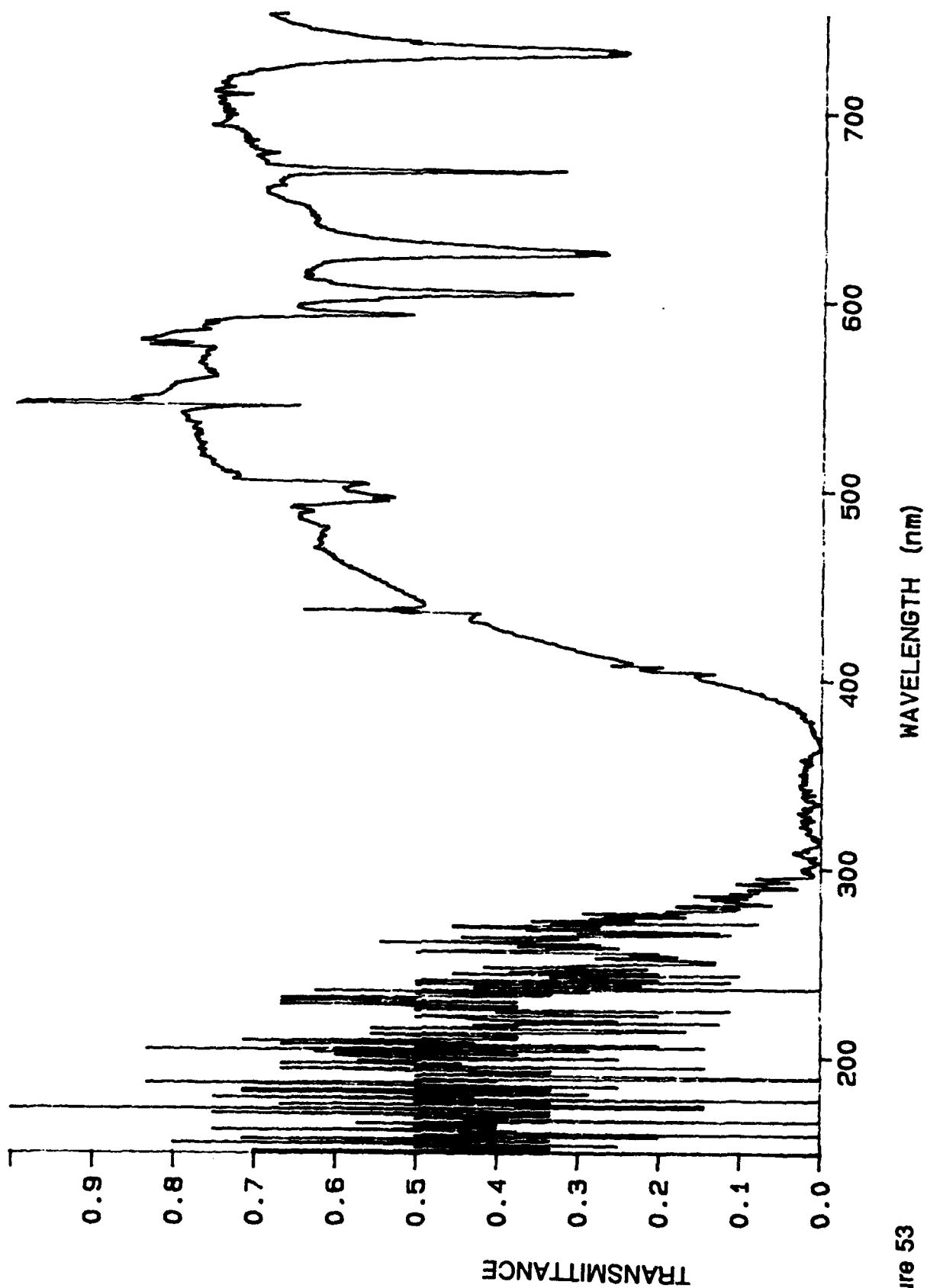


Figure 53
Transmittance of Long Pass Filter 6

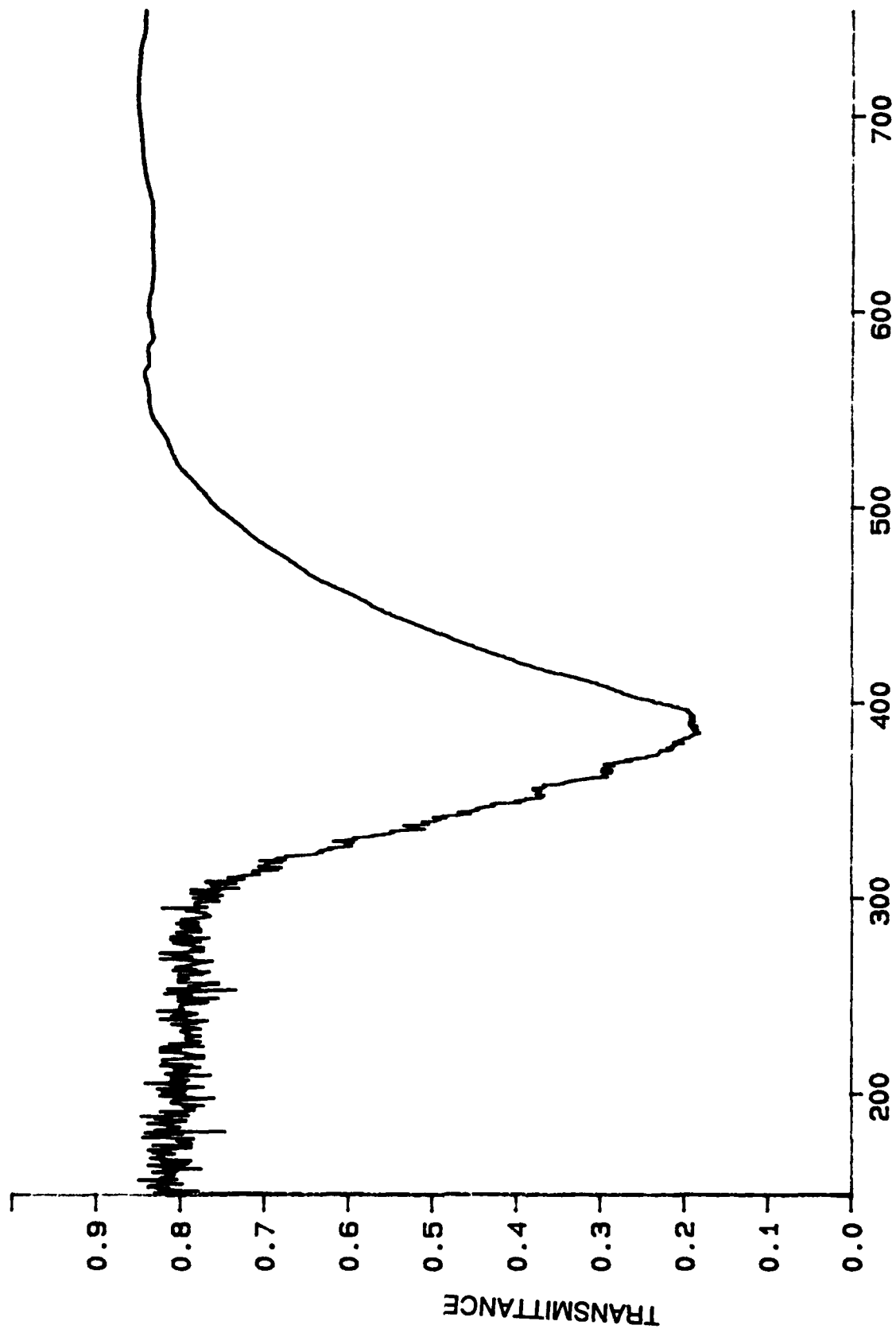


Figure 54
Transmittance of Filter 6 Using 100 W Sylvania Bulb

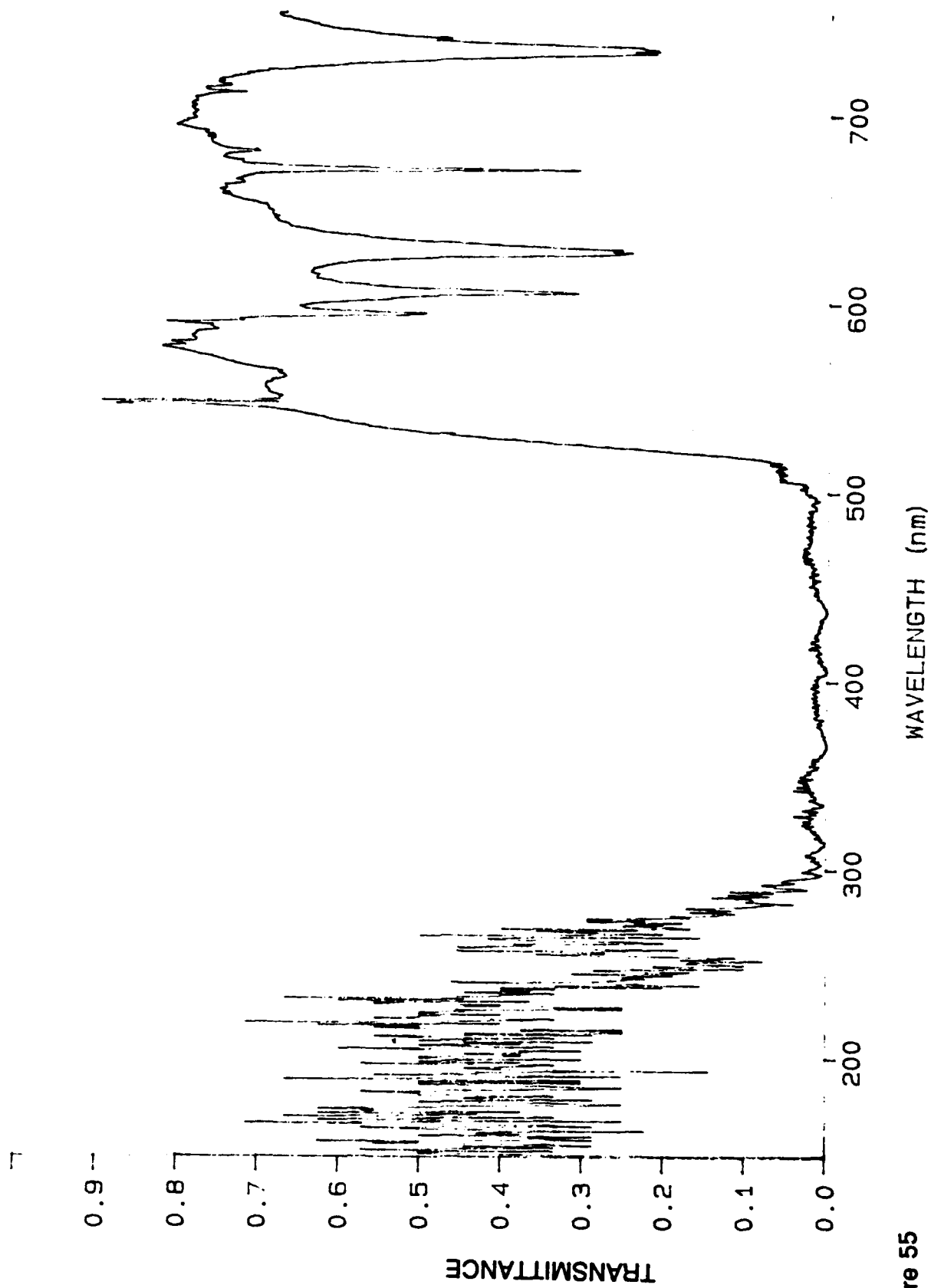


Figure 55
Transmittance of Long Pass Filter 7

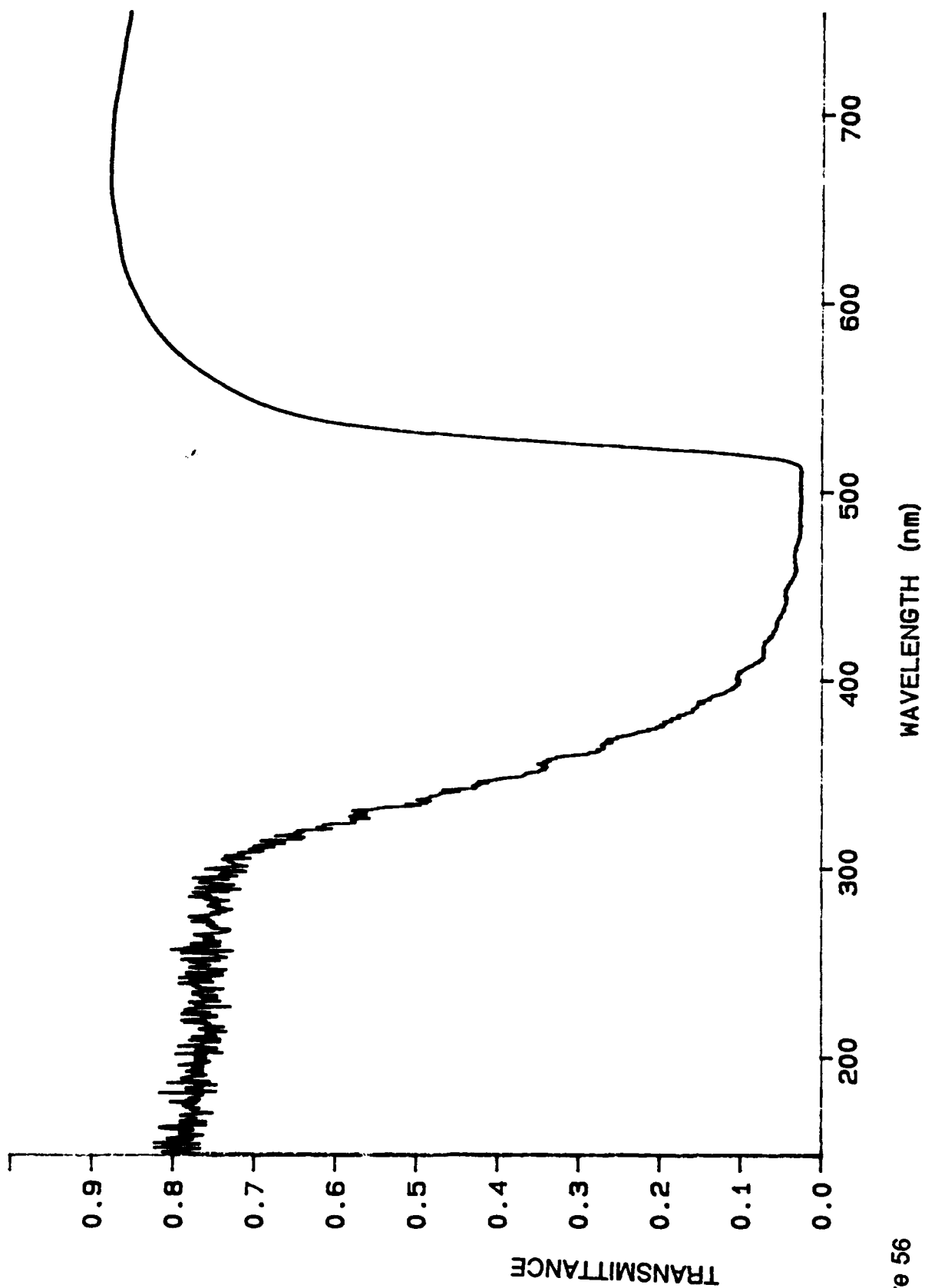


Figure 56

Transmittance of Filter 7 Using 100 W Sylvania Bulb

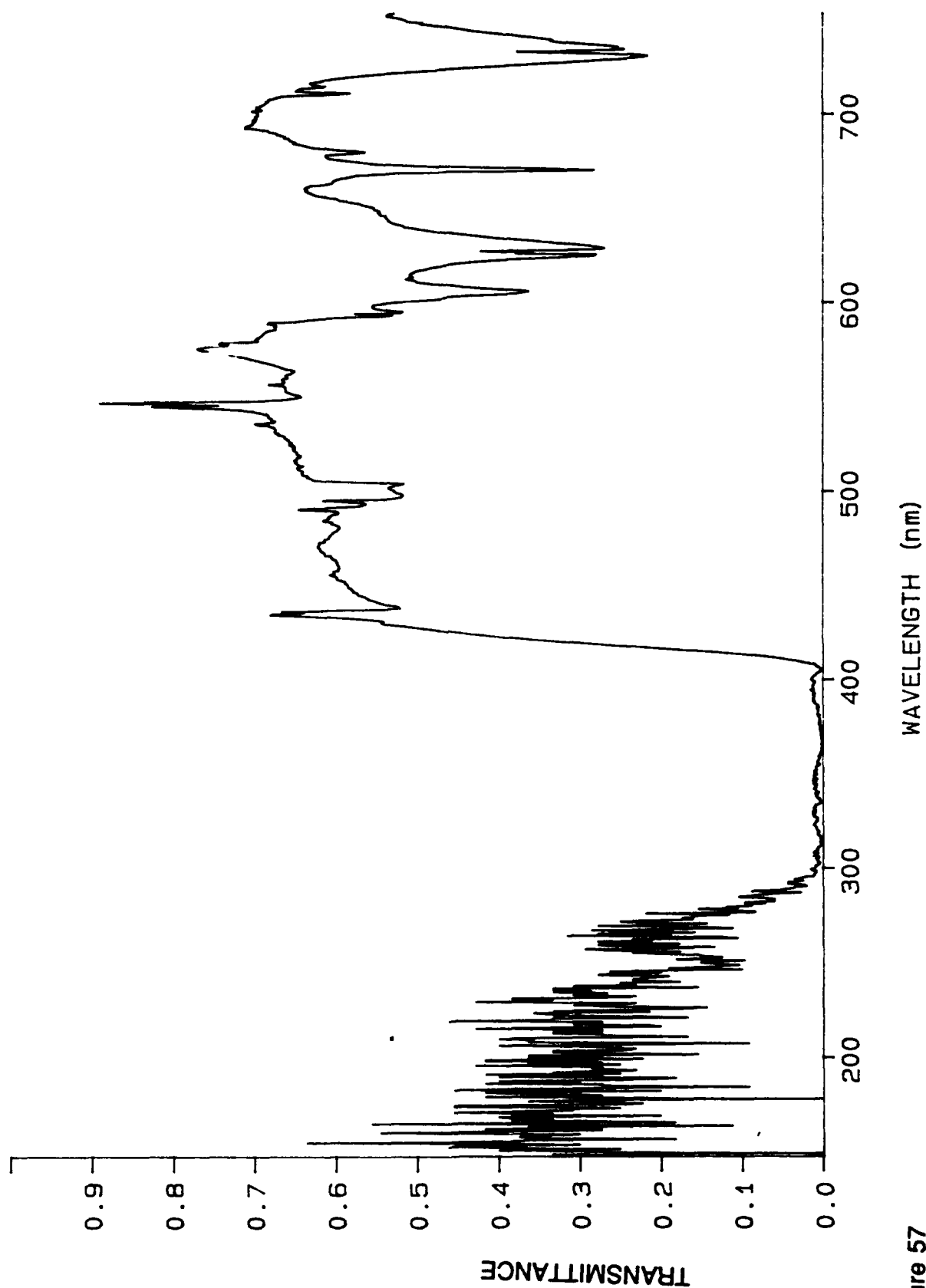


Figure 57
Transmittance of Safety Glasses

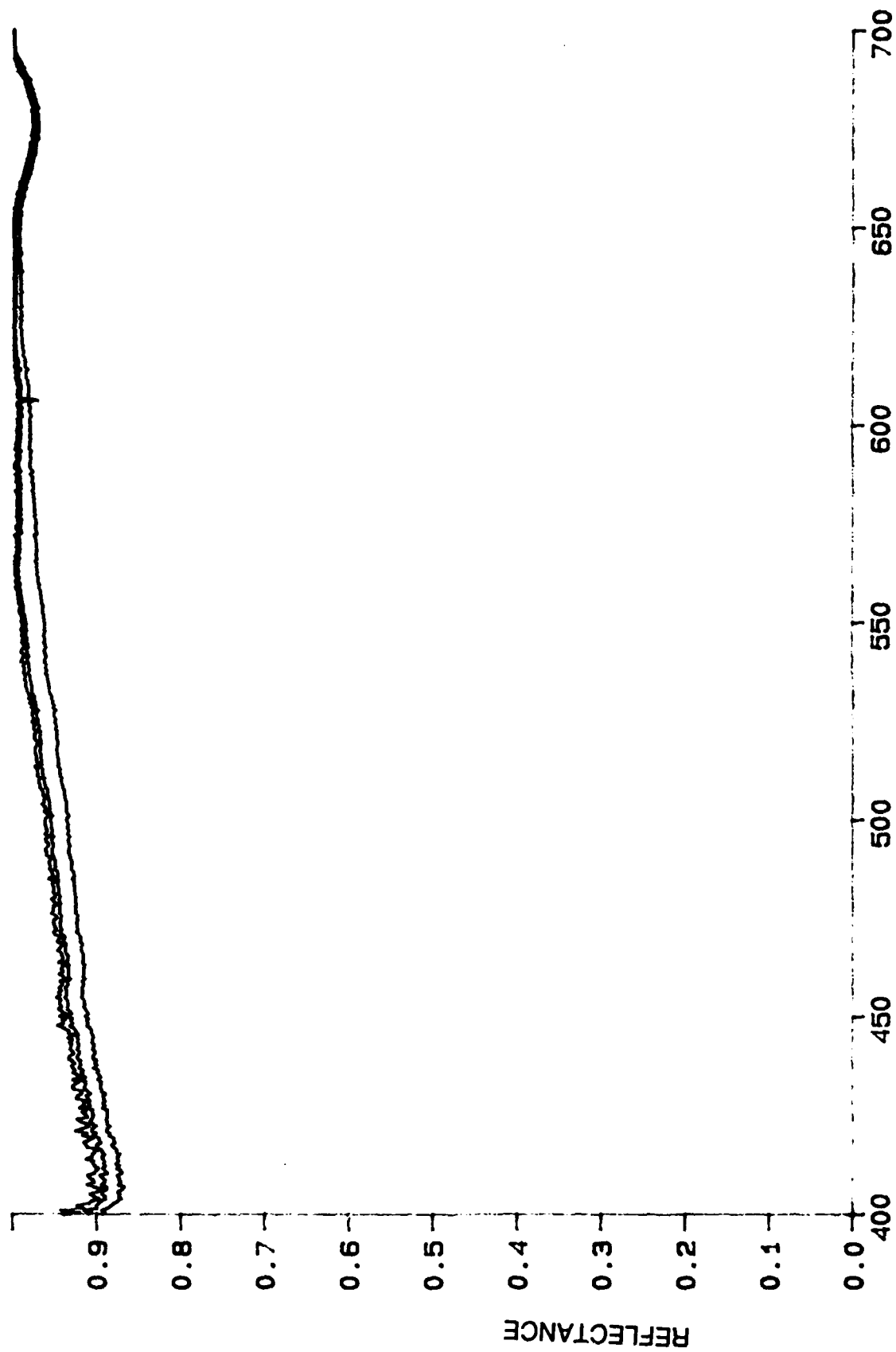


Figure 58
Reflectivity of Polished Aluminum Showing Additive Dispersion Effect

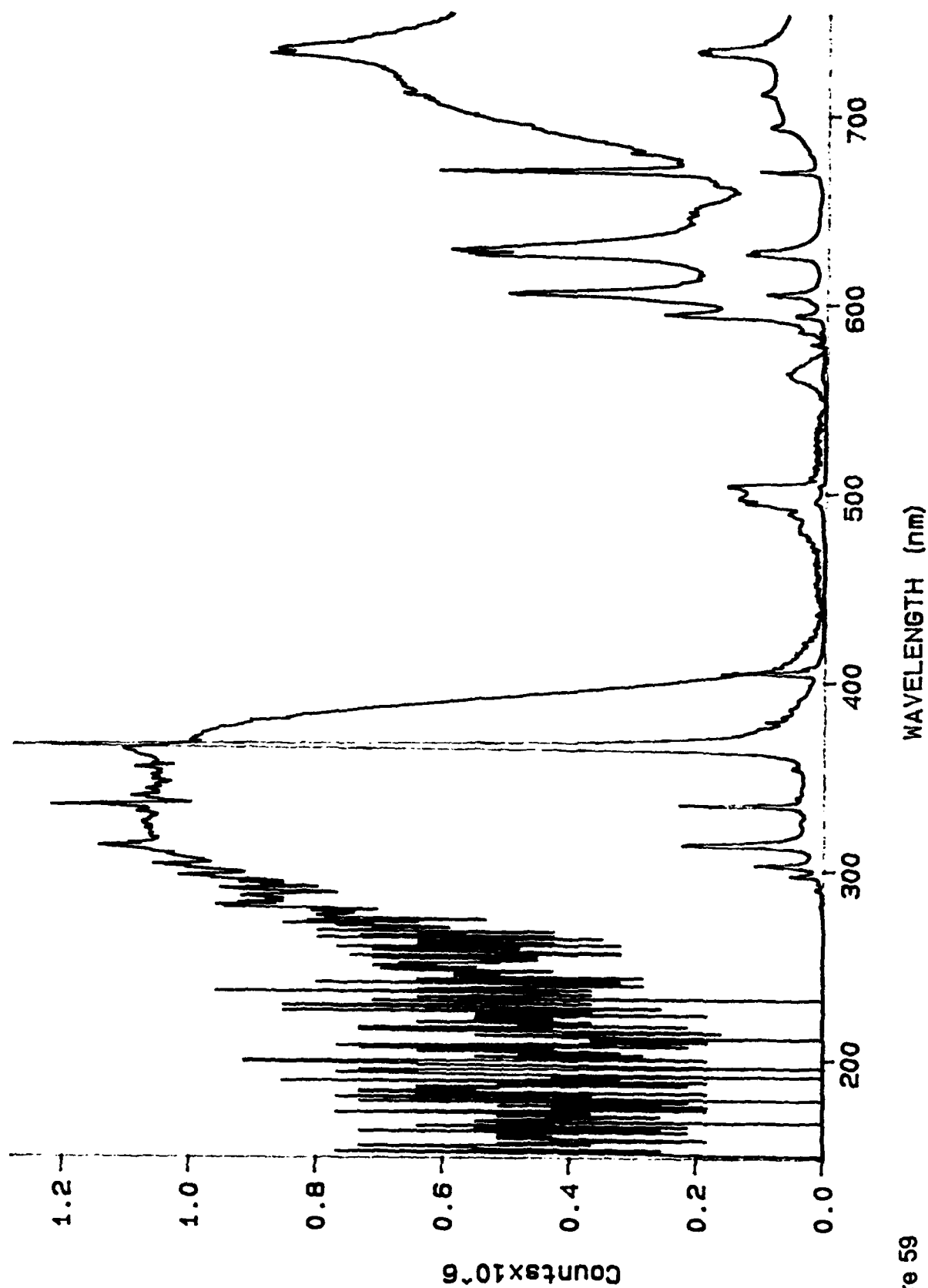


Figure 59
Mercury Arc Lamp Through Filter 3172 Off Polished Copper & Direct

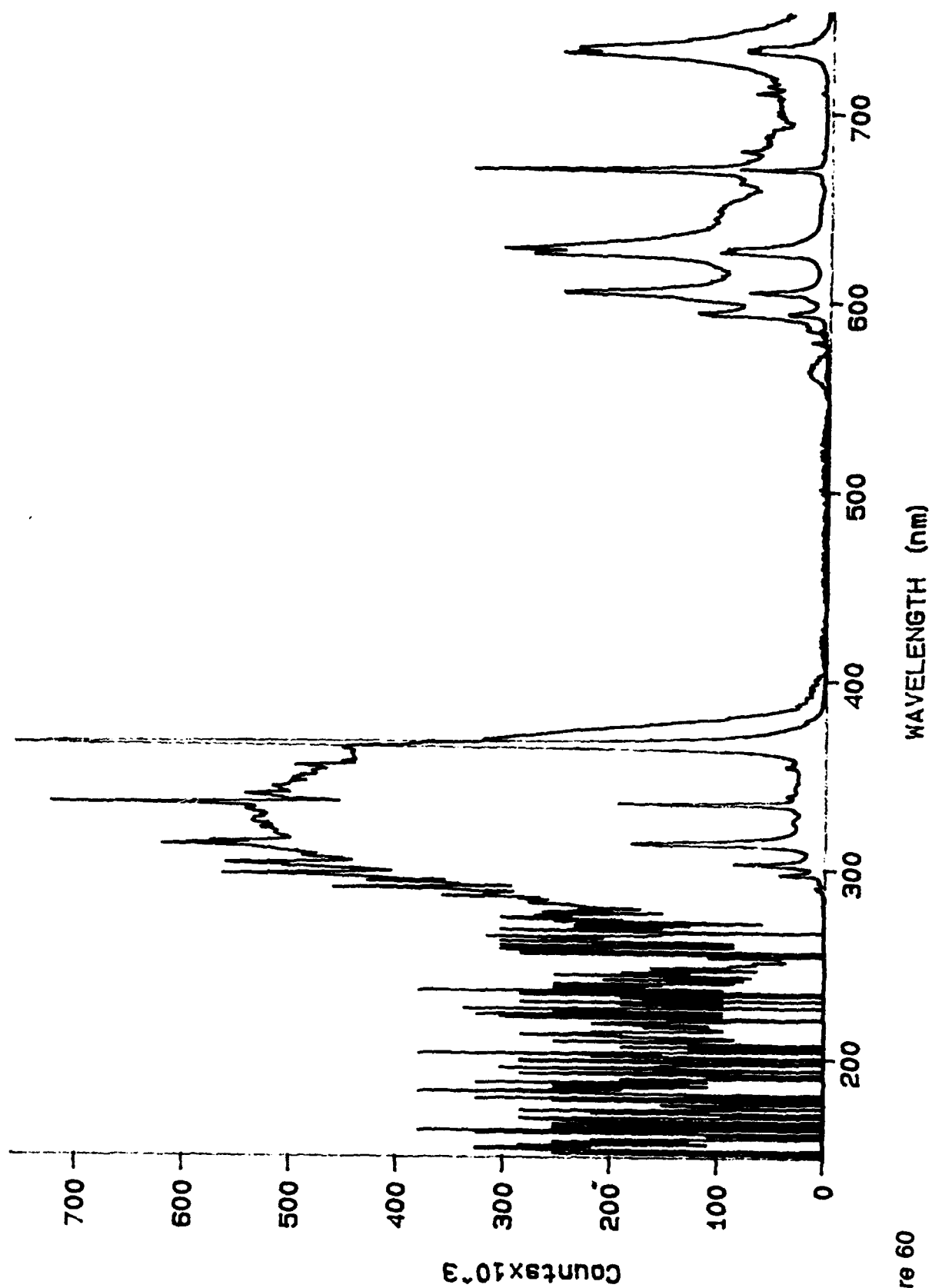


Figure 60
Mercury Arc Lamp Through Filter 3174 Off Polished Copper & Direct

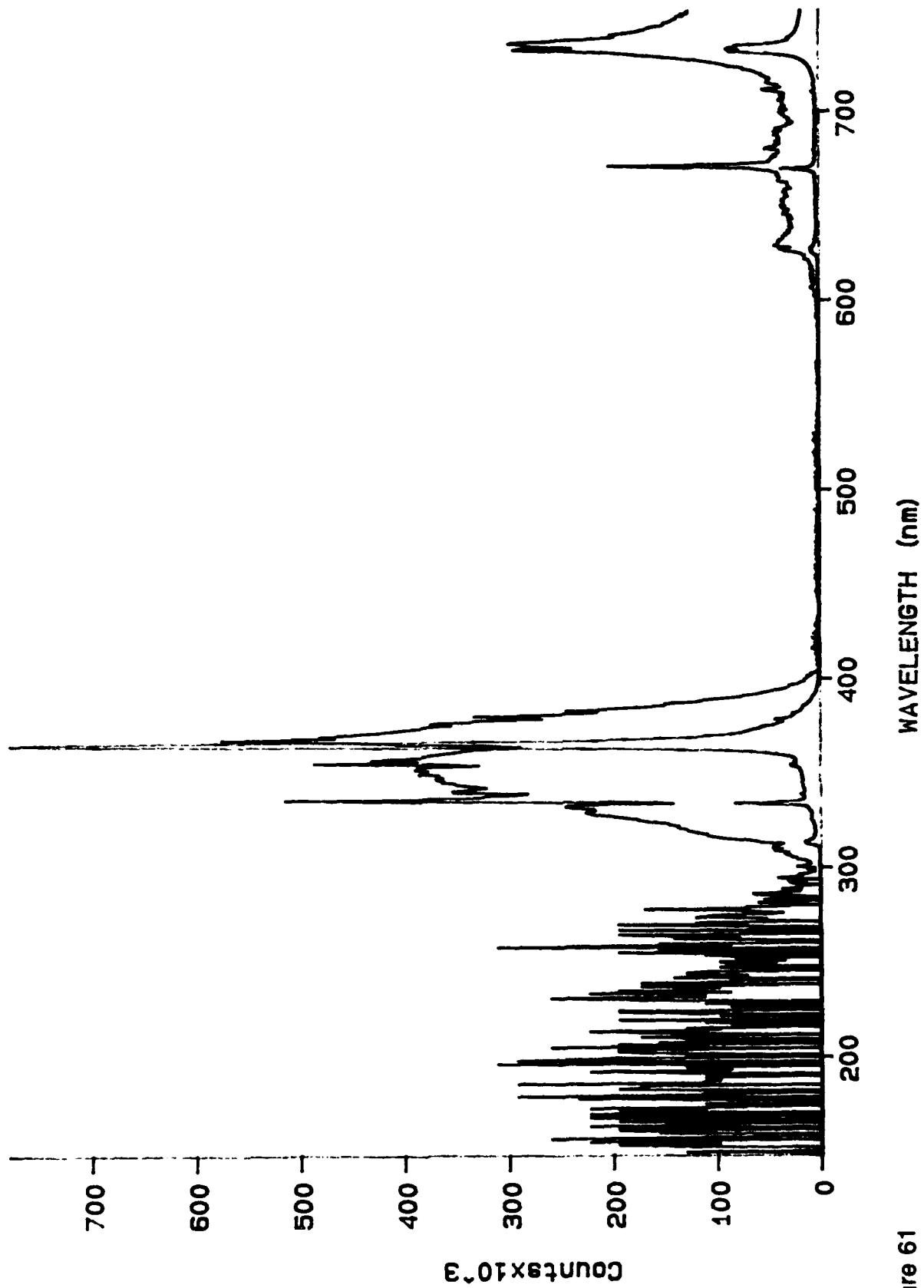


Figure 61
Mercury Arc Lamp Through Filter 3176 Off Polished Copper & Direct

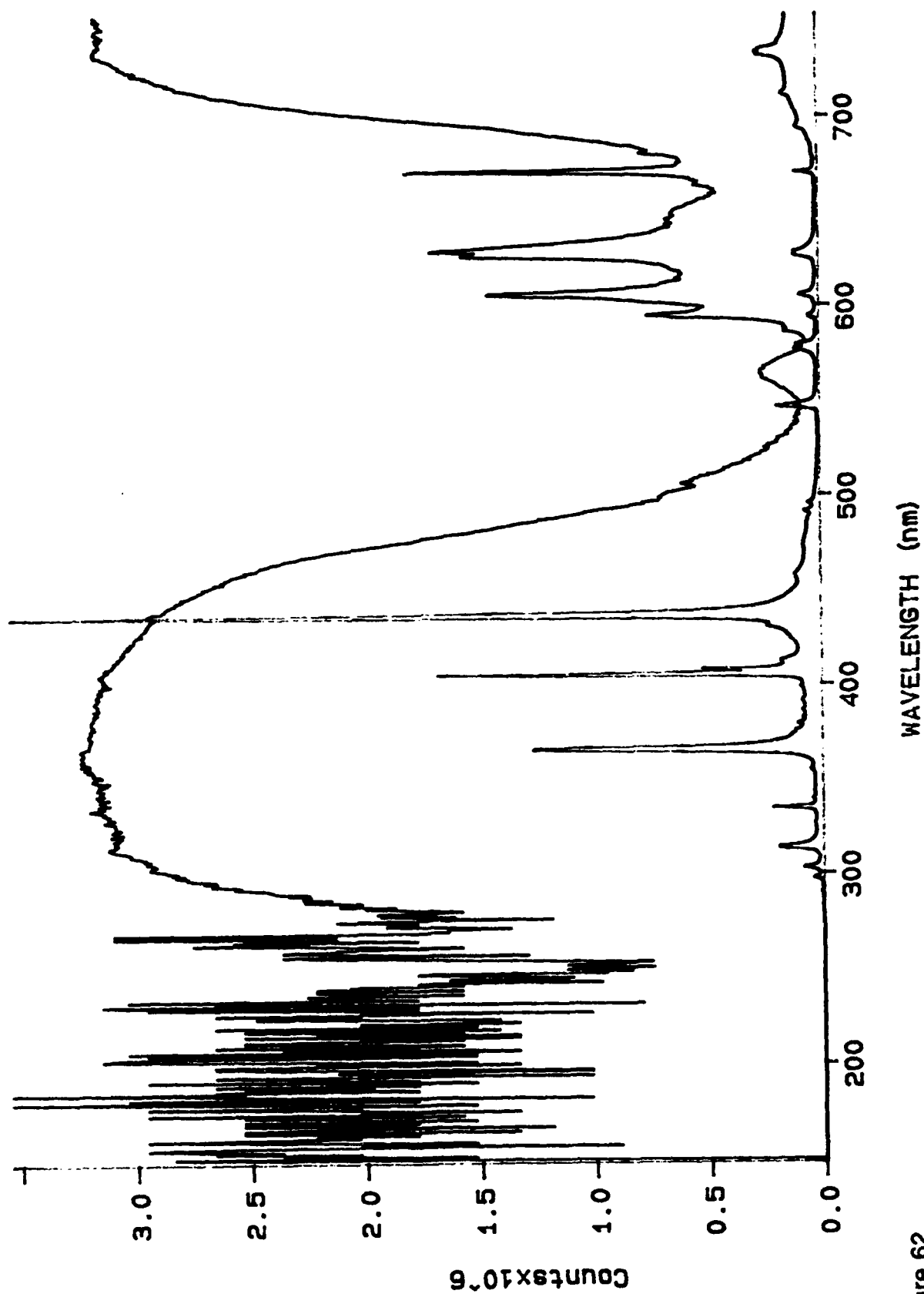


Figure 62
Mercury Arc Lamp Through Filter 3178 Off Polished Copper & Direct

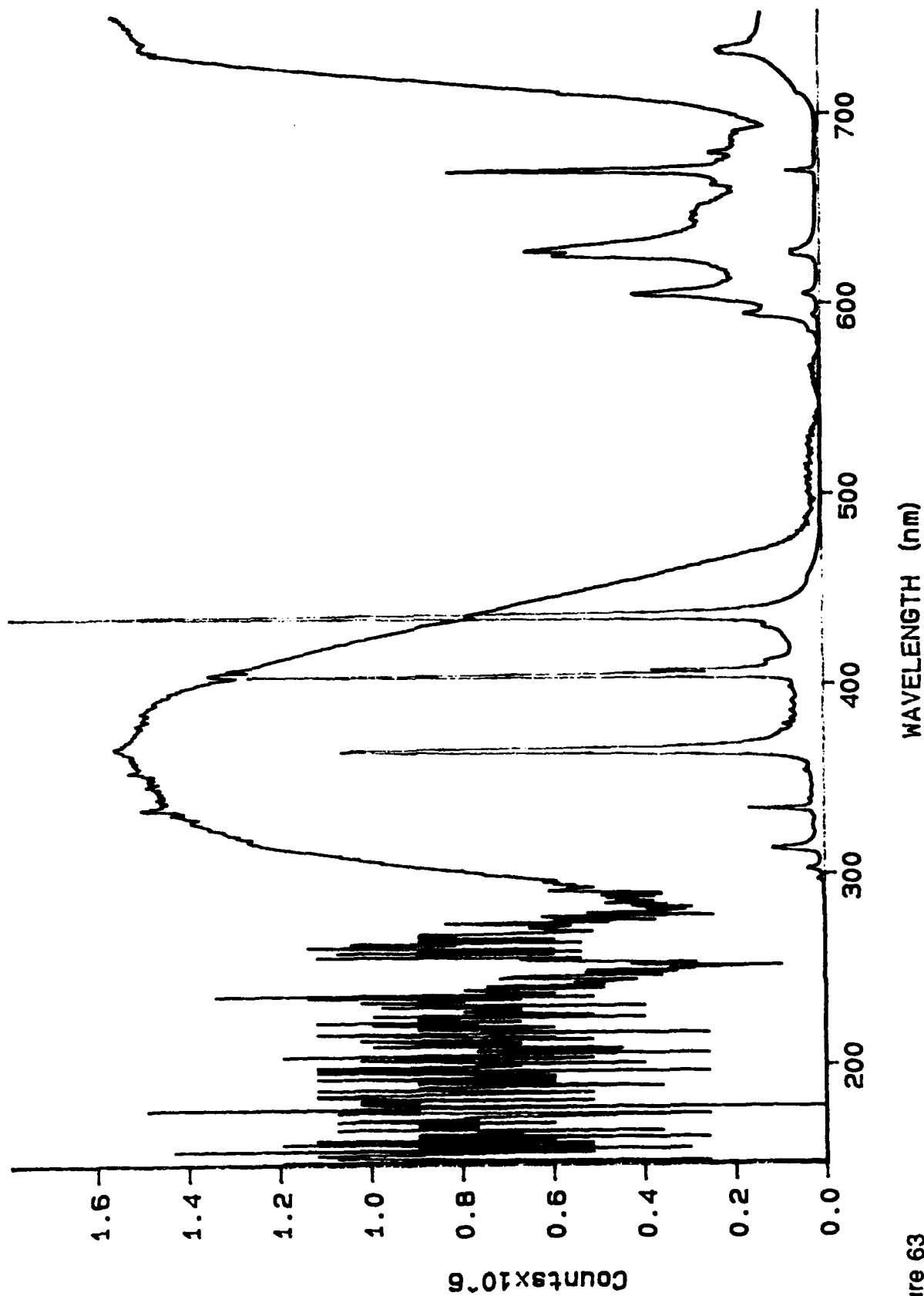


Figure 63
Mercury Arc Lamp Through Filter 3180 Off Polished Copper & Direct

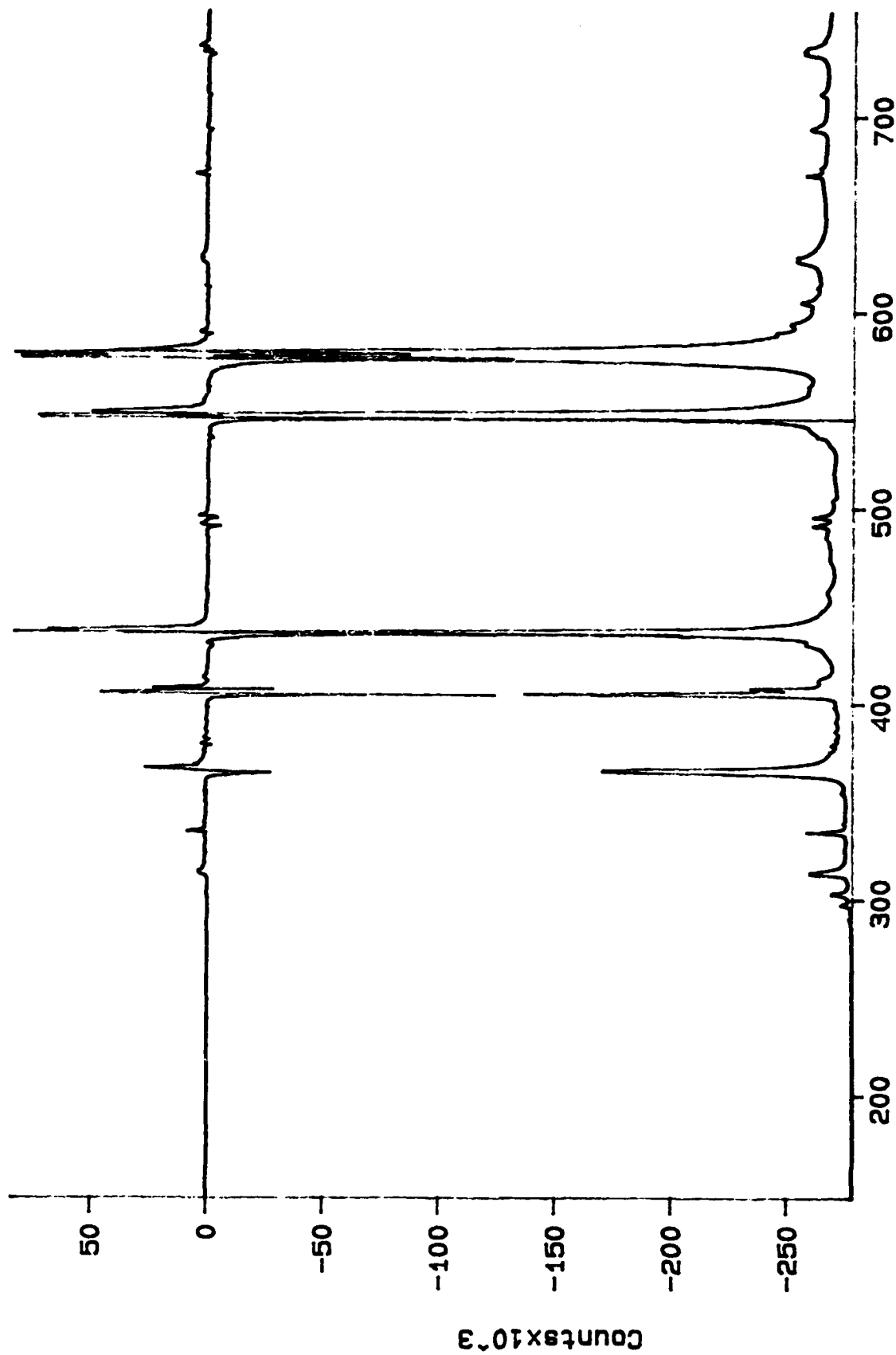


Figure 64
Luminescence Experiment Difference for Filter 1

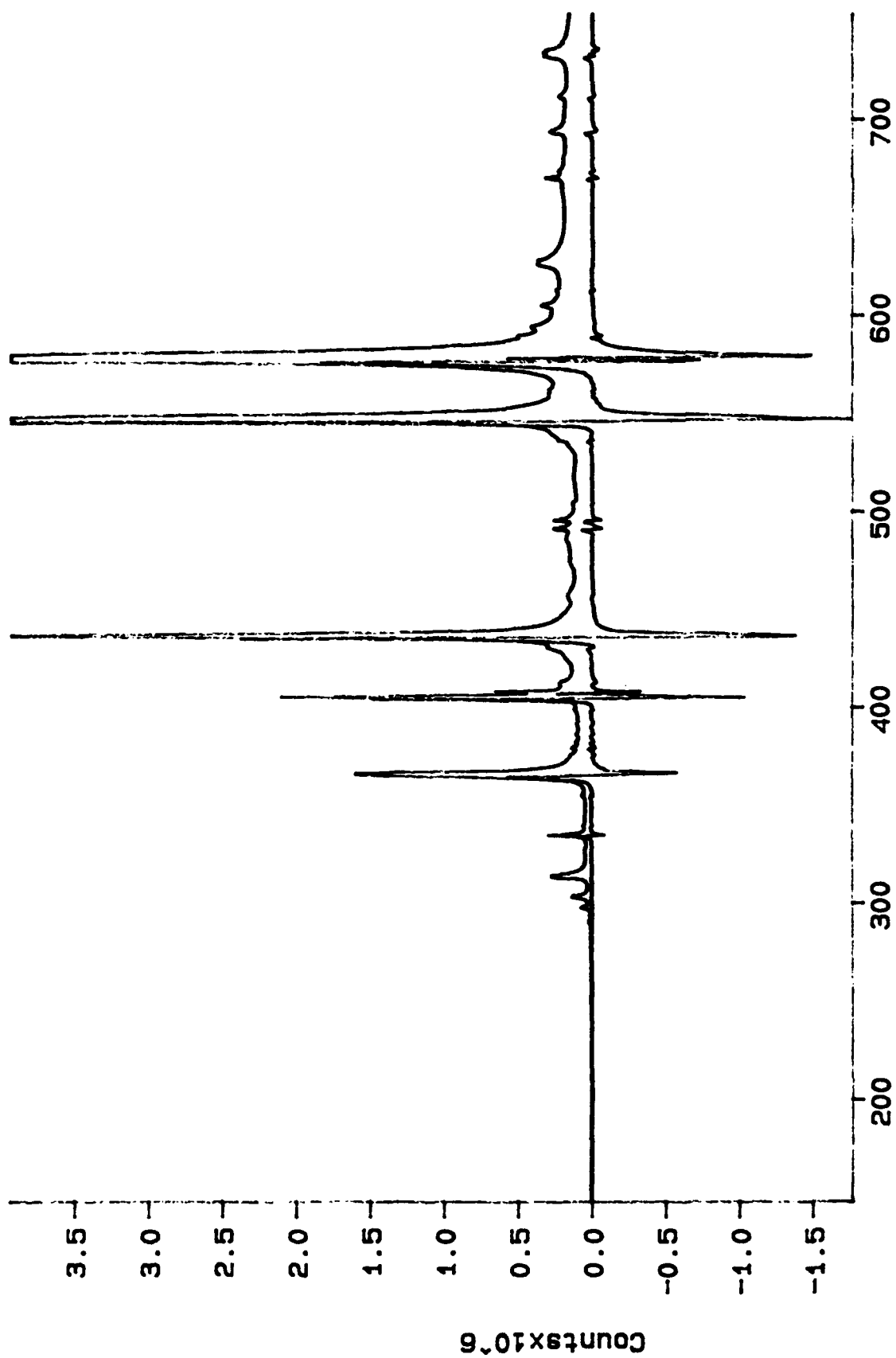


Figure 65

Luminescence, Experiment Difference for Filter 2

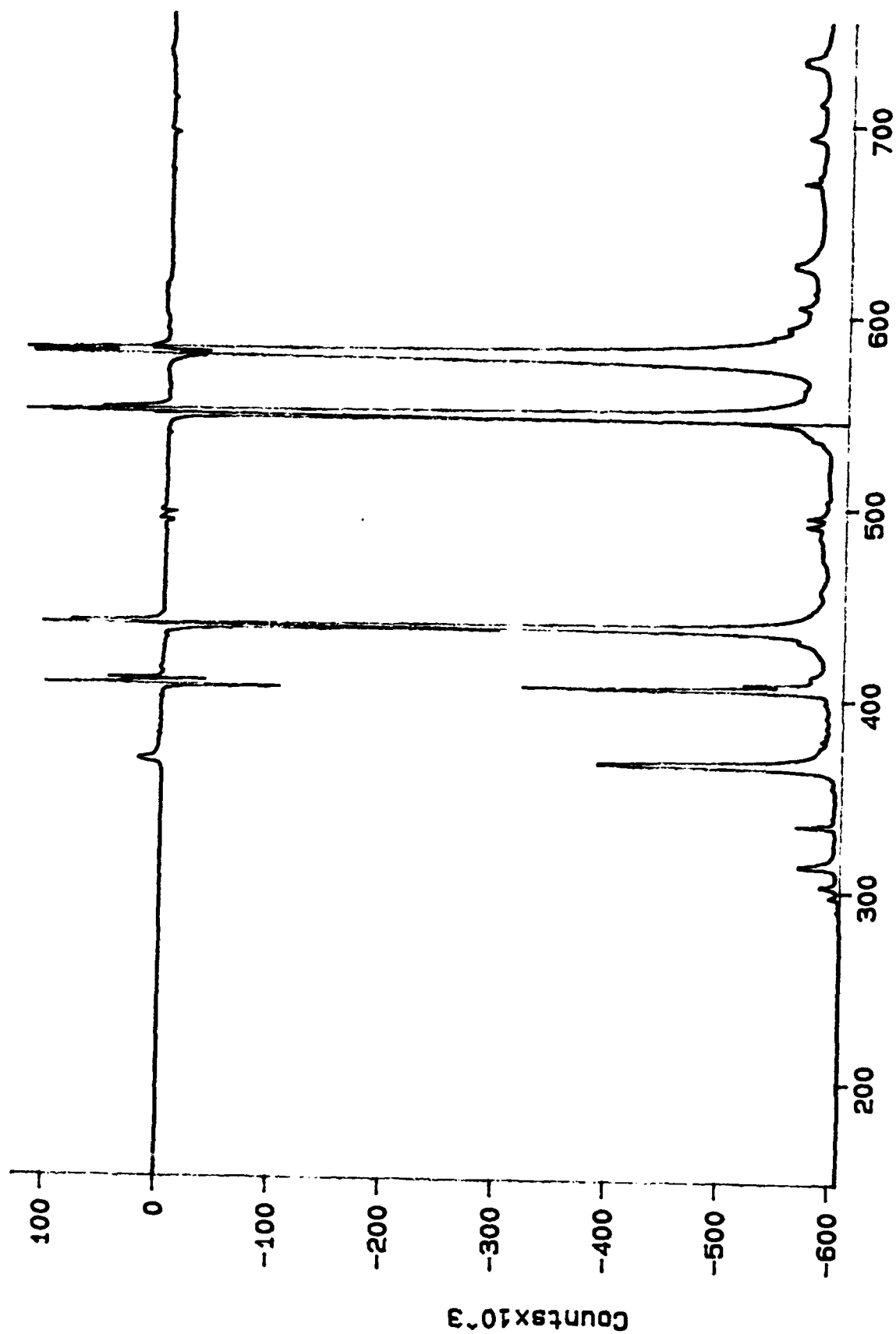


Figure 66
Luminescence Experiment Difference for Filter 3

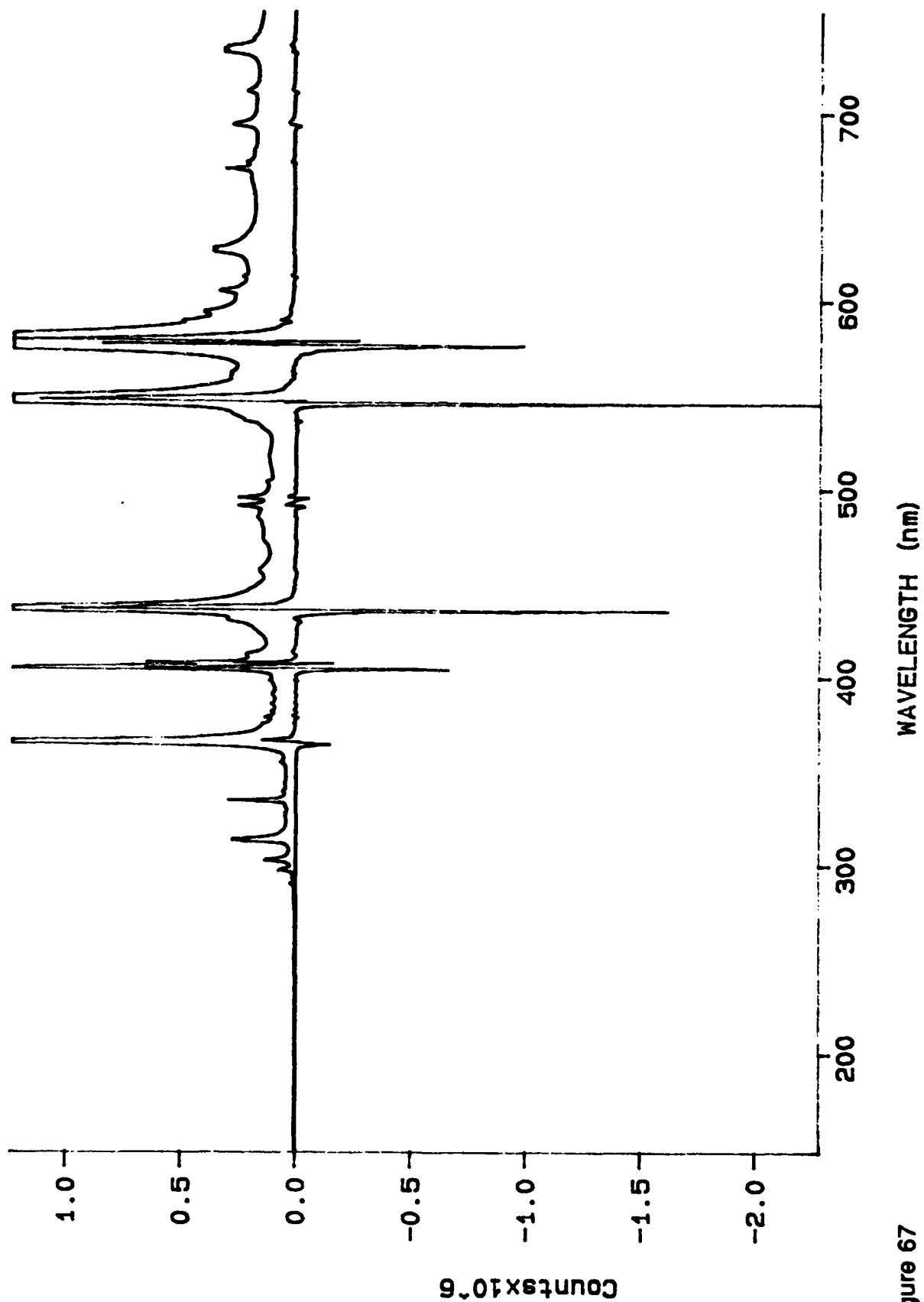


Figure 67
Luminescence Experiment Difference for Filter 4

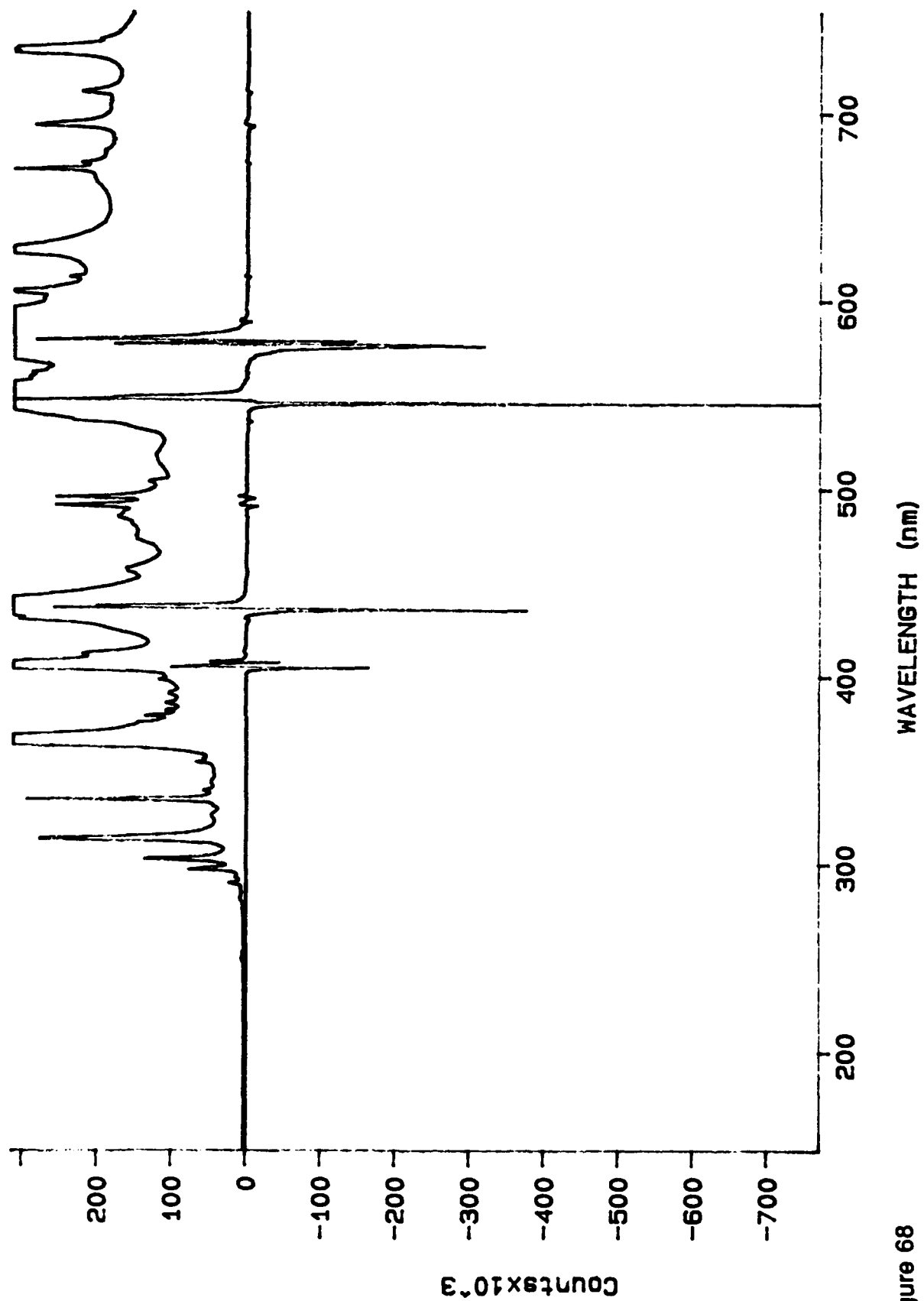


Figure 68
Luminescence Experiment Difference for Filter 5

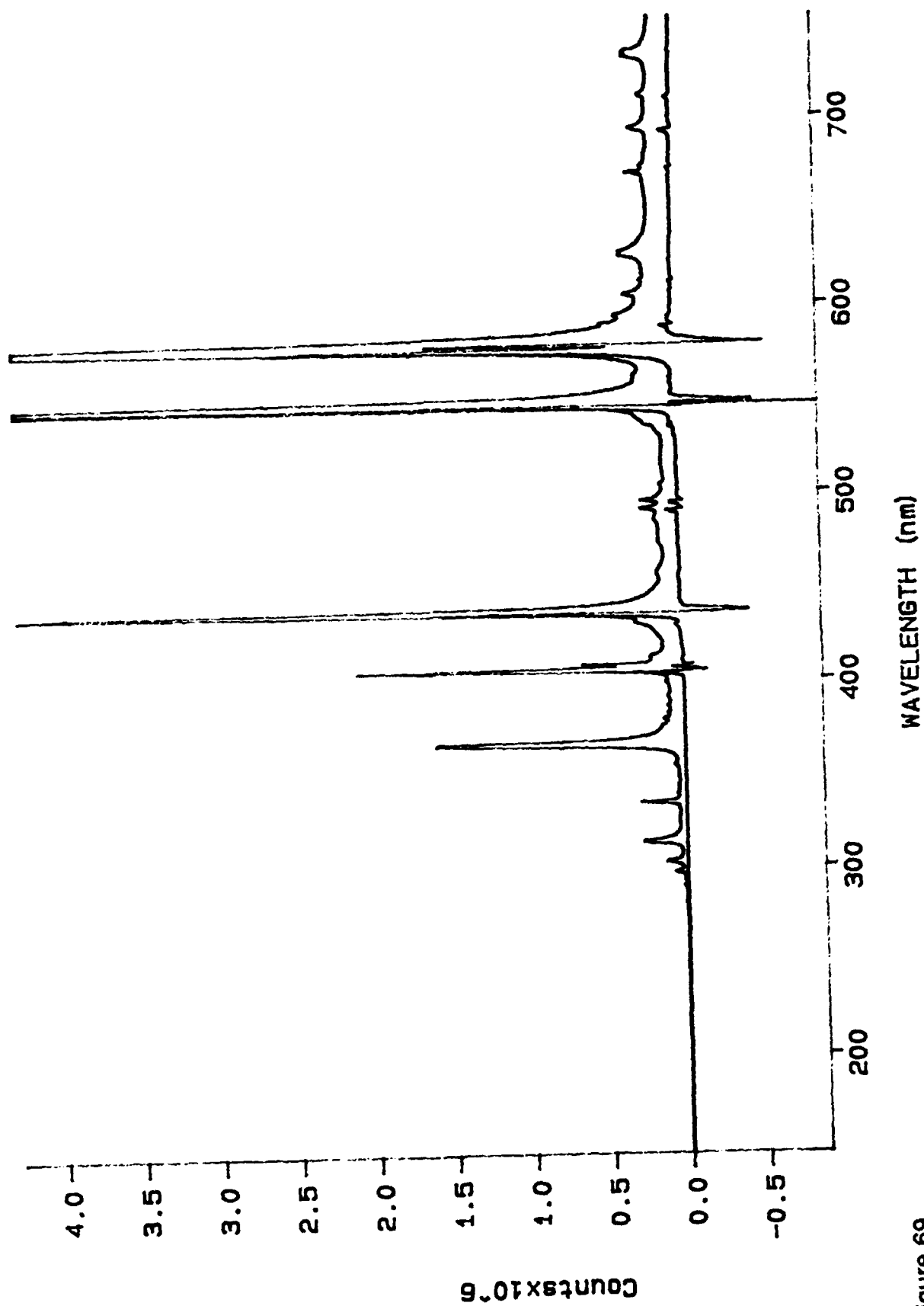


Figure 69
Luminescence Experiment Difference for Filter 6

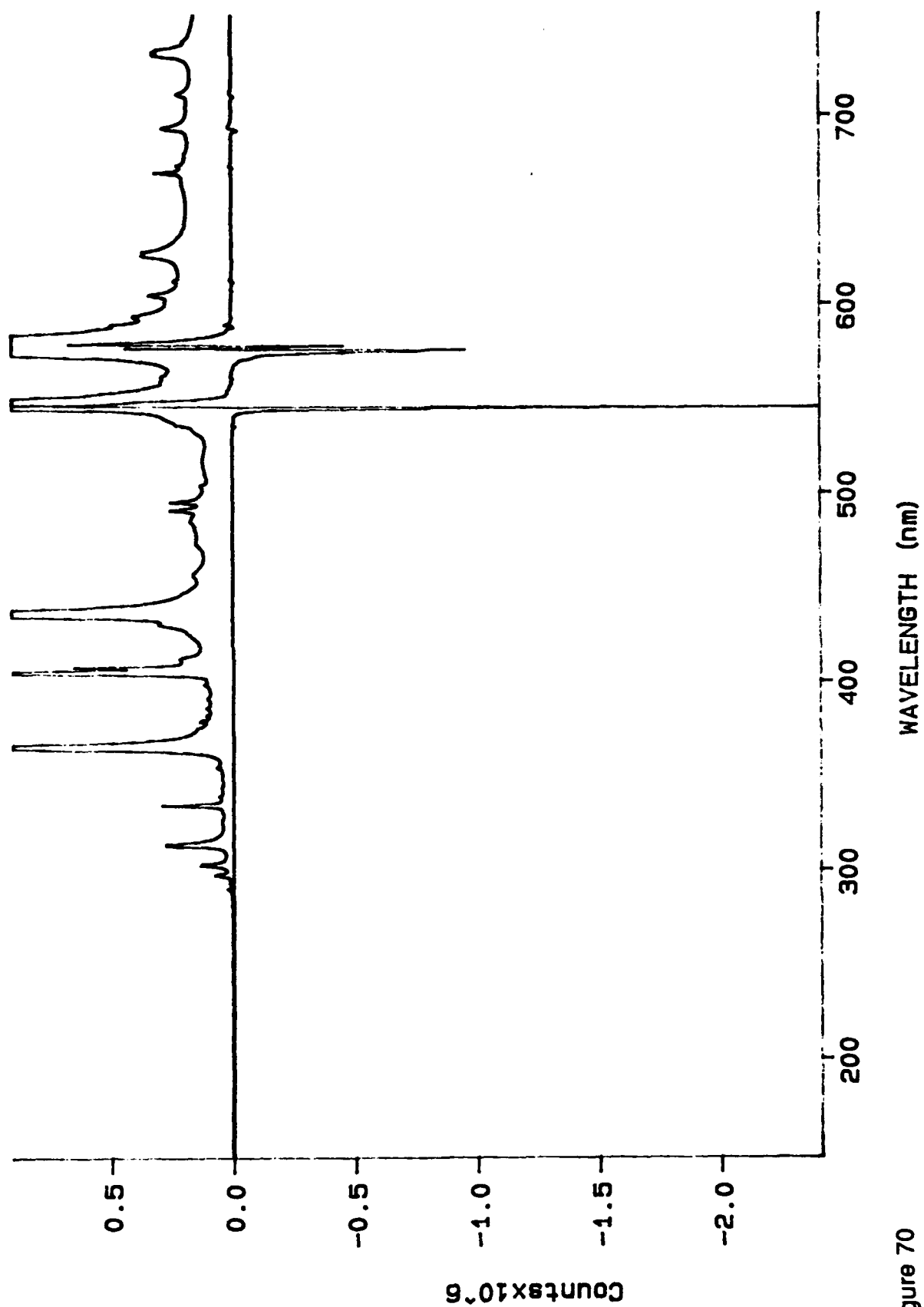


Figure 70
Luminescence Experiment Difference for Filter 7

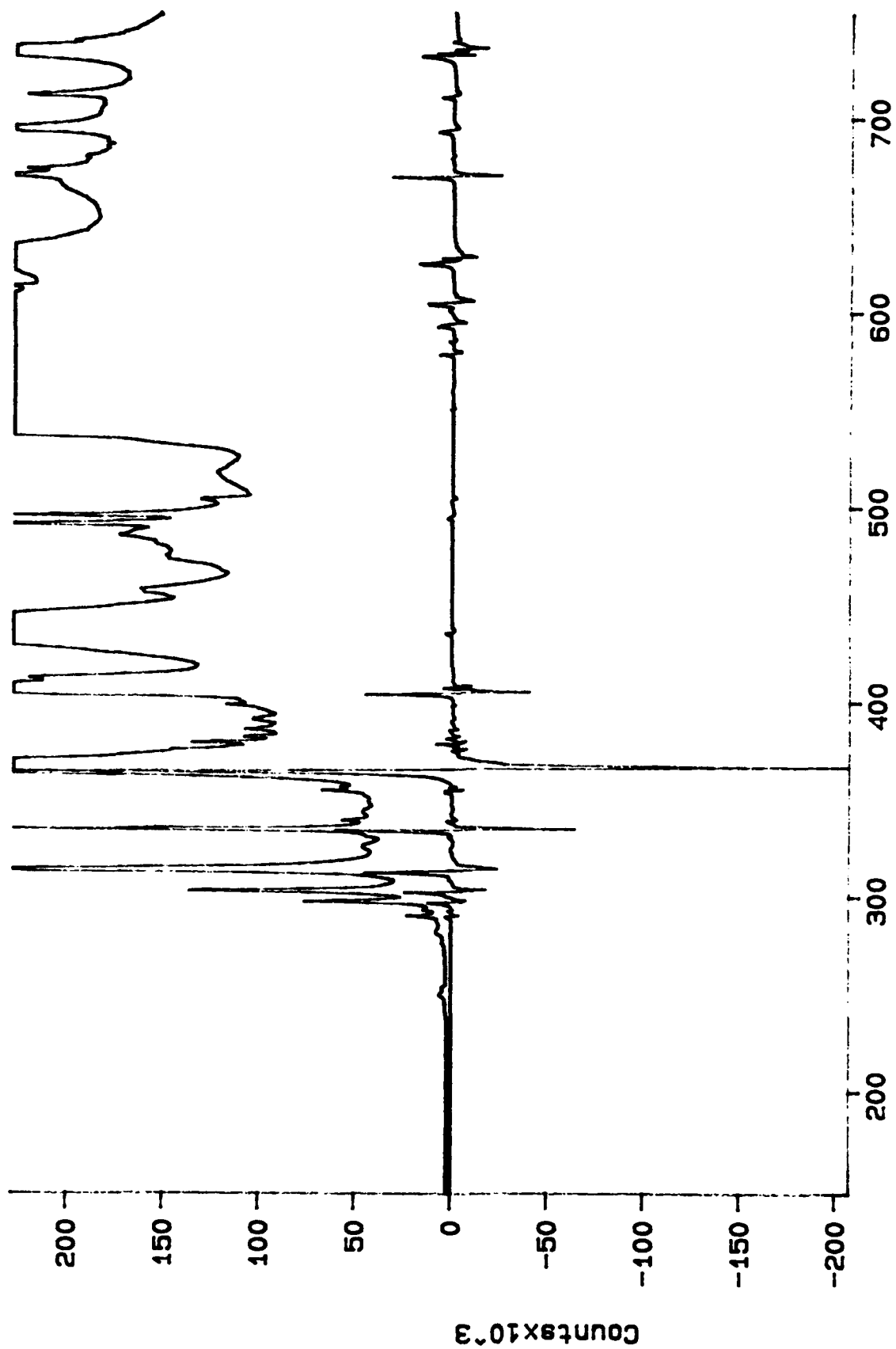


Figure 71

Luminescence Experiment Difference for Filter 3172

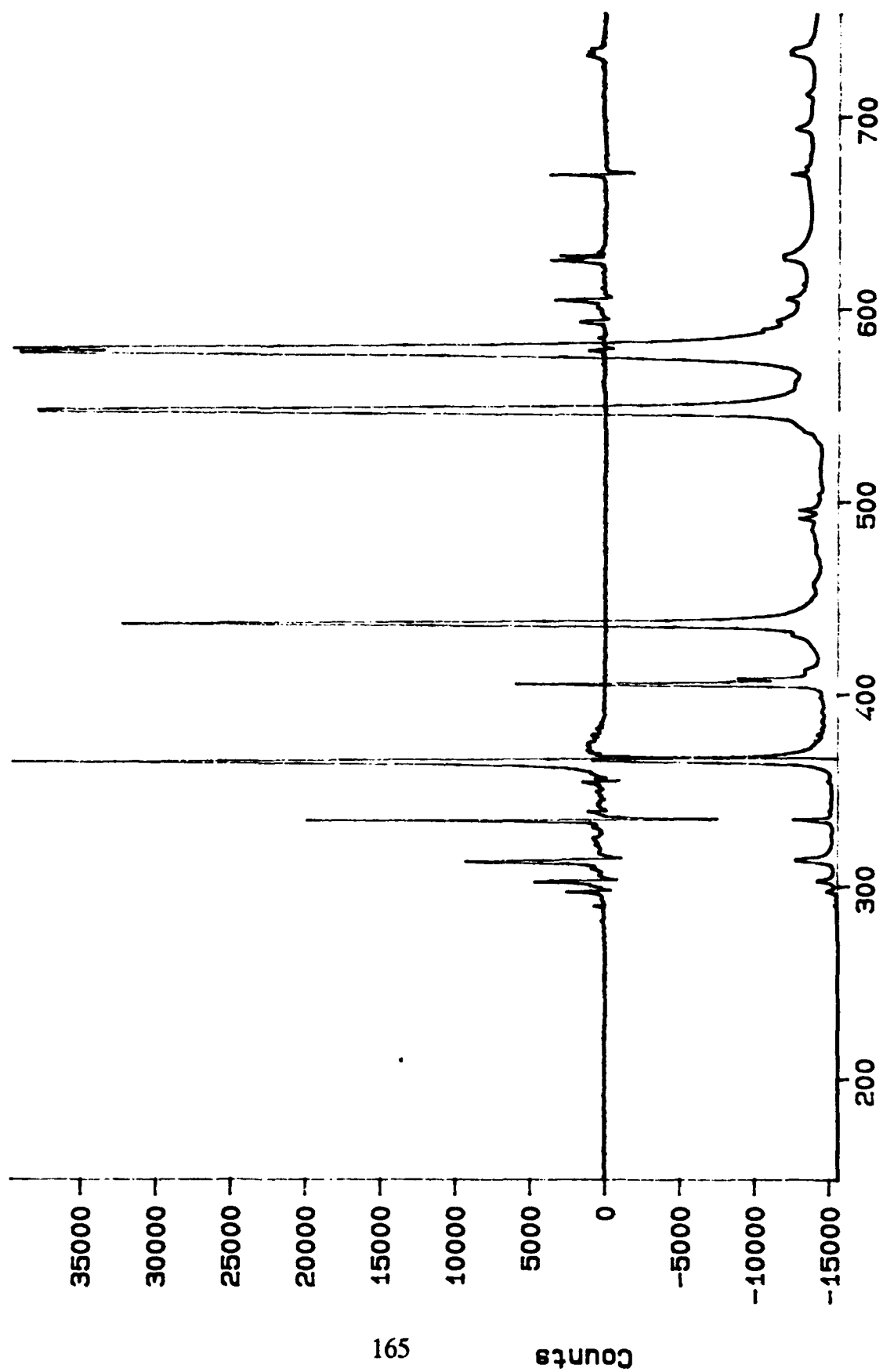


Figure 72

Luminescence Experiment Difference for Filter 3174

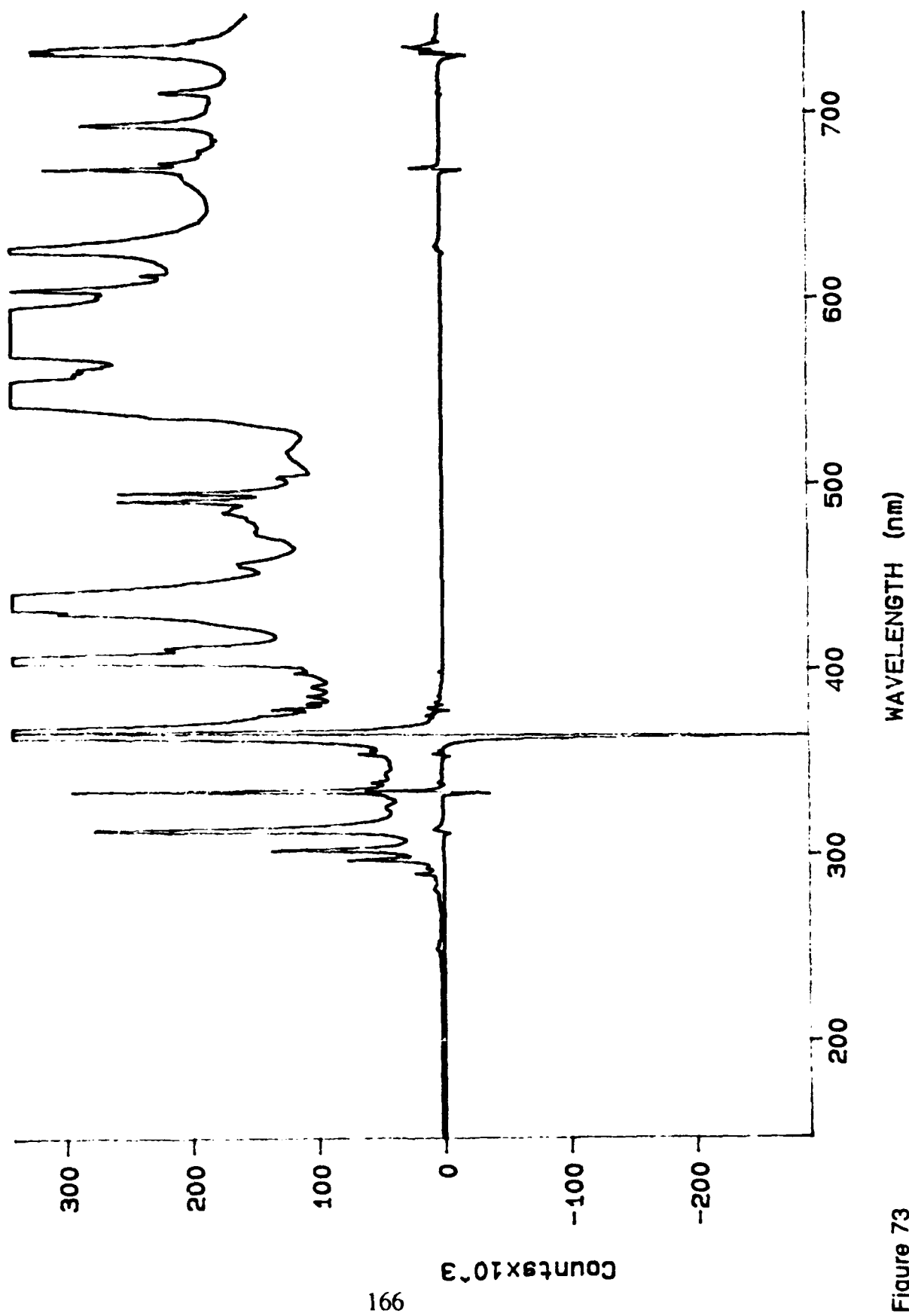


Figure 73

Luminescence Experiment Difference for Filter 3176

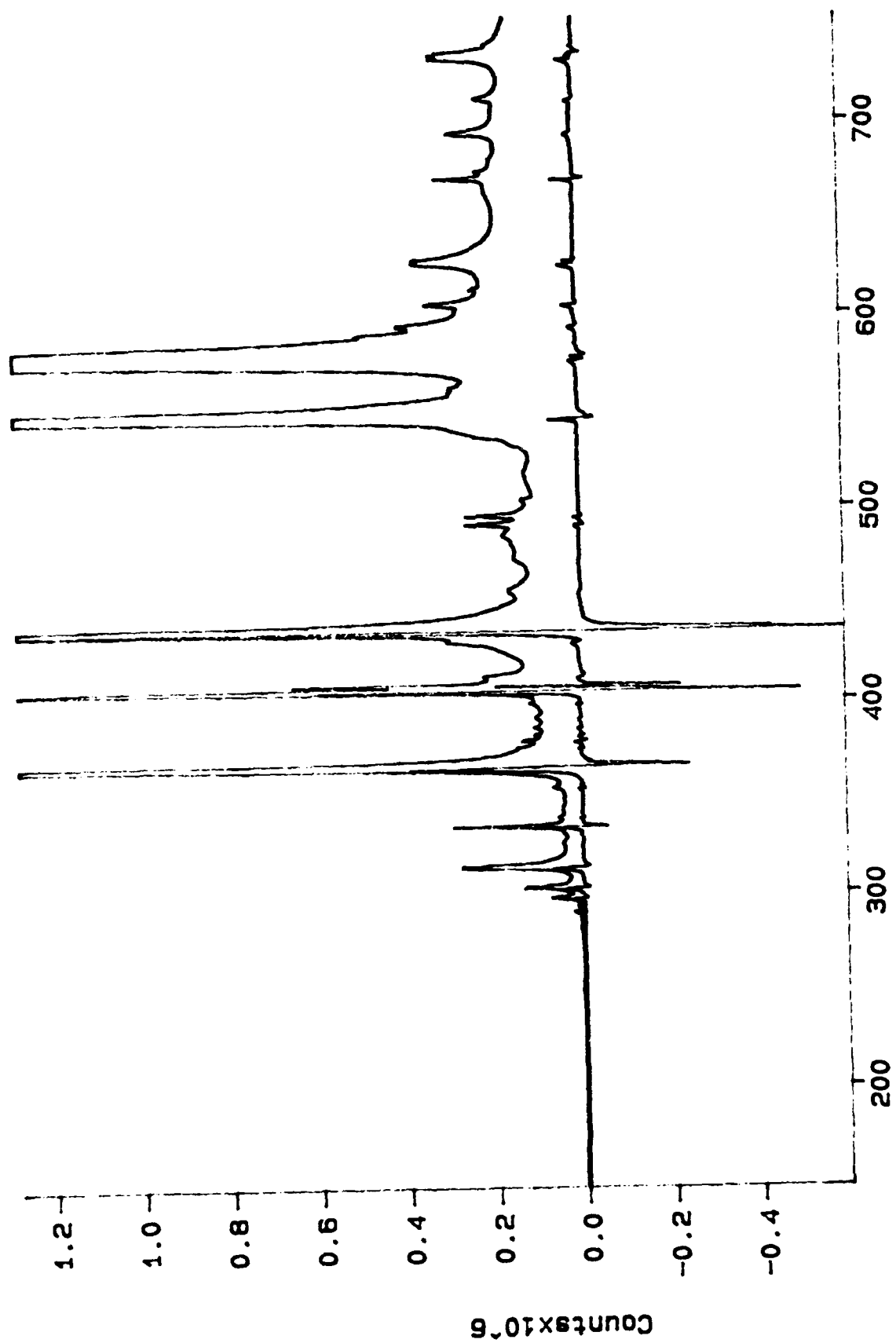


Figure 74
Luminescence Experiment Difference for Filter 3178

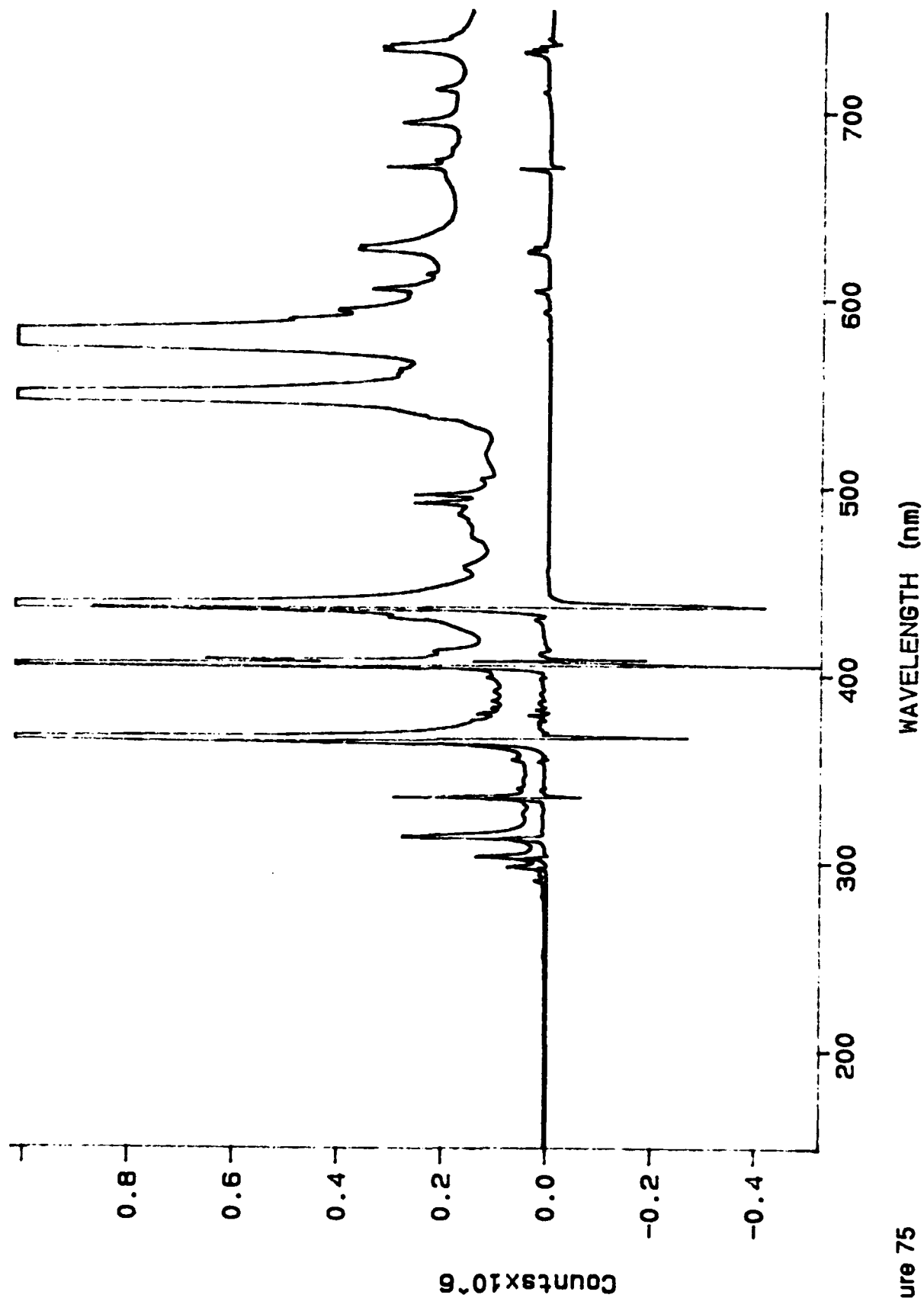


Figure 75

Luminescence Experiment Difference for Filter 3180

Source: F210372.DAT, Mem 1

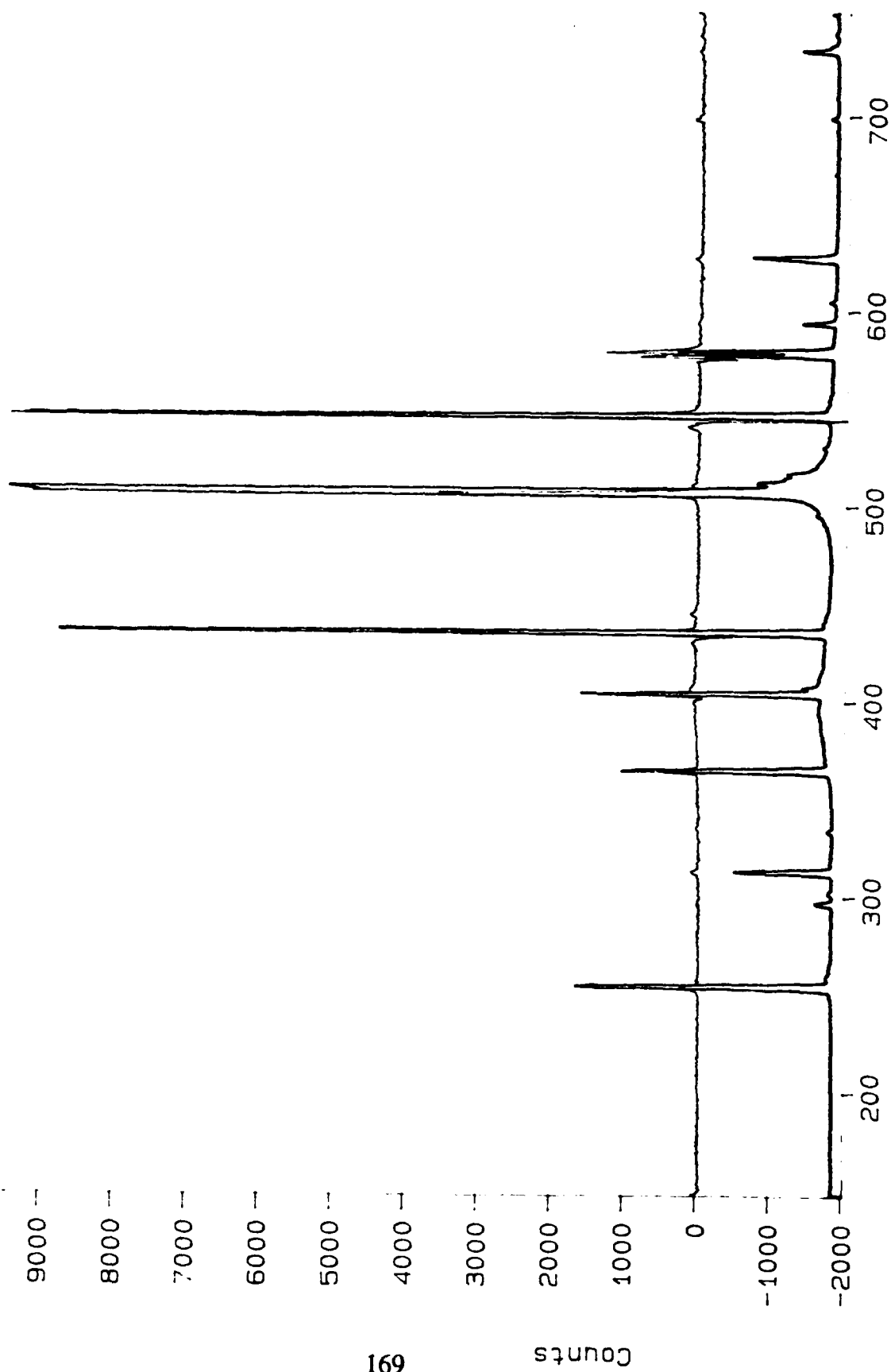
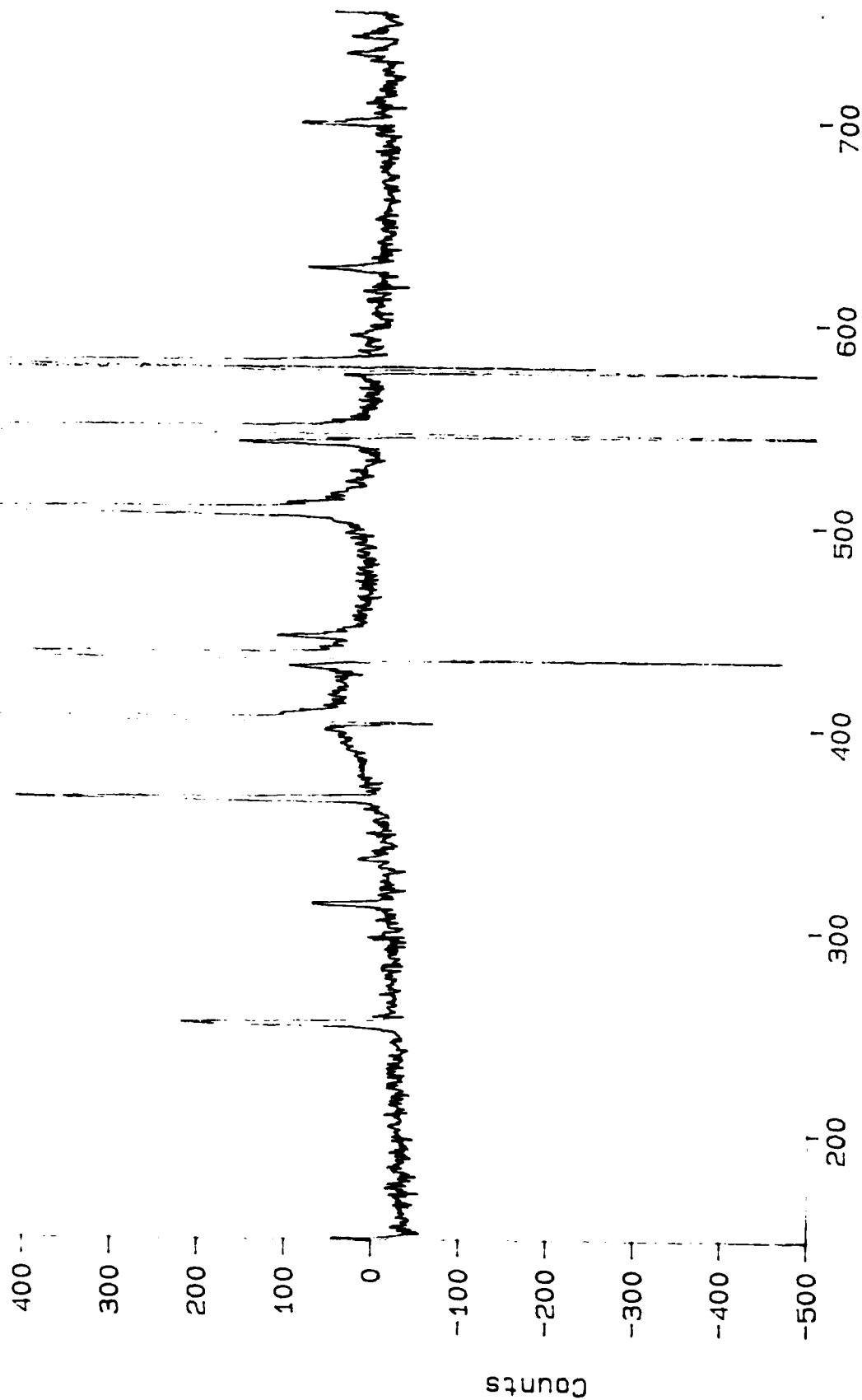


Figure 76

Copper Luminescence Experiment Using Chopper and Mercury Cal. Lamp

Source: F210372.DAT, Mem 1



170

Figure 77

Copper Luminescence Experiment Using Chopper and Mercury Cal. Lamp

REFERENCES

1. Wooten, F., *Optical Properties of Solids*, Academic Press, 1972.
2. Born, M., and Wolf, E., *Principles of Optics*, 6th ed., Pergamon Press, 1980.
3. Moon, P., *Scientific Basis of Illuminating Engineering*, Dover Publishing, Inc., 1961.
4. Jenkins, F.A., and White, H.E., *Fundamentals of Optics*, 4th ed., McGraw-Hill Book Company, 1976.
5. Hecht, E., *Optics*, 2nd ed., Addison-Wesley Publishing Company, 1989.
6. Tipler, P.A., *Physics*, 2nd ed., Worth Publishers, Inc., 1982.
7. Halliday, D., and Resnick, R., *Fundamentals of Physics*, 2nd ed., John Wiley & Sons, 1986.
8. Becker, R.S., *Theory and Interpretation of Fluorescence and Phosphorescence*, Wiley Interscience, 1969.
9. *McGraw-Hill Encyclopedia of Physics*, McGraw-Hill Book Company, 1983.
10. Biblarz, O., "Modification to Thermal Emissions by Clusters on Their Own Metallic Surface," *Journal of Vacuum Science Technology*, A8(1), pp.127-133, January / February 1990.
11. Duncan, M.A., and Rouvray, D.H., "Microclusters," *Scientific American*, pp. 110-115, December 1989.
12. Hayashi, C., "Ultrafine Particles," *Physics Today*, pp. 44-51, December 1987.
13. Baldwin, C.W., *Cluster Model Of Polarization Upon Reflection From Metallic Surfaces*, Master's Thesis, Naval Postgraduate School, Monterey, California, December 1991.
14. Princeton Applied Research Corp., *System Configurations Manual Models 1460 & 1461 (17508-A-MNL-A, 4200-0243)*, Princeton Applied Research Corp., 1988.
15. Allied Analytical Systems, *Jarrell-Ash MonoSpec 27 Monochromator / Spectrograph Models: 82-497, 82-498, 82-499 Operator's Manual*, Allied Analytical Systems, November 1985.

16. Princeton Applied Research Corp., *Models 1452A, 1453A, 1454A, 1453XR and 1452NIR Silicon Photodiode Detectors Instruction Manual (217484--A-MNL-C)*, Princeton Applied Research Corp., 1990.
17. Princeton Applied Research Corp., *Model 1462 Detector Controller and Model 1462/99 14-Bit A/D Converter Instruction Manual (17484-A-MNL-A, 4200-0242)*, Princeton Applied Research Corp., December 1986.
18. Princeton Applied Research Corp., *Model 1460 Optical Multichannel Analyzer Reticon Operating Manual (17631-A-MNL-E, 4200-0251)*, Princeton Applied Research Corp., 1988.
19. Ultra-Violet Products, Inc., *Pen-Ray Lamps ... Ultraviolet Sources for Research and Industry*, Ultra-Violet Products, Inc., 1977.
20. Hewlett-Packard Co., *HP ColorPro Graphics Plotter Operating Manual*, Hewlett-Packard Co., April 1987.
21. Seiko Epson Corporation, *FX-86e / 286e User's Manual*, Seiko Epson Corporation, 1986.
22. *Metals Handbook*, 9th ed., v. 9, pp. 48-56 and 399-401, American Society for Metals, 1985.
23. Thompson-Russell, K.C., and Edington, J.W., *Monographs in Practical Electron Microscopy in Materials Science*, v. 5, pp. 37- 45, Philips, 1977.

INITIAL DISTRIBUTION LIST

	No. Copies
1. Defense Technical Information Center Cameron Station Alexandria, Virginia 22304-6145	2
2. Library, Code 52 Naval Postgraduate School Monterey, California 93943-5002	2
3. Chairman Department of Aeronautics and Astronautics, Code AA Naval Postgraduate School Monterey, California 93943-5000	1
4. Professor Oscar Biblarz Department of Aeronautics and Astronautics, Code AA/Bi Naval Postgraduate School Monterey, California 93943-5000	2
5. Professor David Cleary Department of Physics, Code PH/CI Naval Postgraduate School Monterey, California, 93943-5000	1
6. Chairman Space Systems Academic Group, Code SP Naval Postgraduate School Monterey, California 93943-5000	1
7. Chairman Department of Physics, Code PH/Wh Naval Postgraduate School Monterey, California, 93943-5000	1
8. Professor Brij Agrawal Department of Aeronautics and Astronautics, Code AA/Ag Naval Postgraduate School Monterey, California 93943-5000	1
9. Dr. D. Decker, Code 3816 Physics Division Naval Weapons Center China Lake, California 93555	1

- | | | | |
|-----|--|---|--------|
| 10. | Professor Alfred Cooper
Department of Physics, Code PH/Cr
Naval Postgraduate School
Monterey, California 93943-5000 | 1 | |
| 11. | LCDR David T. Moroney
c/o Professor Oscar Biblarz
Department of Aeronautics and Astronautics, Code AA/Bi
Naval Postgraduate School
Monterey, California 93943-5000 | 1 | ✓
✓ |